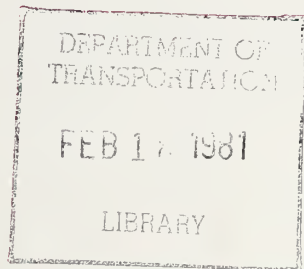


TE
662
.A3
no.
FHWA-
RD-
79-116
c.2

Report No. FHWA-RD-79-116

FEASIBILITY OF A GRADE SEVERITY RATING SYSTEM

August 1980
Final Report



Document is available to the public through
the National Technical Information Service,
Springfield, Virginia 22161



Prepared for
FEDERAL HIGHWAY ADMINISTRATION
Offices of Research & Development
Environmental Division
Washington, D.C. 20590

FOREWORD

This report describes the development of a grade severity rating system. The prototype system developed consists of a grade rating model and a speed selection model. With these models, a "grade severity rating" and a safe descent speed may be calculated and posted on steep downgrades in order to assist truck operators in negotiating the grades. The report will be of interest to those concerned with truck safety and safety of roadway design.

The report presents the results of a study in Project 1U, "Safety Aspects of Increased Size and Weight of Heavy Vehicles," of the Federally Coordinated Program (FCP) of Research and Development. The study was conducted for the Federal Highway Administration, Office of Research, Washington, D.C., under Contract DOT-FH-11-9253, and covers the period of research from September 1976 to April 1978.

Sufficient copies of this report are being distributed to provide a minimum of one copy to each FHWA regional office, one copy to each FHWA division office, and one copy to each State highway agency. Direct distribution is being made to the division offices.



Charles F. Scheffey
Director, Office of Research
Federal Highway Administration

NOTICE

This document is disseminated under the sponsorship of the Department of Transportation in the interest of information exchange. The United States Government assumes no liability for its contents or use thereof. The contents of this report reflect the views of the contractor, who is responsible for the accuracy of the data presented herein. The contents do not necessarily reflect the official views or policy of the Department of Transportation. This report does not constitute a standard, specification, or regulation.

The United States Government does not endorse products or manufacturers. Trade or manufacturers' names appear herein only because they are considered essential to the object of this document.

662
 .43
 20,
 FHWA
 RD-
 9-116
 e.2

1. Report No. FHWA-RD-79-116		2. Government Accession No.		3. Recipient's Catalog No.	
4. Title and Subtitle FEASIBILITY OF A GRADE SEVERITY RATING SYSTEM				5. Report Date August 1980	
				6. Performing Organization Code	
7. Author(s) Thomas T. Myers, Irving L. Ashkenas, Walter A. Johnson				8. Performing Organization Report No. TR-1106-1 R	
				9. Performing Organization Name and Address Systems Technology, Inc. 13766 South Hawthorne Boulevard Hawthorne, California 90250	
12. Sponsoring Agency Name and Address Federal Highway Administration Office of Research Environmental Division Washington, D.C. 20590				10. Work Unit No. (TRAIS) 31U2 032	
				11. Contract or Grant No. DOT-FH-11-9253	
15. Supplementary Notes FHWA Contract Manager: Michael Freitas (HRS-43)				13. Type of Report and Period Covered Final Report March 1977 to August 1979	
				14. Sponsoring Agency Code	
16. Abstract The objective of this study has been to determine the feasibility and format of a grade severity rating system (GSRS) so that existing countermeasures can be more rationally applied and the need for new countermeasures can be established. The study as conducted consisted of a literature review, the development of a truck downgrade braking model, a series of field tests to validate the model and the final development of a prototype grade severity rating system. With the grade severity rating system a downgrade may be given a numerical rating based on the severity of the grade. A speed selection model was also developed that can be used to determine a safe speed of descent based on the grade severity rating and the weight of the truck.					
17. Key Words Highway alignment Truck Highway grades Brake fade Downgrades Downgrade accidents			18. Distribution Statement No restrictions. This document is available to the public through the National Technical Information Service, Springfield, Virginia 22161.		
19. Security Classif. (of this report) Unclassified		20. Security Classif. (of this page) Unclassified		21. No. of Pages 194	22. Price



TABLE OF CONTENTS

	<u>Pages</u>
I. INTRODUCTION.	1
A. Objective of the Project	1
B. Overview of the Program.	1
C. Conclusions.	2
D. Organization of the Report.	2
II. THE TRUCK DOWNGRADE ACCIDENT PROBLEM.	4
A. Previous Grade Severity Rating Systems.	4
B. Introduction to the Grade Descent Problem.	7
C. Analysis of Heavy Truck Braking Systems	10
D. Grade Characteristics in the U.S.	24
III. THE TRUCK DOWNGRADE BRAKING MODEL.	30
A. The Brake Temperature Equation	30
B. Brake Force Required.	32
C. Integration of the Brake Temperature Equation	34
D. Determination of Parameters and Model Validation in the Field Test Program	40
E. Physical Implications of the Downgrade Braking Model	44
IV. THE GRADE SEVERITY RATING SYSTEM	57
A. The Temperature Limit Concept.	57
B. The Grade Descent Control Problem	60
C. The Maximum Safe Descent Speed	63
D. The Grade Severity Rating Concept	70
E. The Gear/Speed Selection Model	79
F. Alternatives to the SSM/CAB Card Concept	91
REFERENCES	100
APPENDIX A. DERIVATION OF THE BRAKE TEMPERATURE EQUATION	A-1
APPENDIX B. FIELD TEST PROGRAM	B-1

	<u>Page</u>
APPENDIX C. EXTENSION OF THE TRUCK DOWNGRADE BRAKING MODEL TO COMPLEX GRADES	C-1
APPENDIX D. DERIVATION OF \bar{V}_{max} APPROXIMATION	D-1
APPENDIX E. EXTENSION OF THE GSRS TO MULTIGRADE HILLS	E-1

LIST OF FIGURES

	<u>Pages</u>
1. The Grade Severity Rating System Proposed by Hykes.	4
2. The Grade Severity Rating System Proposed by Lill	6
3. Compilation of Published Data on Total Drag Force	12
4. Average Weight-Power Ratios and Gross Weights for Commercial Vehicles, 1963 Brake Test	13
5. Simplified Diagram of a Truck Air Brake System (only one trailer brake branch shown)	14
6. Characteristics of the Williams Air Controls 318A Adjustable Tractor Protection Valve.	15
7a. The S-Cam Brake	17
7b. The Wedge Brake	17
8. Mobile Brake Dynamometer Data from Ref. 10 Plotted Three Different Ways to Show the Effects of Line Pressure, Speed, and Brake Temperature.	20
9. Hypothesized Variation of Lining Friction Coefficient with Speed	21
10. Typical Power Absorption and Retarding Torque for a Six Cylinder Diesel Engine with an Engine Brake.	23
11. Distribution of Severe Grades in United States	25
12. Definition of Grade Geometry Limit Line from Severe Grade Data.	27
13. Altitude and Slope Profiles of the Donner Grade.	29
14. Equilibrium of Forces During Descent	34
15. Fluid Analogy of Brake Heat Transfer	35

16.	United States Truck Weight and Length Limits	40
17.	Variation of the $\bar{V}_{\max} = 55$ mph Boundaries with Weight.	41
18.	Comparison of Measured Time History of Average Brake Temperature with Profile Computed from Truck Downgrade Braking Model.	45
19.	Brake Temperature Response Due to Grade Variables	47
20.	Slope Threshold for Power into Brakes	50
21.	Brake Temperature Response Due to Truck Weight and Speed	51
22.	Brake Temperature Variation with Speed.	52
23.	Illustrative Progressive Buildup in Brake Temperature Variation with Speed (No Retarder)	54
24.	Generic Brake Fade Effects	58
25.	\bar{V}_{\max} Contours as a Function of Grade Slope and Length	65
26.	Maximum Slopes for Given \bar{V}_{\max} and Grade Length	67
27.	Optimal Gear Selection Strategy	70
28.	Definition of GSR Categories	74
29.	\bar{V}_{\max} Contours for 70,000 and 80,000 lb.	75
30.	Hill Length Effect on GSR-Induced Final Temperature Errors	78
31.	Example Cab Card	79
32.	Comparison of the \bar{V}_{\max} Approximation with the Exact \bar{V}_{\max} Contours	82
33.	Temperature Error Contours for 60,000 lb Truck and $\theta_{\text{ref}} = 0.06$	86
34.	Temperature Error Contours for 80,000 lb Truck and $\theta_{\text{ref}} = 0.06$	87
35.	Speed Error Contours for 80,000 lb Truck and $\theta_{\text{ref}} = 0.06$	88

	<u>Pages</u>
36. Plot for Definition of WSS Weight Classes.	95
37. Possible Formats for Weight Specific Speed Signs	97
38. Progressive (Burma-Shave) WSS Signs.	98
39. WSS Signs for Multilane Highway	99

LIST OF TABLES

1. Literature Review Topics	3
2. Analogous Quantities in Viscous Funnel Flow vs. Truck Brake Heating.	36
3. Summary of Truck Downgrade Braking Model	43

SYMBOLS

a_x	Longitudinal acceleration, ft/sec ²
A	Vehicle frontal area, ft ²
A_c	Effective heat transfer area of brake system, ft ²
C	Specific heat capacity, ft-lb/slug
e	Base for natural logarithms
$f_1, f_2,$ f_3	Brake torque functions
F	Force, lb
F_{drag}	Total drag force (Eq. 5), lb
F_{eng}	Engine braking force, lb
F_B	Total brake force, lb
F_{NB}	Non-brake force (Eq. 6), lb
g	Gravitational constant (32.2 ft/sec ²)
G_D	Differential gear ratio
G_{T_i}	Transmission gear ratio in ith gear
GSR	Grade severity rating
GSRS	Grade severity rating system
GW	Gross vehicle weight, lb
h	Effective heat transfer coefficient of brake system, lb/ft-°F-hr
HP	Power, hp
HP_B	Power absorbed by brakes, hp
HP_{eng}	Engine power absorption, hp
K_{ret}	Retarder effectiveness constant (Eq. 23)
K_1	$hA_B/m_B C, hr^{-1}$

K_2	$(hA_B)^{-1}$, hp/°F
L	Grade length, mi
m	Vehicle mass, slugs
m_B	Effective thermal mass of brake system, slugs
N	Number of forward transmission gears (Eq. 31)
p	Brake pressure, psi
P_{max}	Maximum brake pressure, psi
q	Heat flux, hp/ft ²
Q'	Rate of heat generation within a system, hp/ft ³
R	Tire rolling radius, ft
SSM	Speed selection model
t	Time, hr
T	Brake temperature, °F
T_f	Final brake temperature, °F
T_{lim}	Brake temperature limit, °F
T_o	Initial brake temperature, °F
T_{rway}	Brake temperature at which a runaway occurs (Fig. 24), °F
T_{ss}	Steady-state brake temperature, °F
T_{stop}	Maximum brake temperature for which an emergency stopping criterion can be met (Fig. 24), °F
T_e	Brake temperature error, °F
T_∞	Ambient temperature, °F
V	Vehicle speed, ft/sec
\bar{V}	Vehicle speed, mph
\bar{V}_{max}	Maximum safe descent speed, mph
\bar{V}_{rec}	Recommended speed (from SSM), mph

W	Total track weight, lb
W_{ref}	Reference weight
WSS	Weight specific speed
x	Distance along grade from top, mi
x_D	Drum thickness, ft
α	Thermal diffusivity, ft^2/hr
Δ	Transmission gear ratio increment (Eq. 31), percent/100
ΔW	Vehicle weight increment, lb
θ	Grade angle (approximate slope), rad
θ_0	Brake force threshold slope (Eq. 24), rad
θ_{ref}	Reference grade, rad
κ	Thermal conductivity, lb/hr
μ_{static}	Static brake lining friction coefficient
μ_{∞}	High speed brake lining friction coefficient
ρ	Density, slugs/ ft^3
ω_{opt}	Engine speed for maximum power absorption, rpm

SECTION I

INTRODUCTION AND SUMMARY

A. OBJECTIVE OF THE PROJECT

The objective of this project, as stated in the Federal Highway Administration's Statement of Work (Refs. 1 and 2) is "to determine the feasibility and format of a grade severity rating system (GSRS) so that existing countermeasures can be more rationally applied and the need for new countermeasures can be established." To accomplish this goal, it was envisioned that two analytical models would be developed and analyzed:

- 1) A grade severity rating model (GSRM) which accepts as inputs the relevant geometric characteristics of any highway downgrade and assigns a resulting (single number) grade severity rating (GSR).
- 2) A gear selection model (GSM) which converts the GSR through suitable in-cab, truck-specific, look-up charts to the corresponding highest gear for safe grade descent at a given weight.

B. OVERVIEW OF THE PROGRAM

The program began with a review of the published literature and trucking industry practice relevant to the downgrade braking problem. This review included previous GSRS systems, truck braking system design and operation, and grade characteristics in the U. S. From the information obtained, a truck downgrade braking model was developed to predict brake temperature during grade descents. A series of field tests was then conducted with a representative instrumented heavy truck to validate the model and obtain numerical values for specific parameters. The model in final numerical form was then used to gain deeper quantitative insight into the downgrade braking problem. It was further used in conjunction with a brake temperature limit to compute the maximum safe speed for a reference truck weight which then became the basis for formulating a grade severity rating and analyzing its effectiveness as a driver aid.

The maximum safe speed concept was also used to formulate possible gear (speed) selection models to be used as the basis for in-cab driver

aids. Problems with the potential accuracy and acceptance of in-cab aids lead to the development of an alternative aid in the form of weight-specific speed (WSS) signs.

C. RESULTS AND CONCLUSIONS

The results and conclusions fully developed in Sections III and IV are presented here to serve both as a summary for the casual reader and as early orientation to those more deeply interested.

- 1) A truck downgrade braking model has been developed and verified through instrumented field test. The model form is generally applicable, although the constants involved are expected to vary with truck and brake system design parameters.
- 2) Brake "fade," although dependent also on material and drum/shoe design, is primarily a brake temperature phenomenon. Accordingly, for purposes of GSR development, a brake temperature limit can be used to investigate potential downgrade fade problems.
- 3) A grade severity rating (GSR) procedure has been developed from the truck downgrade braking model to produce a GSR, based on a representative truck, which is a function of grade parameters only. This GSR, when posted on downgrades, can be used by a truck driver for speed selection on a comparative-intuitive basis within acceptable brake temperature limits. It appears, therefore, that GSR signs by themselves may be sufficiently useful to the driver, compared to conventional signing, to warrant further consideration and evaluation.
- 4) A gear/speed selection model which utilizes only a single grade parameter, specifically GSR, to serve as a basis for in-cab speed selection aids, will have inherent inaccuracies due to fundamental physical problems. These inaccuracies override any practical problems and indicate that in-cab devices are not feasible at the present time.
- 5) The weight-specific speed sign is an alternative which overcomes specific problems with the GSR-only-based in-cab devices. The WSS sign(s) appear sufficiently feasible to warrant further consideration and evaluation.
- 6) Procedures were developed for rating multigrade hills within the concept of the WSS signs and comparative-intuitive GSR. These procedures warrant application and further evaluation in continued research.

- 7) For single-grade hills in the U.S. the maximum existing slope as a function of grade length can be represented by a limit boundary on a plot of grade vs. length for U.S. hills. This grade geometry limit line is useful in setting the range of GSR/WSS considerations and applications.

D. RECOMMENDATIONS

As indicated above, the GSR/WSS signing concept deserves further evaluation and assessment in future follow-on efforts. In particular, such efforts should cover the applicability and utility of the concept to a population of truck types and models different from the "representative truck" used to generate the GSR/WSS signs. Assuming such utility and applicability are demonstrated on one or more single-grade hills, the research should be expanded to cover further analysis and experimental evaluation on multigrade hills.

E. ORGANIZATION OF THE REPORT

To aid in understanding and following the development of the above important results and ideas, a brief outline of the report is presented below. While not specifically noted in the outline, the background literature of pertinence to the project is reviewed, not in a separate section, but rather along the way where most appropriate. Gathering the necessary information required not only reviewing the published literature but also many personal contacts with truck operators, equipment manufacturers, highway patrol personnel, state highway officials, and trucking industry organizations. A listing of the most important topics on which information was gathered and the section of this report in which they are discussed is given in Table 1.

The organization of the report is outlined below.

Section II reviews the truck downgrade accident problem including: previous grade severity rating systems; the downgrade braking problem; truck brake systems; and grade characteristics in the U.S.

TABLE 1. LITERATURE REVIEW TOPICS

TOPICS	SECTION	PAGES
1. Previous grade severity rating systems	II-A	4-6
2. Non-brake power absorption	II-C-1	10-13
3. Truck brake design practice	II-C-2	13-16
4. Brake torque generation and fade	II-C-3	16-22
5. Retarders	II-C-4	22-24
6. Characteristics of downgrades in U.S.	II-D	24-28
7. Brake thermodynamics and heat transfer	III-A	30-40
8. Field test methods	App. B	

Section III presents the development of the truck downgrade braking model, a summary of results from the field test program and a discussion of model implications.

Section IV discusses the Grade Severity Rating System including: formulation and format of the GSR; the problems with the gear selection concept; and an alternative driver aid — the WSS sign.

Appendices A through E present derivations, field test details, and procedures for extending the GSRS to multi-grade hills.

SECTION II

THE TRUCK DOWNGRADE ACCIDENT PROBLEM

A. PREVIOUS GRADE SEVERITY RATING SYSTEMS

One of the first grade severity rating systems was proposed in the early 1960's by Hykes (Ref. 4). This system was an extension of the U.S. Bureau of Public Roads (USBPR) grade categories. The USBPR had divided all grades into the following categories: 1) greater than 3 percent and longer than 10 mi (16 km); 2) greater than 6 percent and longer than 1 mi (1.6 km); and 3) greater than 10 percent and longer than 1/5 mi (0.3 km). Hykes proposed an expansion of this categorization which allowed finer gradations of grade severity (see Fig. 1).

A second grade severity rating system was proposed by Lill (Ref. 5) in 1975. This system introduced three important new ideas:

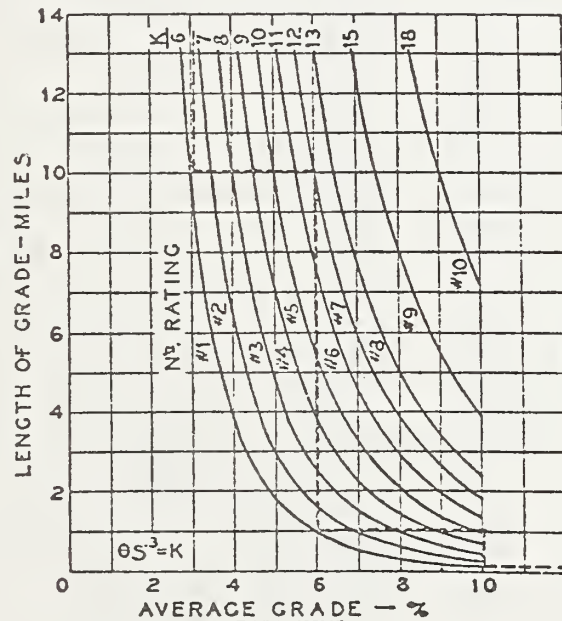


Figure 1. The Grade Severity Rating System Proposed by Hykes (Ref. 1)

- The concept of rating hills by their effect on a representative truck.
- The inclusion of the effect of hill length through consideration of brake fade effects.
- The use of a stopping distance criterion as a measure of available braking capacity.

Lill's method is based on the Work-Kinetic Energy equation applied to braking on a grade. This equation can be solved for the descent speed which will allow stopping in a criterion distance. For use in this equation the total retarding force must include brake and non-brake terms. Lill derived the brake terms for unfaded brakes from field test results and modified these for fade effects by use of a brake fade factor developed by Hykes. This brake fade correction was derived from temperature measurements made during brake dynamometer tests. To use this brake fade factor, Lill introduced the concept of brake equivalent time, which is defined as the hill descent time multiplied by the percent brake use. This analysis results in a maximum safe speed (i.e., the speed which will allow stopping within his criterion of 250 ft (66 m) which varies with length and slope of the hill. Grade severity ratings were then created corresponding to various speed bands, the higher speed band corresponding to least severe, the low speed to most severe, Fig. 2.

There are two primary limitations in Lill's analysis. First, the non-brake forces are considered to be constant, whereas they are known to be functions of velocity. More importantly, the brake fade factor is an empirical fit to specific test data and does not explicitly show the effect of such variables as ambient temperature, initial temperature of the brakes, brake heat capacity and heat transfer characteristics. Because of these limitations and the Federal Highway Administration's desire to review all pertinent analysis and research, this research program was essentially "started from scratch." Thus, the research began with an examination of the problem encountered in operating heavy trucks on severe grades.

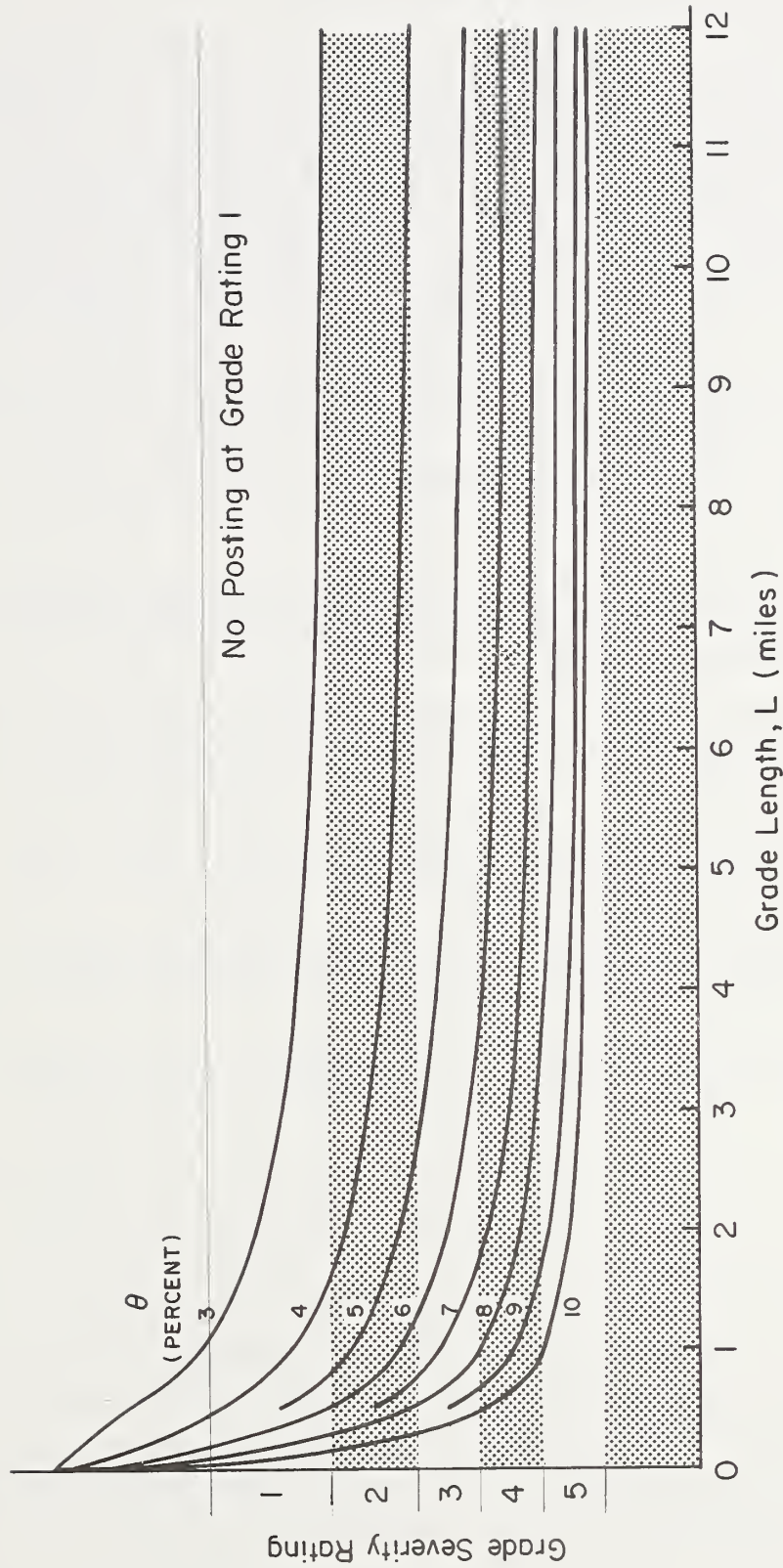


Figure 2. The Grade Severity Rating System Proposed by Lill, Ref. 2

B. INTRODUCTION TO THE GRADE DESCENT PROBLEM

Lill, in Ref. 6, summarizes the investigations made by the Bureau of Motor Carrier Safety (BMCS) of unusually severe truck accidents from 1973 to 1976. His analysis identifies the "runaway accidents on downgrades" and classifies them by state, route, and location. The BMCS study included 497 investigations of severe truck accidents nationwide; of these, 28 (6 percent) were identified by Lill as downgrade accidents. Colorado had the highest percentage of downgrade accidents; out of a total of 24, 10 (41 percent) were downgrade accidents. Furthermore, these accidents contained 40 percent of all the severe truck accident fatalities. A review of Ref. 6 reveals five primary factors which appear repeatedly and are characteristics of truck downgrade accidents:

- 1) Failure to downshift on the grade, improper shifting, or the use of excessive speed (in 82 percent of the downgrade accidents).
- 2) Drivers who were inexperienced or at least unfamiliar with the specific area (in 43 percent of the accidents).
- 3) Defective truck brakes or improper brake adjustment (in 36 percent of the accidents).
- 4) Indications of driver impairment such as the use of alcohol or fatigue due to excessive driving time (in 21 percent of the accidents).
- 5) Inadequate signing for the downgrade; better signing was recommended (in 14 percent of the accidents).

The conclusions to be drawn from the above data are that, grade geometry aside, failure to downshift and defective brakes appear to be the two primary factors in downgrade accidents; and inadequate signing and driver inexperience or impairment enter the picture primarily by causing a failure to downshift and/or excessive speed. These considerations essentially define the requirements for a GSRS. Obviously, a GSRS cannot solve the problem of defective brakes or impaired drivers but rather is intended to aid drivers in choosing the correct speed and gear through the use of improved signing with special emphasis given to the inexperienced driver.

Choosing the correct speed/gear for trucks descending highway grades is fundamental to maintaining a safe margin of braking capacity, both for emergency stopping and to prevent "runaways" on the grade. Other vehicle/roadway factors may also constrain the maximum safe speed on a grade. For instance, road surface conditions such as ice or defective vehicle equipment may all produce problems during grade descent. However, even in the absence of these other factors, there is always a potential problem with inadequate braking capacity on a severe grade.

The problem arises when a truck's service brakes must absorb a large amount of the potential energy that is dissipated in a grade descent. The brakes convert this energy to heat, and the accompanying brake temperature rise produces a decreased braking effectiveness known as "brake fade." For example, an 80,000 lb truck descending a 6 percent grade at 50 mph requires an energy dissipation rate of about 350 hp. If the heat rejection capacity of the truck's brakes (typically only several hundred horsepower) were less than 350 hp, brake temperature would rise continuously during the grade descent and could become critical on a long grade. By way of contrast, the same 80,000 lb truck making a 0.45 g stop (on level ground) from 50 mph requires an average energy dissipation rate of 4800 hp, most of which will be accomplished by the brakes. However, because the 0.45 g stop would last only about 5 seconds, the associated temperature rise would not be critical. These example numbers are intended to show that a hill descent situation is typically much more demanding in terms of brake heat dissipation than a single high performance stop on level ground. And this has a significant impact on safety.

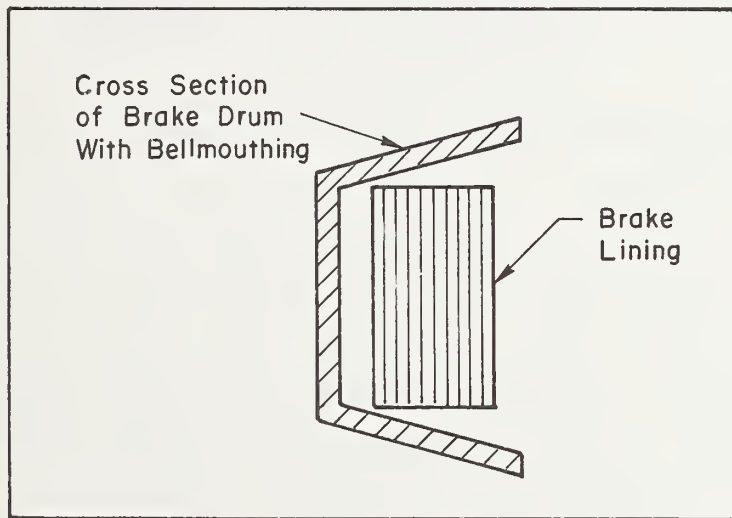
Despite a great deal of research and many improvements by brake designers, the problem of brake fade during hill descent still exists. In particular, as noted in Ref. 7, the extensive efforts involved in meeting FMVSS 121 (Ref. 8) have improved emergency stopping capability but have not necessarily improved heat rejection capability for grade descents. This is because "121" brake system design changes are primarily concerned with generating maximum, usable brake force rather than in improving brake heat rejection. Also, analysis and prediction of brake fade is very difficult, since detailed data are generally not available on specific brake systems.

This is due to a number of factors: the proprietary nature of the data; the variability of characteristics from unit to unit of a given model; and the inherent difficulties in the testing and analysis of friction brakes.

However, it is possible to understand the basic physics of brake operation and fade if we recognize that there are two distinct aspects to brake fade phenomena. First, there is the relation of the brake system temperature to the power input to the brakes, which in turn depends on the hill descent time history. Secondly, there is the relationship of braking friction force to the brake system temperature. These two relationships are essentially independent. That is, they involve different physical phenomena and different parameters of the braking system. In particular, for the case of hill descent at steady speed, the brake system temperature is determined only by the thermodynamic and heat transfer properties of the brakes and can be determined without a knowledge of the friction characteristics of the brake linings and drums. On the other hand, the relation of braking effectiveness to brake temperature depends only on the variation of the friction characteristics of the lining material with temperature, and the mechanical and thermal distortion characteristics of the brake mechanism. For completeness and clarity a brief digress to discuss these items is included here.

The variation of brake lining friction characteristics as a function of brake temperature is due to several phenomena. Two are mentioned here. First, at elevated temperature the lining material may produce a gaseous discharge that tends to "lubricate" the rubbing interface between the lining and the drum. Although significant, the reduction in direct friction properties is believed to be secondary in importance to the effects of mechanical and thermal distortion. The two primary distortion effects are expansion of the drum (due to elevated temperatures) and distortion of the drum shape (due to elevated temperature and large braking forces). At very high temperatures the expansion of the drum away from the brake lining can exceed the available brake shoe travel (even if the slack adjusters are set properly). This situation will also occur at only moderately high temperatures when the slack adjusters are not properly set. This effect is relatively simple to visualize; not quite as easy to visualize is the

(additional) effect of drum distortion — called "bellmouthing." As the drum expands due to heat, and the forces exerted by the lining against the drum expand it even farther, the "open" front of the drum will expand more than the "closed" back of the drum. This produces a somewhat flared opening of the drum causing it to resemble the shape of a bell (hence the name bellmouthing). The significance of this flared shape is that the brake lining can no longer make good contact with the drum wall. The full surface-to-surface contact of the lining on the drum is reduced to only the edge of the lining making contact with the drum rubbing surface. To visualize this, think of a cylinder (the lining) expanding inside a cone (the drum) as the following sketch suggests. With a greatly reduced contact area between lining and drum the braking efficiency is significantly degraded.



Getting back to the original train of thought, as will be shown later, it is possible to develop the grade severity rating system and gear selection model by considering only the first aspect of the brake fade phenomenon — the relation of brake system temperature to hill descent time history. This is crucial since the brake temperature can be determined from basic energy balance considerations requiring only data determinable from relatively simple field tests.

In contrast, it is much more difficult to quantitatively define the loss in brake effectiveness with temperature, as indicated by the foregoing digress and discussed further later. Whereas the details of brake fade are difficult to define, it is possible to establish a limit brake temperature below which safe grade descents can be made. From this viewpoint, the fundamental grade descent problem is to descend without exceeding the limit brake temperature. However, most operators do not have devices to monitor brake temperature and need other information to make a safe descent. Certain "nominal" braking information can be developed through analysis and generalized data, as discussed next.

C. ANALYSIS OF HEAVY TRUCK BRAKING SYSTEMS

1. Non-Brake Forces and Power Absorption

The forces which retard truck motion on the downgrade but do not originate in the service brakes are termed "non-brake forces," F_{NB} . The forces that comprise the total non-brake force include:

- Aerodynamic drag
 - Rolling resistance
 - Chassis friction
 - Engine braking force
- } F_{drag}
- F_{eng}

It is often convenient to deal with the sum of the first three forces (referred to as the total drag force, F_{drag}). This is because most field test procedures yield the total drag. Furthermore, only total drag is actually needed in the calculations pertinent to the purposes of this project.

The primary source of drag data used in previous studies was Ref. 9, which presents empirical formulas derived from a large number of truck field tests. The drag components are given in terms of power as:

$$\text{Aerodynamic drag power} = \frac{0.002A\bar{V}^3}{375} \quad (\text{hp}) \quad (1)$$

$$\text{Rolling resistance power} = \frac{(7.6 + 0.09\bar{V})\bar{V}W}{375,000} \quad (\text{hp}) \quad (2)$$

$$\text{Chassis friction power} = 1 + 2(10^{-7})(\text{rpm})W \quad (\text{hp}) \quad (3)$$

The power absorbed by a retarding force is equal to the force multiplied by the vehicle speed. Thus, the conversion from horsepower to force is given by:

$$\begin{aligned} F &= 375\text{HP}/\bar{V} = 550 \text{ HP/V} & (\text{lb}) \\ &= 249.7\text{HP/V} & (\text{kg}) \end{aligned} \quad (4)$$

When the drag power formulas (Eqs. 1-3) are converted to forces and summed (using typical values of engine speed = 2000 rpm and $A = 120 \text{ ft}^2$), the total drag force is given by:

$$\begin{aligned} F_{\text{drag}} &= \underbrace{(375 + 0.15W)/\bar{V}}_{\text{Chassis Friction}} + \underbrace{(0.0076 + 0.00009\bar{V})W}_{\text{Rolling Resistance}} + \underbrace{0.24\bar{V}^2}_{\text{Aero-dynamic Drag}} & (\text{lb}) \\ &= (170.3 + 0.068W)/\bar{V} + (0.00345 + 0.0000409\bar{V})W + 0.109\bar{V}^2 & (\text{kg}) \end{aligned} \quad (5)$$

Total drag (lb) is plotted versus speed in Fig. 3. Some additional data are available in Ref. 10 for a 3-S2 truck at GVW = 32,000 lb (14.5 Mg) in the 35-50 mph (56-80 km/h) speed range. These data conform nicely to the shape of the SAE curves but are somewhat lower in magnitude. Since the SAE procedure was last revised in 1958 and the Ref. 10 data were obtained about 1973, the lower drag in the latter case may be the result of truck improvements to reduce drag.

During grade descent the throttle is closed and the engine absorbs power input through the driveline to produce a braking effect. Data on engine power absorption capacity are considered proprietary by manufacturers and are not generally available. The only data found in the literature are given by Hykes, Ref. 4. From a survey of manufacturers, Hykes estimated power absorption at 35 percent of maximum output horsepower for gasoline engines and up to 33 percent for diesel engines. However, some manufacturers indicate that engine design changes in recent years make it invalid

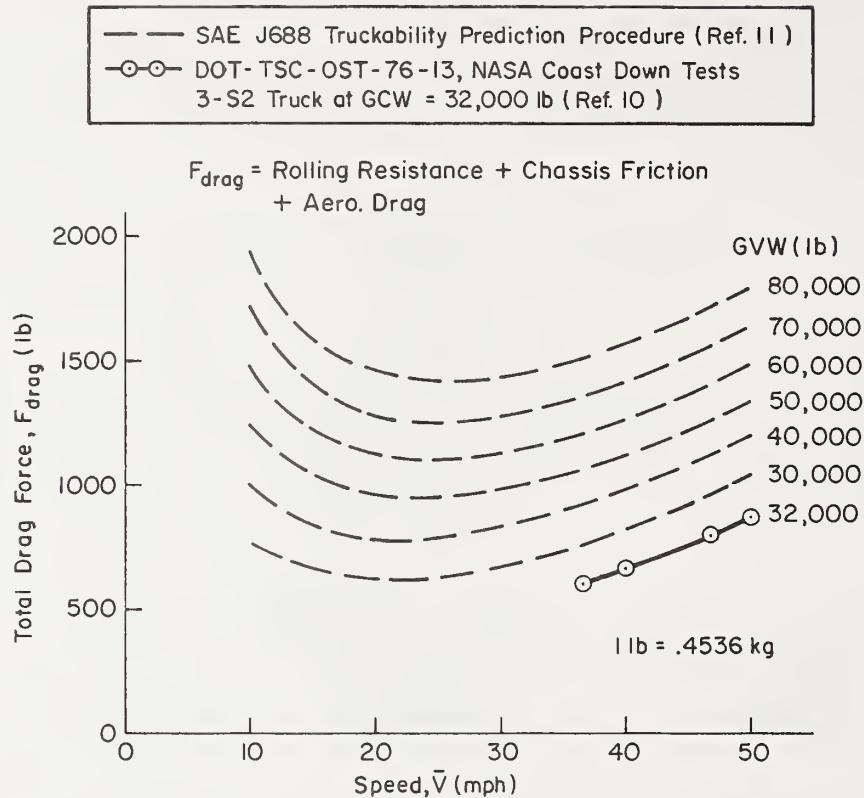


Figure 3. Compilation of Published Data on Total Drag Force

to specify power absorption as a fraction of maximum engine power. Instead, power absorption is specified as a function of engine speed. In general, power absorption increases with engine speed, and thus it is usually recommended that descents be made near the maximum allowable engine speed. Under these circumstances power absorption again depends primarily on maximum engine power.

The ratio of gross vehicle weight to engine power is therefore a significant indicator of the greater tendency for heavy (Class 8) trucks to have more "runaway" incidents or braking problems than light trucks and passenger vehicles. This may be better understood by considering the following. Because most heavy truck use is on nominally level highways, and because weight is only a secondary factor in affecting drag, it is understandable that engine power for heavy trucks is comparable (within a factor of 2) to that for light vehicles. (On upgrades, where the weight of heavy trucks is a significant factor, trucks are simply driven in a very low gear.)

Therefore, even though the braking capacity per pound may be comparable for light vehicles and heavy trucks (because the number of axles generally increases with GVWR). The fact that engine power does not scale up with GVWR (see Fig. 4) means heavy trucks have the least favorable total retardation characteristics.

During grade descents engine speed is determined by the vehicle speed and transmission gear. Thus, the non-brake force is the sum of the total drag and engine braking forces

$$F_{NB} = F_{drag} + 375HP_{eng}(G_{T_i}, \bar{V})/\bar{V} \quad (6)$$

where $HP_{eng}(G_{T_i}, \bar{V})$ is the engine power absorption function.

Measurements of F_{drag} and HP_{eng} were made for the primary test vehicle of this program. The results will be presented in Section III.

2. The Service Brake System

Service brakes for the tractor/trailer vehicles commonly used in line haul applications are universally air mechanical brake systems. Figure 5 is a simplified diagram of a typical air brake system showing only the basic components. Compressed air for operation of the system is generated by an engine-driven air compressor and stored in the main supply reservoir.

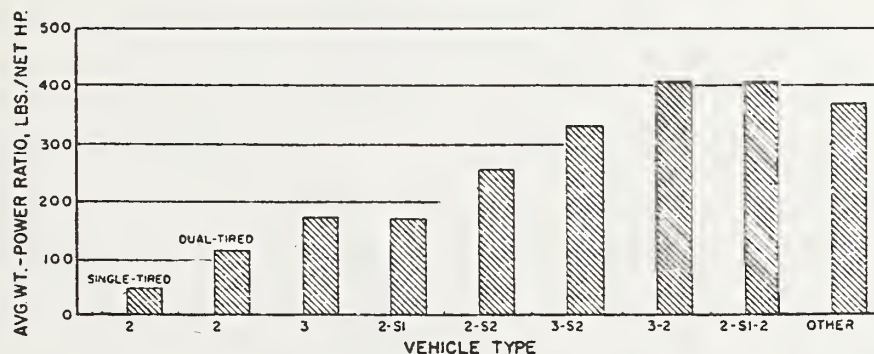


Figure 4. Average Weight-Power Ratios for Commercial Vehicles, 1963 Brake Test (Ref. 11)

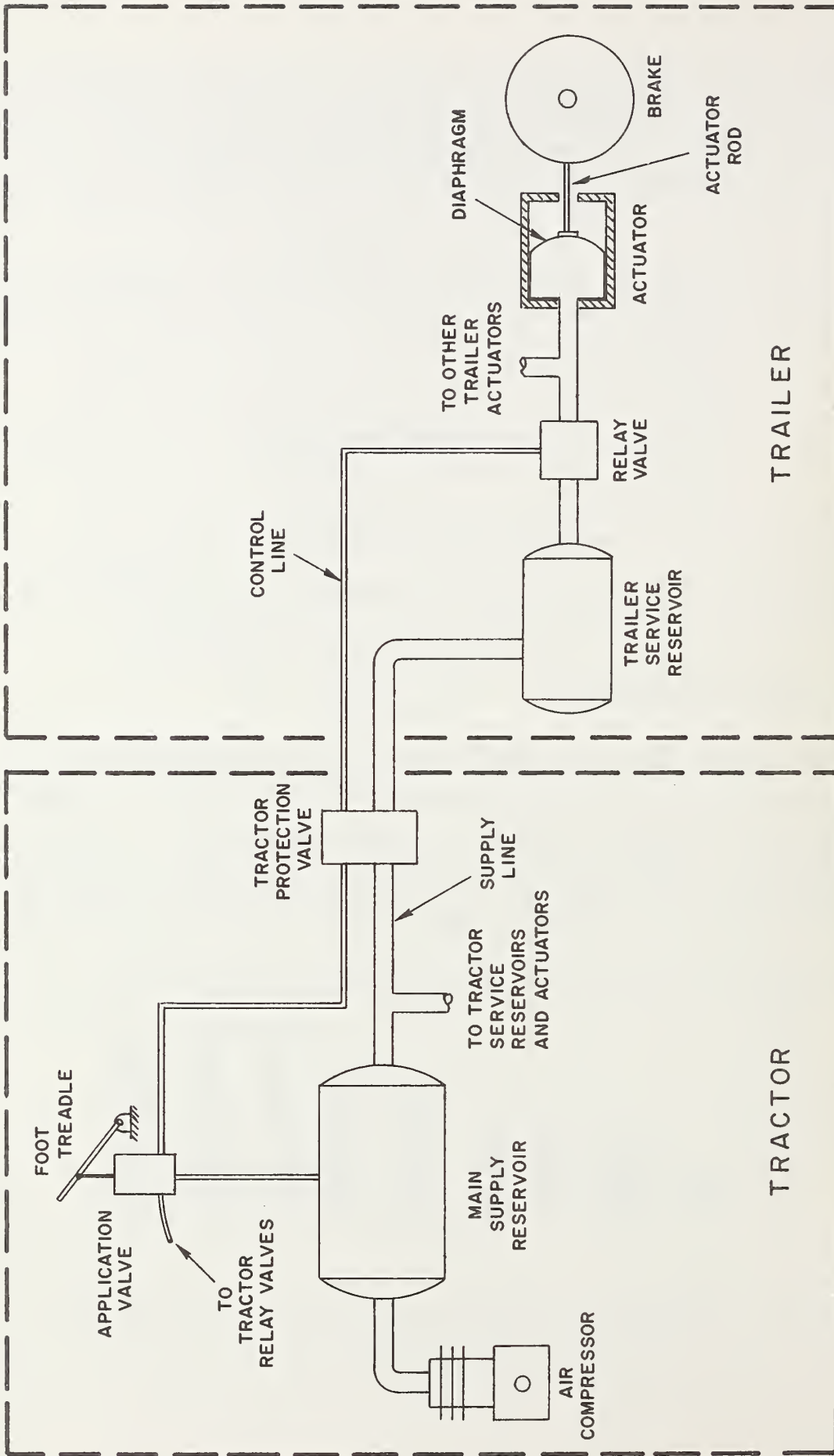


Figure 5. Simplified Diagram of a Truck Air Brake System (only one trailer brake branch shown)

In most systems, the brakes are not directly actuated by air from the main supply tank. This is to prevent long time delays in actuation which would result if a large volume of air were to be transported from the main supply tank in the tractor to the trailer brakes. Instead, trailer brakes and usually the tractor rear brakes are supplied from service reservoirs located nearby. The service reservoir is connected to the brake actuators by a "relay" valve controlled pneumatically by the application (treadle) valve which is operated by the driver. When the application valve is opened, a pressure pulse (as opposed to a large air flow) "trips" the relay valve and allows "supply air" from the service reservoir to flow into the brake actuator. Air pressure acting against the rubber diaphragm in the actuator forces an actuator rod to operate the brake mechanism.

Trailer brakes are typically connected to the tractor air brake system through a tractor protection (TP) valve. A primary function of this valve is to seal off the tractor air supply when it is not connected to a trailer. This would include those instances of accidental trailer separation from the tractor. However, some TP valves also allow the maintenance of an adjustable pressure difference between the tractor and trailer. Such adjustable TP valves are used to achieve brake force balance on combination vehicles. A typical valve, the Williams Air Controls 318A, was used on the Phase I test vehicle, as will be explained in Appendix B. The characteristics of this valve are shown in Fig. 6.

The service brakes used on almost all heavy trucks in the U.S. are of the drum type. There is presently considerable interest in air-operated disc brakes for heavy trucks, but it appears (Ref. 13) that it will be at least several years before disc brake systems are in general use. When disc brake systems do become operational it is expected that they will constitute a significant advancement in braking capability. Thus, drum brake systems will likely remain the "worst case" until they are no longer in use. For this reason the developments in this project have been based on trucks with drum brake systems.

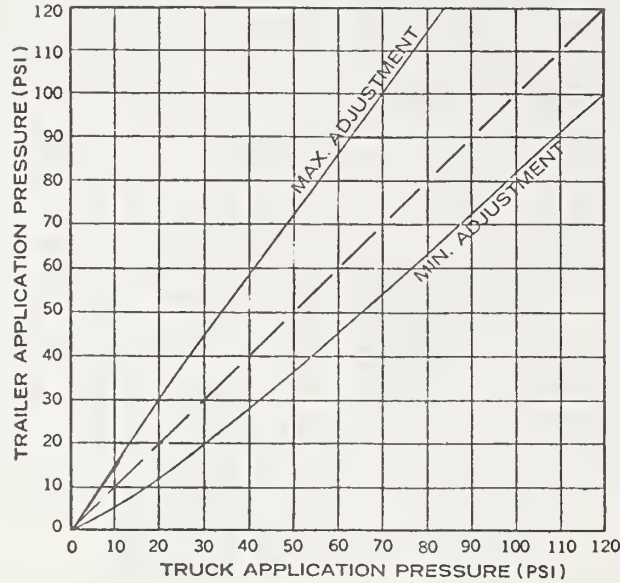


Figure 6. Characteristics of the Williams Air Controls 318A Adjustable Tractor Protection Valve (Ref. 12)

Two types of drum brakes are in general use on heavy line-haul trucks: the "S-cam" brake and the "wedge" brake. In the S-cam brake, Fig. 7a, the actuator rod is connected to a bellcrank ("slack adjustor") which is, in turn, connected to a shaft-mounted S-shaped cam. When the brake is actuated the S-cam rotates and forces both brake shoes out against the brake drum.

In its simplest form, the wedge brake replaces the single S-cam mechanism by a wedge on the end of the actuator rod. In a more common type of wedge brake, the shoes are not pinned to the backing plate but, rather, two wedge mechanisms are used between both ends of the shoes, Fig. 7b.

3. Available Brake Force

For purposes of this project the primary interest in brake performance is with regard to brake fade. Thus, we are concerned with how the available brake force decreases with temperature. However, for any braking situation there is a certain brake force required to accomplish the task. If the maximum available brake force is less than the required brake force because of fade, the braking task cannot be accomplished. In the case of a grade descent this could lead to a runaway or the inability to make a safe emergency stop.

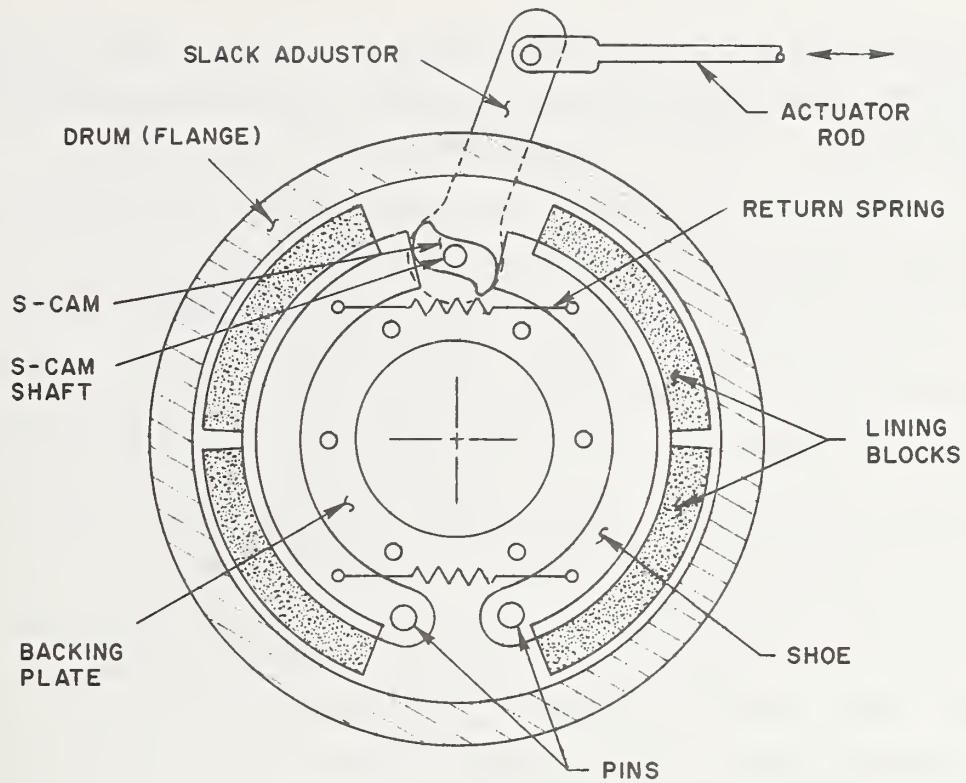


Figure 7a. The S-Cam Brake

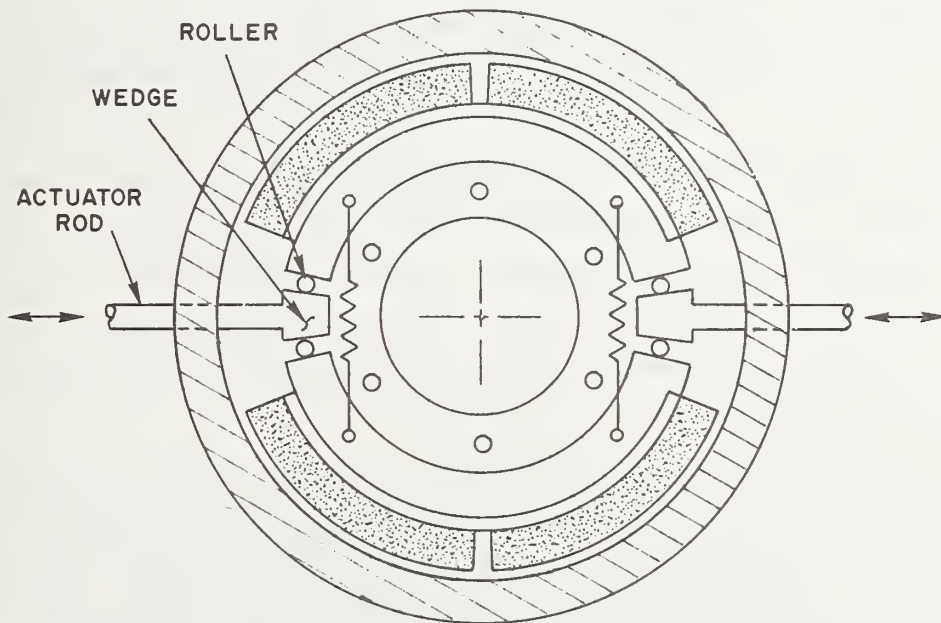


Figure 7b. The Wedge Brake

In this subsection the factors affecting the available brake force will be discussed. The determination of the required brake force will be discussed in Section III.

The brake force at each wheel is developed in the tire/road interface. It is equal to the torque developed by the brake divided by the effective wheel radius as long as the braking force is below a limiting value. Wheel lockup and skidding begin when this limiting brake force is exceeded. This can occur in high deceleration stops if antilock brakes are not used. However, in a steady grade descent (for any conceivable truck and hill), the brake forces will be well below this limit. Consequently, brake force will be directly proportional to brake torque in a grade descent.

When a brake is actuated, the brake lining is pressed against the drum and frictional shearing stresses are produced in the lining/drum interface. The brake torque is the integral of the shearing stress over the lining surface area multiplied by the drum radius. In principle, the shearing stress at any point on the lining surface can be determined from the lining friction coefficient and the normal stress at that point. The lining friction coefficient is the ratio of shearing stress to normal stress and can be measured in tests on small samples of lining material.

The more difficult problem, because it involves complex thermoelastic distortion of both the drum and the shoe, is that of predicting the distribution of normal stress over the lining surface. Because of these complexities, direct calculation of brake torque is apparently not possible, and engineering data are usually obtained directly from dynamometer and field tests of actual brakes. Nevertheless, it is clear that temperature can affect brake torque in at least two ways: first, by affecting the lining friction coefficient; and second, by changing the normal stress distribution over the lining surface.

Other parameters are also involved and, in general (Ref. 14), brake torque is considered to be a function of three variables and possibly their time derivatives: line pressure, brake temperature, and speed. This is true both in steady grade descents and in high deceleration stops, but the form of the function and its time variation may be somewhat different in

these two cases. While test data often indicate that this functional dependence is complex and not easily defined, a common assumption for engineering analysis is that brake torque can be treated as a product of three single variable functions (Ref. 16):

$$\text{Brake torque} = f_1(p) f_2(V) f_3(T) \quad (7)$$

The appeal of this idealization is that the effect of each variable can be characterized independently.

Obtaining quantitative data on the torque generating capabilities of actual brakes is very difficult since data are considered proprietary by manufacturers. It is known that characteristics can vary significantly depending on the lining material and drum design. Significant unit-to-unit variations can also occur within a production run of a given model. The traditional procedure for laboratory testing of truck brakes involves the use of an inertia dynamometer, Ref. 17. In this procedure the brake to be tested is connected to a large flywheel. Measurements of torque, temperature and line pressure are made as the brake brings the spinning flywheel to rest. The test lasts only a few seconds and thus corresponds more to emergency stopping than to continuous braking on a downgrade. In addition, the air flow and heat transfer characteristics do not simulate downgrade braking conditions.

Downgrade conditions are simulated more closely with mobile dynamometers. These devices typically consist of a special trailer towed by a truck which carries a test tire-wheel-brake assembly and necessary instrumentation. In operation the trailer is towed at a constant test speed. The test brake can be operated and its torque and temperature measured as the test wheel turns at constant speed. The only useful mobile dynamometer data found in the literature search are that of Ref. 18. Brake torque measurements were made at three speeds, three application pressures, and three initial temperatures. These 27 data points have been plotted in Figs. 8a, 8b, and 8c in three different ways corresponding to the independent torque functions f_1 , f_2 , and f_3 . The effects of application pressure, speed, and brake temperature can thus be examined and are summarized below.

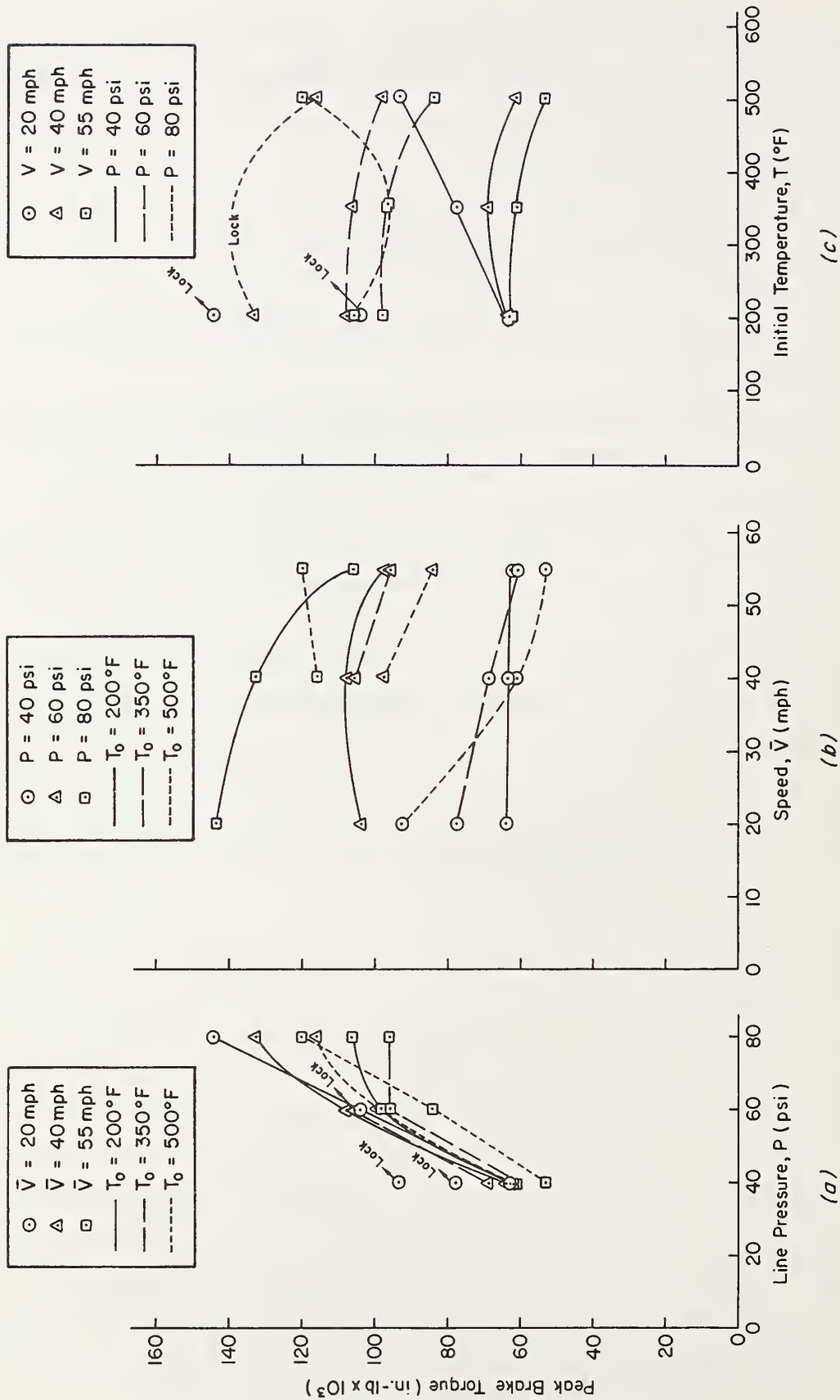


Figure 8. Mobile Brake Dynamometer Data From Ref. 18 Plotted Three Different Ways To Show the Effects of Line Pressure, Speed, and Brake Temperature. Brake tested was an S-cam brake with a cast iron drum.

a. Line Pressure

The dominant trend in the variation with pressure seen in Fig. 8a is a roughly linear increase in brake torque with pressure. There is some non-linearity at high pressure; however, it should be noted that pressures in the region of 80 psi would be used only in a high deceleration stop. During grade descents pressures are typically in the 5-10 psi range. Extrapolating the data linearly to zero torque indicates that a threshold pressure of approximately 8 psi must be reached before a brake torque is produced. This is to be expected since such thresholds or "pushout" pressures are well known (Ref. 19) and can give rise to brake balance problems during grade descent. Thus, in summary, the data indicate that brake torque is roughly linear with pressure over some region but in any case increases monotonically.

b. Speed

The variation with speed, Fig. 8b, is more complex. At $T = 200$ °F and $p = 40$ psi, the brake torque is constant with speed. Under other conditions there is generally a decrease in torque with speed. Such an effect is recognized in the literature and termed "speed fade"; however, little quantitative data are available on the subject. Reference 14 indicates that the lining friction coefficient decreases from a static level to some high speed level in an exponential way, Fig. 9. However, from the data available it is difficult to make any generalizations about the speed fade effect other than that it probably exists.

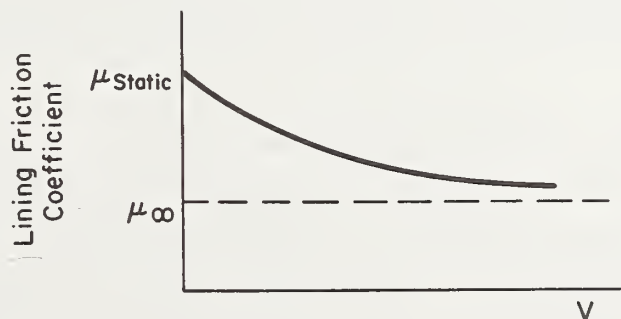


Figure 9. Hypothesized Variation of Lining Friction Coefficient with Speed (Ref. 14)

c. Brake Temperature

The effect of brake temperature is the most important effect for this program since the decrease in brake torque-generating capability with temperature, i.e., brake fade, is the fundamental problem in grade descent. Brake fade is a widely known phenomena, but it is very difficult to obtain quantitative fade characteristics on specific brakes from manufacturers. Contact with manufacturers did reveal that a wide variety of fade characteristics can occur, with lining composition being the most important consideration. For instance, some linings show a definite increase in brake torque with temperature up to the temperature for fade onset. Some linings show a fairly gradual fade with temperature, while others produce a discontinuous drop in brake torque when they fade. The data in Fig. 8c show somewhat conflicting trends; however, at the higher speeds and lower pressures there is evidence of fade onset above 350 deg.

4. Retarders

Trucks operating in mountainous regions have for many years used "retarder" devices to reduce the load on service brakes during long downgrades. There are a number of different types of these devices, all characterized by the ability not only to absorb energy but also to dissipate it effectively, thereby permitting long periods of continuous operation (e.g., on long downgrades). This characteristic is what gives the retarder its basic advantage over truck service brakes on long downgrades. Retarders have been used in the U.S. for over fifteen years but were introduced in Europe over forty years ago and have been widely used since. About five years ago European regulations made retarders standard on trucks built for sale there (Ref. 20).

Three general types of retarders are in current use: engine brakes, compression or exhaust brakes, and drive line brakes. The engine brakes are typified by the Jacobs Engine Brake or "Jake" brake (Ref. 21). When activated, this device modifies the engine valve timing to effectively turn the engine into an air compressor. Specifically, when a piston reaches the top of its compression stroke the exhaust valve is opened, dropping the chamber pressure to atmospheric pressure. Thus, during the power stroke there

is no net pressure acting on the piston to force it back down. This results in a net power absorption by the engine during its operating cycle. Engine brakes are typically installed on diesel engines, both four and two cycle. Typical engine brake power absorption characteristics are shown in Fig. 10. The "rule of thumb" for engine brake performance (Ref. 22) is that the gear for descent of a grade with an engine brake is in general the gear appropriate for ascent of the same grade. The Jacobs Manufacturing Co. estimates that up to 50 percent of the heavy trucks in the Western U.S. have engine brakes. They are particularly popular with owner-operators.

Compression brakes are typified by the Williams "Blue Ox" Compression brake. In this device a slide valve closes off the exhaust system during hill descent, creating a 30-45 psi back pressure which exerts a retarding force on the engine (Refs. 20, 23, 24). The retarding capability of compression brakes is somewhat lower than engine brakes, and they are generally installed only on four cycle diesel engines. According to the Williams Air Controls Co., the "Blue Ox" compression brake is installed on less than 10 percent of the U.S. truck fleet.

Three types of drive line retarders are in general use: hydraulic, electric, and liquid-cooled disc brakes. The Caterpillar "Brake Saver" (Ref. 25), is a typical hydraulic unit. A rotor is mounted between the engine driveshaft and flywheel in a housing which can be filled with oil. During grade descent the rotor is driven by the drive line and converts mechanical energy into thermal energy in the oil by the action of viscous shearing stresses on the rotor. The oil is continuously circulated through a heat exchanger to dissipate the absorbed energy. Similar "add on" hydraulic units are available which can be mounted in the drive line between the transmission and rear axle (Ref. 26). Electric retarders are all similar to the Jacobs Electric Retarder, in which mechanical energy is converted to thermal energy via an electric eddy-current generator (Ref. 27). The thermal energy is then dissipated by cooling fins. The liquid-cooled disc brake devices are similar to disc brakes used in regular truck service brakes. However, they are drive line mounted and have the basic advantage of better heat dissipation characteristics provided by the liquid cooling, which is not practical on truck service brakes.

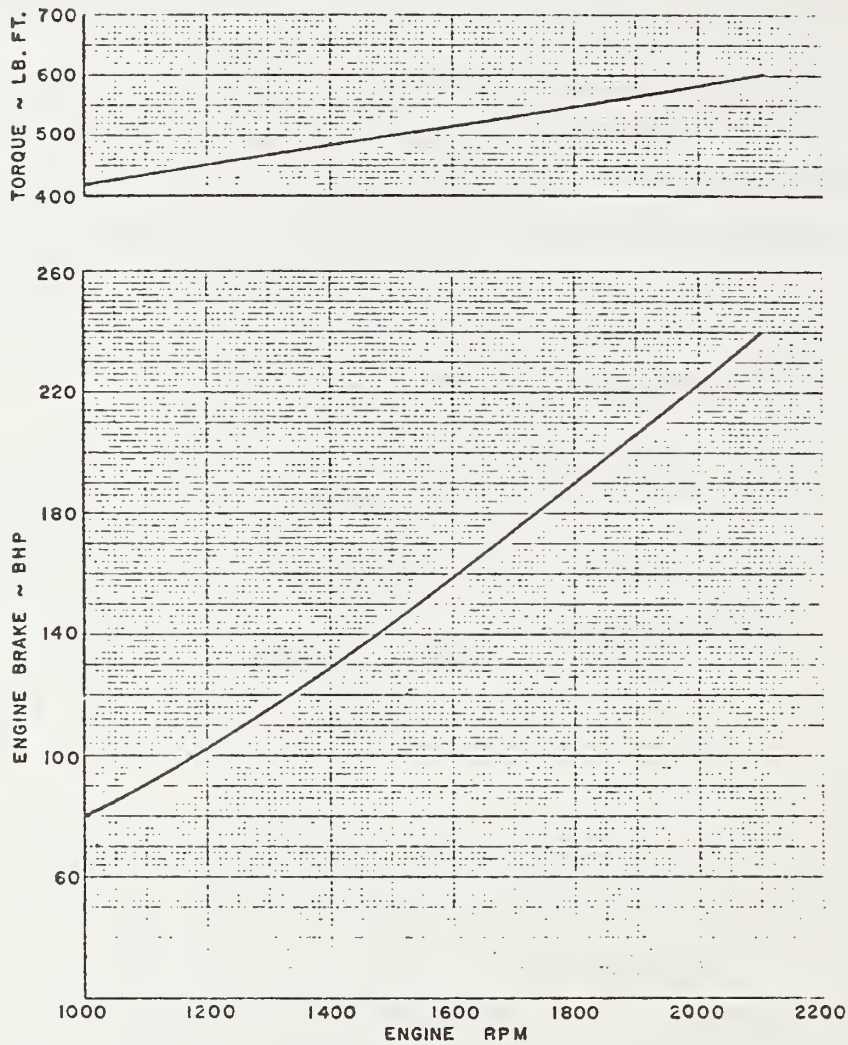


Figure 10. Typical Power Absorption and Retarding Torque for a Six Cylinder Diesel Engine with an Engine Brake (Ref. 21)

In general, the price of retarders increases with their power absorption ability. The least effective devices are the exhaust brakes, which cost \$500-600. Next are the engine brakes, which cost from \$800 to \$1000 and are generally rated as having power absorption capability equal to 100 percent of the output horsepower of a four cycle normally aspirated engine. The drive line retarders, which can absorb up to several hundred horsepower, cost up to several thousand dollars.

D. GRADE CHARACTERISTICS IN THE U.S.

The final element in the truck downgrade accident problem is the highway grade itself. To define the range of grade geometric characteristics in the U.S., grade data were gathered from a number of sources (Refs. 28-31). Unfortunately, most of these data are minimal, i.e., grades are specified in terms of a single slope and length for each hill; nevertheless, they are useful in defining the extremes of grade geometries in the U.S. Subsets of the data available, representing the more geometrically severe grades, are shown for the eastern U.S. in Fig. 11a and for the western U.S. in Fig. 11b. It appears that in terms of maximum slope, grades of comparable steepness can be found in either the eastern or western United States. There is some indication that steep grades may be somewhat more common in the eastern United States. The primary distinction between the eastern and western United States, however, is in terms of length. In the eastern U.S., four extreme grades were found greater than 6 mi in length, and only one of these was greater than 10 mi in length; in the western U.S. a number of grades were found which were longer than 10 mi.

The data from Figs. 11a and 11b are combined in Fig. 12 to form a composite of extreme grade characteristics for the U.S. A "grade geometry limit line" has been established from this plot and represents the locus of the maximum slope occurring at any specific grade length. Thus, for purposes of GSRS development, we need only consider grades (θ, L pairs) lying below this line.

Actual grades are not as uniform or as well identified as the plotted points in Figs. 11 and 12. In fact, examination of the available grade data has shown that the slope and length of a particular highway downgrade may vary widely depending on measurement conventions. For instance, in Ref. 28 there are three different representations of the same section of highway in the Great Smoky National Park. Apparently, the same grade has been reported in three different ways depending on the length over which the grade was averaged. Examples can also be found in comparing Pennsylvania Motor Truck Association (PMTA) data, Ref. 29, with those of Ref. 28. The PMTA data show at least five grades which appear to have severe geometric characteristics but which do not appear in the Ref. 28 data. In addition, the grade west

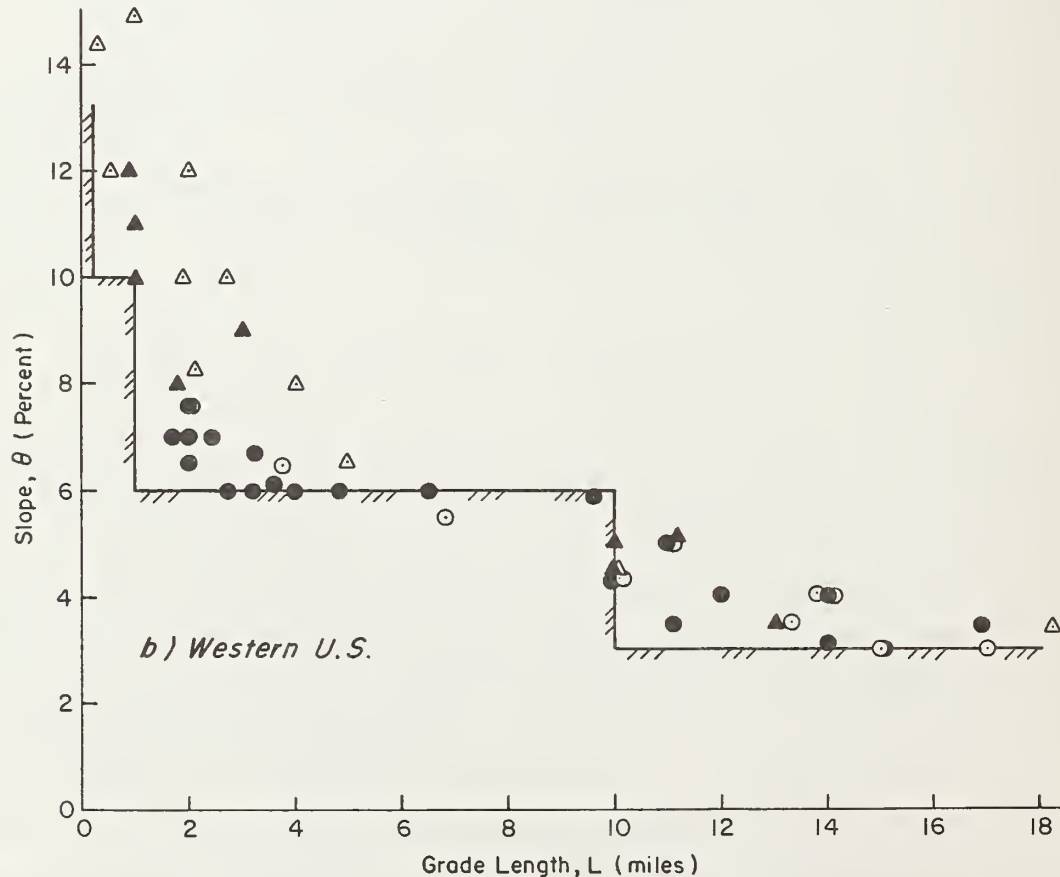
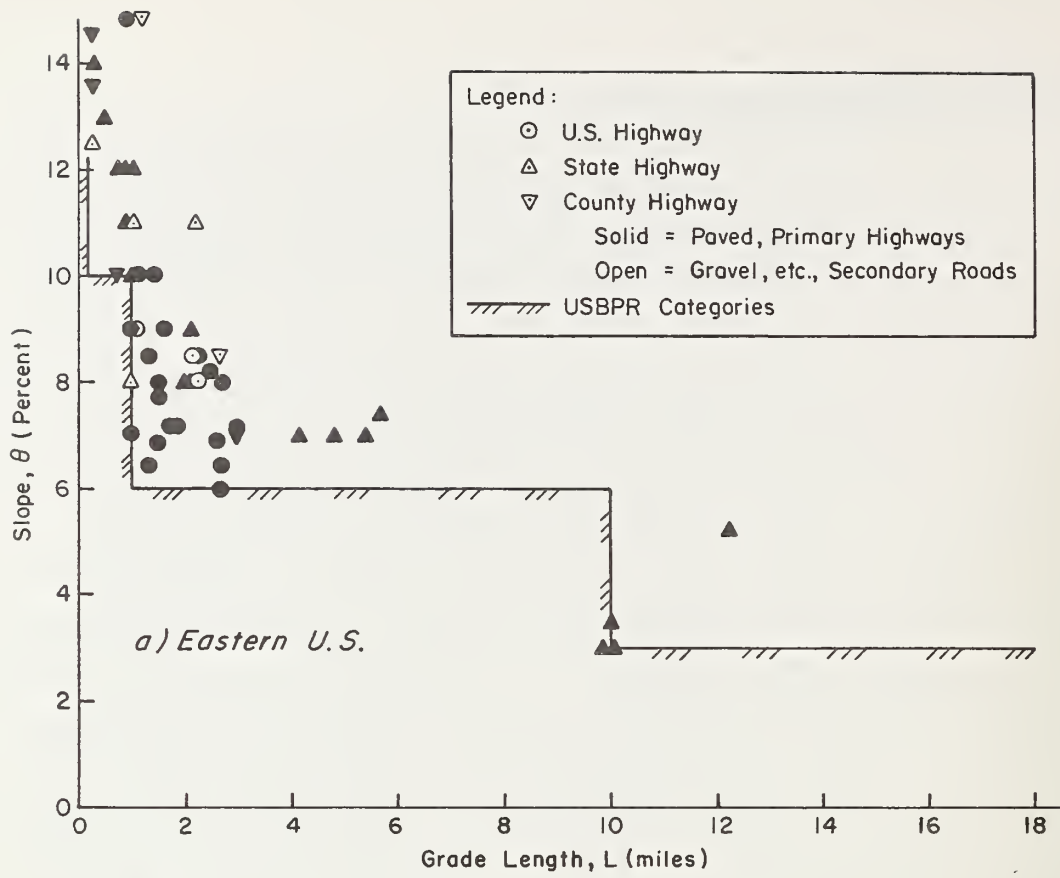


Figure 11. Distribution of Severe Grades in United States

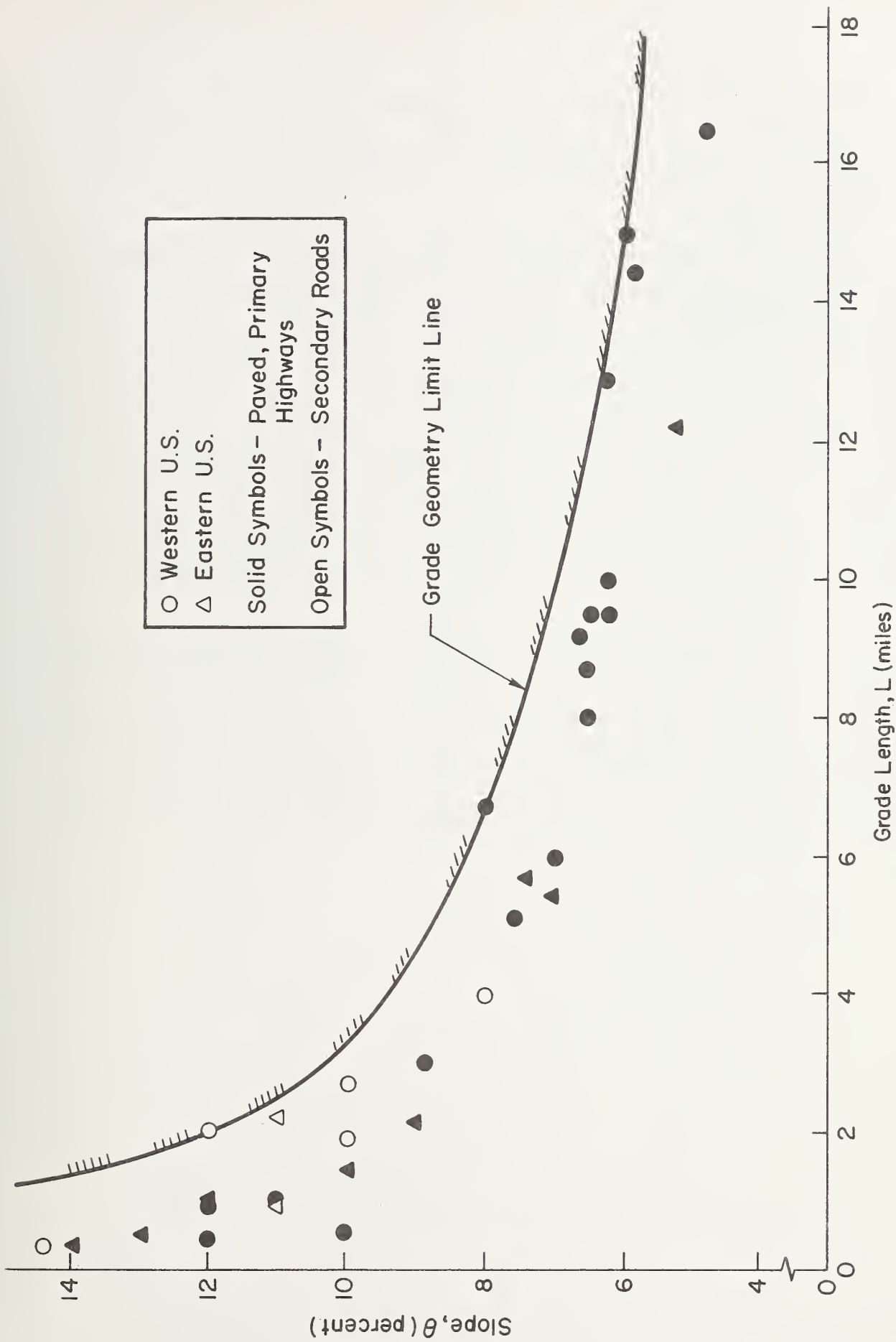


Figure 12. Definition of Grade Geometry Limit Line from Severe Grade Data.

of Fort Loudon, Pennsylvania, on U.S. Highway 30 is reported by Ref. 28 as 3 percent for 10 mi and also 8 percent for 1.23 mi. However, this grade is reported as 9 percent for 3.5 mi by the PMTA, which is considerably more severe.

Beyond such inconsistencies, there is the more fundamental question of the validity of representing a grade by a single constant slope, since slope varies continuously along any real grade. Hills which have significant regions where braking is not required are of particular interest, since partial brake cooling may occur in these regions. Braking is required on a downgrade, only after a threshold slope, θ_0 , is exceeded. Sections of the hill where this occurs (locally) are referred to as "braking intervals"; the remaining sections, with local slopes less than θ_0 , are "non-braking intervals." A grade which contains significant non-braking intervals, thereby allowing partial brake cooling, is referred to as a "multiple grade hill" or "multigrade."

The 58 mi section of I-80 west from Donner Summit to Auburn, California, known as the Donner grade, has been used as an example multigrade in this program. The vertical profile of this grade was determined by the pressure altimeter measurement technique discussed in Appendix B and is shown in Fig. 13a. The corresponding slope profile is shown in Fig. 13b, where the braking and non-braking intervals are separated by the $\theta_0 = 0.023$ line.

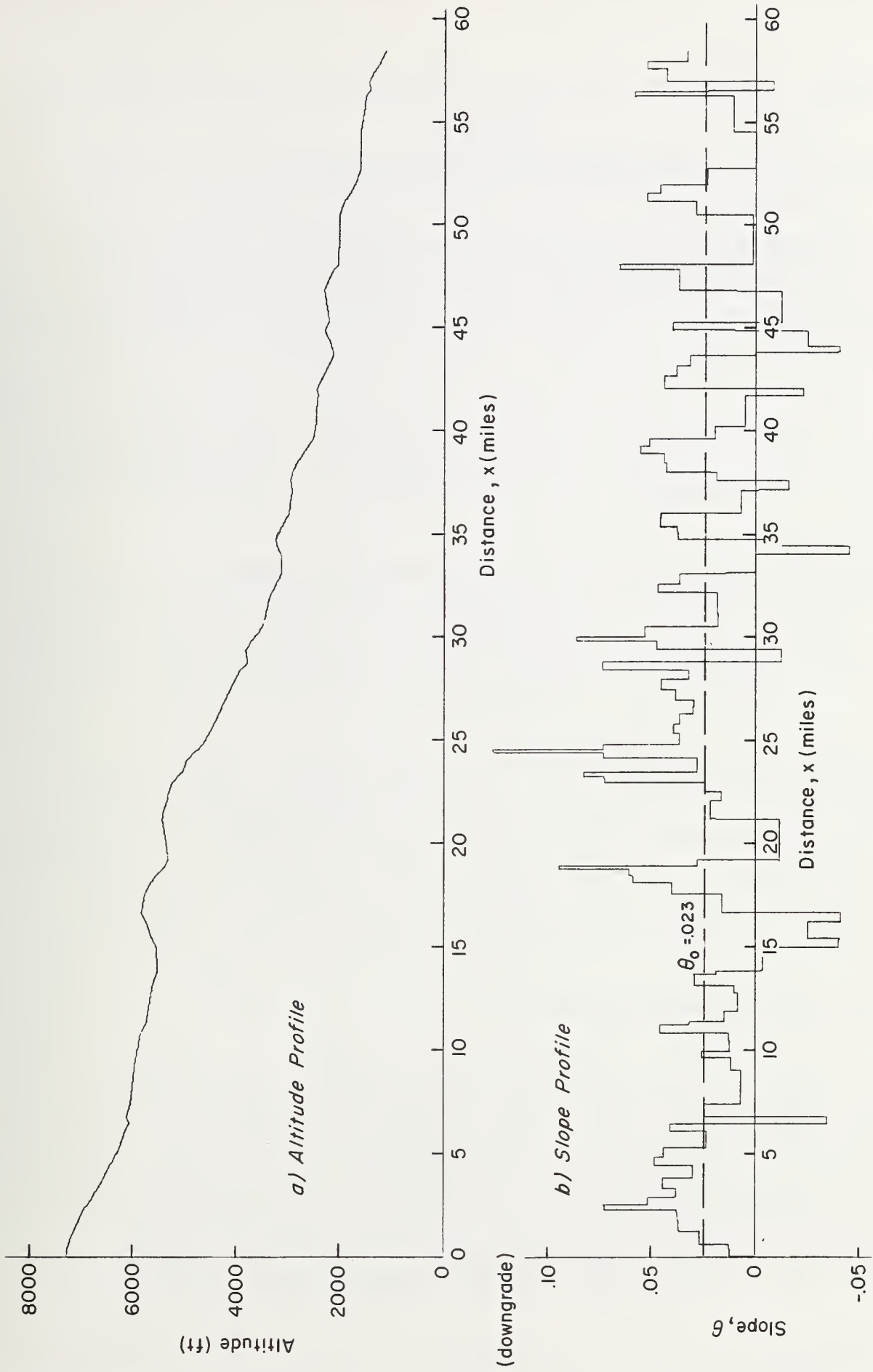


Figure 13. Altitude and Slope Profiles of the Donner Grade

SECTION III

THE TRUCK DOWNGRADE BRAKING MODEL

In Subsection II.B it was stated that a grade severity rating system could be based on a mathematical model that predicts brake temperature during a grade descent. In this section, such a model, the truck downgrade braking model, will be developed. Particular emphasis will be placed on the case in which the speed and gear are held constant during descent. This idealization is useful in analyzing many real grade descent situations, since even for any series of grades of varying severity, drivers will often attempt to drive sections of the grade at constant speeds. This fact is related to basic truck characteristics. As noted previously, a driver should descend grades with engine speed near the maximum to obtain maximum engine retardation. Thus, if the driver wishes to reduce his speed on a grade he must downshift; but since engine speed will be near the maximum he must first reduce the vehicle speed by braking. In a critical brake fade situation he may not be able to do this. A possibility which is even worse is that the driver may get the transmission into neutral but not be able to get it back into gear, resulting in the loss of all engine braking. Thus, in general, downshifting is to be avoided; this implies that grade descent should be made at a safe, constant speed in a single gear. Furthermore, if the GSRS works, as intended, to prevent truck runaways (as opposed to aiding the driver after a runaway), it is legitimate to assume there will always be adequate braking capacity for the driver to maintain speed constant.

A. THE BRAKE TEMPERATURE EQUATION

The truck downgrade braking model may be derived by considering the energy transfer processes which occur during grade descent. When a truck begins descent it has potential energy by virtue of its altitude. During the descent part of this energy is absorbed by the engine and part is dissipated by the action of the drag forces. The rest of the energy must be absorbed by the brakes. If the brakes cannot absorb all of the excess energy because they have faded, the excess energy will become kinetic

energy — that is, the truck speed will increase uncontrollably in a "run-away."

Brakes function by converting mechanical energy to thermal energy through the action of frictional shearing stresses in the drum/lining interface. This thermal energy is absorbed by brake components, thus increasing their temperature and then transferred out of the brakes by convection, radiation, and conduction. This process may be represented by an energy balance equation:

$$\left(\begin{array}{l} \text{Rate of change of} \\ \text{internal energy} \\ \text{in brake system} \end{array} \right) = \left(\begin{array}{l} \text{Rate of conversion} \\ \text{of mechanical} \\ \text{energy to heat} \\ \text{in brake system} \end{array} \right) - \left(\begin{array}{l} \text{Rate of heat} \\ \text{transfer from} \\ \text{brake system} \end{array} \right) \quad (8)$$

This equation considers the gross energy balance in the braking system but does not explicitly involve the spatial distribution of temperature in an individual brake or the distribution of braking effort among the brakes. A "lumped parameter" model such as this is appropriate for development of the GSRS.

To gain a deeper understanding of the influences of the details of brake temperature and braking effort distributions, Eq. 8 is derived from first principles, in Appendix A. For the lumped parameter model this derivation also shows that the internal (thermal) energy in the brakes is proportional to the temperature with the total heat capacity, $m_B C$, as the proportionality constant; and the rate at which mechanical energy is converted to thermal energy in the brakes is equal to the power input to the brakes, HP_B . Heat transfer from the brakes is by convection, conduction, and radiation. However, data in Ref. 14 indicate that most of the heat is transferred from the outer surface of the drum by convection into the surrounding airstream. Thus, the heat transfer rate is approximately $hA_C(T - T_\infty)$, which is the well known expression for convective heat transfer (Newton cooling). As a practical matter, the relatively small effects of convection and radiation are lumped with convection, and an "effective" convective heat transfer coefficient is used. Under these assumptions, Eq. 8 may be written as a first-order linear ordinary differential equation:

$$\underbrace{m_B C \frac{dT}{dt}} = \underbrace{HP_B} - \underbrace{hA_C(T - T_\infty)} \quad (9)$$

Rate of internal energy change Power into brakes Heat transfer rate

When the initial brake temperature is specified in conjunction with this equation, we have an initial value problem which may, in principle, be solved to give an analytic expression for brake temperature. The effective brake mass (m_B), the effective brake system area (A_C), and the specific heat capacity (C) of the brake system are constants independent of speed. However, the effective heat transfer coefficient (h) is a function of speed, which makes Eq. 9 difficult to solve if speed varies with time.

Because, as noted previously, we may assume a constant descent speed for at least some portion of a grade, the resulting linear differential equation with constant coefficients can be solved by standard techniques. However, we must first have a means for specifying the value of the forcing function, i.e., the power into the brakes, which is related to the brake force and speed by:

$$HP_B = F_B \bar{V} / 375 \quad (10)$$

Our primary problem is thus to develop a means of computing brake force.

The difficulties of computing available brake force from its constituent variables (pressure, speed, and temperature) have been noted in Subsection II.C. However, if a GSRS is to work, then the available brake force (at the appropriate pressure for a given speed and temperature) will just equal the brake force required. Therefore, our task is to develop a formula for the brake force required for the downgrade braking situation.

B. BRAKE FORCE REQUIRED

During grade descent, sufficient braking capacity must be available to: maintain a steady descent speed, i.e., prevent a runaway; and allow emergency stopping on the grade. The emergency stopping requirement is the more

severe in that it requires a higher braking force and is particularly critical in high traffic density situations. If the traffic density is low the driver may be able to avoid the necessity of stopping in a downgrade emergency; but if a runaway occurs, speed will rise and there may be a problem maneuvering in traffic or on a curve.

An emergency stop, by definition, involves high deceleration, e.g., on the order of 0.5 g. This is large compared to the downhill component of gravitation, which for an average 5 percent grade would be 0.05 g. Thus, the emergency stopping requirements are approximately the same on a grade as on a level road. Such requirements are often specified in terms of a stopping distance; however, for a constant deceleration rate the stopping distance is directly related to the deceleration rate, so that either may be used to quantify the stopping criterion. In field tests of truck stopping capability, such as those demonstrating compliance with FMVSS 121, it is more convenient to measure stopping distance than deceleration rate. However, for our purposes here, it is more convenient to work in terms of deceleration rate. Since the prevention of a runaway requires maintaining $a_x = 0$, any downgrade braking requirement may be stated as a specified value of a_x .

The braking force required for either an emergency stop or prevention of a runaway may be determined from the dynamic equilibrium of forces acting on the truck. A free body diagram showing the forces acting on a truck during a grade descent is shown in Fig. 14. The angle θ is sufficiently small for any normal grade to permit the "small angle approximations,"

$$\sin \theta \doteq \theta \text{ rad} \doteq \text{slope of grade}$$

$$\cos \theta \doteq 1$$

Since $\cos \theta \doteq 1$, the tire normal load, and hence the rolling resistance, is the same on the grade as on a level road. Thus, the dynamic equilibrium of forces along the grade is:

This is the "funnel" analogy suggested by Hykes, in which the flow of thermal energy through a truck brake system can be likened to the flow of a viscous fluid* (heavy oil) through a funnel with a small orifice at the bottom (see Fig. 15). The analogy between the funnel and a truck brake may be seen from the analogous quantities in the two cases (Table 2).

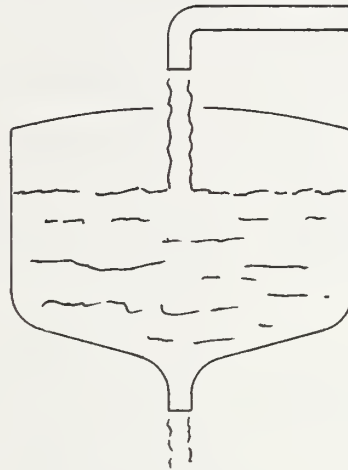


Figure 15. Fluid Analogy of Brake Heat Transfer

As fluid flows into the funnel at a constant rate, the level of fluid in the tank will rise until a "steady state" or equilibrium condition is reached in which the flow rate out of the orifice just equals the flow rate of fluid into the tank. In a similar manner the steady input of power into the brakes will cause temperature to rise until the temperature difference ($T - T_{\infty}$) reaches an equilibrium level, and the heat transfer out of the brakes just equals the power into the brakes. If the fluid level rises over the top of the tank before equilibrium is reached, the tank will overflow just as the brakes fade if temperature rise is too high. It can be

*For a viscous fluid the discharge rate is directly proportional to the head; whereas for a fluid such as water, where the inertial forces dominate the viscous forces, the discharge rate is proportional to the square root of the head.

TABLE 2

ANALOGOUS QUANTITIES IN VISCOUS FUNNEL
FLOW VS. TRUCK BRAKE HEATING

FUNNEL FLOW	TRUCK BRAKE
1. Volume flow rate into tank	Rate of flow of energy (power) into brakes, HP_B
2. Fluid head (depth)	Temperature difference, $T - T_\infty$
3. Area of tank base	Total effective heat capacity, $m_B C$
4. Volume of fluid in tank	Internal energy, $m_B C T$
5. Orifice discharge coefficient	Effective heat transfer coefficient, h
6. Orifice area	Total effective heat transfer area, A_C
7. Volume flow rate out	Heat transfer rate, $h A_C (T - T_\infty)$

seen that a large tank area implies that more fluid can be stored for a given fluid depth. Similarly, high heat capacity or brake mass implies that more thermal energy can be stored in the brake system for a given temperature level. A high discharge coefficient or large orifice area results in a high flow rate out of the funnel, implying that a lower head is required to balance a given input flow rate. Similarly, a high heat transfer coefficient or area reduces the temperature required to balance a given power input. Finally, note that a high discharge coefficient for the funnel means that the steady-state fluid level will be approached rapidly as the fluid does not have to rise very high. In a similar way, high brake heat transfer coefficients cause the brake system to respond quickly to brake power inputs because the (low) steady-state temperature will be approached rapidly.

The qualitative ideas gained from the funnel analogy may now be made quantitative by formally solving the brake temperature initial value problem

for the constant speed/constant slope case. The differential equation (Eq. 9) may be integrated using standard techniques (Ref. 32) to give:

$$T(t) = T_0 + [T_\infty - T_0 + K_2 HP_B][1 - e^{-K_1 t}] \quad (13)$$

where $K_1 = hA_C/m_B C$ is the inverse thermal time constant and $K_2 = 1/hA_C$ is the inverse of the total heat transfer parameter, both functions of speed through h . This result has previously been given by Limpert, Ref. 33.

In the development of the GSRS we will often be concerned with the brake temperature at some distance x from the summit. In particular, we will often be interested in the temperature at the bottom of the grade, T_f , where $x = L$. For a constant speed descent, $t = x/\bar{V}$; thus, Eq. 13 may be rewritten in terms of distance as:

$$T(x) = T_0 + [T_\infty - T_0 + K_2 HP_B][1 - e^{-K_1 x/\bar{V}}] \quad (14)$$

As distance becomes infinite, the exponential term $[1 - e^{-K_1 x/\bar{V}}]$ goes to 1 and brake temperature approaches its steady-state value:

$$T_{ss} = T_\infty + K_2 HP_B \quad (15)$$

If we temporarily make the reasonable approximation that $T_0 = T_\infty$, the temperature rise, $T - T_\infty$, may be approximated from Eq. 14 as the ratio of the power into the brakes, HP_B , divided by the total heat transfer coefficient, $1/K_2 = hA_C$, all multiplied by an exponential factor

$$T - T_\infty = \frac{HP_B}{hA_C} [1 - e^{-(hA_C/m_B C)(x/\bar{V})}] \quad (16)$$

It can be seen that, all other things being equal, increasing the power input into the brakes or reducing the heat transfer out of the brakes will increase brake temperature. Note also that the exponential factor, which is characteristic of first-order systems, determines how close T will come to steady state on a hill of finite length, x .

It is useful at this point to classify the variables and parameters in the downgrade braking model according to their physical significance. Brake temperature may be considered the "controlled variable" in that the driver will attempt to control brake temperature to prevent brake fade. Speed and transmission gear may be thought of as "control variables," because they are modulated by the driver to control brake temperature. There are two grade geometry parameters, slope and length, which completely characterize any straight single grade hill of constant slope. T_0 and T_∞ may be thought of as environmental parameters characteristic of a downgrade site. Certainly, T_∞ is characteristic of a specific grade site; however, T_0 is, in a sense, a truck parameter. But, it is largely determined by highway characteristics near the beginning of the grade and thus it is reasonable to treat T_0 as an environmental parameter which is the same for all trucks. The remaining quantities (W , K_{ret} , K_1 , K_2 , F_{drag} , HP_B) are parameters and functions specific to the truck. Of these, truck weight is unique in that it is the only truck parameter that normally varies from day to day for a specific truck, and thus it is the truck variable. The other parameters are really truck population variables in that they vary among trucks but are nominally constant from day to day for a specific truck.

In much of the development that follows we will consider only the "worst case" truck which has no retarder. Thus, except where noted, $K_{ret} \equiv 0$ and is not treated as a variable in the problem. This implies that HP_{eng} is only a function of engine speed or, equivalently, only a function of vehicle speed and transmission gear for a given truck. K_1 , K_2 , and F_{drag} are functions of speed, and F_{drag} may also be a function of W through the weight effects on chassis friction and rolling resistance noted previously, Eq. 5. However, as noted in Appendix B, it appears that weight effects on F_{drag} are negligible, and this will be assumed for the following developments.

One final simplification will be made for purposes of GSRs development. That is, it will be assumed that constant standard values of T_0 and T_∞ may be used for all trucks and all (single grade) hills.

Under the above assumptions, brake temperature is reduced from a function of eleven parameters and functions to a function of four independent variables

$$T = T(\theta, x, W, V)$$

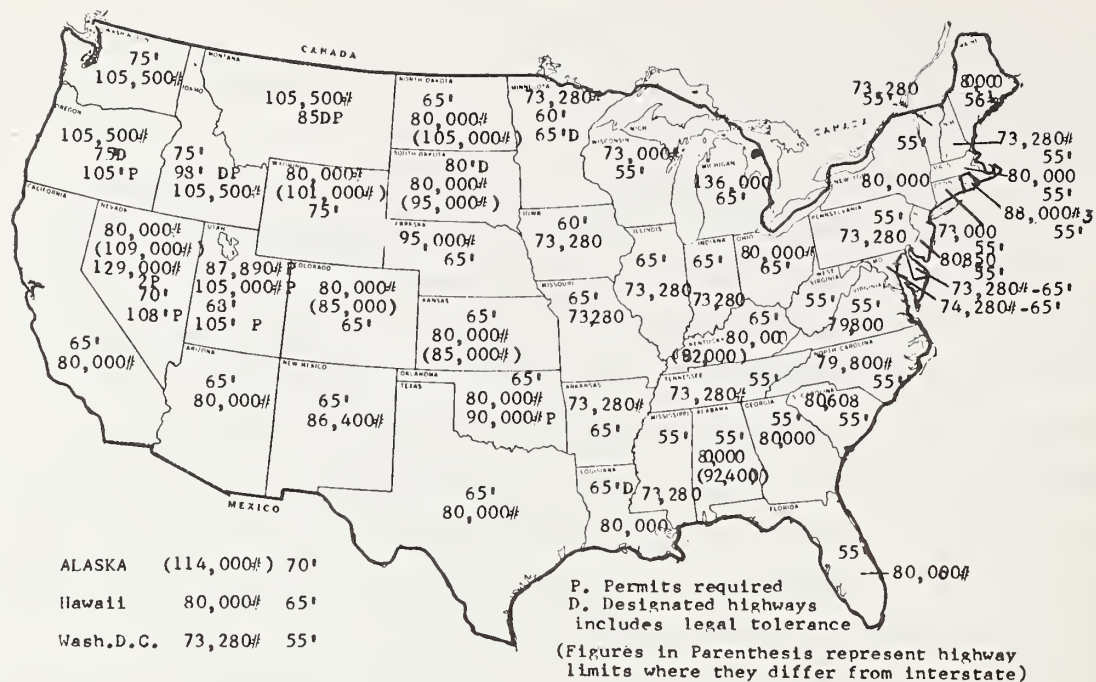
where W is now the only truck variable.

Because formulating a workable GSRS is not simple, it is important to avoid unrealistic values of the independent variables; otherwise, a potentially workable GSRS might appear to be unworkable (e.g., too inaccurate). Consequently, it is very important to define the "domains of interest," relevant to the downgrade problem for the four independent variables.

The upper limit on speed considered in this program is the national maximum highway speed limit of 55 mph. Any severe grade will of course require speeds well under 55 mph for heavily loaded trucks. Ten mph was taken as a minimum speed, since grade descents below 10 mph are generally not feasible because of the dangers of traffic congestion and rear-end collisions by faster trucks. If a maximum safe speed is computed to be less than 10 mph for some trucks, then a ban of such trucks might be warranted. Maximum values for the grade geometry parameters (θ and L) for single grades are specified by the grade geometry limit time discussed in Subsection II.D. The maximum length of any realistic single grade hill appears to be less than 12 miles. Any grade longer than 12 miles will be a multigrade hill.

The upper limit on weight was established by examining the truck weight limits in effect in the United States. According to Ref. 26, the Federal Aid Highway Amendment of 1974, signed into law on 4 January 1975, provides for a total gross weight limit on interstate highways of 80,000 lb. Prior to the passage of this act, however, a few states had weight limits that exceeded the new federal maximums. These limits have been grandfathered into federal law along with state weight limits lower than 80,000 lb. The weight limits in effect in the United States are summarized in Fig. 16. For purposes of analysis in this program a weight of 80,000 lb has been used. For higher weights additional calculations would have to be made using the same basic equations.

An absolute lower limit on weight is established by the empty weight of typical combination vehicles, approximately 30,000 lb. However, there is a greater lower bound on W as grade geometry produced by the physics of grade descent. This is given by the locus of θ, L values for which a grade may be descended at 55 mph for any weight. These boundaries are shown in



- Prior to July 1, 1956, some states have had weight limits in effect which exceeded the new federal maximums. These practices have been "grandfathered" into law by the Federal Highway Act of 1975.
- Requires 9 axles spaced 101' overall.
- 3-axle truck and 3-axle trailer.
- P Permits are required.

Figure 16. United States Truck Weight and Length Limits (Ref. 26)

Fig. 17 for the nominal temperature conditions and brake, drag, etc., parameters generally assumed for GSRs development. Note that the 40,000 lb line parallels the grade geometry line, indicating that for grades longer than about 4 miles the practical lower bound on weight is about 45,000 lb.

D. DETERMINATION OF PARAMETERS AND MODEL VALIDATION IN THE FIELD TEST PROGRAM

To determine the values of the parameters in, and validate the form of, the downgrade braking model, we conducted Phase I field tests with a typical truck. Since the structure of the model was developed before these tests, we were able to develop and use specific procedures designed to extract the unknown parameters from the test data and to validate the braking model. The details of these tests are presented in Appendix B, but an overview of the tests will be given here.

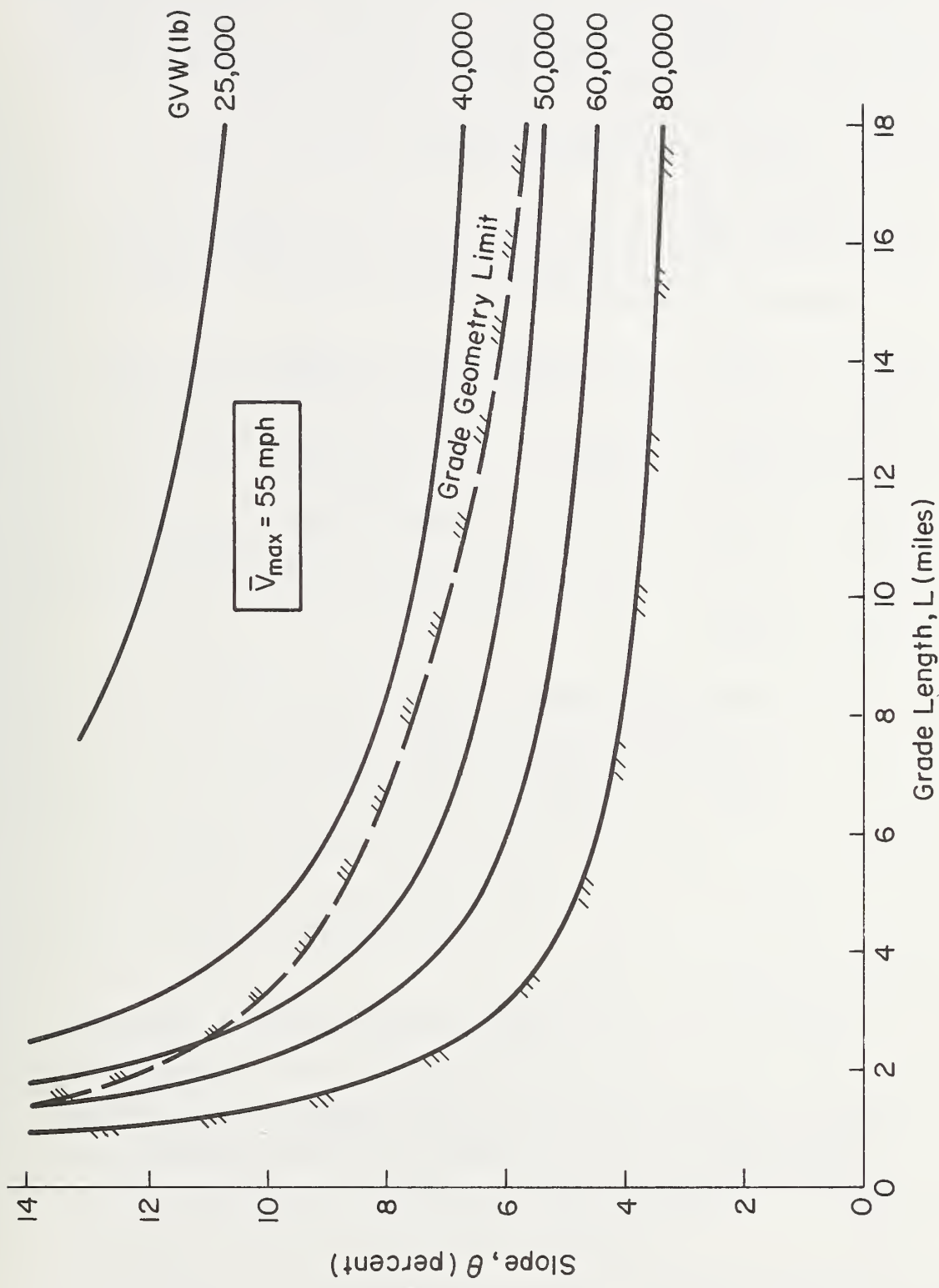


Figure 17. Variation of the $\bar{V}_{max} = 55$ mph Boundaries with Weight

The tests were performed using a fully instrumented 3-S2 tractor-semitrailer loaded to 75,500 lb GCW (33,175 kg). Temperature sensors (thermocouples) were installed in the lining of each brake; and vehicle speed, engine speed, and brake application pressure were also measured. All data were permanently recorded with an 8-channel chart recorder.

Three basic types of tests were performed:

- Coast-down tests
- Cool-down tests
- Grade descent tests

The coast-down tests were used to define the drag forces and engine power absorption characteristics. The process involved accelerating to the test speed (approximately 40 mph) on a level test area, closing the throttle, shifting the transmission to neutral, and allowing the truck to decelerate under the action of the drag forces. The magnitude of F_{drag} is then calculated from the time history of the truck speed. The engine power absorption was determined in a similar manner except that the tests were performed with the transmission in gear.

The cool-down tests were performed to define the inverse thermal time constant, K_1 . These tests involved "dragging" the brakes until they reached moderately high temperatures. The brakes were then released and the truck was driven at a constant test speed until the brakes cooled to approximately ambient temperature. K_1 was then computed from the brake temperature time histories. By performing the tests over a range of test speeds, the variation of K_1 with speed was defined. It is noted that these empirical values of K_1 include the effects of radiation.

The grade descent tests in conjunction with the results of the coast-down and cool-down tests allowed the determination of the final truck parameter, K_2 . These tests consisted of descending grades of known, constant slope at constant speed. By conducting tests at various retarder settings on several grades of different slope it was possible to define K_2 as a function of speed.

The Truck Downgrade Braking Model and the numerical values for the parameters are summarized in Table 3.

TABLE 3. SUMMARY OF TRUCK DOWNGRADE BRAKING MODEL

$$T(x) = T_0 + [T_\infty - T_0 + K_2 HP_B][1 - e^{-K_1 x / \bar{V}}] \quad ^\circ F \quad (18)$$

$$HP_B = F_B \bar{V} / 375 = (W\theta - F_{drag}) \frac{\bar{V}}{375} - HP_{eng} \quad (19)$$

where the slope θ is in radians, the total truck weight is in pounds, the distance x is in miles, and the speed is in miles per hour. The truck parameter functions are:

$$K_1 = \frac{hA_c}{m_B C} = 1.23 + 0.0256\bar{V} \quad 1/hr \quad (20)$$

$$K_2 = \frac{1}{hA_c} = (0.100 + 0.00208\bar{V})^{-1} \quad ^\circ F/hp^* \quad (21)$$

$$F_{drag} = 450. + 17.25\bar{V} \quad lb^\dagger \quad (22)$$

$$HP_{eng} = 73. + 100K_{ret} \quad hp \quad (23)$$

where

$$K_{ret} = \begin{cases} 0 & \text{engine brake off} \\ 0.5 & \text{engine brake low} \\ 1. & \text{engine brake high} \end{cases}$$

$$T_\infty = 90 \quad ^\circ F$$

$$T_0 = 150 \quad ^\circ F$$

*For convenience the energy flow rate is written directly in "mechanical" units (hp) rather than "thermodynamic" units (BTU/hr).

†Note that non-braking drag is considered independent of weight here rather than weight-dependent as shown in Eq. 5 and Fig. 3. This approximation is consistent with the relatively small range of practical weights to be considered, i.e., 80,000 to 45,000 lb (see Fig. 17) and the apparent reduction in weight sensitivity due to recent truck improvements.

Following the analysis of the data from the Phase I tests, a second set of Phase II tests was performed to validate the model. These tests involved only constant speed grade descents. In addition to the test vehicle used in the Phase I tests, a second truck, an instrumented 2-S1-2 "doubles" unit, was tested at 78,000 lb (35.1 Mg) GCW. These tests confirmed that the prediction of brake temperature from the downgrade braking model was accurate. An example of the comparison between an actual brake temperature profile measured on the No. 1 test truck and a profile predicted by the downgrade braking model is shown in Fig. 18.

So far, the downgrade braking model has been developed for single grades of constant slope. However, if the grade is a true multigrade hill, with significant braking and non-braking intervals, the speed will in general vary along the grade. For instance, downshifting on non-braking intervals may be necessary if there are sections of upgrade. The previously noted prohibition against downshifting still applies to braking intervals, but the descent speed may vary among such intervals. Thus, the integrated form of the brake temperature equation, Eq. 18, cannot immediately be applied to the multigrade case, since both the assumptions of constant slope and constant speed are violated. However, Eq. 18 can be applied to each individual grade (measurement) segment in the grade profile since θ and \bar{V} are approximately constant. A brake temperature profile may then be calculated sequentially from the summit by noting that the initial brake temperature on a grade segment is equal to the final temperature on the previous segment. This concept has been developed into an organized sequential calculation procedure and programmed on a digital computer (see Appendix C).

E. PHYSICAL IMPLICATIONS OF THE DOWNGRADE BRAKING MODEL

The truck downgrade braking model, as summarized in Table 3, is complete and may be used as a basis for developing a GSRS. However, before this is done it is useful to exercise the model to gain greater insight into the physics of downgrade braking. This may be done by plotting brake temperature as a function of the independent variables. Obviously, even with the independent variables reduced to four, it is not possible to make a single plot including all four variables. The best that can be done in terms of

Test Vehicle No. 1
 Grapevine, Run No. 665
 Speed = 20.3 mph
 RPM = 1900
 Total Weight = 75,500 lb
 Retarder Off
 Grade = 5.8 Percent

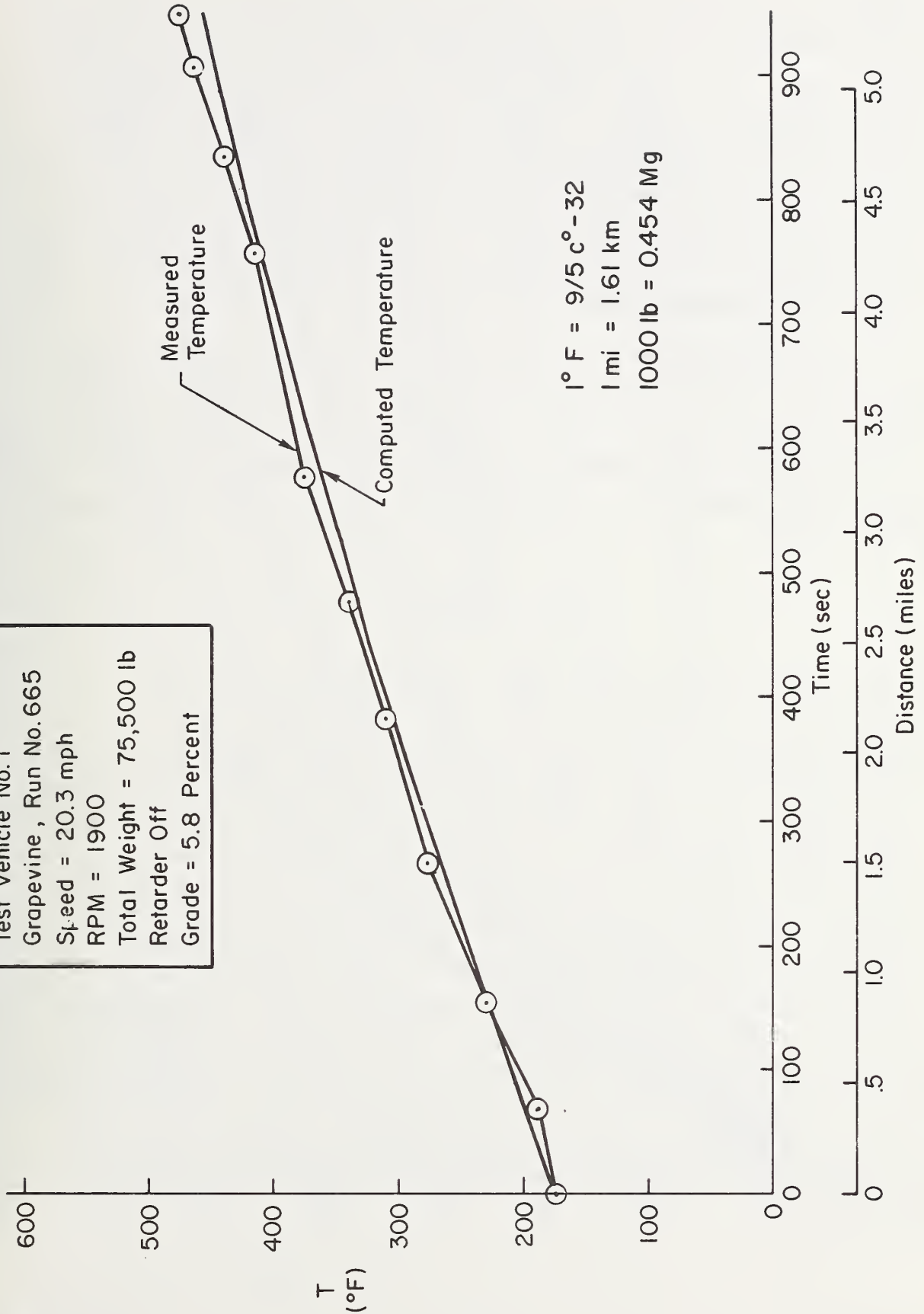


Figure 18. Comparison of Measured Time History of Average Brake Temperature with Profile Computed from Truck Downgrade Braking Model

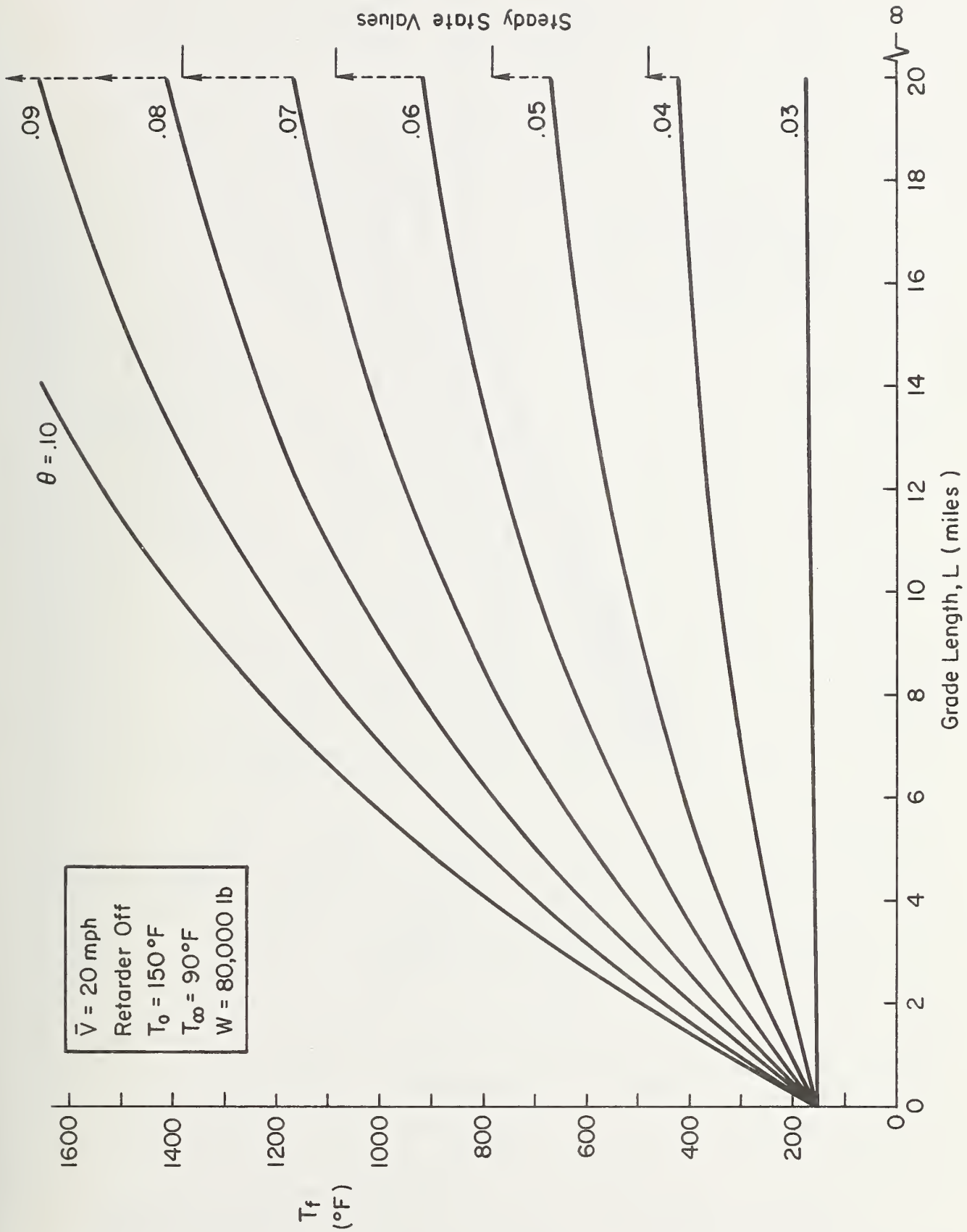
graphical representation is to consider brake temperature as a function of two of the independent variables for fixed values of the other two variables. In this manner brake temperature could conceivably be shown as a surface over a two parameter (e.g., θ , L) plane. However, easier visualization and better understanding result from three 2-dimensional plots formed by "slicing up" the temperature surface with planes normal to each of the three axes. Of the six possible pairs of independent variables, three parameter planes are particularly revealing and will be examined briefly. These are the grade parameter plane, the W, V plane, and the V, L plane.

From the variation of brake temperature in the grade parameter plane, Figs. 19a, 19b, 19c, it may be seen that there is a "threshold" value of downgrade slope, θ_0 , which must be exceeded before there is an increase in brake temperature on the grade. θ_0 represents the steepest downgrade slope for which zero brake force is required, i.e., from the brake force required equation, Eq. 12,

$$\theta_0 = F_{NB}/W \quad (24)$$

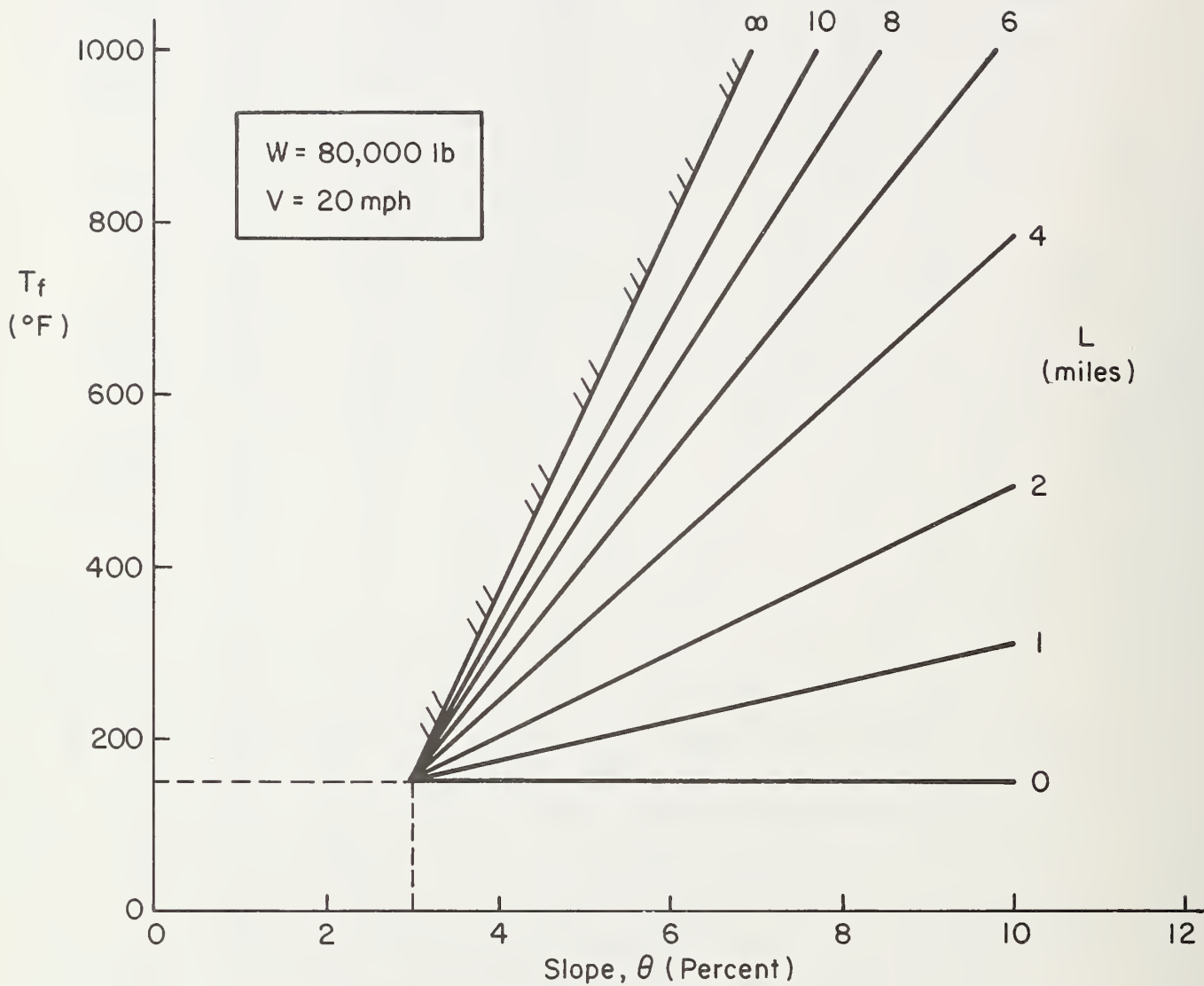
θ_0 is a function of weight and speed, as shown in Fig. 20.

Other insights from Fig. 19 are, in Figs. 19a, the "distance response" of brake temperature which shows a rapid initial rise followed by an asymptotic approach to a steady state value. This first-order characteristics of the temperature response, i.e., temperature increasing monotonically with distance along the grade, is of special significance, as discussed later. Figure 19b shows the variation of brake temperature with slope. It can be seen that for a given grade length the final brake temperature varies linearly with slope, that is, a given increment in slope always produces the same increment in brake temperature. This increment increases with grade length, asymptotically approaching the steady-state value for an infinitely long grade. The constant final temperature contours in the grade parameter plane, Fig. 19c, show a roughly hyperbolic shape. Thus, for a given final brake temperature, a steep hill must always be shorter than a shallower hill.



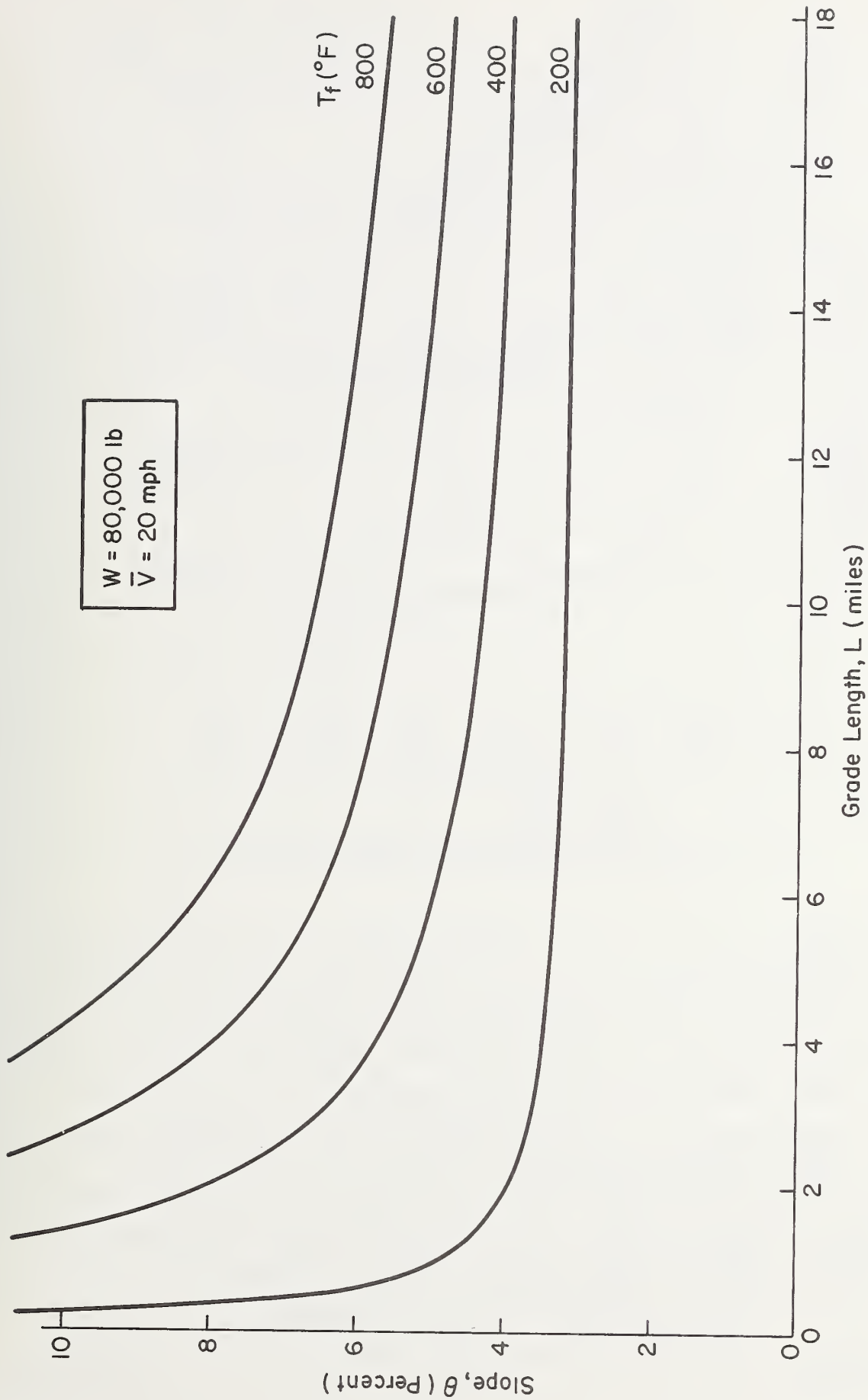
a) Length Effects With Grade as a Parameter

Figure 19. Brake Temperature Response Due to Grade Variables



b) Grade Effects With Length as a Parameter

Figure 19. (Continued)



c) Isotherms as a Function of Grade and Length

Figure 19. (Concluded)

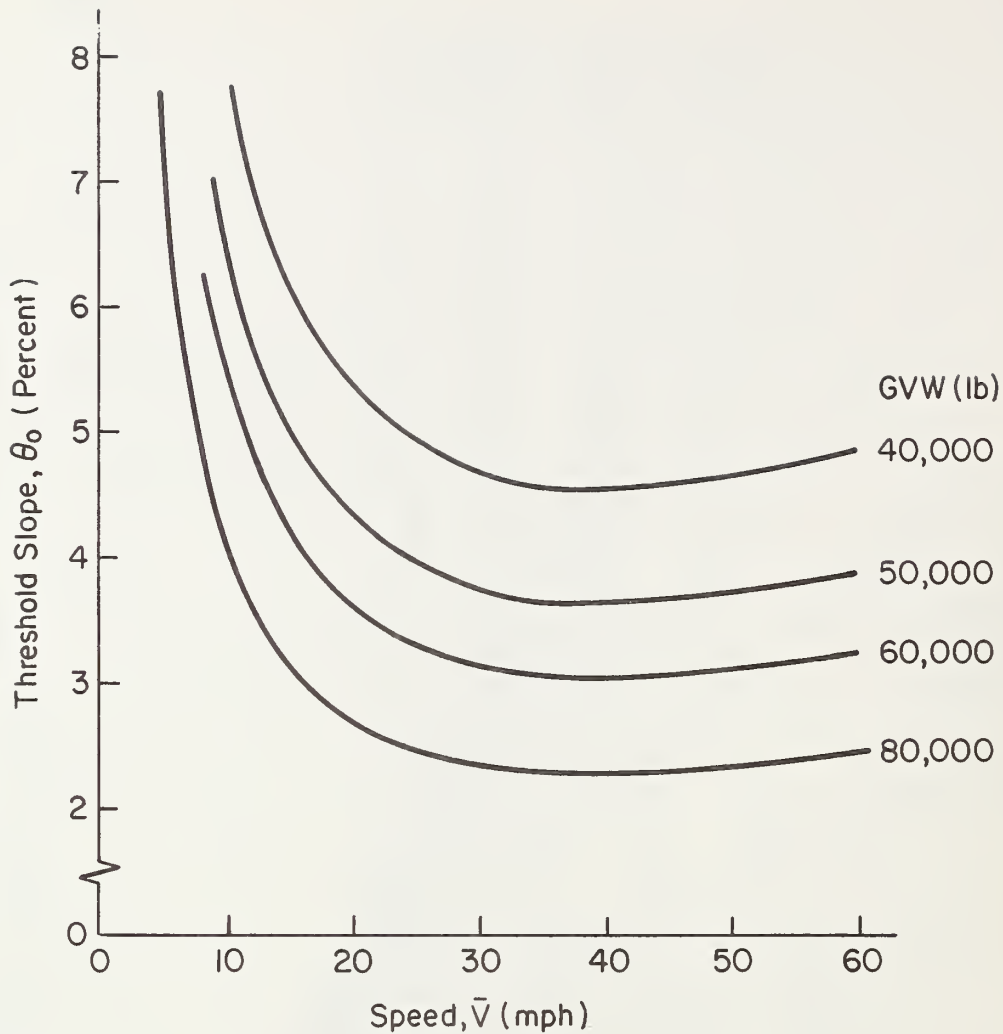
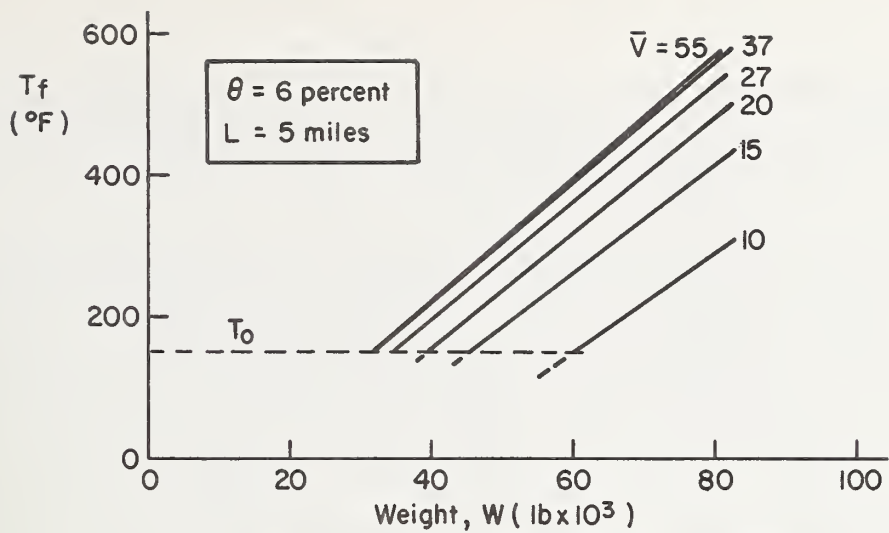
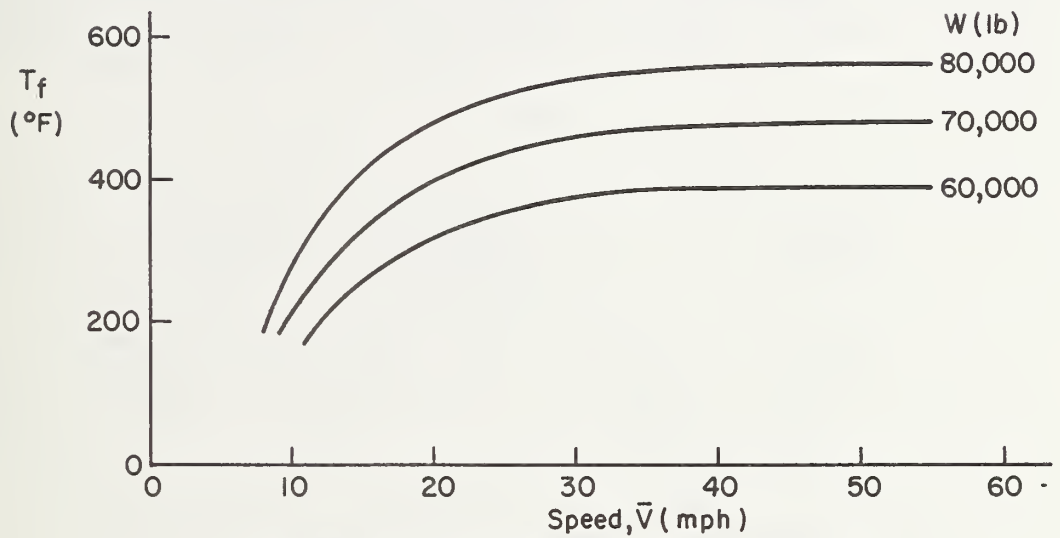


Figure 20. Slope Threshold for Power into Brakes

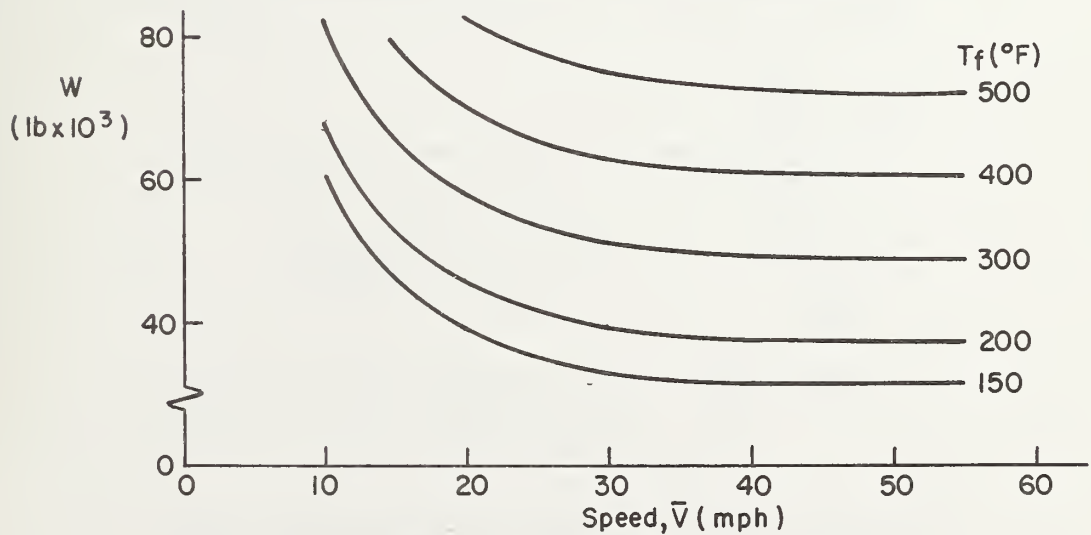
Figures 21a, 21b, and 21c show the variation of brake temperature with the truck variable, W , and the control variable, \bar{V} . Figure 21a shows that brake temperature is linear with truck weight at a given speed. This linear variation is related to the linear variation of temperature with slope shown in Fig. 19b. Both of these variations result from the fact that in the brake temperature and power equations, Eqs. 18 and 19, weight and slope enter in only one place and appear as a product, $W\theta$, which represents the downgrade component of weight. This effect results in an inherent "coupling" between slope and weight which will be seen to have important consequences for the development of a GSRS. Figure 21c shows isotherms in the W, V plane;



a) Weight Effects With Speed as a Parameter



b) Speed Effects With Weight as a Parameter



c) Isotherms as a Function of Weight and Speed

Figure 21. Brake Temperature Response Due to Truck Weight and Speed

as in the grade parameter plane (Fig. 19c), they have a roughly hyperbolic characteristics, an increase in truck weight requiring a decrease in speed to maintain the same brake temperature.

The variation of brake temperature in the V,L plane is seen from the plot of T_f versus \bar{V} in Fig. 22. For a grade of given length the final brake temperature increases rapidly with descent speed in the low speed region. However, at higher descent speeds ($\bar{V} > 30$ mph), the final brake temperature is roughly constant or decreases with increasing speed over a wide range of speeds. This nonlinear variation of brake temperature with speed is primarily related to the speed variation of the heat transfer coefficient. Since this effect has important consequences for the development of a GSRS it is worth examining in more detail. This may be done in an

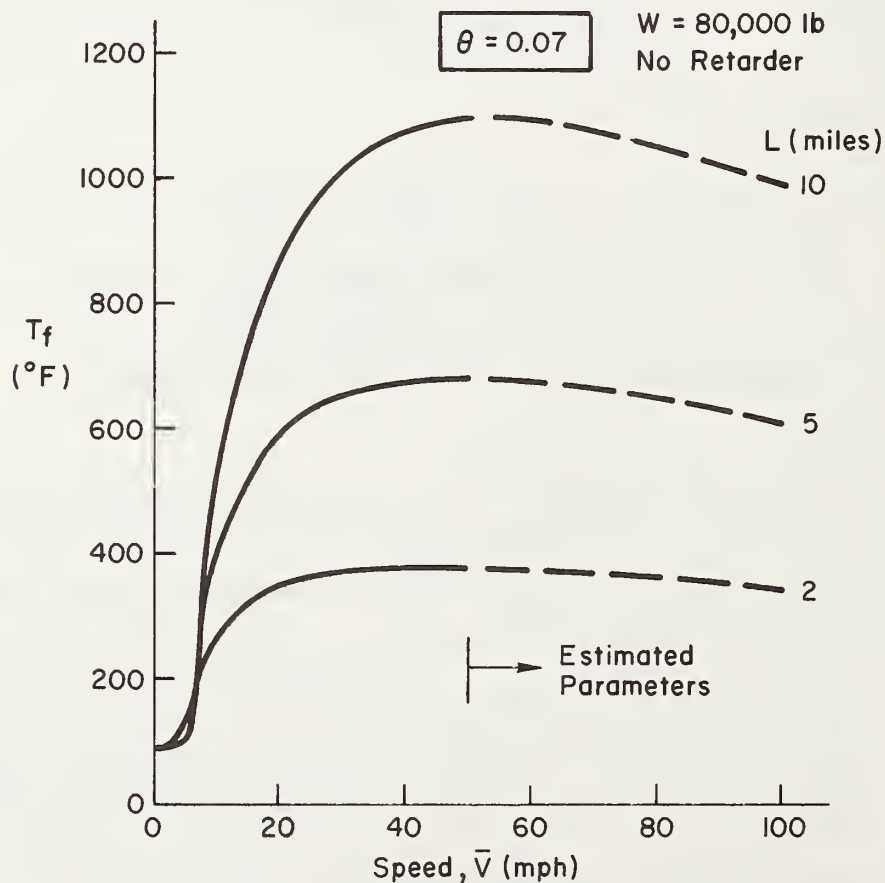
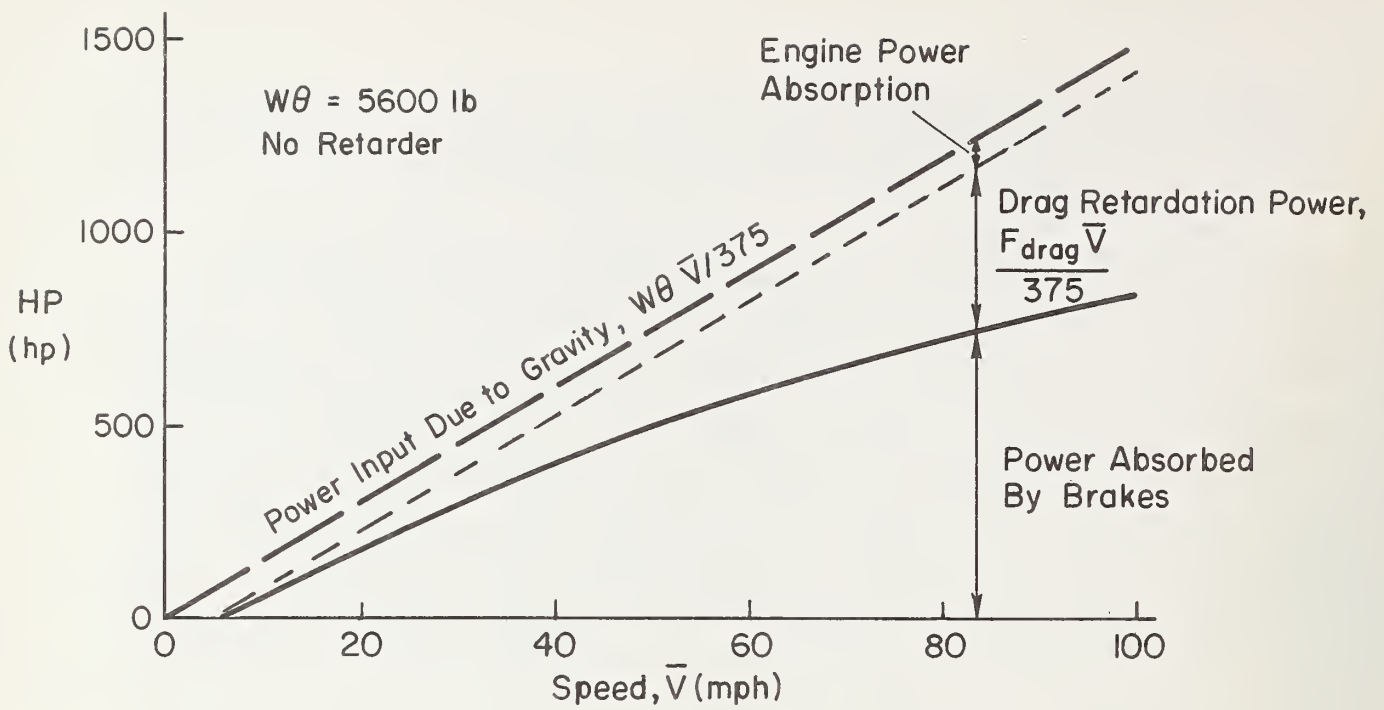


Figure 22. Brake Temperature Variation with Speed

insightful way by "building up" the variation of T_f with \bar{V} from the basic factors in the approximate temperature rise expression, Eq. 16.

To begin, we examine first the braking power balance as depicted in Fig. 23a for $W\theta = 5600$ lb. It may be seen that for typical descent speeds most of the "gravitational power" must be absorbed by the brakes. Figure 23b shows the power absorption by the brakes for several levels of the downgrade component of weight, $W\theta$. It may be seen that increasing either the weight of the truck or the slope of the grade will increase the power absorbed by the brakes at any descent speed. More important to our present example, for any but the lowest level of $W\theta$, the power absorption increases almost linearly with speed. However, the variation of the total effective heat transfer parameter, hA_C , with velocity, Fig. 23c, limits the steady-state ($L \rightarrow \infty$) brake temperature as shown in Fig. 23d. The greater curvature of the $W\theta$ lines here (over those in Part b) shows that the brake temperature flattens out at high speed, despite the increased power absorption, because of the increasing heat transfer rate with speed. The inverse thermal distance constant, K_1/\bar{V} , given in Fig. 23e has an additional flattening effect directly shown by the shape of the exponential, finite length factor also shown in Part e. When the exponential factors are multiplied by the steady-state temperature curves (Part d) for $\theta = 0.07$, we have (approximately) the complete T_f curves of Fig. 22. We see therefore that the nonlinear shape of the Fig. 22 final temperature curves is strongly influenced by the shapes of the heat transfer functions in Figs. 23d and 23e.



a) Brake Power Balance as Influenced by Speed

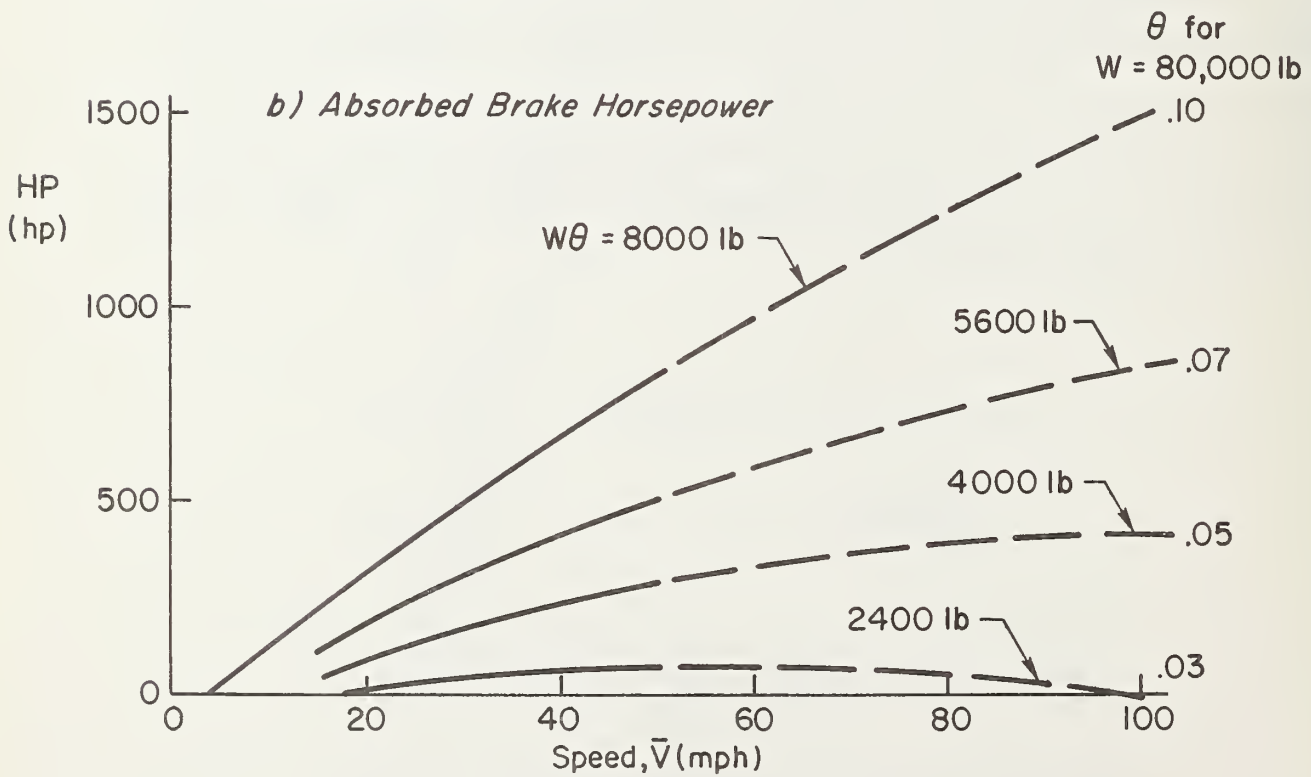
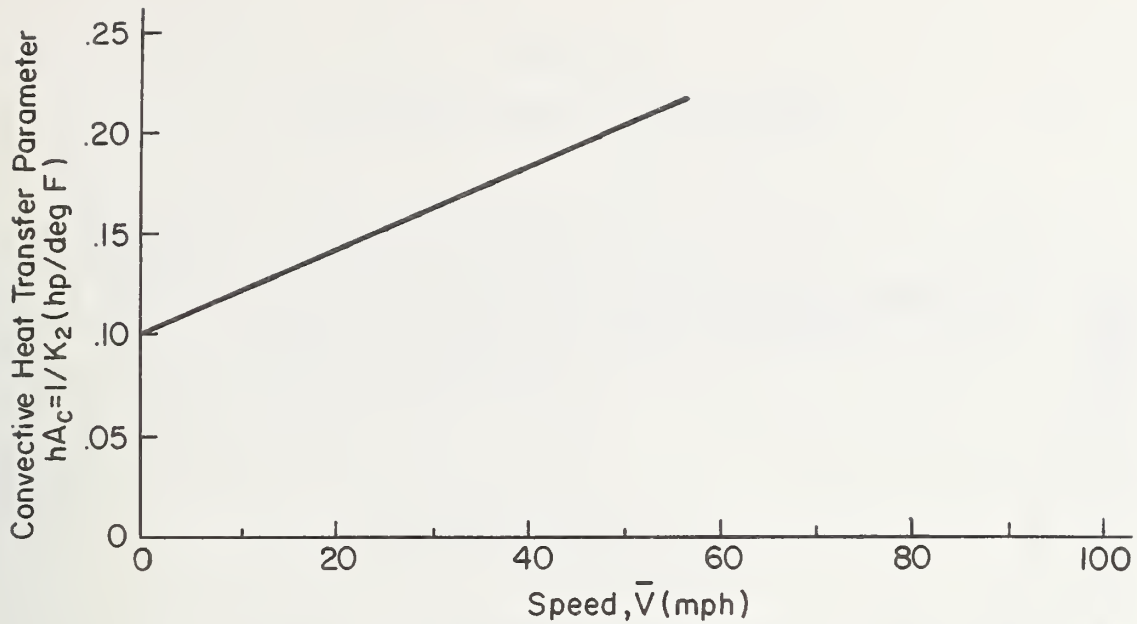
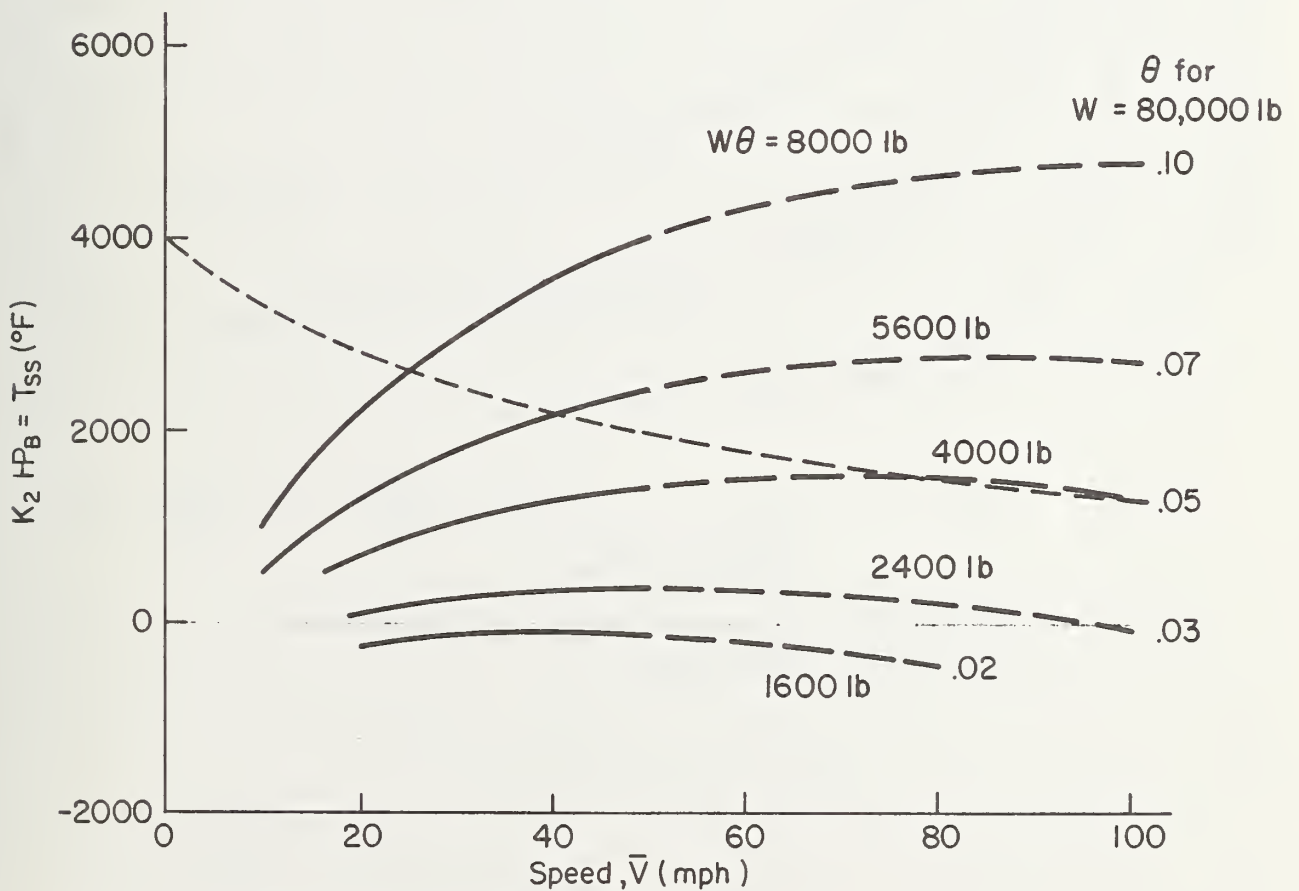


Figure 23. Illustrative Progressive Buildup in Brake Temperature Variation With Speed (No Retarder)

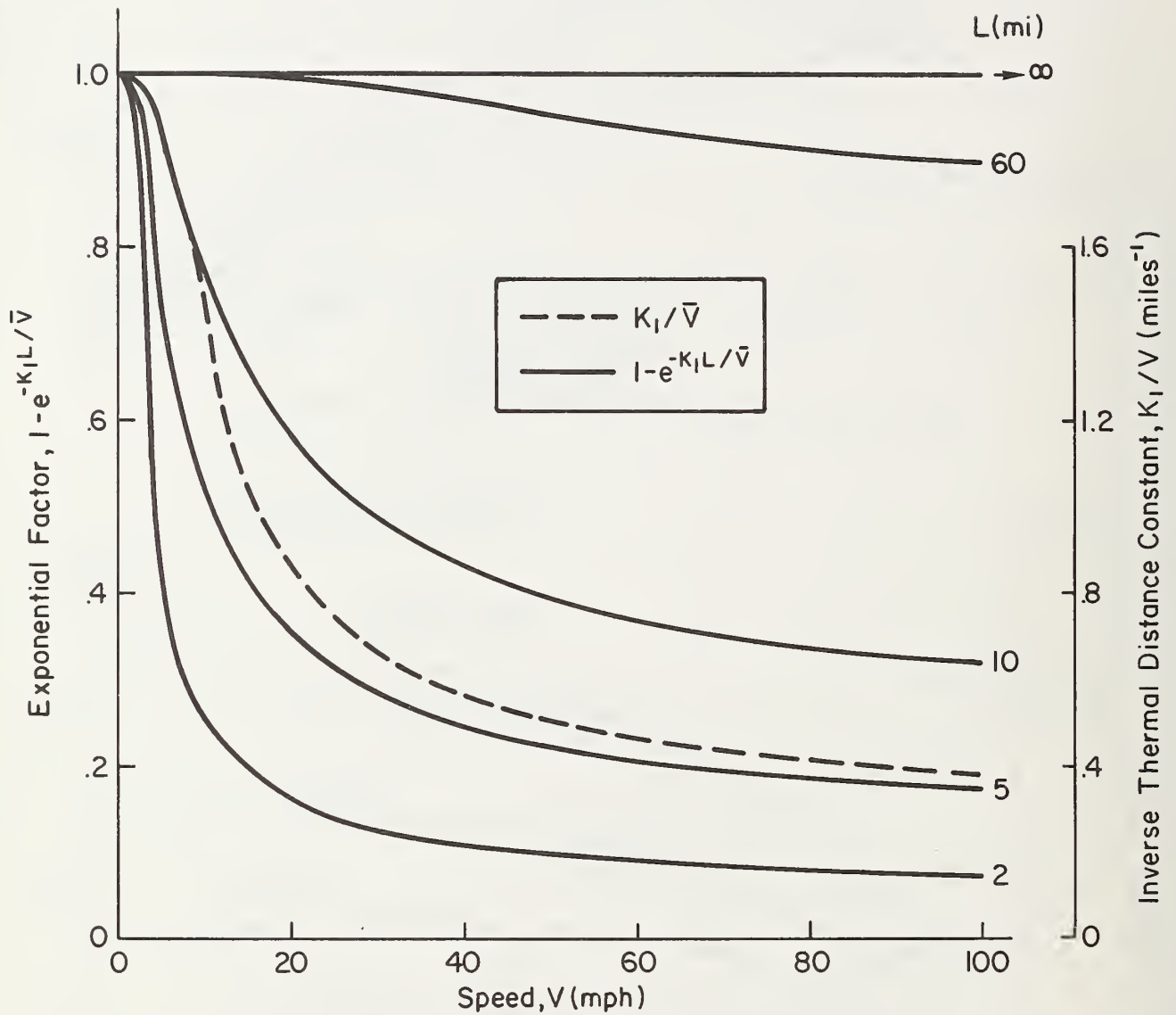


c) Variation of the Convective Heat Transfer Parameter, hA_c , With Speed



d) Steady State Brake Temperature

Figure 23. (Continued)



e) First-order Exponential Variation of Final Form
Steady State Temperature

Figure 23. (Concluded)

SECTION IV

THE GRADE SEVERITY RATING SYSTEM

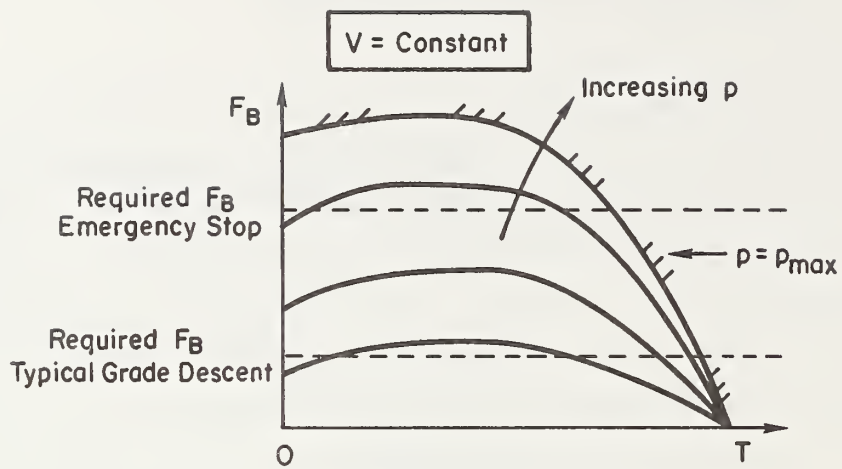
We now have a model which predicts brake temperature on downgrades and provides some insight into brake thermodynamics. In this section we will exercise this model to develop a GSRS. However, as stated in the Introduction, it will be found that, for a variety of reasons, the GSRS as originally conceived is not feasible. The problem lies in the gear selection model (cab card) concept which is not workable because of a combination of conceptual problems and practical considerations.

The conceptual problems will be addressed first to see if it is even theoretically possible to formulate a gear selection model structured according to the original concept. Here it will be shown that an exact mathematical formulation of the gear selection model from the downgrade braking model is not feasible. Instead, it is necessary to make further approximations, beyond those of the downgrade braking model, which produce inherent and significant inaccuracies in the resulting gear selection model.

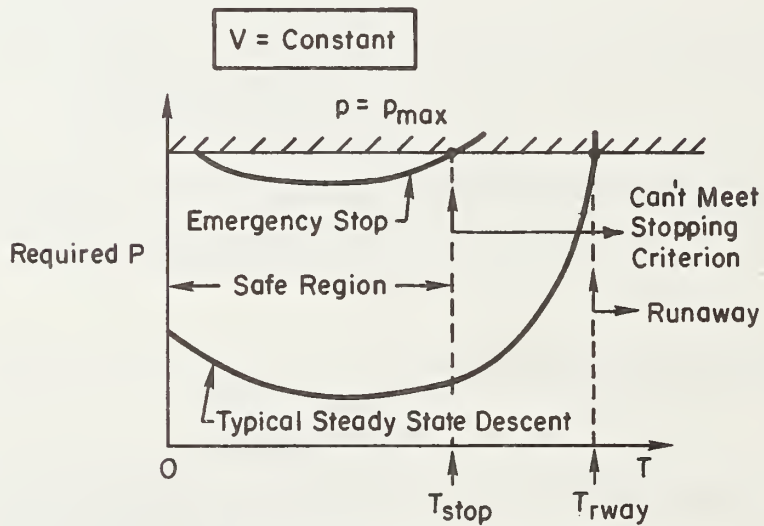
Once the conceptual problems are understood, we will consider the practical problems which combine with the inherent inaccuracy to make the gear selection model infeasible. Here the concern will be with problems of cab card format and human factors as well as general user acceptance of the cab card concept. Finally, an alternative to the gear selection model will be developed.

A. THE TEMPERATURE LIMIT CONCEPT

A logical first step in the GSRS development is to consider the consequences and implications of reduced braking capacity (fade) with increasing brake temperature. Figure 24a sketches the brake capacity (force available) variation with temperature as a family of constant application pressure lines (solid lines) per the discussion in Subsection II.C. A change in descent speed will modify the curves due to speed fade, but for a given speed they will remain unchanged during the descent — at least until a runaway occurs.



a) *Temperature and Pressure Effects On Available Braking Force*



b) *Braking Pressure Variations With Temperature*

Figure 24. Generic Brake Fade Effects

Specific downgrade braking force requirements (e.g., Eq. 12) are represented as horizontal (dashed) lines in Fig. 24a. For a given braking task, the brake force available must equal the brake force required; thus, as the brake temperature increases during grade descent the brake pressure required will increase, as shown by the Fig. 24b crossplot. It can be seen that as brake fade develops the pressure required to achieve a given braking requirement increases ever more rapidly. Since there is a limit, P_{max} , on the brake pressure available, there will be a limiting brake temperature beyond which any given braking task can no longer be accomplished. As shown in Fig. 24b, this limiting temperature is lowest for the emergency stopping requirement. That is, when the brake temperature, T_{stop} , is exceeded, the emergency stopping criterion can no longer be met. However, the truck will not have run away at this temperature. An additional temperature increase, to T_{rway} , will be required before a runaway occurs.

The logical implication of these considerations is that, for a given constant descent speed and a particular brake pressure limit, the "no stop" and runaway situations can be completely specified in terms of brake temperature. Accordingly, we see that, for a given speed, the use of temperature to specify downhill braking requirements (which are dominated by brake heating considerations) is completely equivalent to the use of stopping distance or deceleration.

While there is some variation in P_{max} among trucks, the variation is probably not significant. The speed fade effect is possibly more important. As noted in Subsection II.C, this effect is not well defined; however, it is known that brake force available decreases as vehicle speed increases. Thus, the greatest loss in brake force occurs at high speeds, i.e., near the speed limit. Consequently, the lowest values of T_{stop} and T_{rway} occur at high speeds. If a driver maintains brake temperature at or below some temperature limit, T_{lim} , which is less than or equal to T_{stop} at 55 mph, he would be assured of being able to meet all braking requirements during grade descent. This logic leads to the temperature limit concept in which the GSRS is seen as a system to aid the driver in maintaining downgrade brake temperature at or below T_{lim} ; and a single value of T_{lim} is used for all truck loads and speeds. Obviously, the use of a single minimum value of T_{lim} is somewhat

conservative; however, it appears that the range of variation of the temperature limit with speed or among trucks is comparable to the range of uncertainty with which the limit can be determined for any specific truck and speed.

The temperature limit concept, evolved as above from the physics of braking, also has some independent validity. That is, the idea of using a limiting brake temperature is widely accepted in the trucking industry. In fact, it parallels common practice which involves watching (in the rear view mirror) for smoking brakes as a harbinger of brake fade.

The example value used to illustrate GSRS trends, concepts, feasibility, etc., in the following developments is $T_{lim} = 425$ °F; this conservative, average value recognizes that because of the brake imbalance, intentional or otherwise, prevalent in most truck rigs,* individual brake temperatures may be 200 deg hotter. If we later find that the example limit value should be changed, this is unlikely to affect the conclusions reached regarding GSRS feasibility and form. That is, the results of the analyses and their overall implications are not dependent on the exact value of T_{lim} used.

B. THE GRADE DESCENT CONTROL PROBLEM

Within the context of the temperature limit concept, the driver's task during grade descent is to control brake temperature, the controlled variable, by choosing the correct speed and gear, the control variables. Thus, a temperature constraint equation may be written which must be satisfied during grade descent:

$$T(x) \leq T_{lim} \quad (26)$$

This constraint simply states that the brake temperature may never exceed the temperature limit during the grade descent. One possible control law or strategy which will satisfy this constraint would be for the driver to

*A preliminary finding of Ref. 3.

pick a speed and gear such that the steady-state temperature (which is only slope dependent) is less than or equal to the temperature limit:

$$T_{ss} = T_{lim} \quad (27)$$

This is obviously too conservative (e.g., compare Figs. 22 and 23c) and would require the driver to descend a grade at a much lower speed than is actually necessary (considering grade length) to keep the brake temperature below T_{lim} . For example, the descent of a 5 mi long, 6 percent grade in a 70,000 lb truck such that $T_{ss} = T_{lim}$ requires a speed less than 13 mph. In fact, it would be possible to descend this grade at 28 mph without exceeding the temperature limit. Thus, it is important to consider the length of the grade as well as the slope of the grade in determining the maximum safe descent speed.

There is a more fundamental idea here; specifically, that it is not sufficient for a GSRS to merely maintain the brake temperature below the temperature limit. It is also necessary that the GSRS allow the driver to descend the grade as rapidly as possible consistent with safety. A system which is overly conservative, and requires unrealistically low descent speeds, will very likely be ignored by drivers. Thus, we have not just a temperature control problem, but rather an optimal control problem. That is, maximum brake temperature must be controlled consistent with the minimization of a "cost function" (descent time).

For a single grade hill of constant slope the solution of this optimization problem is quite simple. Recalling that brake temperature increases monotonically along the grade in a constant speed descent (Fig. 19a), it follows that the maximum brake temperature will always occur at the bottom of the grade. The final brake temperature also increases monotonically with descent speed (at least for the speeds used on severe downgrades, see Fig. 22). Thus, a descent speed is selected which makes the final brake temperature just equal to the temperature limit, the maximum safe speed will have been selected for that downgrade and thus the descent time will be minimized.*

*However, it will be shown later that the optimization problems is much more complex for multigrade hills.

The control requirement for the optimal descent of a single grade hill may therefore be written as

$$T_f = T_{lim} \quad (28)$$

It may be seen that this requirement is equivalent to the steady-state strategy (Eq. 27) in the limit as grade length approaches infinity.

The control requirement above, as well as many of the other developments so far, is based on a constant descent speed. In fact, the integrated form of the downgrade braking model is strictly valid only for a constant speed descent. The justification for this will now be considered more fully.

If a truck driver always had a good idea of his brake temperature, he might simply begin the descent of a grade at relatively high speed and modify his speed if he sees that brake temperature is rising too rapidly. This would constitute "closed loop" control of brake temperature and represents the sort of feedback process on which a furnace thermostat is based. In this case, the "man in the loop" would be acting as the thermostat. This closed-loop control approach has a number of attractive features; in particular, it could theoretically handle differences in trucks, load, and grade without any prior knowledge of their actual characteristics. However, closed-loop control of descent is not practical for several reasons. First, drivers do not generally have a good indication of brake temperature during grade descent.* Their most common (basically qualitative) feedbacks are smoke from the brakes and diminished deceleration for familiar levels of brake pedal application. Furthermore, these cues appear at brake temperatures well into the fade region and thus occur too late to aid the driver. On trucks equipped with a brake application pressure gauge, experienced drivers can maintain pressure below 10-15 psi during descent. If the pressure rises above this level, it indicates the onset of brake fade and the driver then downshifts (if possible). This brake pressure feedback is related to brake pressure temperature feedback (see Fig. 24b). Unfortunately, brake pressure

*A few trucks operating under special conditions have brake-monitoring thermocouples, but such installations are rare because of additional cost, complication, and maintenance.

application gauges are not installed on all trucks. Assuming the quality and application of such feedbacks could be improved, there is a more fundamental problem with closed-loop control of brake temperature. This is, as noted in Section III, it is generally impractical or dangerous to downshift on a severe downgrade. Accordingly, even if a driver did have good feedback of brake temperature, he would not generally be free to modulate speed and transmission gear.

These considerations imply that, in general, the driver will be required to control brake temperature "open loop." That is, he will be required to pick his speed and gear before (or at least shortly after) beginning descent and to maintain them all the way down the grade.* The primary disadvantage of open-loop control with respect to closed-loop control is that it does not automatically compensate for variations in grade geometry or truck parameters, in particular weight. Thus, the driver and the highway designer face the formidable task of determining the correct speed for a large number of possible grade geometries, trucks, and loads. It is precisely this problem that the GSRS is intended to solve.

C. THE MAXIMUM SAFE DESCENT SPEED

It is useful, at this point, to formally define the maximum safe descent speed, \bar{V}_{\max} , as follows. \bar{V}_{\max} is the (constant) descent speed, less than or equal to the speed limit (55 mph) which produces a maximum brake temperature equal to the temperature limit when maximum engine retardation is used. Hence, for a single grade of constant slope, \bar{V}_{\max} is the speed which satisfies the optimal control requirement, Eq. 28. T_f is given by Eq. 18, with $x = L$; thus, the control requirement, Eq. 28, becomes:

$$T_f = T_0 + [T_\infty - T_0 + K_2 HP_B][1 - e^{-K_1 L / \bar{V}_{\max}}] = T_{\text{lim}} \quad (29)$$

where HP_B is based on maximum engine retardation.

*When a driver uses open-loop control of brake temperature with speed he does, however, employ closed-loop control of speed with brake pressure. That is, he monitors longitudinal acceleration and modulates brake pressure to maintain $a_x \doteq 0$.

In principle, we could solve this equation explicitly for \bar{V}_{\max} . However, because of the complexity of the functional relationships involving speed (K_1 , K_2 , HP_B), it is not possible to do this exactly. For computational purposes, an indirect approach which avoids this problem is to solve Eq. 29 explicitly for L , i.e.,

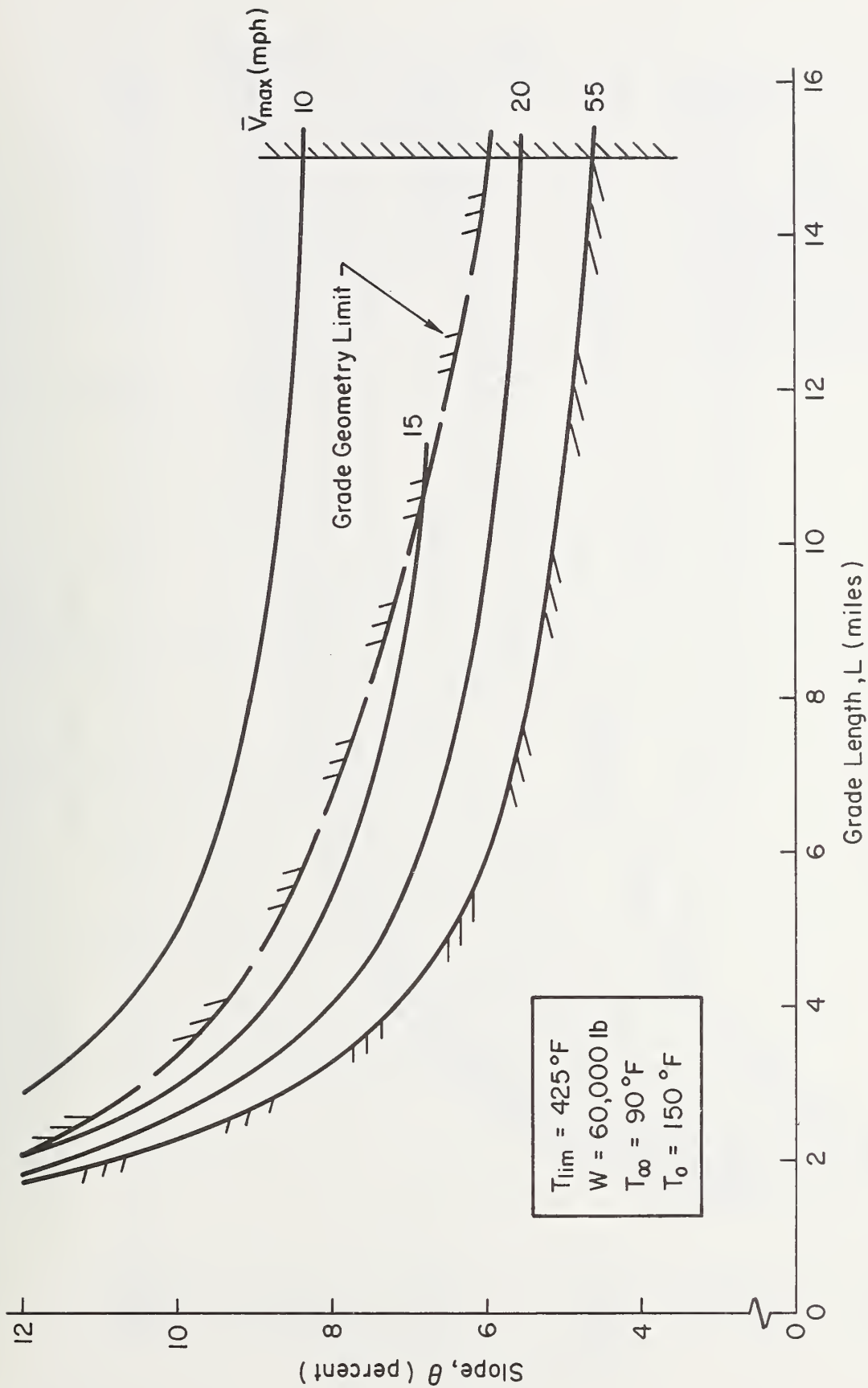
$$L = -\frac{\bar{V}_{\max}}{K_1} \ln \left[1 - \frac{T_f - T_o}{T_\infty - T_o + K_2 HP_B} \right] \quad (30)$$

We can now substitute a particular value of \bar{V}_{\max} into Eq. 30 from which L is evaluated for a sufficient number of θ 's to define the \bar{V}_{\max} contour. Example plots are shown in Figs. 25a and 25b. It may be seen that \bar{V}_{\max} decreases as we move from the origin, implying that as the geometric severity (θ and/or L) of the grade increases, the maximum safe speed decreases. In addition, for any given \bar{V}_{\max} , the corresponding safe slope decreases with grade length.

A "crossplot" of Fig. 25 into the V, L plane (Fig. 26), which will later be important, may also be directly computed using Eq. 30, i.e., by substituting a particular value of θ and corresponding HP_B and computing L for a number of values of \bar{V}_{\max} . Given any hill, i.e., any θ, L pair, we can immediately determine \bar{V}_{\max} from such plots.

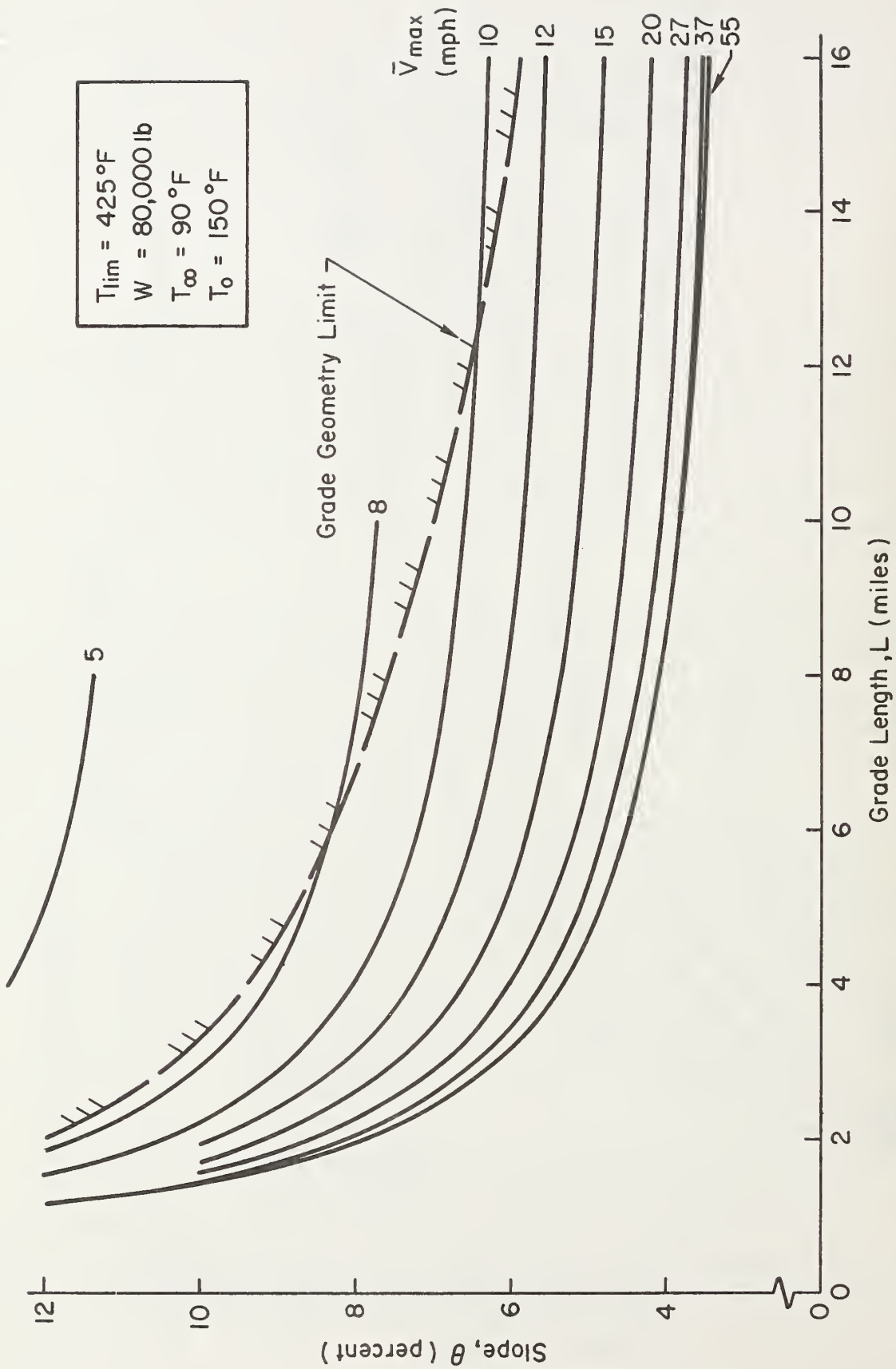
Examination of Figs. 26a and 26b shows that above speeds of 35 to 40 mph the slope contours become essentially vertical or even curve backwards. This phenomenon is simply a manifestation of the speed effect on brake temperature discussed previously in Subsection III.E. The implications here, however, are interesting. From Fig. 26b, for instance, a 5 percent grade less than 4.6 mi long may safely be driven at any speed up to, or even beyond, the 55 mph speed limit. For a 6 percent grade, this is true for any grade less than 3.2 mi long.

It should be noted at this point that the maximum safe speed as defined above is related only to the effect of the vertical plane grade geometry on brake temperature. There are other possible constraints on the maximum safe speed, for instance, sharp curves. If the maximum safe speed for negotiating horizontal curves on a grade is lower than the recommended safe speed as



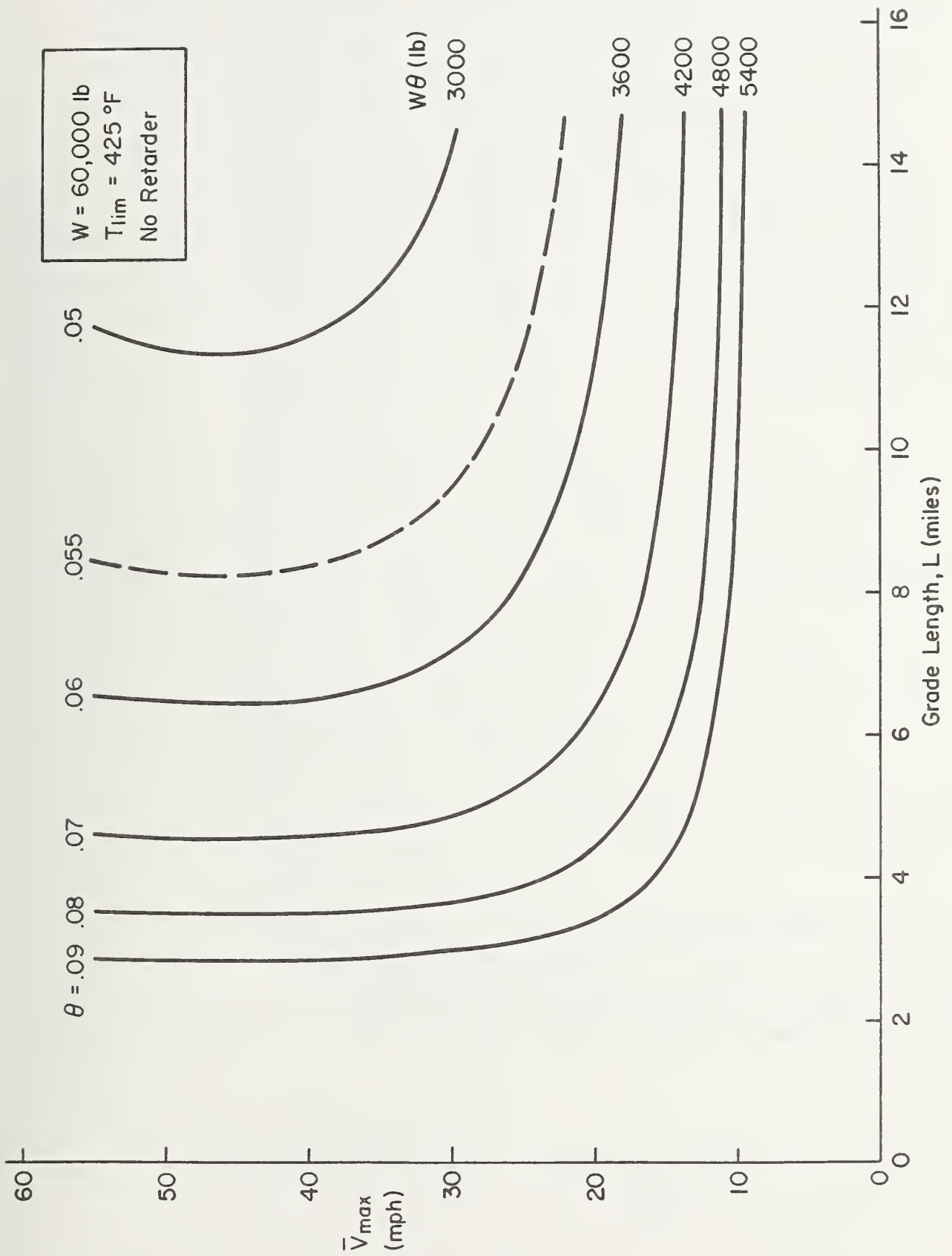
a) Weight = 60,000 lb

Figure 25. \bar{V}_{max} Contours as a Function of Grade Slope and Length



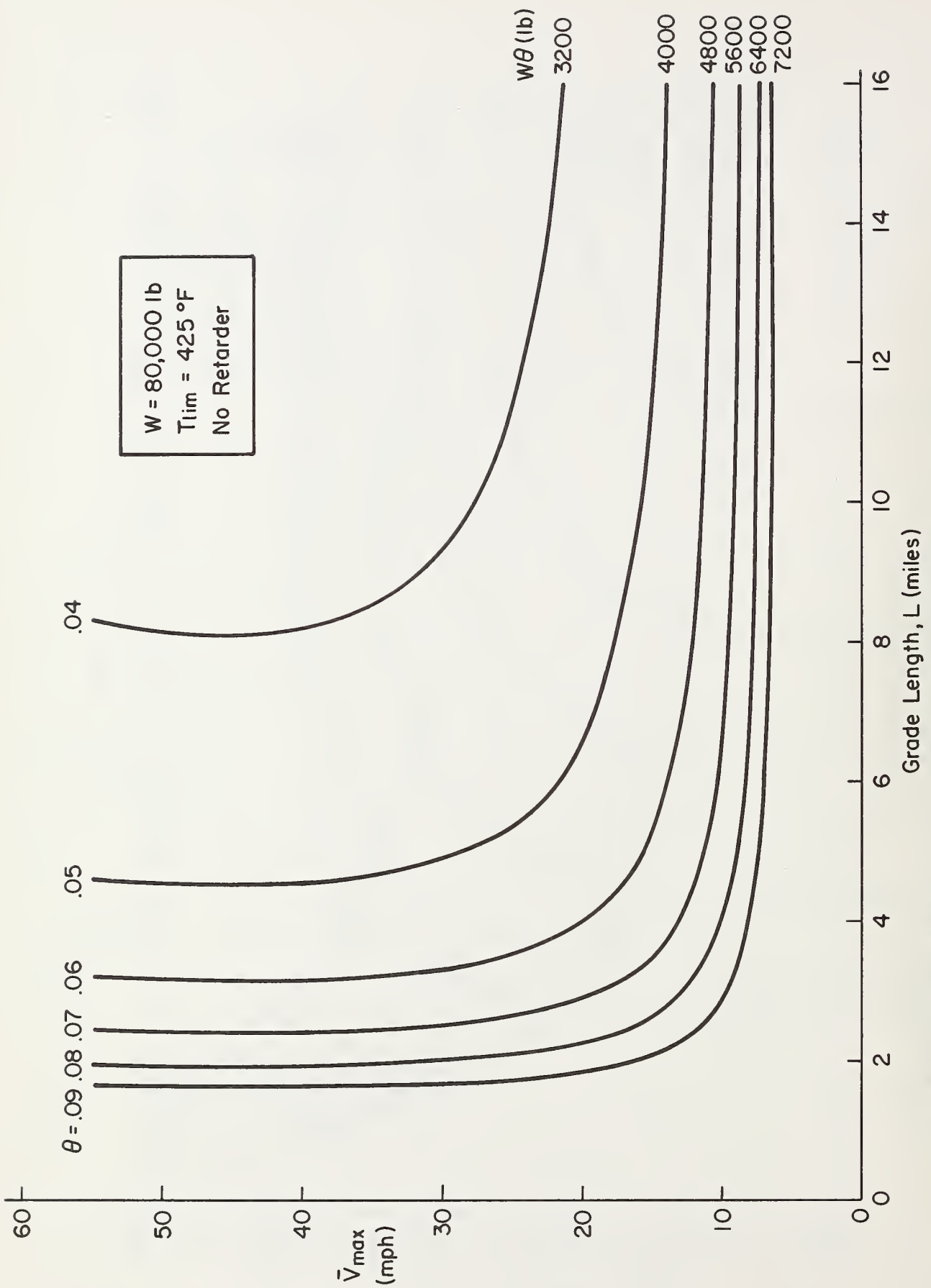
b) Weight = 80,000 lb

Figure 25. (Concluded)



a) Weight = 60,000 lb

Figure 26. Maximum Slopes for Given \bar{V}_{max} and Grade Length



b) Weight = 80,000 lb

Figure 26. (Concluded)

determined from the above brake temperature considerations, then the posted speed would be the lower of the two. However, lateral curvature is not in itself a significant aspect of the downgrade accident problem. That is, provided a runaway has not occurred, a curve in the highway is no more severe on a downgrade than on a level road. Thus, on highways designed so that curves may be negotiated at high speeds, curves should not pose a problem. The only exception would be those instances following a runaway where the increased speed could prevent the driver from negotiating a curve. However, since we are seeking to develop a system aimed at preventing runaways, what happens after a runaway begins is irrelevant, strictly speaking. Thus, the GSRS development in this report will be based only on the effects of vertical grade profile on braking.

One final point should be considered here; that is, how the second control variable, transmission gear, is to be specified. It has been established that the particular engine speed which produces maximum power absorption should always be used during grade descent. Thus, ideally the transmission gear selected should be that which produces \bar{V}_{\max} at the optimum engine speed. Since there are only a finite number of transmission gears (usually from 6 to 15), there are only an equal number of descent speeds available which satisfy the engine speed constraint; thus, it will generally not be possible to obtain the exact optimum match between engine and vehicle speeds. The gear selection strategy which will be used to cope with this is the conservative one — namely, selection of the highest gear which gives a descent speed less than or equal to \bar{V}_{\max} at the optimum engine speed. This strategy is shown graphically in Fig. 27.

This "discretizing" effect of the transmission is not of fundamental importance in the development of the GSRS and may be neglected for the time being. It reenters the picture at the final stage of development where it influences the range of speeds (V_{\max}) assigned a given GSR number.

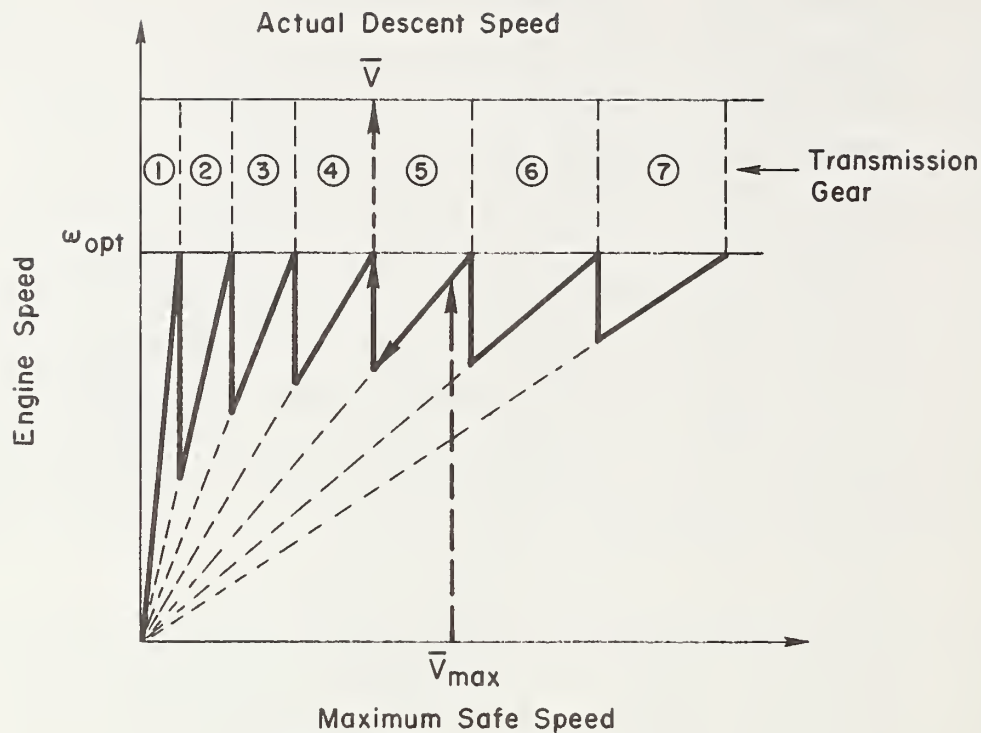


Figure 27. Optimal Gear Selection Strategy

D. THE GRADE SEVERITY RATING CONCEPT

In principle, we could now advise a truck driver of the correct speed for the descent of any grade by giving him a package of " \bar{V}_{\max} versus L and θ " plots for a number of weights (e.g., Fig. 26) and posting θ and L on all grades. Obviously, such a procedure would distract the driver, be subject to error, and otherwise be totally unacceptable for on-the-road use. To develop an acceptable, practical GSRS we must solve both the optimal control problem posed in the preceding article and the human factors problem — namely, to make the system convenient for use by a busy driver. The basic problem in this regard is that there are too many variables (θ , L , W) for the driver to accurately manage. However, sacrifices in accuracy can result in simplified, perhaps manageable, presentations.

Such considerations led to the GSRS initially envisioned in Ref. 1. This simplified concept, still based on \bar{V}_{\max} , derives from the work of Hykes and Lill and combines the two basic grade parameters, slope and length, into

a single (scalar) metric, the GSR, which then characterizes the grade. The idea is that grades which differ geometrically may still have the same "severity." Therefore, if the GSR were posted on all grades, drivers could immediately rank grades on the basis of their relative severity. Since a driver relates severity to how fast he can descend the grade, the obvious quantification for the GSR is in terms of \bar{V}_{\max} or, more generally, some function of \bar{V}_{\max} . However, there is a problem with relating the GSR directly to \bar{V}_{\max} , because \bar{V}_{\max} is, strictly speaking, a measure of "absolute" grade severity. That is, it measures the grade severity of a particular grade for a specific truck. What is really needed is a "relative" GSR which is dependent on the grade parameters only.

Such a relative rating may be formulated from \bar{V}_{\max} by using Lill's (Ref. 5) concept of a representative truck, in which the GSR for any grade is related to the \bar{V}_{\max} for the representative truck (or rather the truck mathematical model). In the context of the truck downgrade braking model used here, the definition of the representative truck is a matter of picking a reference weight. The choice of reference weight was considered carefully and led to our selecting $W_{\text{ref}} = 80,000$ lb, as explained shortly. Accordingly, the GSR could now be simply defined as \bar{V}_{\max} at 80,000 lb (e.g., Fig. 26b). However, because the operational value of \bar{V}_{\max} is still truck type-dependent, it is desirable and necessary to assign simple numerical GSR values by partitioning the \bar{V}_{\max} axis values into discrete intervals.

There are several considerations involved in such partitioning and rating number assignment. First, the numerical GSR values should be integers which increase sequentially with grade severity and cannot easily be confused with speed limit numbers. Second, the number of GSR categories should be minimized but without excessive loss of information. Finally, we should recognize that there is no advantage to having more than one GSR number (band), on the average, within the speed range covered by a single transmission gear in a typical truck.

This last consideration leads to the idea of relating the GSR bands to the gearing of typical truck transmissions. As noted in Ref. 26, transmission gear ratios are ideally chosen so that each ratio is a constant

percentage increase, Δ , over the previous ratio. For an N-speed transmission, the gear ratio in the i th gear, G_{T_i} , is thus given by the formula:

$$G_{T_i} = (1 + \Delta)^{N-i} \quad (31)$$

based on the standard condition that $G_{T_N} = 1$. The vehicle speed at optimum engine rpm, ω_{opt} , in the i th gear is given by the formula

$$\bar{V} = 0.0714 \frac{R\omega_{opt}}{G_{T_i}G_D} \quad (32)$$

where

R is tire rolling radius (ft)
 G_D is differential gear ratio

The \bar{V}_{max} axis may now be "naturally" partitioned by the following procedure.

- 1) Assume a 12 speed transmission ($N = 12$).
- 2) Assume $\bar{V} = 55$ mph in top gear, then from Eq. 32:

$$0.0714 \frac{R\omega_{opt}}{G_D} = 55$$

- 3) Assume minimum speed, 10 mph, occurs at the top of second gear; then using Result 2, above, and Eq. 31 in Eq. 32:

$$\frac{55}{(1 + \Delta)^{12-2}} = \bar{V}_2 = 10$$

which implies $\Delta = 0.186$.

- 4) Compute the top speed in each gear from

$$\bar{V}_i = \frac{55}{(1.186)^{12-i}}$$

as tabulated below:

<u>Gear</u>	<u>Speed (mph)</u>
1	8.4
2	10.0
3	11.8
4	14.0
5	16.7
6	19.8
7	23.4
8	27.8
9	33.0
10	39.1
11	46.4
12	55.

and partition the \bar{V}_{\max} axis accordingly, i.e.,

- 5) Assign GSR = 1 to the $i = 12$ to 10 band.
- 6) Assign GSR = 2 through 9 to the $i = 10-9$ through 3-2 bands.
- 7) Assign GSR = 10 to $\bar{V}_{\max} \leq 10$ mph (grade geometry limit).

This procedure leads to the ten category GSR shown in Fig. 28.

The GSR, as formulated above, is a function of grade geometry only, and thus allows a driver to make severity comparisons among grades. But the driver's real task is to select a safe descent speed, i.e., to estimate \bar{V}_{\max} , for a specific grade. Since \bar{V}_{\max} varies with weight on any given grade, the driver must combine GSR and weight in some way to do this. A driver with general grade experience, but unfamiliar with a specific site, could to some extent do this intuitively using his knowledge of the correct speed and gear for familiar situations with comparable weight and GSR. This idea of using the GSR to extend a driver's experience from a familiar, reference grade to a new grade puts a special requirement on the GSR function, i.e.,

If a driver knows the correct descent speed for a grade at a given weight, that speed must be appropriate for all other grades of the same GSR at that weight.

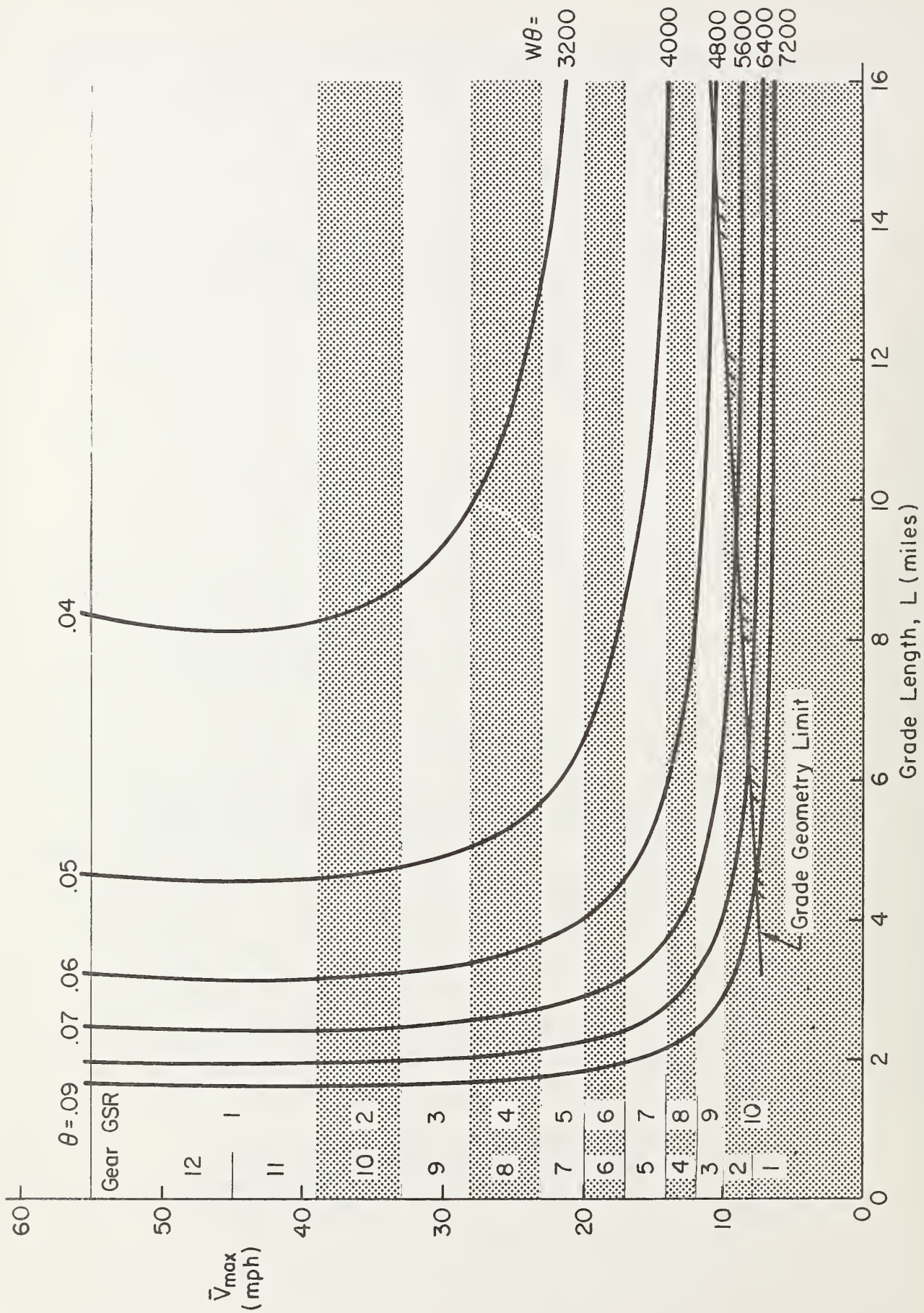


Figure 28. Definition of GSR Categories

This might be called the "speed uniqueness" requirement and is a necessary but not sufficient condition for logical speed selection to be possible. That is, satisfying the uniqueness requirement is not a sufficient guarantee that the driver will actually know the correct speed for any grade. The relative GSR formulated above from \bar{V}_{\max} for a reference weight will certainly have speed uniqueness when used for a truck at the reference weight. The subtle question is whether or not this is true for weights other than the reference weight.

This question may be answered by examining \bar{V}_{\max} contours for $W = 80,000$ and $70,000$ lb (Fig. 29). It may be seen that Grade A can be descended at 14 mph in an 80,000 lb truck and at 20 mph in a 70,000 lb truck. If the GSR is based on an 80,000 lb reference weight, then any grade on the 14 mph contour, B for instance, would have the same GSR as A. Thus, if a driver encounters Grade B in an 80,000 lb truck, he should descend at 14 mph, which would in fact be the correct speed. Note, however, that at 70,000 lb there is no

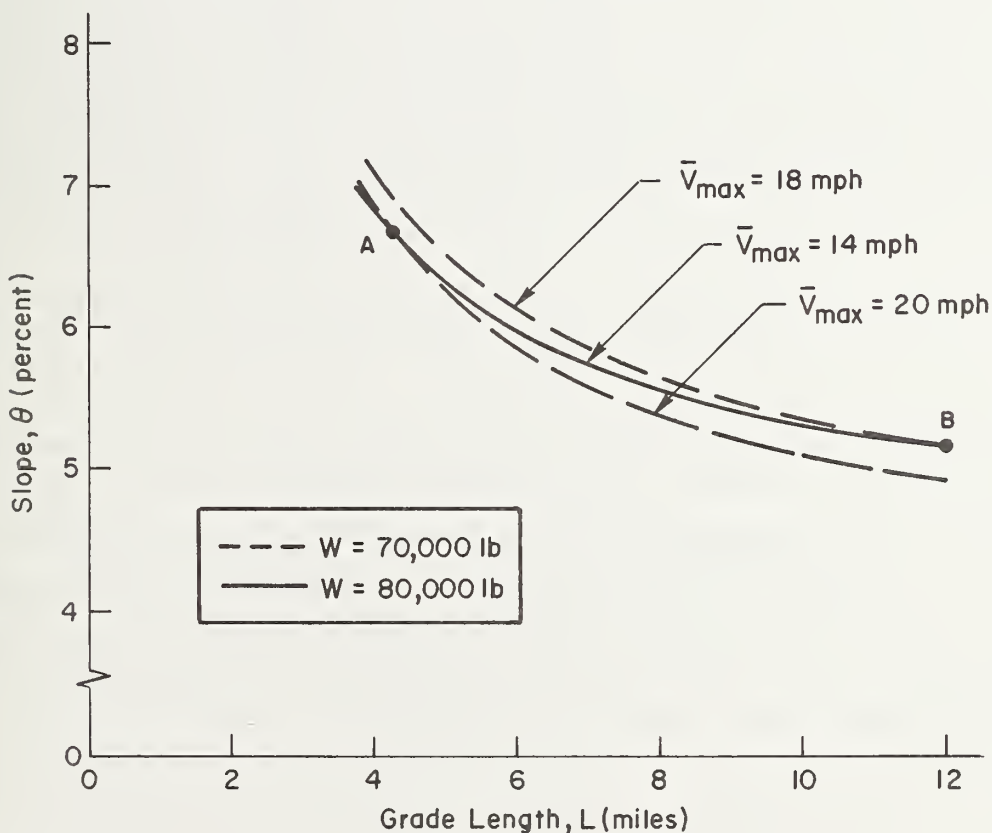


Figure 29. \bar{V}_{\max} Contours for 70,000 and 80,000 lb

single \bar{V}_{\max} curve through Grades A and B, but rather $\bar{V}_{\max} = 20$ passes through A and $\bar{V}_{\max} = 18$ passes through B. Accordingly, the driver's 70,000 lb experience with Grade A would lead him to descend B 2 mph too fast, i.e., at 20 mph rather than at 18. Conversely, his 70,000 lb experience with B would lead to a descent 2 mph too slow for A.

This demonstrates that a GSR based on \bar{V}_{\max} meets the speed uniqueness requirement exactly only for trucks at the reference weight. For any other weight, some conservative (slow) or unconservative errors will occur. It might be expected that the choice of reference weight could be optimized in some way to minimize such errors. For instance, we might base the GSR on $W_{\text{ref}} = 70,000$ lb; but then Fig. 29 shows that the driver's 80,000 lb experience at B would again result in a 2 mph error at A (18 rather than the "correct" 20 mph for $W = 70,000$ lb). Thus, it can be seen that it is not possible to significantly reduce the overall speed errors inherent in the system through the choice of reference weight. Instead, the reference weight should be picked to minimize errors at the most critical, i.e., the maximum, weight. While the usual maximum weight in the domain of interest is 80,000 lb, there are a few states which allow higher weights and, perhaps equally important, trucks are sometimes operated illegally above the weight limit. Thus, the use of an 80,000 lb reference weight appears to be a good compromise.

The foregoing has demonstrated that the GSR does not, strictly speaking, satisfy the speed uniqueness requirement. However, for the example shown, the speed errors do not appear too significant. It would be desirable to understand the physical origin of these errors and this will be demonstrated later; our immediate concern is with the larger question of how the lack of speed uniqueness affects intuitive speed selection by a driver using GSR signing. In particular, it would be desirable to determine, over the grade and weight domains of interest, the brake temperature error, T_e , between the desired final brake temperature, T_{lim} , and that which results from the driver's speed choice. That is, we wish to compute

$$T_e = T_f(\text{Chosen } \bar{V}) - T_{\text{lim}} \quad (33)$$

To do this analytically would require predicting the speed chosen by a driver in a given case, which would ultimately require simulation and/or field requirements. However, we can gain some insight into potential accuracy by making a simple assumption about the driver's intuitive use of the GSR. Specifically, we will assume that at each GSR level there is a set of reference hills for which the driver knows the proper speed at any weight. For concreteness in the analysis, we will assume that the driver is completely familiar with 5 mi hills of any GSR. Because the 80,000 lb-based GSR signs will be correct at that weight for all grades, the error analysis of interest is for a weight considerably lighter but still significant, specifically 60,000 lb.

For simplicity in the analysis, the effect of using discrete GSR categories will be neglected by considering grade severity to be simply \bar{V}_{\max} for $W_{\text{ref}} = 80,000$ lb. Hills A and B in Fig. 30 have the same $\bar{V}_{\max} \doteq 11$ mph at 80,000 lb and thus are rated at the same grade severity. A 60,000 lb truck has a \bar{V}_{\max} of 20 mph at A and since we are assuming the driver knows this he will also drive hill B, having the same (GSR) severity, at 20 mph. However, it may be seen in Fig. 30 that the true 60,000 lb \bar{V}_{\max} for B is less than 20 mph; and that, if driven at 20 mph, the final brake temperature will exceed T_{lim} by 60 deg, i.e.,

$$T_e = T_f(\bar{V} = 20) - T_{\text{lim}} = 60 \text{ } ^\circ\text{F}$$

If this calculation is repeated for a number of points in the hill parameter (θ, L) plane, contours of temperature error (vertical dashed lines in Fig. 30) can be defined over the grade domain of interest. The temperature error contour lines are essentially linearly spaced with hill length and, being vertical, are not much affected by speed changes and associated variations in the 80,000 lb \bar{V}_{\max} (GSR) level. They show that the assumed ideal driver with "perfect" knowledge of the weight correction for certain hills would incur brake temperature errors on the order of ± 50 $^\circ\text{F}$ over the entire grade domain. How close an actual driver, after long exposure to GSRS, would come to this acceptable level of accuracy is of course debatable. Nevertheless, the "ideal" errors are sufficiently

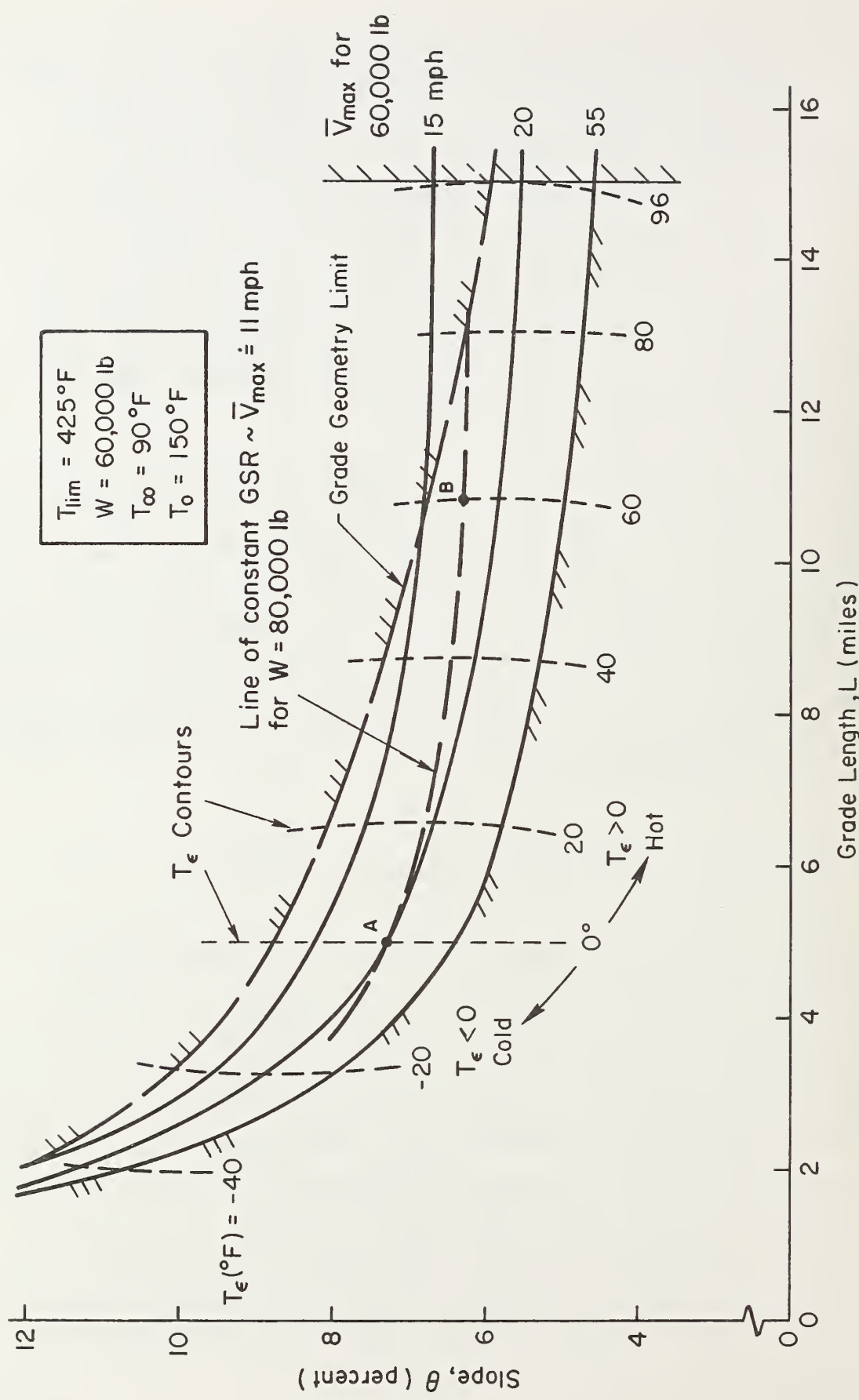


Figure 30. Hill Length Effect on GSR-Induced Final Temperature Errors

small to suggest that the use of GSR signs is feasible and warrants further consideration.

E. THE GEAR/SPEED SELECTION MODEL

We have just shown that GSR signs may be a viable aid in speed selection for experienced truck drivers. However, since drivers with little or no downgrade experience may represent a significant factor in the downgrade accident problem, it would be highly desirable to formulate a GSRS which would provide specific speed and/or gear recommendations for all, including inexperienced, drivers.

This need led to the second element of the Ref. 1 GSRS concept — the "gear selection model." In its original conception, this model would form the basis for a driver aid device combining GSR and weight to obtain a recommended gear for safe descent. It was envisioned that the device would be an "in-cab" driver aid specifically formulated for each truck model or type to account for such constant (but different) truck parameters as retarder capability, drag characteristics, etc. The basic concept for this driver aid was a card (a "cab card") containing a matrix of recommended gears for any combination of GSR and weight, as indicated in Fig. 31.

A highly desirable requirement for the cab card is that the only grade parameter required is the GSR. This simplifies the card by making it

		Weight →				
		W ₁	W ₂	W ₃	W ₄	W ₅
← GSR	1	G _T	G _T	G _T	-	-
	2	G _T	G _T	-	-	-
	3	G _T	-	-	-	-

Figure 31. Example Cab Card

two-dimensional (GSR and W) instead of three-dimensional (θ , L, and W). Furthermore, a single posted GSR could then serve for speed selection using either a cab card or intuition. Drivers who were experienced with operation on severe downgrades, but who were unfamiliar with a particular area, could use the GSR intuitively without reference to the cab card, which would be used primarily by drivers who were basically inexperienced with driving in mountainous regions.

The Ref. 1 GSRS concept was also supposed to "determine the appropriate gear the truck should be in before it starts down the grade....". However, discussions with drivers and others in the trucking industry have indicated that the idea of a system which would produce a recommended gear for descent is generally disliked, and probably would not be accepted. Actually, there is nothing unique to the downgrade problem which makes it more necessary to specify gear for the driver than for any of the other driving situations he encounters. Instead, the real issue is for the driver to descend at a safe, efficient speed (e.g., \bar{V}_{\max}) using the optimum engine speed to produce maximum engine retardation. Here there does appear to be a need to provide specific information, because some drivers do not use the optimum engine speed in descent. This is due to their belief that lower engine speeds during descent lead to extended engine life — not generally true for modern truck engines. Consequently, a device which would be simpler and much more acceptable than a cab card specifying gear would be a simple placard installed on the instrument panel to specify the optimum descent engine speed. Using the placard, any competent driver, even without downgrade experience, could pick the correct gear if given \bar{V}_{\max} through the GSRS. Even without the GSRS, the placard would be helpful in guaranteeing the use of maximum engine retardation.

Accordingly, in the developments to follow, the "gear selection model" of the Ref. 1 GSRS concept will be replaced by a "speed selection model" (SSM) which would be used to produce cab cards specifying recommended truck-specific descent speeds. Many approaches to generating a suitable SSM were tried in the course of this program. All of these candidates produced significant speed errors in some region of the grade/weight domain. The best SSM concept was developed from the idea that the SSM should produce a recommended speed, \bar{V}_{rec} , which is as near as possible to \bar{V}_{\max} . This implies that

the SSM should be developed from an explicit, literal formula for \bar{V}_{\max} . Not only does this approach lead to the best formulation for an SSM/cab card system, but it also gives a physical understanding of the inherent accuracy problem and makes it possible to decide when a best SSM has, in fact, been found. Also, this approach provides a deeper understanding of the GSR speed uniqueness problem and the requirements for intuitive speed selection.

To exercise this approach requires an explicit, literal \bar{V}_{\max} formula; but earlier (Subsection III.C) we saw that such a formula could not be derived exactly. The exact Eq. 30 can be used for general computations; but our present purpose requires the development of an approximate literal expression for \bar{V}_{\max} . A number of different approximations was examined until one was found which appeared to be the most accurate over the entire variable domain of interest. The details of the derivation of this approximation are given in Appendix D. Two intermediate approximations were required to formulate this approximate expression for \bar{V}_{\max} . The first was to approximate the power absorbed by the brakes, HP_B , as a linear function of descent speed. The second was to approximate the exponential factor in Eq. 29 with a modified Pade function, as is common in dynamic analysis, Ref. 34. These simplifications result in the approximate expression for \bar{V}_{\max} :

$$\bar{V}_{\max} = \frac{-482 + 1.415(T_{\infty} - T_0) - .984(T_f - T_0)}{53.6 - .0367W\theta - .0294(T_{\infty} - T_0) + (T_f - T_0/L)} \text{ mph} \quad (34)$$

For a single grade, using "standard" values of $T_f = T_{\text{lim}} = 425^\circ$, $T_0 = 150^\circ$, and $T_{\infty} = 90^\circ$, this is further simplified to:

$$\bar{V}_{\max} = \frac{-837.5}{55.4 - .0367W\theta + 275/L} \text{ mph} \quad (35)$$

All of the terms in Eq. 35 are significant in some region of the variable domains of interest; thus, the approximation cannot be simplified further without greatly compromising its accuracy. The accuracy of this approximation may be assessed by using it to generate constant \bar{V}_{\max} contours in the grade parameter plane and comparing these with the exact \bar{V}_{\max} contours as in Fig. 32. It may be seen that the approximate contours follow the trends in

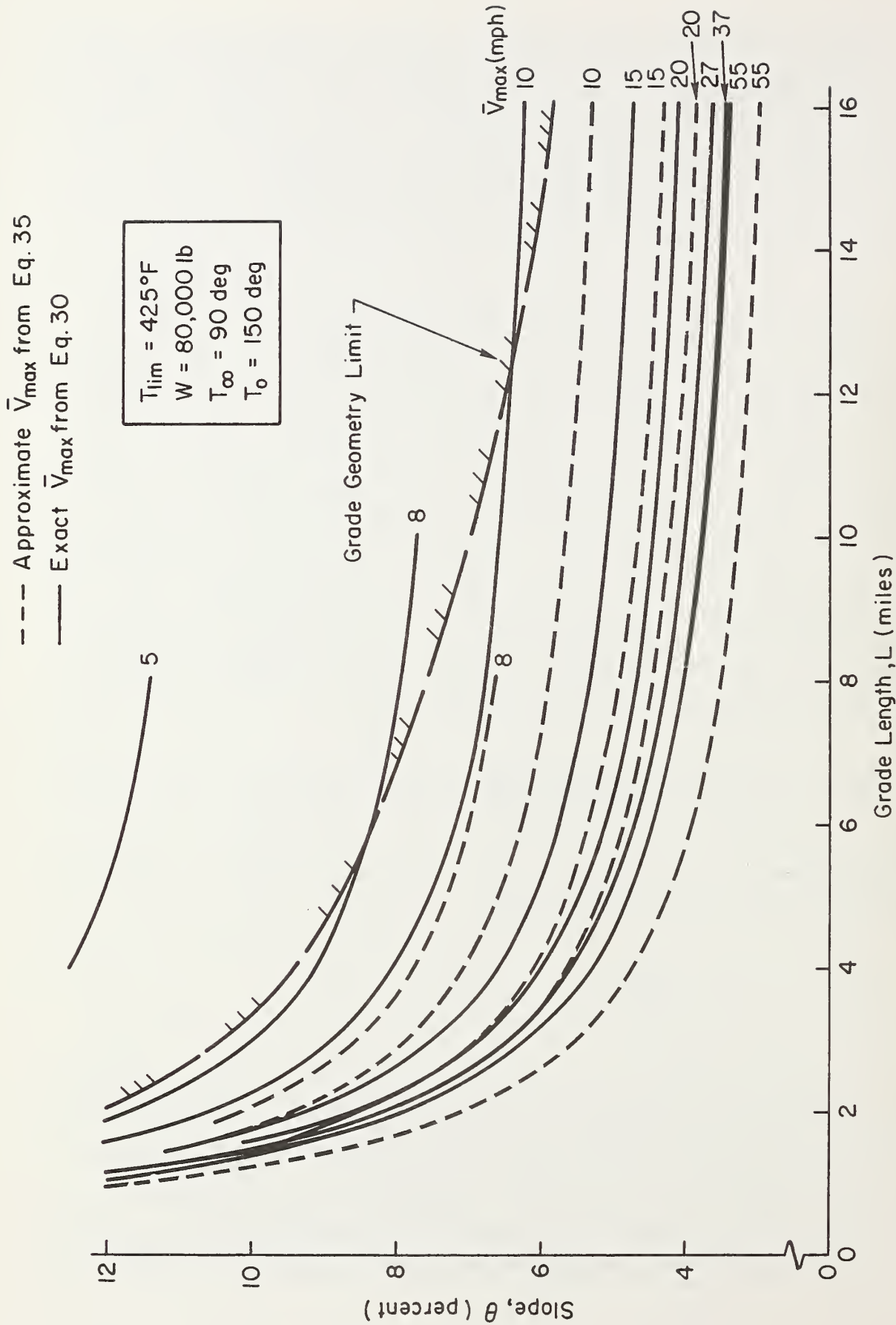


Figure 32. Comparison of the \bar{V}_{max} Approximation (Eq. 35) With the Exact \bar{V}_{max} Contours

the exact contours quite well. However, in many cases the approximate curves show absolute errors which are rather large. As will become clearer in the following discussion, these errors are less important than the fact that the approximation reproduces the basic behavior of \bar{V}_{\max} . In fact, the real value of Eq. 35 is that it is a literal expression for \bar{V}_{\max} rather than a complex formula in terms of \bar{V}_{\max} , and this is extremely useful in understanding the physics of the SSM problem.

When we attempt to separate truck and grade variables to form an SSM, we have an immediate problem with the second term in the denominator of Eq. 35, because the truck variable (W) and the grade variable (θ) are inherently coupled. This problem can be attacked by representing truck weight as the sum of the reference weight and a weight increment (ΔW):

$$W = W_{\text{ref}} + \Delta W \quad \text{lb} \quad (36)$$

Then Eq. 35 becomes

$$\bar{V}_{\text{rec}} = \frac{-837.5}{\underbrace{[55.4 - .0367W_{\text{ref}}\theta + 275/L]}_{g(\theta, L)} - .0367\Delta W \theta} \quad (37)$$

The bracketed denominator term is a function of the grade parameters only and thus satisfies the requirements for separation of truck and grade parameters. In fact, g is inversely proportional to the approximation for \bar{V}_{\max} and thus g is an approximation to the "true" (continuous) GSR, i.e., g and GSR are conceptually equivalent (within a constant factor). In principle, the driver could now enter ΔW for his truck into the second denominator term, add this to the posted GSR, and then divide the sum into -837.5 to determine \bar{V}_{rec} .

However, there is still a fundamental physical problem — specifically, to evaluate the ΔW term the driver must know not only ΔW but also a grade parameter, θ . That is, he must be given two independent grade parameters (GSR and θ), and this violates the requirement that GSR is to be the only grade parameter required by the SSM.

It is important to recognize that this coupling between θ and W is not merely an artifact of the particular approximation for \bar{V}_{\max} , but rather has a real, i.e., physical, explanation. If we consider two different grades with the same GSR — one short but steep, the other long but more shallow — the steeper grade will have the much greater sensitivity to truck weight increments. This is because the weight component pulling the truck down the grade, $W\theta$, is much greater on the steep grade; hence, weight increments are much more critical as grade slope increases. This phenomenon apparently has not been previously appreciated in considerations of the cab card (SSM) concept. Instead, it was implicitly assumed that any corrections necessary to apply the GSR to a specific truck could in fact be accomplished with a cab card. It may now be seen that, strictly speaking, this is an invalid assumption. The fact is that accurate (continuous \bar{V}_{\max}) severity ordering of a series of downgrades will change with truck weight; in other words, perfect speed uniqueness is impossible regardless of GSR/SSM concepts or formulations.

Given this understanding of the $W\theta$ problem on any SSM, the "real world" problem is to determine if an approximate SSM can be formulated with sufficient accuracy to be useful. To this end, several candidate SSMs were developed based on further approximations of Eq. 37. The best of these is based on the use of a constant value for slope, θ_{ref} , in the ΔW term of Eq. 37, resulting in

$$\bar{V}_{\text{rec}} = \frac{-837.5}{g(\theta, L) - .0367\theta_{\text{ref}}(\Delta W)} \quad (38)$$

To evaluate the accuracy of this SSM, an error analysis was performed to determine, in a quantitative way, the speed and brake temperature errors over the entire grade/weight domain.

$$\bar{V}_e = \bar{V}_{\text{rec}} - \bar{V}_{\text{max}} \quad (39)$$

$$T_e = T_f(\bar{V}_{\text{rec}}) - T_{\text{lim}} \quad (40)$$

These quantities were calculated in a manner similar to that used in the analysis of Subsection III.D. For example, if the SSM is based on $\theta_{\text{ref}} = 0.06$ (a "typical" value), $\bar{V}_{\text{rec}} = 13.9$ mph for a 60,000 lb truck on a 6 mi, 7 percent grade, which results in a final brake temperature, $T_f = 340$ °F. However, the true \bar{V}_{max} for this grade and weight is 18.9 mph. Thus,

$$\bar{V}_\epsilon = 13.9 - 18.9 = -5.0 \text{ mph} \quad (\text{slow}) \quad (41)$$

$$T_\epsilon = 340 - 425 = -85 \text{ °F} \quad (\text{cold}) \quad (42)$$

The above error calculations, performed over the entire grade domain for a 60,000 lb truck, result in the constant temperature error contours of Fig. 33; conservative (cold) temperature errors of more than 150 °F are indicated for near-limit grades. A fairly obvious way to improve accuracy in the 60,000 lb region would be to use a GSR based on a 60,000 lb reference weight; but then, as seen from Fig. 34, the temperature errors for an 80,000 lb truck, while changed in distribution (from Fig. 33), are in general a little larger. Accordingly, the error is minimized by using the larger, more critical reference weight (as indicated earlier in Subsection III.D). The corresponding speed error contours for the 60,000 lb reference weight case are shown in Fig. 35, from which it can be seen that at 80,000 lb, speeds recommended by the SSM may be up to 20 mph (33 percent) too slow for relevant grades.

By similar examples and reasoning, it may be shown that a change in θ_{ref} will not eliminate errors, but simply move them in the grade plane.

While the errors produced by the SSM are conservative (slow and cold), their magnitudes are large enough to make the value of a cab card questionable. However, it should be noted that the error in \bar{V}_{rec} is due partly to the original approximations involved in Eq. 35 and partly to the further approximation (the use of θ_{ref}) required to create the SSM of Eq. 38. For instance, in the previous ($W = 60,000$ lb) example, Eq. 35 yields

$$\bar{V}_{\text{max}} \doteq \frac{-837.5}{55.4 - .0367(60,000)(.07) + 275/6} = 15.8 \text{ mph} \quad (43)$$

--- T_e Contours

$T_{lim} = 425^\circ\text{F}$
$W = 60,000\text{ lb}$
$W_{ref} = 80,000\text{ lb}$
$T_{\infty} = 90^\circ\text{F}$
$T_o = 150^\circ\text{F}$

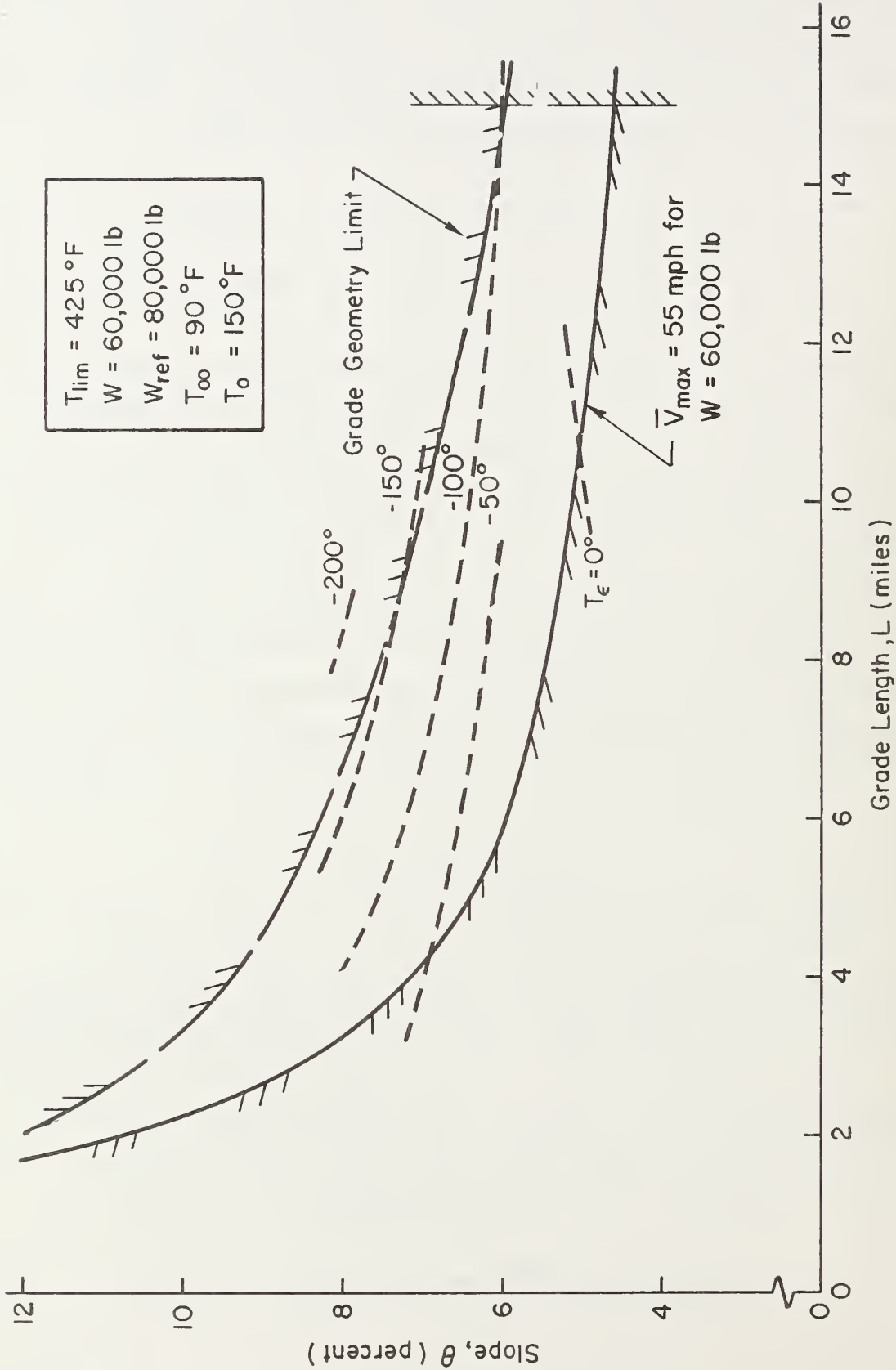


Figure 33. Temperature Error Contours for 60,000 lb Truck and $\theta_{ref} = 0.06$

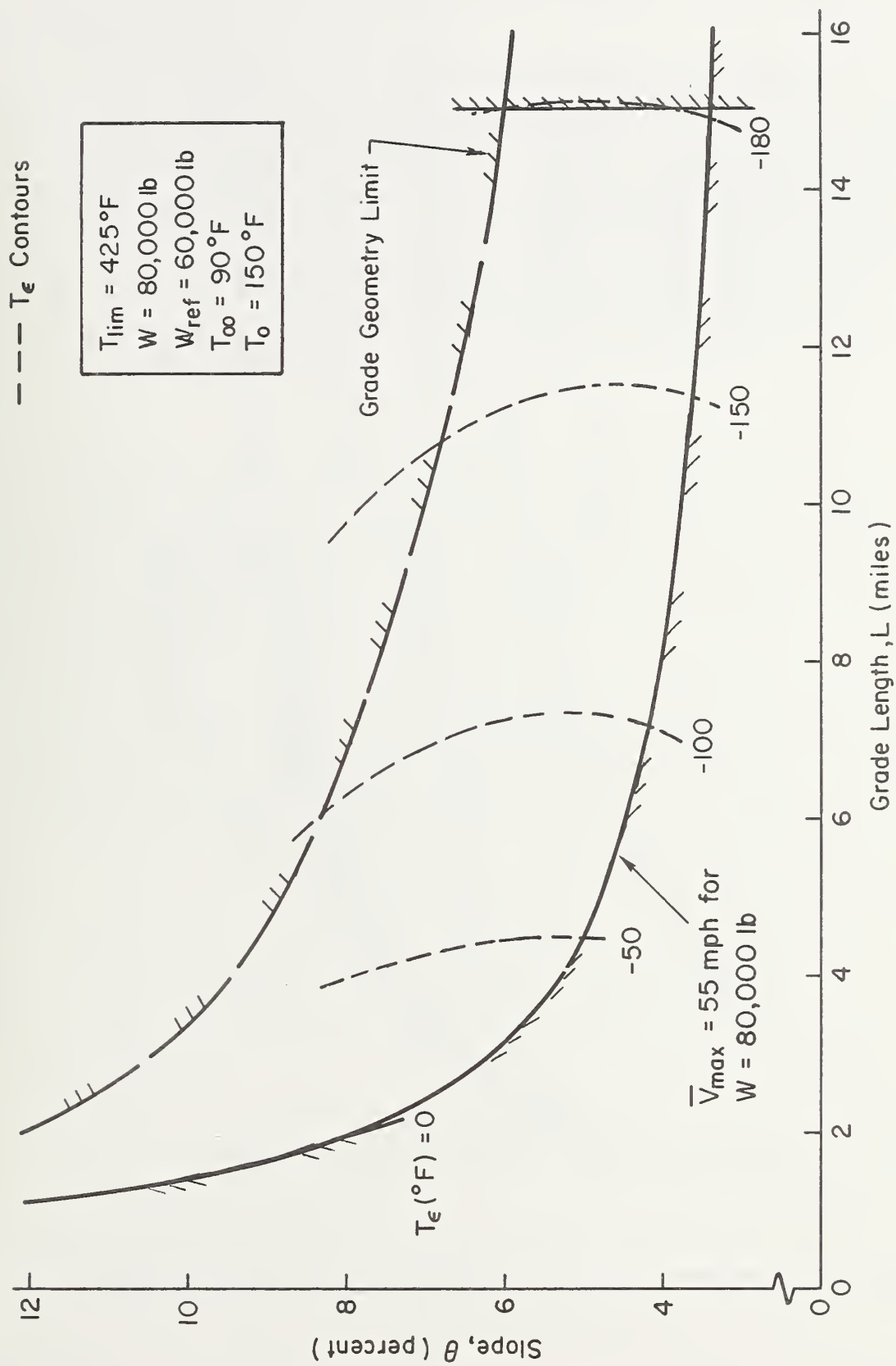


Figure 34. Temperature Error Contours for 80,000 lb Truck and $\theta_{ref} = 0.06$

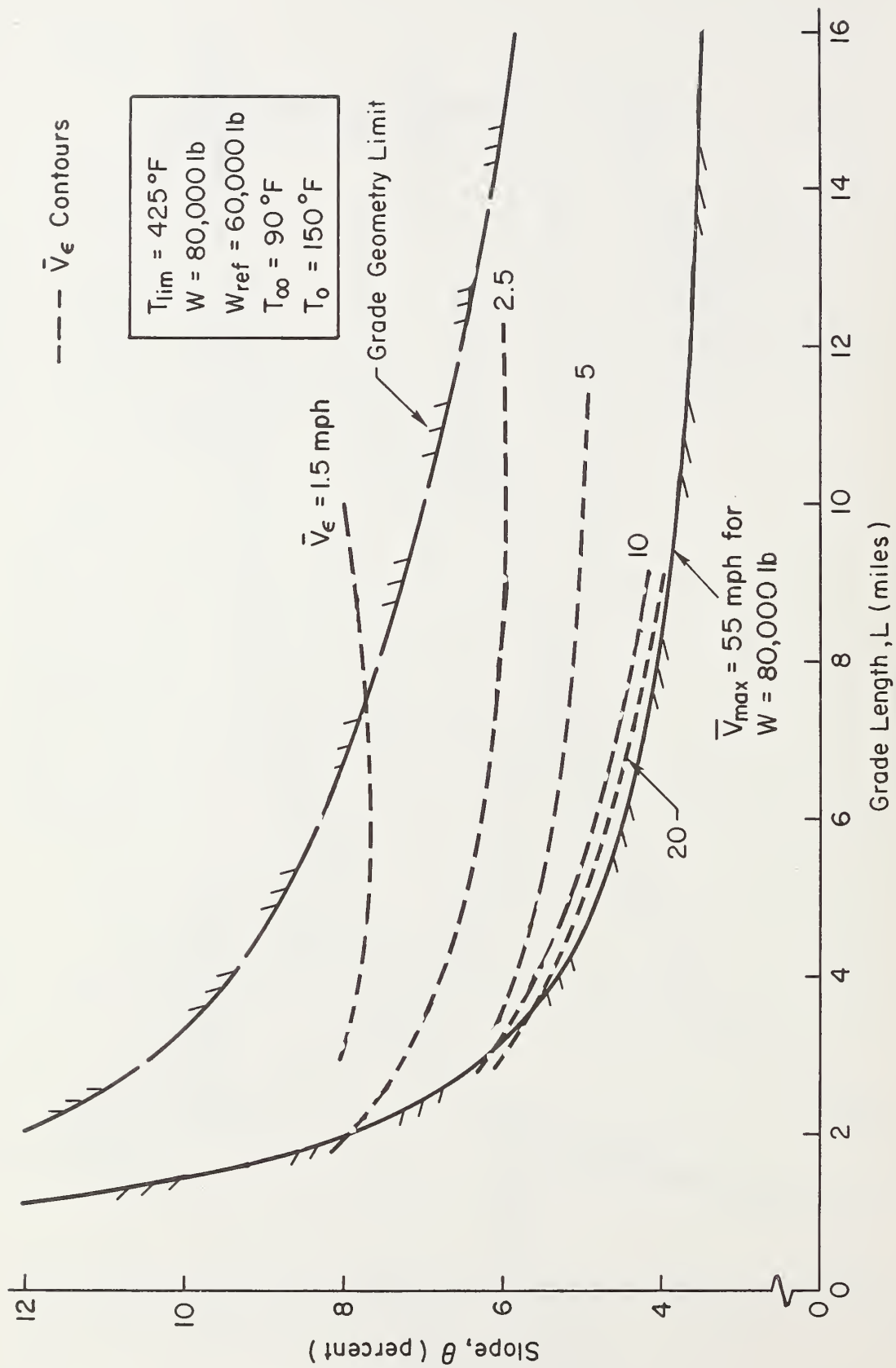


Figure 35. Speed Error Contours for 80,000 lb Truck and $\theta_{ref} = 0.06$

Consequently, $15.8 - 13.9 = 1.9$ mph (38 percent) of the above-noted 5.0 mph error is due to the essential SSM approximation and the rest is due to the original \bar{V}_{\max} approximation in Eq. 35.

For actual generation of cab cards it would thus be desirable to at least avoid the " \bar{V}_{\max} approximation" errors that result from Eq. 35. This can be done by simply using the exact value of \bar{V}_{\max} for the selected "reference" grade for each GSR,W element in the cab card matrix. This procedure is conceptually equivalent to the reference grade concept used as the basis for error analysis of the intuitive speed selection process in Subsection III.D. Therefore, we can expect that it would produce comparable speed and temperature errors — about one-half the magnitude of those in the SSM error analyses above.

Even such reduced level of error in the SSM/cab card is still high enough to make the usefulness of the concept questionable. In addition, these error analyses are based on continuous GSR and weight variables, but a cab card must be simplified by using only a few discrete values of GSR and weight. This necessary discretizing of the cab card will produce a "loss of information" which will lead to additional errors.

An additional source of error is that due to the effects of multigrades, i.e., grades which have non-braking intervals long enough to safely downshift on, but not long enough for complete brake cooling. Extending the single-grade GSRS to multigrades involves posting GSR signs at the beginning of each braking interval, as discussed in detail in Appendix E. Thus, any cab card must be accurate for each succeeding braking interval and realistic initial brake temperatures, T_{0j} . This adds another problem to the formulation of the SSM, i.e., that in principle it must retain T_0 as a variable, Eq. 34. If we proceed to derive an SSM from this equation, we would write, analogous to the single-grade case,

$$\bar{V}_{\text{rec}j} = \frac{-773 - .431T_{0j}}{g(\theta, L) - .0367\theta_{\text{ref}}(\Delta W)} \quad (44)$$

where $g(\theta, L)$, the generalized GSR function, is

$$g(\theta, L) = (51.0 - .0367W_{\text{ref}}\theta + 425/L) + (.0294 - 1/L)T_{Oj} \quad (45)$$

Since the highway engineer will know the desired T_{Oj} distribution along the grade (see Appendix E) as well as W_{ref} , θ , and L , there is no (conceptual) problem in defining the GSR signs corresponding to the Eq. 45 values of $g(\theta, L)$ for a multigrade. However, the driver cannot be given T_{Oj} (only GSR), and thus he has no way of assessing (through the cab card) the term in the (Eq. 45) numerator. Instead, this term will have to be approximated as a constant using the single-grade value of $T_O = 150$ °F. Since for some multigrades T_{Oj} may approach T_{lim} , this approximation may lead to significant additional errors, i.e., for $T_{Oj} = 400$,

$$\frac{\text{Percent additional error in } \bar{V}_{\text{rec}}}{\text{error in } \bar{V}_{\text{rec}}} = \frac{-.431(400 - 150)}{-773 - .431(400)} \times 100 = 11\% \quad (46)$$

The preceding analyses have shown that, for fundamental physical reasons, any SSM/cab card system which requires only GSR as a grade input will contain intrinsic inaccuracies. These inaccuracies alone are of a magnitude to bring the entire concept into question, e.g., are the speed recommendations good enough to be useful? Then there is the trouble of using even a minimal card, with 10 GSRs and 5 weight classes, requiring at least several seconds of "eyes off the road" examination. Another important issue is the determination of braking parameters (e.g., K_1 , K_2) for each truck model and type. To establish values for these parameters, not generally defined by manufacturers, would require use of the test procedures developed in this program, Appendix B, involving considerably more instrumentation and data analysis than, say, FMVSS 121 compliance testing. Finally, drivers and others in the trucking industry are generally negative toward the cab card concept (but positive toward GSR signs). This attitude is apparently based on the questionable usability of the cab card and the feeling that its use involves transferring the decision-making process from the driver to a system of questionable accuracy. In view of these problems and attitudes, it appears that an in-cab aid based on an SSM is not feasible.

F. ALTERNATIVES TO THE SSM/CAB CARD CONCEPT

Despite the above conclusion, posting GSR signs for intuitive speed selection without cab cards does appear to be useful on either single or multi-grades (see Appendix E). Since the GSR signs are intended to provide information about the grade but not to "recommend" descent speeds, high accuracy in the truck parameters and the braking model are less critical. Also, the use of a single set of generic truck parameters (e.g., the values used in this program) to generate the GSR appears to be reasonable. Accordingly, GSR implementation costs should be comparable to those for conventional downgrade signing, whereas their benefits may be greater.

A good indication of such enhanced benefit is that truck drivers and others in the trucking industry are positive toward the concept. In particular, it seems to be widely felt that GSR signs would be advantageous if only because they represent a uniform system, especially good for heavy, critical weights. (The incorrect ordering or ranking of hills for lighter, less critical weights, as noted earlier, would then have to be considered tolerable.)

The implementation of GSR signs alone will primarily be useful to drivers with some general downgrade/speed experience (e.g., on hills of similar rating). It is also desirable to have some formal system to give inexperienced drivers direct speed selection guidance (the cab card function). Assuming relatively insignificant variations in truck parameters (other than weight), a single generic set (i.e., those used to define GSR) may be used to compute \bar{V}_{\max} for any truck. Consequently, the cab card could conceptually be "taken out of the cab" and posted as a sign on a specific grade. If this were to be done an important simplification would result. Since each sign would be for a specific grade, the speed values on it could be calculated directly from Eq. 30 (by a highway engineer) without the errors attending the use of the discrete GSR. Also, the direct calculation of $\bar{V}_{\max}(W)$ from θ and L would avoid the errors inherent in a cab card due to $W\theta$ coupling. Thus, the sign collapses from a two-dimensional (W , GSR) cab card matrix to a more accurate one-dimensional column of weights (and speeds). Such weight-specific speed (WSS) signs would, neglecting details of format, consist of

discrete weights and corresponding values of \bar{V}_{max} . Furthermore, they could be extended to multigrades without the errors introduced into cab cards by the variation of initial brake temperature on each braking intervals along the grade (see Appendix E).

The advantages of such signs over conventional downgrade signing are that they account for the critical weight effect and they they are based on a rational accurate truck braking model. In contrast, the truck downgrade speed signs now in use are based on informed opinions of competent local officials — a procedure which may well lead to inconsistencies in assigning downgrade speed limits in different states or even within states. Furthermore, it is unclear what weight is used as a basis for conventional speed limit signs, or even if weight is considered.

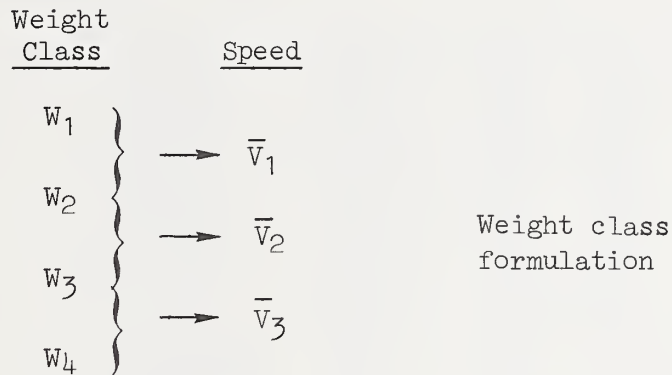
The disadvantage of WSS signs is that they will present more information than conventional truck speed limit signs and thus will be more complex from the driver's standpoint; therefore, the question of format is very important. While a complete study of format issues and possibilities is beyond the scope of this program, a few candidate formats will be suggested in order to set the range of possibilities.

Two possible formulations for the WSS sign suggest themselves. First, a group of discrete weights could be specified with the corresponding values of \bar{V}_{max} , i.e.,

<u>Weight</u>		<u>Speed</u>	
W_1	→	\bar{V}_{max1}	Discrete weight formulation
W_2	→	\bar{V}_{max2}	
W_3	→	\bar{V}_{max3}	
W_4	→	\bar{V}_{max4}	

Since only a few discrete weights are specified, for weights other than those listed, refined speed estimates would require interpolation. As a practical matter, drivers familiar with the WSS sign concept and format could probably interpolate; less confident drivers would simply pick the speed specified for the sign weight just larger than their truck weight.

An alternative formulation would be to specify a speed for a weight class, i.e.,



In this formulation there are several possibilities for assigning speeds to weight classes. In particular, the speed could be the minimum \bar{V}_{\max} for the weight class or perhaps the average \bar{V}_{\max} .

Regardless of whether a discrete weight or weight class formulation is used, the primary consideration is to cover the weight domain of interest for a specific downgrade. Whereas the maximum weight will always be 80,000 lb (say), the minimum weight, generally in the 50-60,000 lb range (Fig. 17 shows that at lower weights brake heating usually is not a problem at the legal speed limit), will depend on the specific grade details. Therefore, the lowest weight specified on a particular sign might vary with grade severity, i.e., more weight classes would be used for severe grades.

The more critical requirement is to standardize the weight classes. This is essential to allow drivers to learn the weight classes and merely concentrate on the listing of speeds. In this way a driver, familiar with the signs, could simply pick the "second speed from the top" rather than take the time to read both weights and speeds. In defining standard weight classes the primary issues are how many classes will be used and how they will be picked, i.e., how the weight spectrum will be partitioned. Obviously, increasing the number of weight classes increases the potential accuracy of the sign; however, this must be traded against the need to make the sign quickly readable. Certainly it is desirable to use "round" numbers for weight, specifically, multiples of 5000 lb.

A rationale for defining weight classes may be found by considering the variation of \bar{V}_{\max} with weight for several hills covering the grade domain, Fig. 36. The general shape of these curves indicates the basic effect of weight on \bar{V}_{\max} , with increasing grade severity shifting the curves downward. The most important aspect of these curves is their asymptotic approach to $\bar{V}_{\max} = 0$ as weight increases; e.g., the marginal change in \bar{V}_{\max} due to a 1000 lb change in W is much smaller at 80,000 lb than at 60,000 lb. This means that variations in class size with weight should be considered. However, the ultimate consideration is the gear to be used in descent; thus, it would be desirable to relate the weight classes to speed ranges corresponding to the gearing of a typical truck. This may be done on the basis of the hypothetical gearing used to develop the GSR categories. These speed ranges in gears are shown as horizontal speed bands in Fig. 36. The intersection of these bands with the grade curves produces "natural" partitions of the weight scale. Obviously, each grade curve produces a slightly different partition; however, the general implication is the same for all grades — namely that the weight class should be wider at higher weights.

When all the above considerations are taken into account a best compromise formulation of weight classes appears to be:

Class 1	50-55,000 lb
Class 2	55-60,000 lb
Class 3	60-70,000 lb
Class 4	70-80,000 lb

With these standard weight classes, speed data for a sign may be immediately generated by a highway engineer from a grade curve in the \bar{V}_{\max}, W plane. For example, the grade curve in Fig. 36 for a 7 percent, 6 mi grade yields the discrete weight \bar{V} 's shown below; the values for the weight class form derive therefrom.

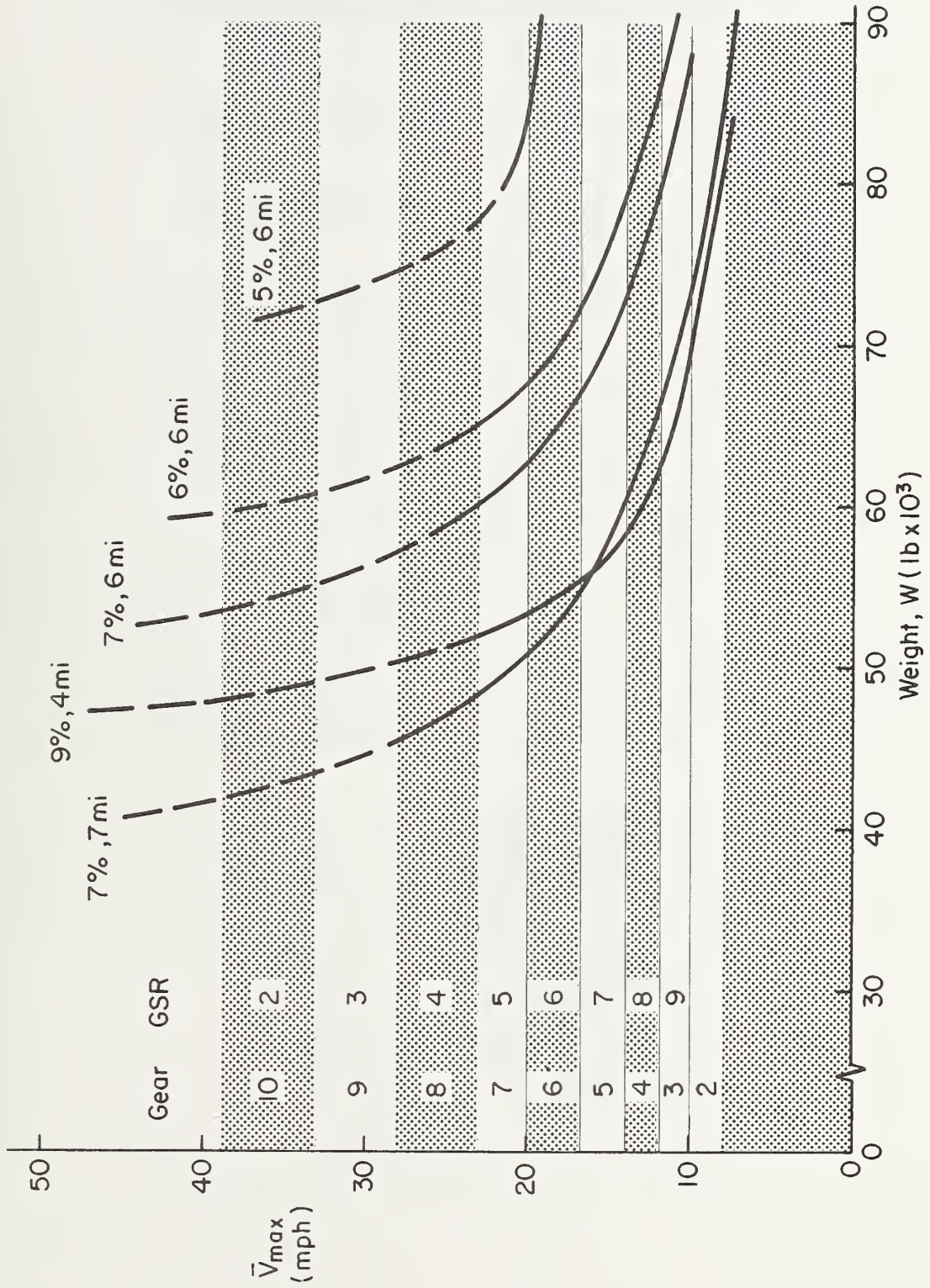


Figure 36. Plot for Definition of WSS Weight Classes

Weight (lb)	Discrete Weight Form, \bar{V}	Weight Class Form	
		Minimum \bar{V}	Average \bar{V}
50,000	55	33	44
55,000	33		
60,000	23	23	28
70,000	16	16	19
80,000	12	12	14

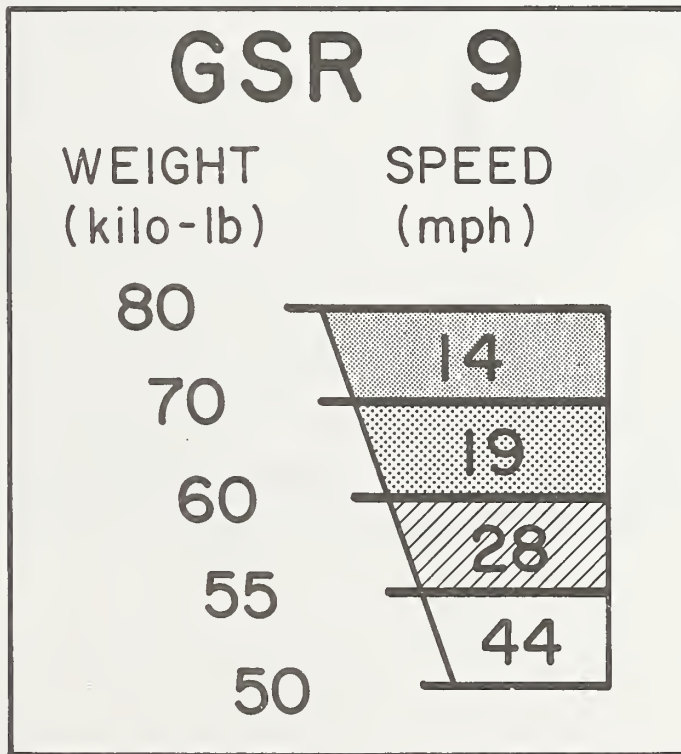
In a single WSS sign the discrete weight formulation might appear as shown in Fig. 37a, a weight class formulation as shown in Fig. 37b. The latter has some additional graphical devices to aid the driver, i.e., size and shading of the trapezoidal speed boxes to suggest the weight range. A possibility for reducing the complexity of individual signs would be to use a "Burma Shave" configuration as shown in Fig. 38.

A final concept for the WSS sign could be particularly applicable for high truck traffic density areas. In such areas it may be unsafe to allow many different levels of truck speed to be used. In fact, it might be desirable to have assigned weight/speed ranges for each truck lane of a multilane highway. This could be accomplished with the form of WSS sign shown in Fig. 39.

Perhaps the ultimate form of the WSS would be to combine it with the GSR. In this approach experienced drivers would primarily use the GSR information but less experienced drivers would tend to use the WSS information.

GSR 9	
WEIGHT	SPEED
80,000 lb	12 mph
70,000 lb	16 mph
60,000 lb	23 mph
55,000 lb	33 mph
50,000 lb	55 mph

(a)



(b)

Figure 37. Possible Formats for Weight Specific Speed Signs

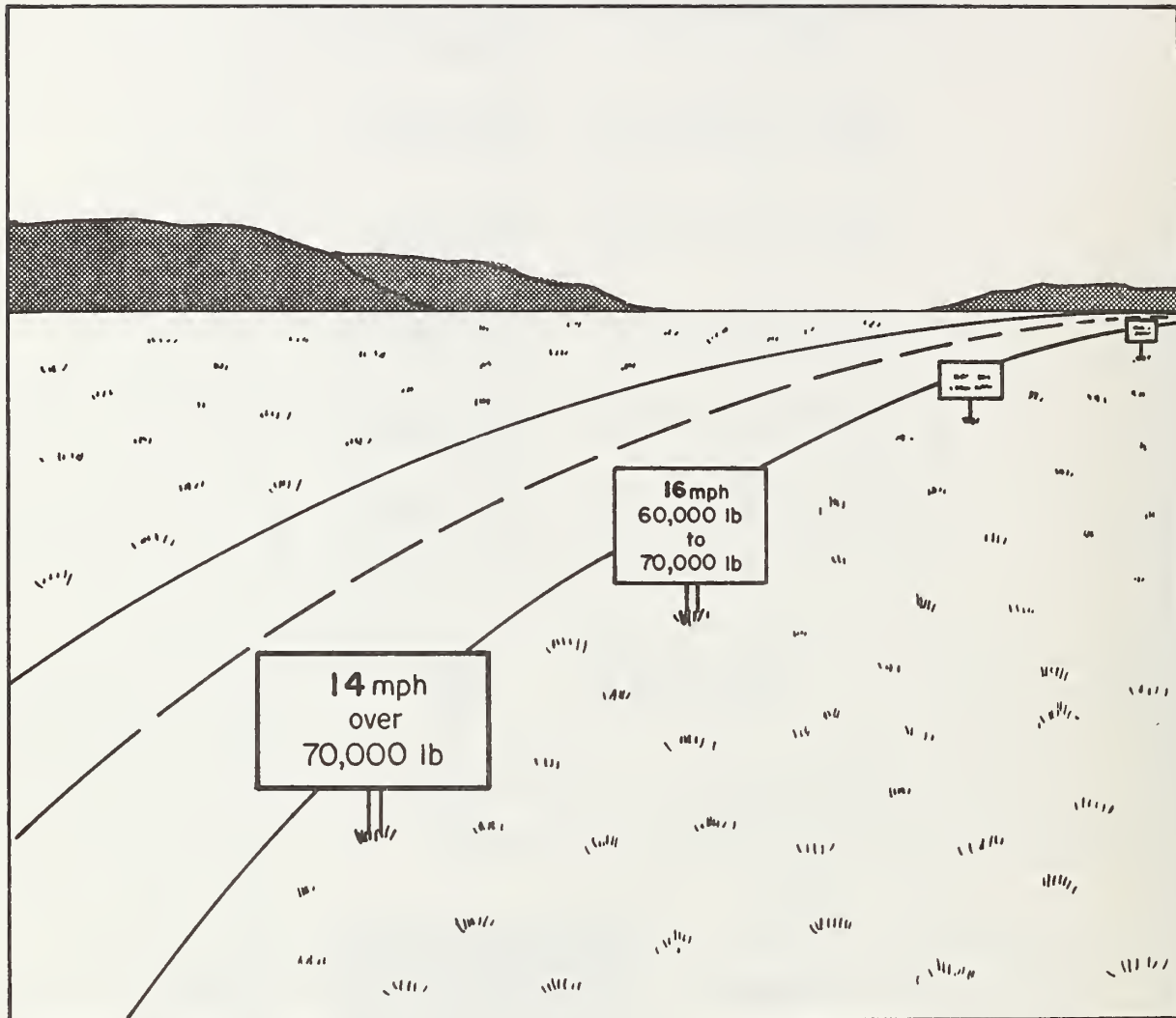


Figure 38. Progressive (Burma-Shave) WSS Signs

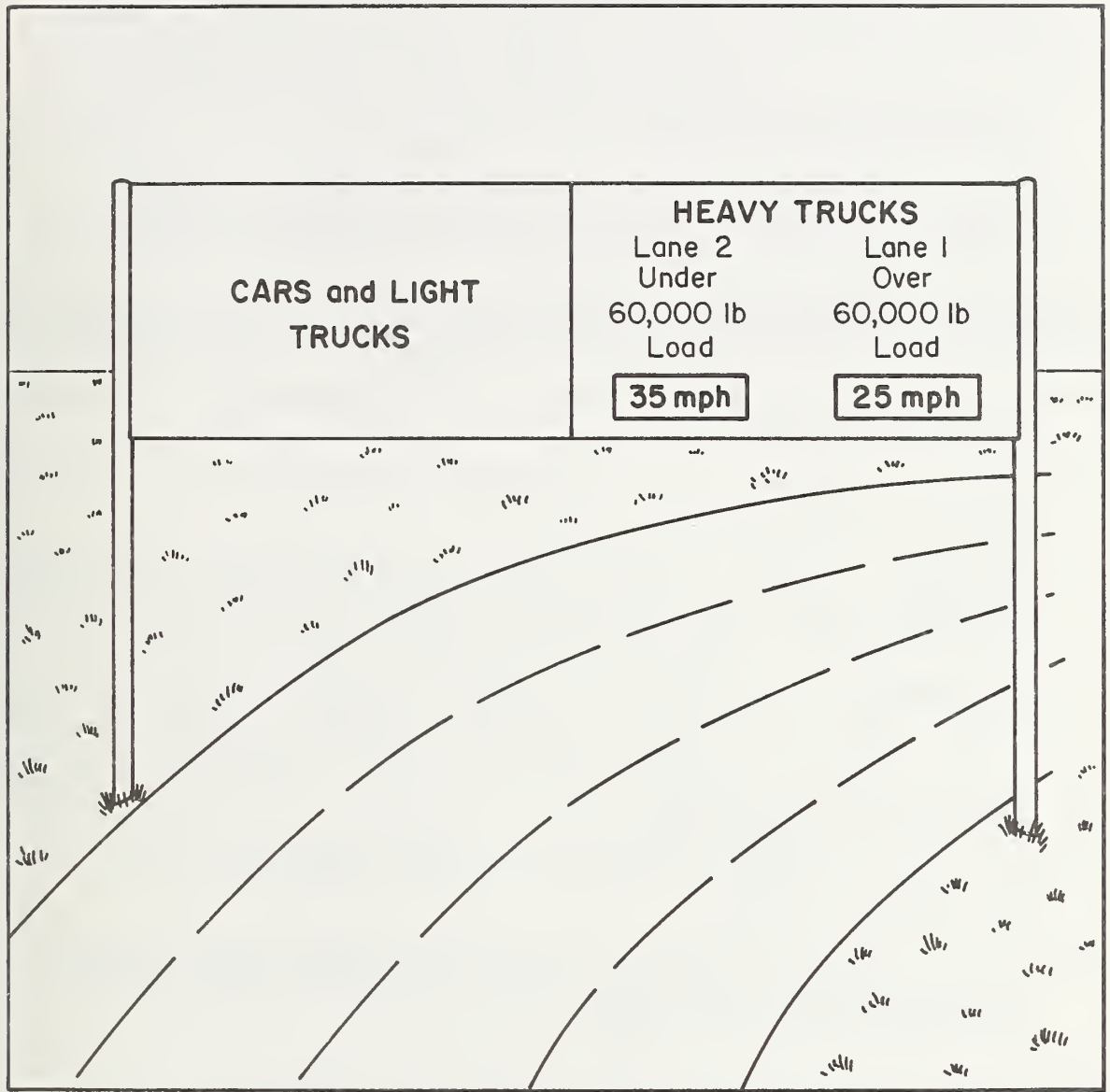


Figure 39. WSS Signs for Multilane Highway

REFERENCES

1. "Grade Severity Rating Systems," Federal Highway Administration, Contract DOT-FH-11-0253, Apr. 1977.
2. "Contract DOT-FH-11-0253 Request for Change of Scope to Develop a Prototype Grade Severity Rating System and Document Results," Systems Technology, Inc. ltr., Ref. S.O. 1106/LP-270, 10 Apr. 1977.
3. "Evaluation of Techniques to Counter Truck Accidents on Steep Downgrades," Federal Highway Administration, Contract DOT-FH-11-9356, 30 Sept. 1977.
4. Hykes, Paul G., "Truck Downhill Control Prediction Procedure," SAE Paper No. 630A, Jan. 1963.
5. Lill, Richard A., "Development of Grade Severity Rating System," American Trucking Associations, Dec. 1975.
6. Lill, Richard A., "Review of BMCS Analysis and Summary of Accident Investigations, 1973-1976 With Respect to Downgrade Runaway Type Accidents," American Trucking Associations, Inc., Memorandum, 13 Sept. 1977.
7. Limpert, Rudolf, "An Investigation of Integrated Retarder/Foundation Brakes Systems for Commercial Vehicles," SAE Paper 750126, Feb. 1975.
8. "Air Brake Systems — Trucks, Buses, and Trailers," Federal Motor Vehicle Safety Std. No. 121, 1975.
9. "Truck Ability Prediction Procedure," SAE J688, SAE Handbook, 1977, pp. 37.02 to 37.04.
10. Steers, L. L., and L. C. Montoya, Study of Aerodynamic Drag Reduction on a Full-Scale Tractor-Trailer, Transportation Systems Center, DOT-TSC-OST-76-13, Apr. 1976.
11. Horsepower Considerations for Trucks and Truck Combinations, Western Highway Institute, Research Comm. Rept. No. 2, Oct 1969.
12. "Williams 318A Tractor Protection Valve Instructions," Williams Air Controls Corp.
13. "The All-Air Disc Brake: Will It Take Over?" Heavy Duty Trucking, Vol. 55, No. 12, Dec. 1976, pp. 36-38.
14. Murphy, Ray W., Rudolf Limpert, and Leonard Segel, Bus, Truck, Tractor/Trailer Braking System Performance, Univ. of Michigan, HSRI-70-101 (PF-101), Mar. 1971.

15. Limpert, Rudolf, "An Investigation of the Brake Force Distribution on Tractor Semitrailer Combinations," SAE Paper 710044, Jan. 1971.
16. Fisher, D. K., "Brake System Component Dynamic Performance Measurement and Analysis," in 1970 International Automobile Safety Conference Compendium, New York, SAE, 1970, pp. 265-287.
17. Mathews, G. P., Art and Science of Braking Heavy Duty Vehicles, SAE SP-251, Jan. 1964.
18. Post, Thomas W., Paul S. Fancher, and James E. Bernard, "Torque Characteristics of Commercial Vehicle Brakes," SAE Paper 750210, Feb. 1975.
19. Winkler, C., et al., Predicting the Braking Performance of Trucks and Tractor-Trailers, Phase III, Tech. Rpt. UM-HSRI-76-26-1, 15 June 1976.
20. "Remember Speed Retarders?" Heavy Duty Trucking, Vol. 55, No. 4, Apr. 1976, pp. 48-52, 54.
21. "The Jacobs Engine Brake," Jacobs Mfg. Co., Jan. 1977.
22. "Jacobs Engine Brake Drivers Manual," Jacobs Mfg. Co., Oct. 1976.
23. "Strong and Silent; Williams Air Control," Weatherhead Company, Feb. 1977.
24. Witconis, Leon, "Baby Your Brake with a Retarder," Owner-Operator, Sept./Oct. 1975, pp. 30-34.
25. "Caterpillar Brake Saver," Caterpillar Tractor Company.
26. Fitch, James William, Motor Truck Engineering Handbook, 1976.
27. "The New Jacobs Electric Retarder," The Jacobs Mfg. Co., Mar. 1977.
28. "Survey of Grades in the United States," transmitted to STI by FHWA, 28 Feb. 1978.
29. "List of Hazardous Hills," Pennsylvania Motor Truck Association.
30. "Grades, Summits and Passes; State Highway System," State of California, Div. of Highways Map.
31. "Grade Data," transmitted to STI by Western Highway Institute, Jan. 1978.
32. Boyce, Wm. E., and Richard C. Di Prima, Elementary Differential Equations and Boundary Value Problems, N.Y., London, 1969.
33. Limpert, Rudolf, "Cooling Analysis of Disc Brake Rotors," SAE Paper 751014, Nov. 1975.
34. McRuer, Duane, Irving Ashkenas, and Dunstan Graham, Aircraft Dynamics and Automatic Control, Princeton University Press, 1973.

35. Eckert, E R. G., and Robert M. Drake, Jr., Heat and Mass Transfer, New York, McGraw-Hill, 1959.
36. Limpert, Rudolf, "The Thermal Performance of Automotive Disk Brakes," SAE Paper No. 750873, Oct. 1975.
37. Letter from Paul G. Hykes, American Trucking Associations, Inc., to Walter Johnson, STI, transmitting simplified procedure for determining brake torque balance at low levels of brake application pressure, 22 June 1977.
38. Walston, William H., Jr., Frank T. Buckley, Jr., and Colin H. Marks, "Test Procedures for the Evaluation of Aerodynamic Drag on Full-Scale Vehicles in Windy Environments," SAE Paper 760106, Feb. 1976.

APPENDIX A

DERIVATION OF THE BRAKE TEMPERATURE EQUATION

The distribution of temperature in space and time for any isolated system is governed by the heat conduction equation, Ref. 35.

$$\frac{Q'}{\rho c} + \alpha \nabla^2 T = \frac{\partial T}{\partial t} \quad (\text{A-1})$$

subject to the boundary conditions

$$-\kappa \nabla T = q \quad (\text{A-2})$$

where the thermal diffusivity, $\alpha = \kappa/\rho c$. To particularize the general boundary value problem for our purpose, the boundary conditions must be written for a brake. This is quite difficult because of the complex geometry of the brake components. The problem has been approached using finite element methods but only after simplifying the geometry, Ref. 36. However, for our purpose it is better to make several conventional assumptions to simplify the analysis.

1. The heat generated in braking is absorbed by the brake drums as a uniform heat flux over the rubbing surface. The thermal gradients in the linings are roughly comparable to those in the drums; however, the iron drums have a much higher thermal conductivity than the linings. Thus most of the heat (typically about 95 percent, Ref. 14) flows into the drums. Since the entire drum rubbing surface continuously moves over the lining blocks, the heat flux distribution is fairly uniform over the drum rubbing surface.
2. All heat is transferred out of the drum by convective heat transfer at the outer surface of the drum flange. Reference 33 indicates that in the operating temperature range of drum brakes, most of the heat transfer is due to convection. The convective heat transfer flux is proportional to the temperature difference between the drum outer surface and the ambient air.

3. Since the drums have large radius compared to their thickness, the drum may be approximated as a flat, infinite, uniformly heated strip.

Under these assumptions the isolated system to be analyzed is the "unrolled" brake drum flange shown below with the system boundary outlined by the dashed line.

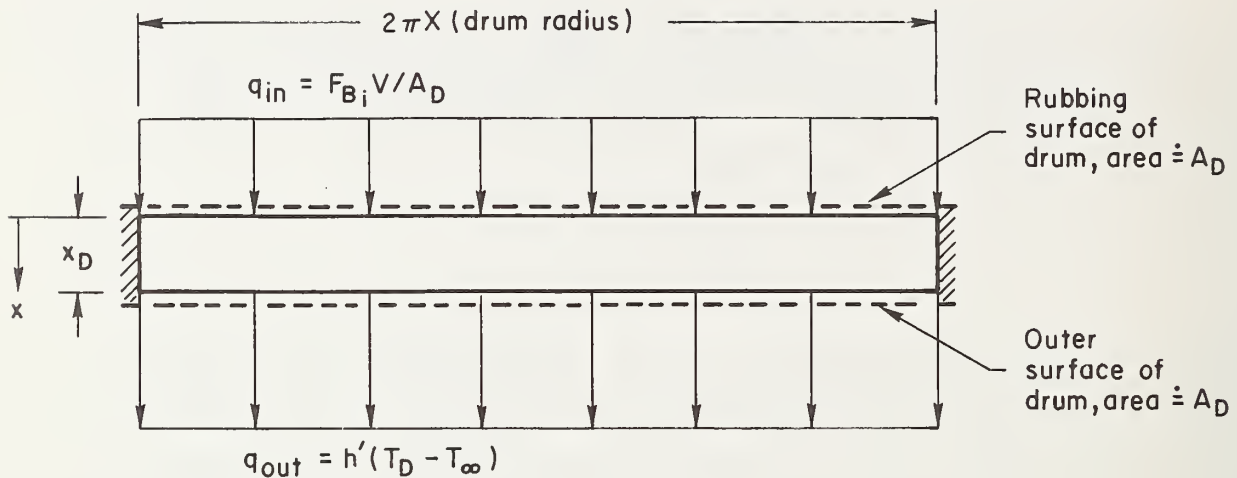


Figure A-1. Heat Transfer Through the Unrolled Brake Drum Flange

In this flat strip the heat flows normal to the rubbing surface (i.e., in the x direction). There are no heat sources within the system (brake drum) and thus $Q' = 0$. The heat conduction equation thus reduces to

$$\alpha \frac{\partial^2 T}{\partial x^2} (x,t) = \frac{\partial T}{\partial t} (x,t) \quad 0 < x < x_D \quad (A-3)$$

The boundary condition at the rubbing surface reduces to

$$\kappa \frac{\partial T}{\partial x} (0,t) = -F_{B_i} \frac{V}{A_D} \quad (A-4)$$

where $F_{B_i} V$ is the portion of the total braking power generated by the brake in question. The boundary condition at the drum outer surface reduces to

The second partial with respect to x in Eq. A-3 can be approximated in terms of the known boundary conditions as

$$\begin{aligned} \frac{\partial^2 T}{\partial x^2} & \doteq \frac{\frac{\partial T}{\partial x}(X_D, t) - \frac{\partial T}{\partial x}(0, t)}{X_D} \\ & = \frac{-h'(T_D - T_\infty) + F_{B_i} \frac{V}{A_D}}{X_D \kappa} \end{aligned} \quad (A-6)$$

This is equivalent to approximating the temperature profiles by straight lines as suggested by the dashed lines in Fig. A-2. It can be seen that the relative errors decrease with time to zero in the steady state. As a practical matter in using the Truck Downgrade Braking Model in field testing, T_D will not be known. Rather some temperature in the lining will be measured by a thermocouple and used as T . If the quantity $T_D - T_\infty$ is assumed proportional to $T - T_\infty$, the error will be comparable to that for the straight line approximation of the temperature profiles. Thus

$$h'(T_D - T_\infty) = h(T - T_\infty) \quad (A-7)$$

where h is the effective heat transfer coefficient incorporating the temperature proportionality constant. The heat conduction equation, Eq. A-3, now reduces to an ordinary differential equation

$$\frac{\alpha}{\kappa X_D} \left[\frac{F_{B_i} V}{A_D} - h(T_D - T_\infty) \right] = \frac{dT}{dt} \quad (A-8)$$

Noting that $A_D X_D \kappa / \alpha = A_D X_D \rho C = m_D C$, this equation may be written as

$$m_D C \frac{dT}{dt} = F_{B_i} V - h A_D (T - T_\infty) \quad (A-9)$$

Since the quantity $m_D c T$ represents the internal heat energy stored in the brake drum, this differential equation can be given the following physical interpretation

$$\left(\begin{array}{c} \text{rate of change} \\ \text{of internal} \\ \text{energy in} \\ \text{brake} \end{array} \right) = \left(\begin{array}{c} \text{rate mechanical energy} \\ \text{is converted to} \\ \text{thermal energy} \\ \text{by brake} \end{array} \right) - \left(\begin{array}{c} \text{rate of heat} \\ \text{transfer out} \\ \text{of brake} \end{array} \right) \quad (\text{A-10})$$

This statement of the gross energy transfer in the brake could have been taken as the starting point for deriving Eq. A-9. However, beginning with the completely general heat conduction equation (A-1) allows us to examine the approximations inherent in the lumped parameter model. In particular we can expect some error in predicting the initial transient temperature due to linearization of the temperature profile through the drum and the use of a thermocouple in the lining.

Equation A-9 when combined with the initial condition $T(0) = T_0$ forms a very simple initial value problem for the case of a steady grade descent. Equation A-9 is a first order linear differential equation with constant coefficients in which the power input, $F_{B_1} V$, is the forcing function. This equation can be integrated by standard techniques, Ref. 32, to yield an equation for brake temperature

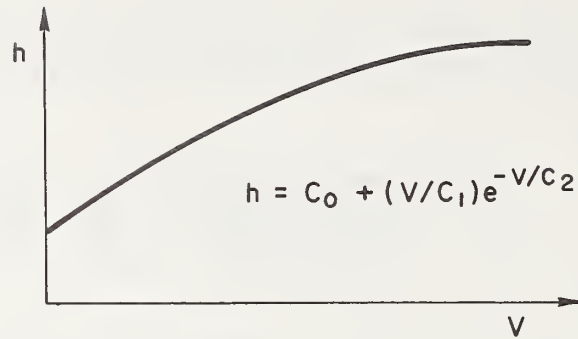
$$T = T_0 e^{-K_1 t} + (T_\infty + K_2 F_{B_1} V)(1 - e^{-K_1 t}) \quad (\text{A-11})$$

where $K_1 = hA_D/m_D c$ and $K_2 = 1/hA_D^*$. Since in a steady grade descent $t = x/V$, this equation may also be written as

$$T = T_0 e^{-K_1 x/V} + (T_\infty + K_2 F_{B_1} V)(1 - e^{-K_1 x/V}) \quad (\text{A-12})$$

It should be noted that the convective heat transfer coefficient, h , (and hence K_1 and K_2) is a function of speed. Reference 33 gives an empirical formula for h .

*The definitions of K_1 and K_2 given here are, strictly speaking, different than used elsewhere in this report in that they are referenced to the drum and speed in feet per second, however they are conceptually the same as defined in Eq. 13.



Equation A-12 gives the temperature of a single brake; however, what is really desired is an overall brake temperature for the whole truck. In general the temperature response will not be the same for all brakes. In fact, field test experience has revealed that there can be temperature differences of hundreds of degrees among the brakes on a given truck during a grade descent. These differences could arise from brake-to-brake differences in thermal parameters (h , A_D , etc.), i.e., "thermal imbalance". However, it appears that the most common cause of differences in brake temperature is a lack of force balance in the brake system. That is, the braking effort is not evenly divided among the brakes. The average brake temperature may be found by averaging Eq. A-12 over all n brakes under the assumption that the thermal parameters are the same for all brakes.

$$\frac{\sum_{i=1}^n T_i}{n} = \frac{\sum_{i=1}^n \left[T_0 e^{-K_1 x/V} + (T_\infty + K_2 F_{B_i} V)(1 - e^{-K_1 x/V}) \right]}{n} \quad (\text{A-14})$$

which reduces to

$$T = T_0 e^{-K_1 x/V} + (T_\infty + K_2 F_B V)(1 - e^{-K_1 x/V}) \quad (\text{A-15})$$

where T is the average brake temperature and $F_B V$ is the total brake power absorption

$$F_B V = V \sum_{i=1}^n F_{B_i} \quad (\text{A-16})$$

APPENDIX B

FIELD TEST PROGRAM

FIELD TEST PREPARATIONS

Test Vehicle

The primary test vehicle (No. 1) was a fully instrumented 3-S2 tractor/semitrailer combination which was used in both the Phase I and Phase II tests. Specifications are given in Table B-1. Test Vehicle No. 1 was tested at 75,500 lb GCW (35,100 kg).

Instrumentation

The instrumentation system used in Test Vehicle No. 1 consisted of sensors, thermocouple reference junctions, switches, a signal conditioning unit, a chart recorder, and power supplies (see Fig. B-1). The quantities measured and the instruments or sensors used were:

<u>Measured Quantity</u>	<u>Instrument or Sensor</u>
1. Brake temperature (each brake)	Thermocouple
2. Vehicle speed	Fifth wheel
3. Engine speed	Tachometer generator
4. Brake application pressure	Electrical pressure transducer
5. Trailer brake pressure	Electrical pressure transducer
6. Ambient temperature	Bulb thermometer
7. Ambient wind velocity	Hand-held wind meter

The first four quantities were recorded automatically on a chart recorder. Since only eight channels were available on the recorder, only five temperature signals (from the five left or five right brakes) were recorded at one time. Switching from left to right thermocouples was accomplished by use of a five pole switch. The trailer brake pressure signal was recorded in place of the engine speed during a few tests.

TABLE B-1

PRIMARY TEST VEHICLE SPECIFICATIONS

Tractor

Make: Ford
Year: 1977
Model: WT9000
Type: Cab over engine (no sleeper)
Wheelbase: 142 inches
Engine: Detroit Diesel V6 2 cycle diesel, Model 6V-92
270 hp
Retarder: Jacobs engine brake, 6V-92, 2 position (one or
both cylinder banks)
Transmission: Fuller 9 speed manual, RT-9509A
Rear Axle: Dual tandem, Rockwell 38SQHD (3.70 ratio)
Service Brakes: Rockwell S-cam, 17 in. diameter drums
Antiskid System: Kelsey-Hayes
Tires: Goodyear Super Hi Miler 10.00-20, load range F

Trailer

Make: Fruehauf
Year: 1977
Model: FB9-F2-45
Type: Van
Size: 8 ft x 45 ft
Axles: Tandem bogie
Brakes: S-cam, 16 in. diameter drums, Carlisle MMD39
linings (SAE EE)
Antiskid System: Kelsey-Hayes Bogie Control
Tires: 10-22, load range F

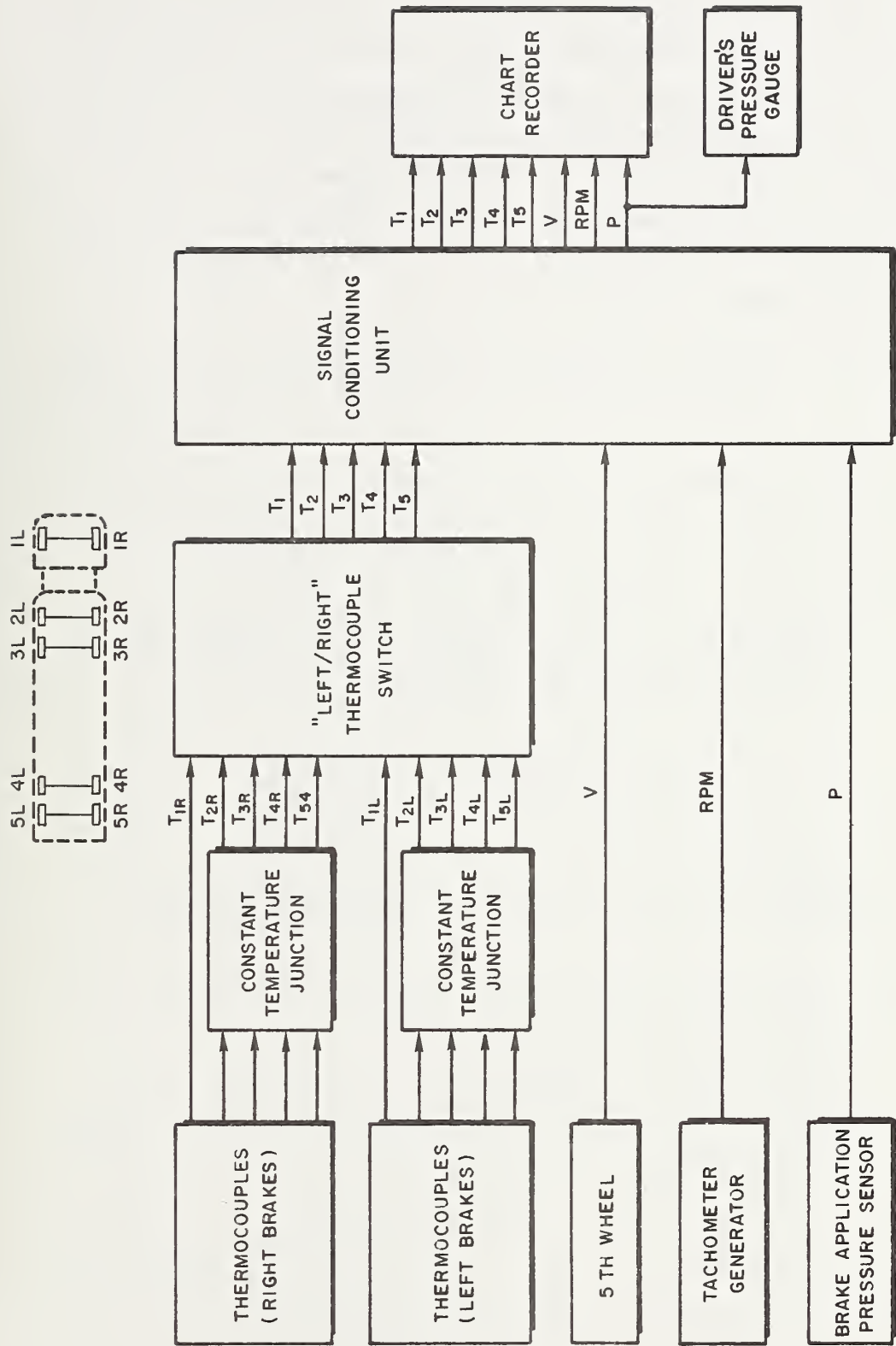


Figure B-1. Instrumentation System Used in Test Vehicle No. 1

The measurement of temperature via thermocouples requires that the temperature of one junction (the "cold" junction) be known. This junction is often left at ambient temperature, but for convenience and increased accuracy, the cold junction can be placed in a "thermocouple reference junction," an electrically controlled device that maintains the cold junction at a pre-set temperature [150 °F (66 °C)]. For this program eight of these devices were available and were used on all but the front tractor brake channels. The cold junctions of the front brake channels were at the (measured) ambient temperature.

The signals from five thermocouple channels plus the vehicle speed, engine speed, and brake application pressure were fed to a signal conditioning unit. This unit filters high-frequency noise from the sensor signals and amplifies them to the proper voltage levels for input to the chart recorder. The conditioned signals were then fed to the chart recorder.

Components of the instrumentation system included:

1. Thermocouple: Iron-constantan J, $32\mu\text{V}/^\circ\text{F}$ nominal sensitivity, one mounted in lining of leading shoe of each brake per SAE J786 recommended practice.
2. Fifth wheel: Tracktest Serial Number 1353, mounted on rear of trailer landing gear.
3. Tachometer generator: Servo Tek, Type 757B-1, 20.6 V/1000 rpm, mounted in tractor tachometer cable.
4. Application pressure sensor: Bourns No. 2005562002, 0-125 psig, mounted in treadle valve control output line.
5. Constant temperature junction: PACE Wiancko, Model LRJR49-8TT, mounted in tractor cab.
6. Chart recorder: MFE Model 28, 8 channel, mounted in tractor cab.
7. Power supply: Powermate 12 V, 500 watt inverter, mounted in tractor cab.
8. Wind velocity meter: Dwyer Portable Wind Meter, 2-66 mph, hand held.
9. Bulb thermometer: Mounted in tractor cab.

All sensors and instruments were precalibrated, and no recalibration of individual sensors was required except for checking the thermocouple sensitivity. The primary task in calibrating the total instrument system was to set the desired scale factors (number of units of each measured quantity to produce full-scale deflection of chart recorder pen) by adjusting gains in the signal conditioning unit and chart recorder. The vehicle and engine speed channels were calibrated on the basis of the known transducer gains. The thermocouple channels were calibrated by immersing a test thermocouple in a boiling water bath. The brake pressure channels were calibrated with pressure gauges mounted near the pressure transducers. Calibrations were repeated as necessary throughout the test program to correct for recorder drift and nonlinearities.

Test Vehicle No. 2 was not instrumented, but temperature measurements were made on the brake drums after each test run using a portable pyrometer temperature probe. A comparison of temperatures measured using the portable probe with those measured via the installed thermocouples in Test Vehicle No. 1 is shown in Fig. B-2. The results indicate that the portable probe measurements are about 60° F (16° C) lower than the thermocouple readings.

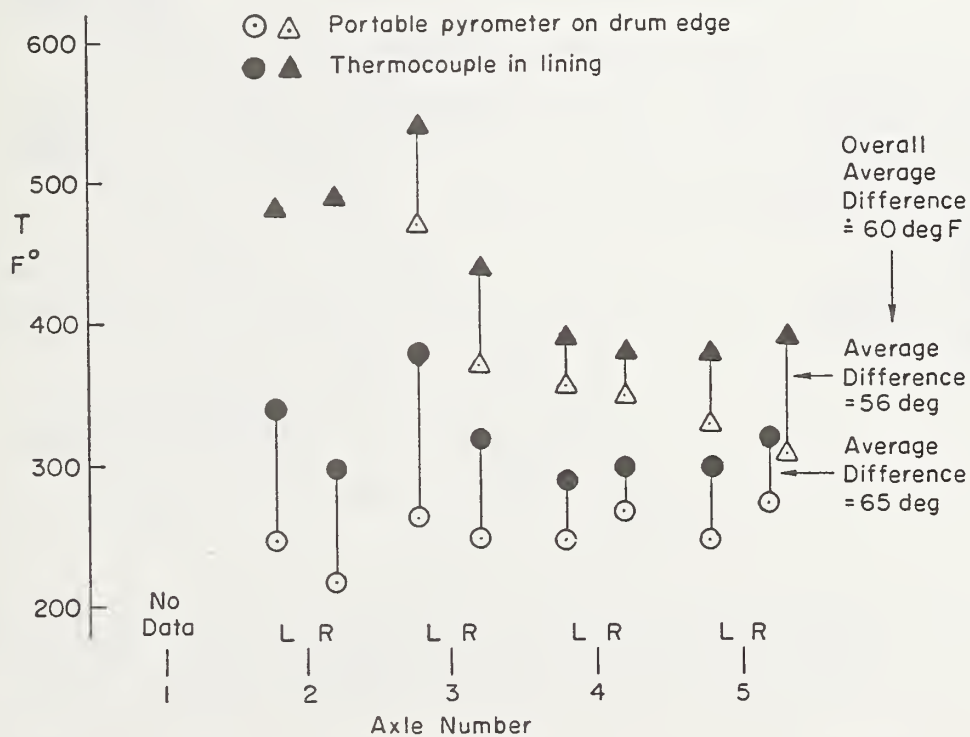


Figure B-2. Comparison of Thermocouple and Portable Pyrometer Readings

Test Vehicle Preparation

In addition to the installation and calibration of instruments, two additional procedures were required on Test Vehicle No. 1 before testing could begin to insure that accurate, repeatable data would be generated in the test program (in particular in the Phase I tests). These consisted of:

- Burnishing the brakes
- Balancing the brake forces

The brake burnish procedure was required because the test tractor and trailer were new. New brakes must undergo many brake application cycles before wear and heating effects cause the brake system to reach a steady state in which a given application pressure and brake temperature result in a unique, repeatable braking force. This effect is shown in Fig. B-3 for a typical 3-S2 vehicle. It can be seen that effectiveness changes of

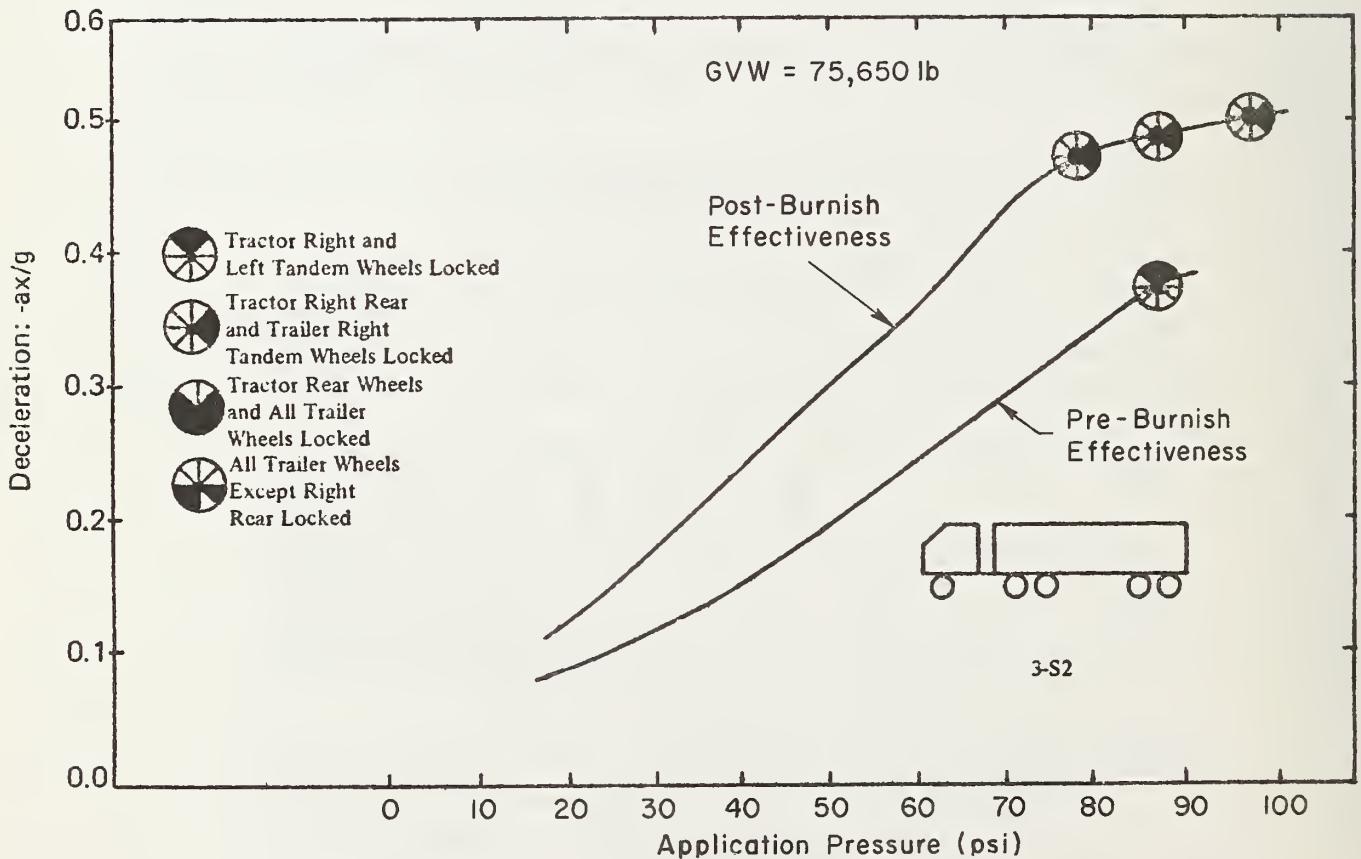


Figure B-3. Effect of Brake Burnishing on Brake Effectiveness (From Murphy Ref. 14)

up to 30 percent occur over the burnish period. While such changes are not of great practical concern to a truck operator (the driver simply controls pressure "closed loop" to obtain the needed deceleration), they would prevent the measurement of accurate, repeatable data. Accordingly, it was considered mandatory in this program to conduct the tests with the brakes properly burnished.

As envisioned in the Phase I Test Plan, a brake force balance test would be performed immediately following the completion of the brake burnish. Brake balance essentially requires that the brake force be distributed among the axles in proportion to the axle loads. A serious force imbalance could result in a large temperature imbalance in the downhill tests and greatly complicate the test program. The brake balance procedure of SAE J880 is commonly used; however, it is conducted at a relatively high brake pressure [42 psi (1549 N/m^2)], whereas during hill descents pressures are usually below 10 psi (368.9 N/m^2). As noted by Hykes, Ref. 37, it is not uncommon to have tractor/trailer balance at 42 psi and to have serious imbalance at 10 psi due to brake system component nonlinearities and incompatibilities between tractors and trailers. Thus it was planned to conduct balance tests at both 10 and 42 psi.

Since problems with brake imbalance between tractors and trailers are common, provision was made for adjusting the brake force distribution. This was done by installing a Williams Air Controls 318A adjustable tractor protection valve which allowed the trailer brake line pressure to be increased or decreased with respect to the tractor line pressure.

After instrumentation checkout and calibration were completed, Test Vehicle No. 1 was driven to the level road test site and brake burnish was begun. In three days 200 burnish runs had been made. The test plan had called for monitoring the change in brake effectiveness (measured by the parameter a_x/P) during the burnish, and terminating the burnish when the brake effectiveness reached a steady-state value (after at least 200 snubs). As can be seen from Fig. B-4, there was no discernible change in a_x/P through 200 snubs, indicating this parameter to be an insensitive measure of the state of brake burnish. In addition, large temperature differences existed

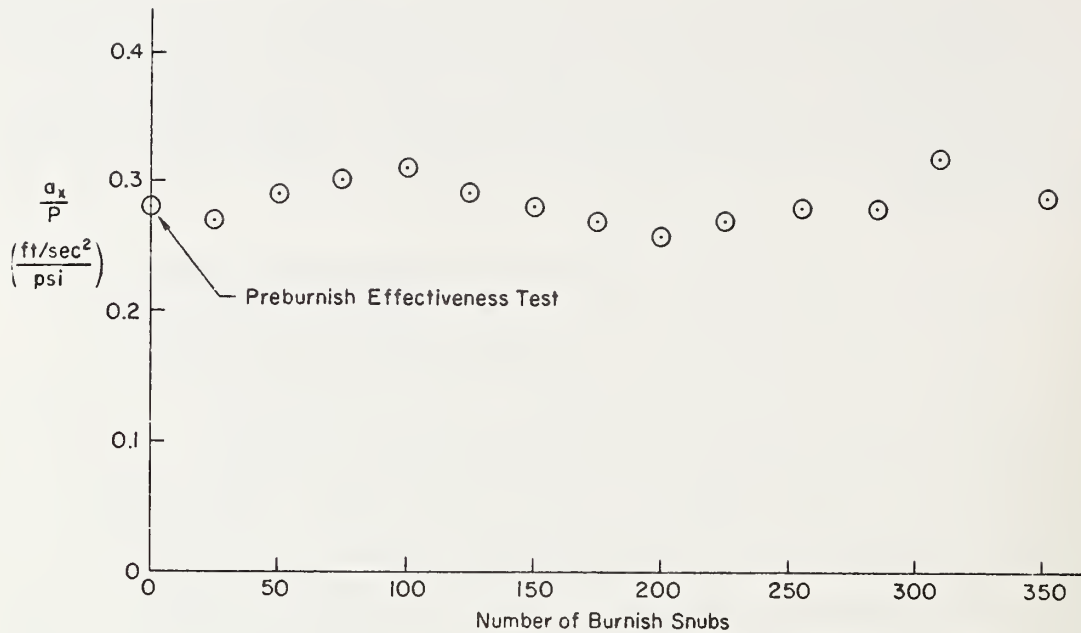
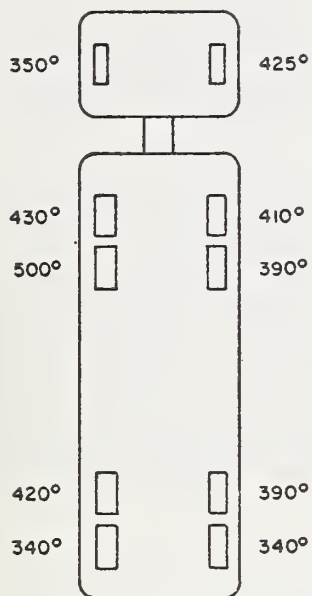


Figure B-4. Variation of Brake Effectiveness During Burnish

among the axles and also between left and right brakes on a single axle; therefore, it was decided to continue the burnish. After 350 snubs the large temperature differences remained (Fig. B-5), indicating that the test truck had significant brake imbalance and a preliminary attempt should be made to correct it. The tractor protection valve was adjusted and additional burnish snubs were run as a check in an attempt to equalize the temperatures between the tractor and trailer. After four adjustment trials, a setting was reached which increased the trailer brake temperatures to an average of 60° F (16° C) less than the tractor average. The brake burnish was terminated after 480 snubs.

Brake force balance was undertaken immediately following the completion of brake burnishing. A balance at 10 psi (368.9 N/m²) was sought because this was considered typical of hill descent braking. The final results indicated that the trailer was supplying slightly more braking effort than the tractor. Since the earlier balance checks based on temperature indicated that the trailer brakes averaged slightly cooler than those on the tractor, it was concluded that the tractor/trailer was



Note: Trailer brakes alone were used to raise the trailer brake temperatures just prior to this run.

Figure B-5. Temperatures After Severe Braking Following Run No. 367

essentially balanced [at 10 psi (368.9 N/m^2)] and that better cooling of the rear brakes kept their temperature low even though they did more work. As will be discussed in Section IV, when the hill descent tests began it was immediately discovered that, in spite of our 10 psi "balance," a serious imbalance still existed during actual downhill operation. This is believed to be due to significant nonlinearities in braking force at pressures around 5 psi (184 N/m^2) (which the downhill tests required).

Burnish and balance procedures are summarized as follows.

Brake Burnish Procedure
(Based on SAE J786a and J880a)

Purpose: To "run in" new brakes to insure that brake force as a function of P, V and T has reached a steady-state relationship.

Controlled and Measured Variables:

1. To be recorded on effectiveness tests and 40-0 mph stops: application pressure, velocity, rpm, and brake temperature on each axle.
2. Deceleration rate monitored with U-tube accelerometer.
3. All snubs and stops made with clutch disengaged.

Procedure: The procedure is shown in the flow chart, Fig. B-6. Completion of burnish is determined by plotting brake pressure required for the 10 ft/sec² stop against stop number. When at least 200 snubs have been made and the pressure for the 10 ft/sec² stop reaches a steady-state level, the burnish will be terminated.

Brake Force Balance Test
(Based on SAE J880a and Ref. 36)

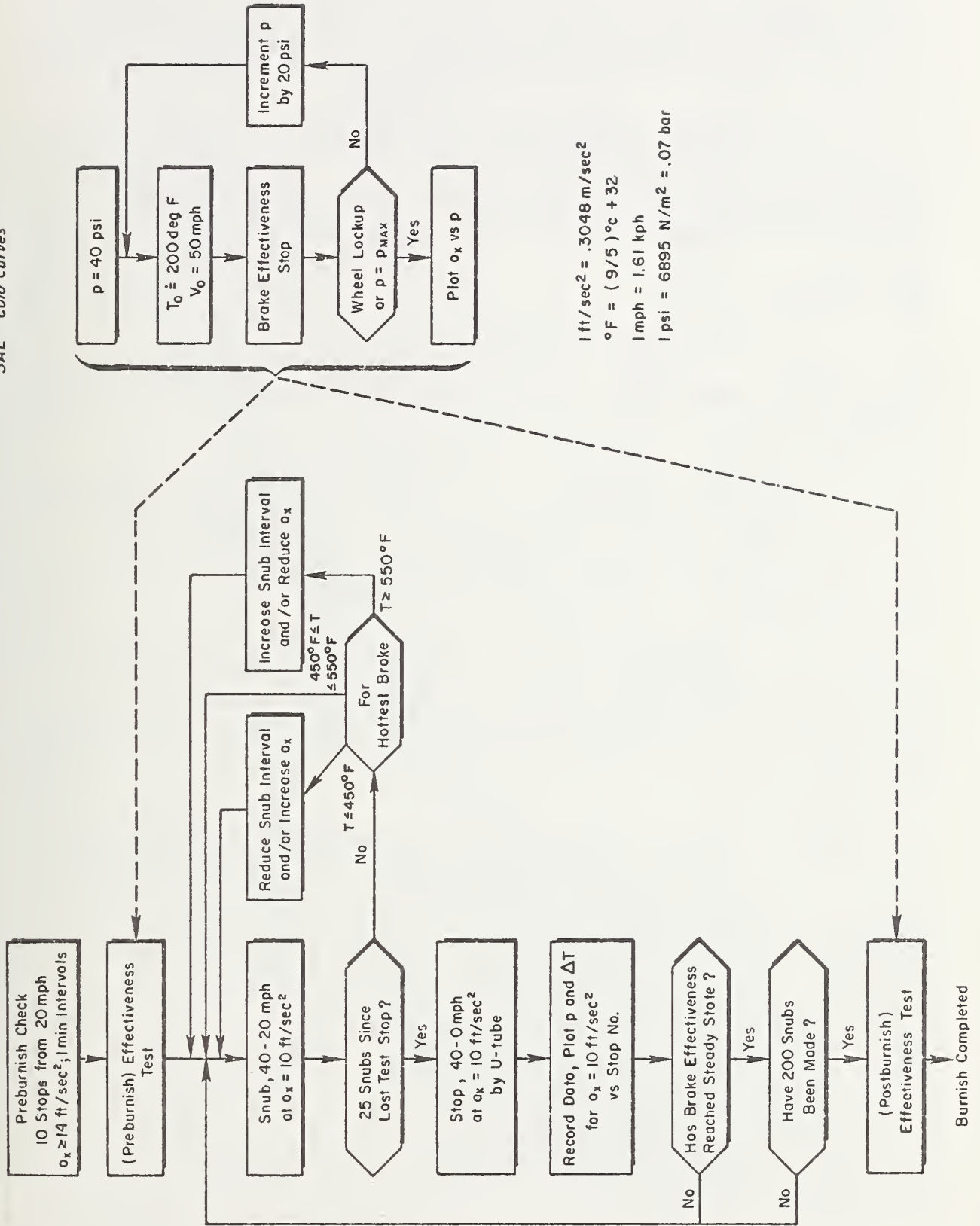
Purpose: To determine if braking effort is properly distributed between tractor and trailer.

Controlled and Measured Variables:

1. Record application pressure, velocity, rpm, and brake temperature on each axle.
2. Monitor brake pressure with application pressure gauge.

Procedure:

1. Temperature condition brakes to 150-200° F on hottest axle.
2. 3 snubs at 10 psi (all snubs are 20-10 mph, 1/4 mi intervals, clutch disengaged).
3. 3 snubs at 42 psi.
4. Manually lock spring brakes and disconnect trailer air lines.
5. 3 snubs at 10 psi.
6. 3 snubs at 42 psi.



1 ft/sec² = .3048 m/sec²
 °F = (9/5) °C + 32
 1 mph = 1.61 kph
 1 psi = 6895 N/m² = .07 bar

Figure B-6. Flow Chart of Brake Burnish Procedure

7. Reconnect trailer air lines and release spring brakes.
8. 3 snubs at 10 psi using trailer hand valve to apply only trailer brakes.
9. 3 snubs at 42 psi using trailer hand valve to apply only trailer brakes.

Data Analysis: Compute distribution of braking effort between tractor and trailer using speed traces and data from "coast-down" tests.

TEST LOCATIONS

Two types of test areas were used in the field tests. For the brake burnish, brake balance and coast-down tests, a level road area was required. This was Adobe Road, a 5 mi (8 km) section of little used paved road near Bakersfield. For the hill descent tests, fairly constant-slope grades several miles long were required. Three mountain grades along Interstate 5 between Los Angeles and Bakersfield were chosen for use in the Phase I tests (Fig. B-7), and a fourth one was used in addition during the Phase II validation tests.

Before the hill descent tests were begun, measurements of the length and steepness of each grade to be used were made using an altimeter (and confirmed with U.S. Department of Interior topographic maps). The results were:

<u>Number</u>	<u>Test Grade</u>	<u>Grade (%)</u>	<u>Length</u>
1	A section of old California 99 between Templin Highway and Pyramid Lake	5.7	3.0 mi (4.8 km)
2	"Grapevine" on I-5 North between the towns of Lebec and Grapevine	5.8	5.1 mi (8.2 km)
3	"5-mile" grade on I-5 South just above Castaic	4.6	5.4 mi (8.6 km)
4	A mountain road near the Templin Highway offramp on I-5 leading to the Castaic power station	7.1	3.2 mi (5.1 km)

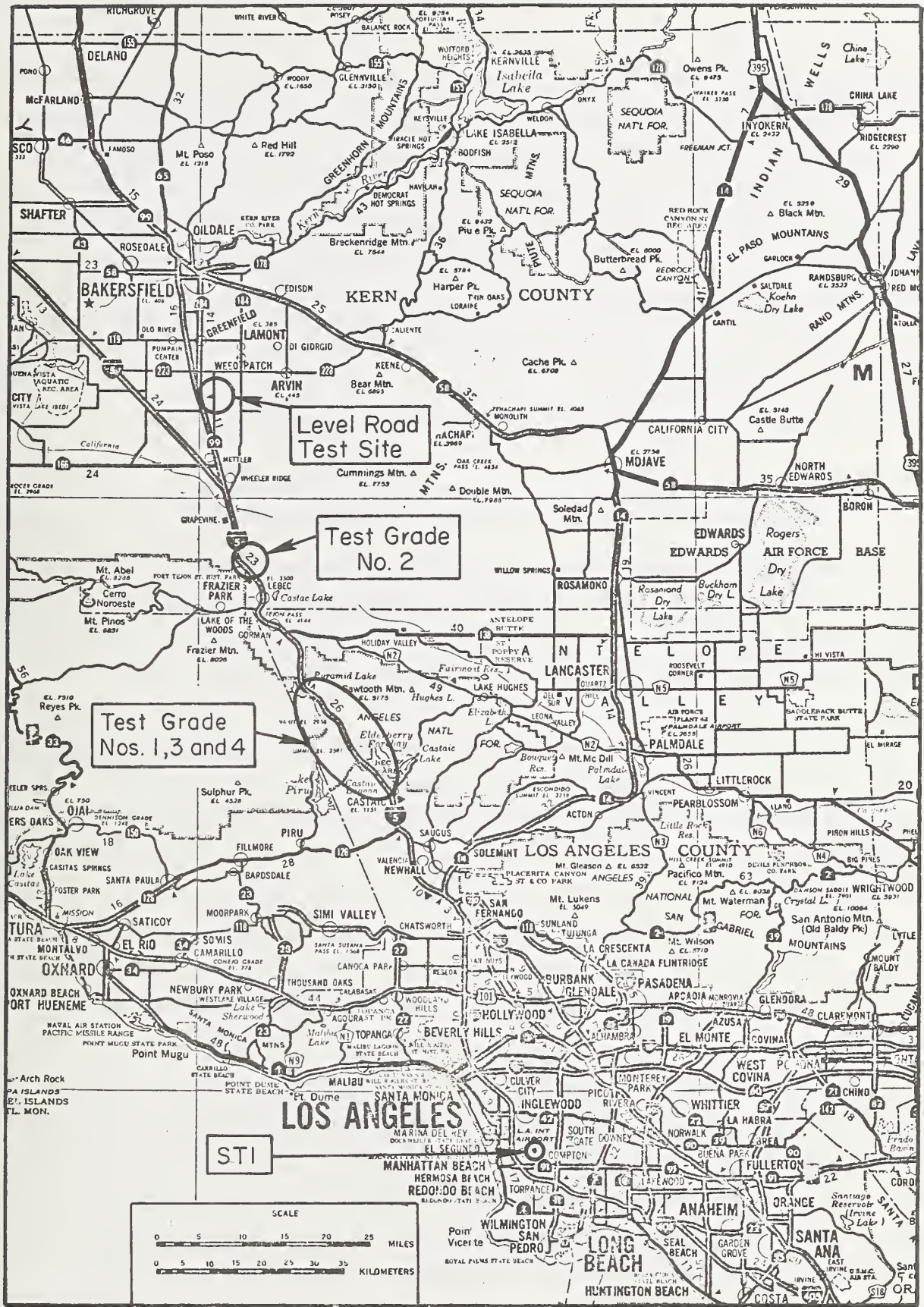


Figure B-7. Test Site Locations

TEST METHODOLOGY

The Phase I tests were conducted primarily to obtain data necessary to quantify and finalize the truck braking model on which the final Grade Severity Rating/Gear Selection Models would be based. In particular, it was desired to verify that the theoretical models were adequate, and also to obtain specific quantitative data on:

- The non-brake forces, including their variation with vehicle speed.
- The variation of braking capability with temperature (brake fade).
- Brake thermodynamic characteristics, including heat transfer coefficients and thermal time constants.

A number of full-scale test methods was available for obtaining the data desired from the Phase I tests. The final choice of methods involved factors such as economy, minimizing complexity, time constraints, accuracy requirements, and compatibility with standardized procedures. When the basic test methods had been chosen, experimental design analyses were used to establish the values of the parameters to be varied, the order of the tests, the accuracy of data measurements and other factors to optimize the test program from the standpoint of obtaining the most information within the money and time constraints. This involved extensive use of data obtained in the literature search and the then current Truck Braking model. The Truck Braking model was very useful in planning the Phase I tests; in particular, the sensitivity of the variables to be measured to the vehicle and hill parameters to be controlled in a given test were predicted by exercising the model.

The basic experimental procedure in the Phase I tests was to descend several hills at various speeds, transmission gears, and retarder settings while measuring the brake temperatures and application pressures. These tests provided verification of the basic model and specific data on the brake thermal properties. In addition, several tests were run on level ground to provide data such as that required to determine the non-brake

forces. Table B-2 gives an overview of the types of tests run and their purposes. The following is intended to give an increased understanding of why the tests were done the way they were.

TABLE B-2. TEST PROGRAM OVERVIEW

TYPE OF TEST	TEST CONDITIONS	PURPOSE OF TESTS
Coast-Down Tests	On flat ground Coast to a stop (no braking)	To determine non-brake forces as a function of speed and gear selected (e.g., rolling resistance, air drag, chassis friction, engine friction, and retarder force)
Cool-Down Tests	At constant speed (no braking)	To determine thermal time constant for brakes
Down-Hill Tests	On constant grade Use braking to maintain constant speed	To determine temperature characteristics of brakes during steady braking

Non-Brake Force Tests

The non-brake forces can be determined by one of three full-scale procedures (Ref. 38):

- Hill rolling tests
- Towing tests
- Coast-down tests

Hill rolling tests are conducted by letting the vehicle roll down a grade at its terminal velocity. This procedure has the advantage of being conducted at constant speed but requires many tests at different weight/grade combinations to define the velocity variation. Towing tests are conducted by towing the test vehicle with a second vehicle using a drawbar instrumented to measure force. The test speed is constant and can be varied easily, but the procedure is expensive and it is difficult to

obtain "noise"-free force measurements (Ref. 14). Coast-down tests are made by recording speed as the vehicle coasts on a level surface and determining drag from the slope of the velocity trace. Since the speed is not constant, the drag force includes a component due to the deceleration of rotating drive line components. This component can be accounted for, however, using available rotational inertia data (Ref. 37). Since this test has the advantage of simplicity and the ability to define drag forces over the entire speed range in one or two test runs, the coast-down procedure was used.

Stopping Capability Tests

The variation of stopping capability with brake temperature is usually determined by making a series of stops on level ground under controlled conditions. While the certification of vehicles for conformance to FMVSS 121 requires the measurement of both deceleration rates and stopping distances, for the purpose of this project deceleration rate is an adequate measure of braking effect, since stopping distance can be computed from a knowledge of the deceleration time history. Furthermore, the FMVSS 121 stopping distance requirements are very nearly equivalent to a constant deceleration capability at all speeds. Deceleration can be determined quickly and simply from the slope of recorded velocity traces and can be controlled by reference to simple cab-mounted instrumentation (e.g., a U-tube accelerometer).

Since it is neither necessary nor desirable to perform stopping tests at the high speeds and deceleration levels used in the FMVSS 121 procedures, the stopping capability test used in this program was essentially the SAE J786 Fade Test. In this test repeated 40-20 mph snubs are made at $a_x = -10 \text{ ft/sec}^2$ (-3 m/sec^2) until an appreciable increase in brake application pressure is required. Pre-heating the brakes by making hill descents prior to the fade tests can be used to overcome the practical problem encountered by Murphy (Ref. 14) in his tests where because of the long time required for the heavily loaded truck to accelerate it was impossible to heat the brakes sufficiently to produce fade.

Brake Heat Transfer Tests

The effective brake heat transfer properties were determined from "cool down" tests. In these tests the brakes were first heated by repeated snubs and the vehicle was then driven at constant speed while temperatures were recorded as the brakes cooled. The tests were performed at several speeds, including zero, to define speed effects on heat transfer.

Hill Descent Tests

The primary consideration in designing the hill descent tests was to decide how the several variables involved would be controlled. The test procedure adopted for the Phase I program is analogous to the technique recommended and used in long haul trucking, i.e., maintenance of a constant descent speed by the driver's modulation of brake pressure. From a "data gathering" standpoint, a constant speed descent is highly desirable because, for a given truck and load, the non-brake force is constant, and hence the required brake force is constant. This brake force can be determined from the steepness of the grade, and the non-brake force (determined from the coast-down tests). This greatly simplifies data analysis and allows a considerable amount of information to be extracted from the hill descent tests as will be seen shortly.

The design of the hill descent tests was the most complex experimental design problem. Perhaps the most convenient way of looking at the problem is to consider the "temperature time history" during a constant-speed hill descent. Such a time history can be predicted from the brake temperature equation (Eq. 5 in Section II).

$$T = T_0 e^{-(hA_c/mBC)t} + \left(T_\infty + \frac{F_B V}{hA_c} \right) \left(1 - e^{-(hA_c/mBC)t} \right) \quad (B-1)$$

The brake force is given by Eq. 12.

$$F_B = W\theta - F_{NB} = W\theta - f(W, V, F_{eng}) \quad (B-2)$$

Thus, for a constant speed hill descent, the required braking force and the power which must be absorbed by the brakes, $F_B V$, are both constant. Furthermore, since the heat transfer coefficient, h , is a function of speed only, the temperature time history is uniquely dependent on F_B and V for a given truck and will have the general character shown in Fig. B-8.

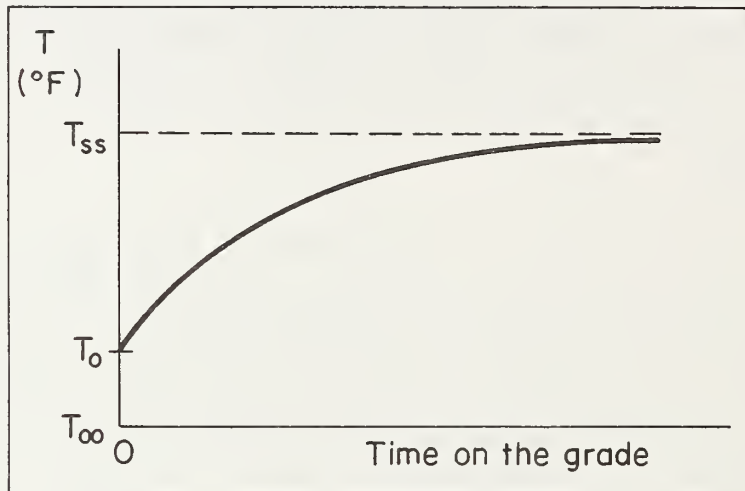


Figure B-8. Sketch of Typical Temperature Time History

Thus, the basic test plan was to conduct descent tests for a number of F_B values for each of several speeds. However, for a given V there are many (infinite) combinations of W , θ , and F_{eng} which will produce the same F_B , and thus the same temperature time history. Conversely, it is possible to use one parameter, such as the engine brake (retarder) setting, to simulate a change in the other two parameters. This might be done to simulate a change in W for a test on a given grade. This is a valuable technique for speeding up testing since engine braking can be changed "at the flip of a switch," whereas changing a load can take most of the day.

TEST PROCEDURES

Coast-Down Test

Purpose: To determine the sum of the "drag" forces on the test vehicle (i.e., rolling resistance, chassis friction, aerodynamic drag, and engine braking) as a function of W and V .

Controlled and Measured Variables: Measure and record speed, rpm, ambient temperature and wind velocity.

Procedure: For each test weight, on the level road test facility,

1. Accelerate to the test speed ($V = 50$ mph).
2. Disengage clutch and idle engine (note change for engine braking test).
3. Allow vehicle to coast to a stop.
4. Repeat steps 1-3 in opposite direction.

Data Analysis:

1. Average velocity traces from all runs at each vehicle weight.
2. Determine a_x from the slope of the averaged velocity trace and plot versus velocity.
3. Correct a_x for inertial resistance.
4. Compute $F_{NB} = (W/g) \times (\text{Corrected } a_x)$ and plot versus V for each test W .
5. Compare results to SAE J688 curves

Cool-Down Test

Purpose: To determine effective total heat transfer coefficient, hA_c , as a function of speed.

Controlled and Measured Variables: Measure and record speed, rpm, application pressure, brake temperature, ambient temperature, and wind velocity.

Procedure: On the level road test facility,

1. Perform a series of snubs to heat brakes to medium/high temperatures.
2. Release brakes and drive at steady test speed until $T = T_\infty$.
3. Repeat Steps 1 and 2 for next test speed.

Data Analysis: For each speed,

1. Average temperatures from all brakes.
2. Plot: $\ln[T - T_{\infty}]/(T_0 - T_{\infty})$ vs. time.
3. Determine $K_1 = hA_C/m_B C$ from slope of curve.
4. Plot K_1 vs. V .

Stopping Capability Tests (SAE J786 Fade Test)

Purpose: To determine the variation of stopping capability with brake temperature from the brake pressure required to produce a specified deceleration.

Controlled and Measured Variables: Measure and record speed, rpm, application pressure, brake temperature, ambient temperature, and wind velocity.

Procedure: On the level road test facility,

1. Temperature condition brakes to $T \doteq 200$ °F.
2. Make three baseline snubs, 40-20 mph, $a_x = 10$ ft/sec² at $T \doteq 200$ °F.
3. Make repeated snubs from 40-20 mph at $a_x = 10$ ft/sec² as rapidly as possible until it is impossible to achieve $a_x = 10$ ft/sec² (all snubs made with clutch disengaged).

Data Analysis:

1. Plot pressure required for $a_x = 10$ ft/sec² and brake temperature vs. snub number.
2. Cross-plot pressure required vs. brake temperature.

Hill Descent Test

Purpose: To find the variation of brake pressure and temperature during a steady hill descent as a function of W , θ , L , engine braking, and descent speed. Also, to determine the total convective heat transfer parameter, hA_C , and the brake force, F_B , as a function of P , V , and T .

Controlled and Measured Variables:

1. Record application pressure, velocity, rpm and brake temperature on each axle.
2. Driver monitors speedometer to modulate brake pressure.
3. V, W, θ , and engine brake per run schedule.

Procedure:

1. Insure that brakes are cool ($T \leq 200$ °F on hottest brake).
2. Descend hill maintaining speed constant by modulating brake pressure.

Data Analysis:

Extraction of total heat transfer parameter, hA_c :

Total heat transfer parameter at each test speed is computed from

$$hA_c = \frac{(W\theta - F_{NB})V}{T_{SS} - T_{\infty}}$$

where $T_{SS} = \lim_{t \rightarrow \infty} T$ is the steady-state brake temperature.

DATA ANALYSIS AND RESULTS

Relation of Vehicle Speed to Engine Speed

The relation of vehicle speed to engine speed in each transmission gear for Test Vehicle No. 1 was determined from speed data recorded as the truck was accelerated through the gears. These data are plotted in Fig. B-9 as the effective total drive line gearing; they show that up-shifting to the next gear when the engine speed reaches 1900 rpm (which is near the upper limit) drops the engine speed to approximately its lower limit, 1400 rpm. Thus it can be seen that the transmission is well matched to the engine.

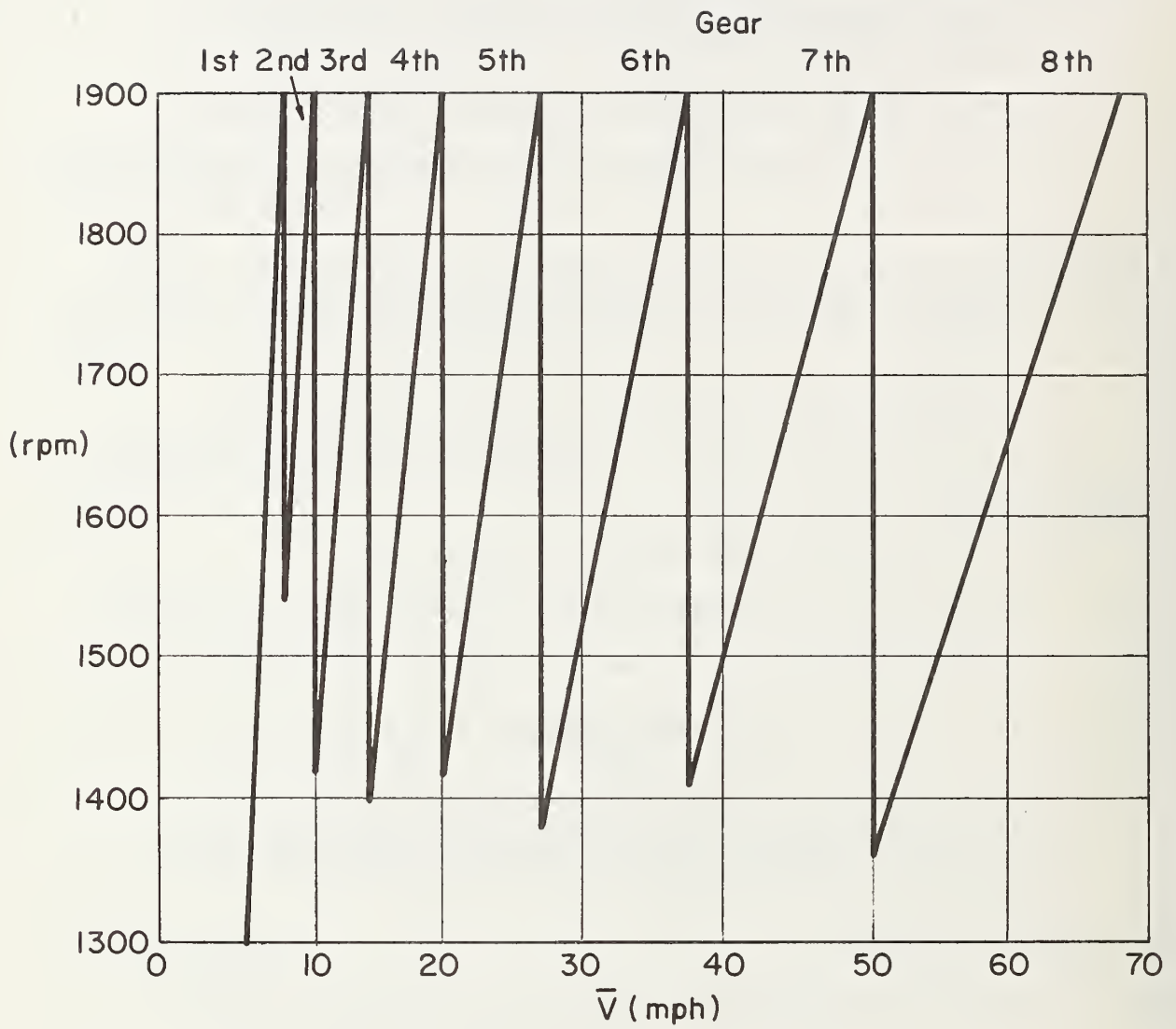


Figure B-9. Speed vs. RPM in Each Gear

Brake Effectiveness and Fade Tests

Brake effectiveness tests were conducted at low brake temperature (SAE "cold curve," $T = 200$ °F) and high temperatures (SAE "hot curves," $T = 500$ °F on hottest brake) with the results shown in Fig. B-10. It can be seen that there is no evidence of brake fade. It was felt that brake effectiveness tests could not be conducted at higher temperatures without undue risk of brake component damage (such as oil seal failure) that would jeopardize later tests. Thus, no further attempts were made to define the brake fade.

Determination of F_{drag}

As used here, the term F_{drag} represents the combined effects of air drag, rolling resistance, and chassis friction. The numerical determination of F_{drag} is based on the variation of speed with time in the coast-down tests (made in neutral) as shown in Fig. B-11. It can be seen that the deceleration is lower for the northbound runs because the road slopes down to the north. If the entire test area were of constant slope, the northbound and southbound data could simply be averaged; however, the slope was steeper at the south end. This change in slope affects the variation of a_x with V and cannot be "averaged out," since at a given point in the test area the truck is moving at different speeds on the northbound and southbound runs. Equipment was not available to measure the slope change directly but an estimate was made from the coast-down tests with engine braking (these tests are discussed in the next section). The coast-down tests in neutral required the entire length of the test area (just over a mile), and only one run could be made in one pass over the test area. Since the truck decelerated much more rapidly with engine braking, three such runs could be made in each pass over the test area. Thus, by taking the difference in decelerations between the northbound and southbound runs on the north, middle, and south ends of the test area, the local slope was estimated from:

$$\theta \text{ in } \% \doteq [(a_{xN'bnd} - a_{xS'bnd})/2g] \times 100 \quad (B-3)$$

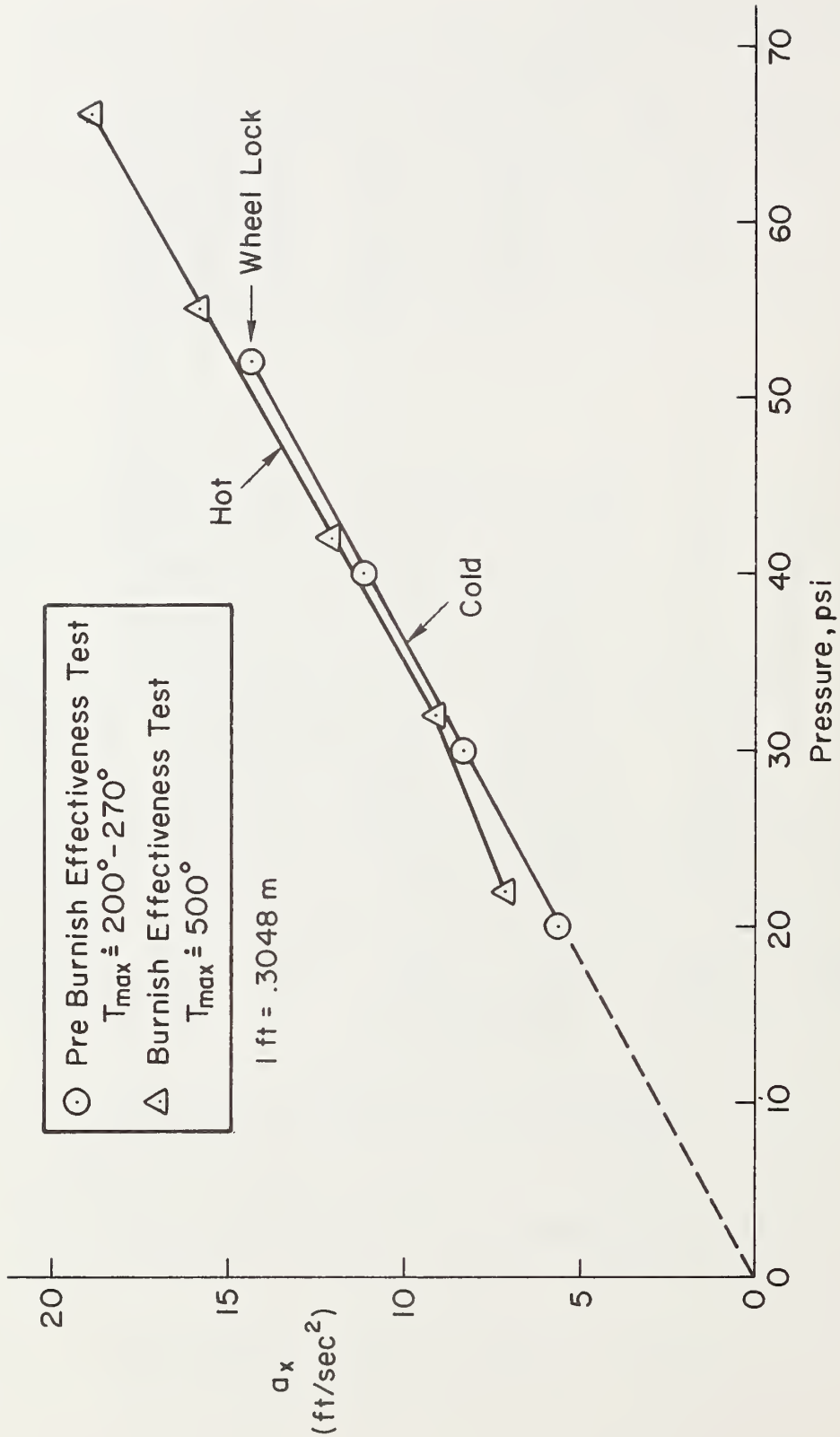
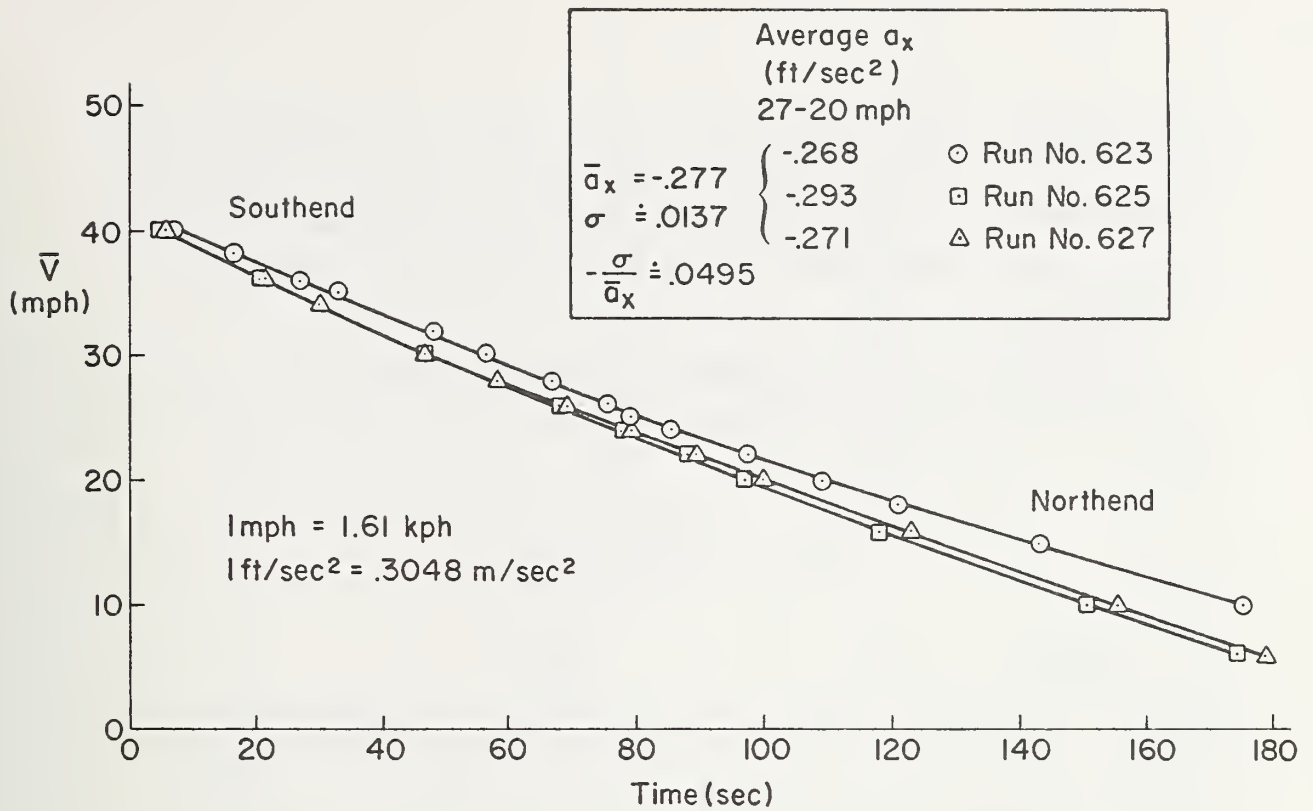
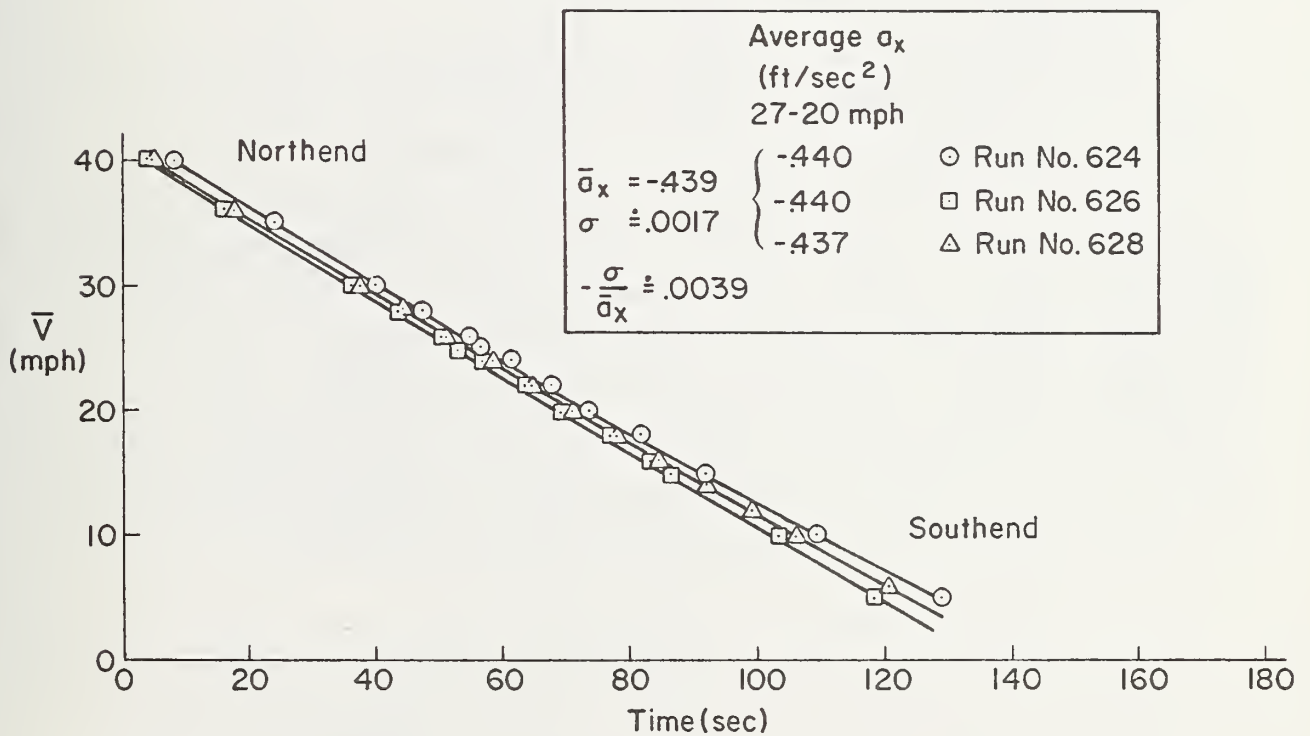


Figure B-10. Brake Effectiveness and Fade Tests



a) Coast Down, Neutral, Northbound



b) Coast Down, Neutral, Southbound

Figure B-11. Coast Down Test Data for Determination of F_{drag}

The results are shown in Fig. B-12. While there is some scatter in the data, it appears that the south end is about 0.26 percent steeper than the north end. This slope change is equivalent to several hundred pounds of longitudinal force, which is significant in terms of the F_{drag} determination.

The effects of rotational inertia on the deceleration was accounted for through the second term of the relation

$$F_{\text{NB}} = \left(\frac{W}{g} + \frac{nI_w}{R} \right) a_x \quad (\text{B-4})$$

which includes only the rotational effect of the decelerating wheel/tire assembly torques. Based on the wheel inertia data of Walston, et al. (Ref. 37), the effect was calculated to be equivalent to a 4 percent increase in vehicle weight. This is consistent with values given by the Western Highway Institute (Ref. 11).

Figure B-13 shows the estimated total drag force, corrected for slope variation and wheel inertia, compared to the SAE J688 estimate and data from Steers and Montoya (Ref. 10). It can be seen that the speed variation of F_{drag} for Test Vehicle No. 1 is consistent with the SAE estimate but that the level of drag is lower. The more recent Steers and Montoya data are closer to present results than the SAE data, indicating that the drag level of line haul trucks has been reduced (as has the sensitivity to weight variation), apparently due to truck improvements aimed at increased operational economy. The increase in F_{drag} at low speeds in the SAE estimates is due to the rolling resistance contribution; however, no evidence of this effect was seen in the present test results.

$$\theta = \left[\frac{(\alpha_{xN} \text{ 'bnd} - \alpha_{xS} \text{ 'bnd}) / 2g}{\bar{\theta}} \right] \times 100$$

Section	$\bar{\theta}$ (%)
North end	.173
Middle	.155
South end	.435
Δ	Denotes Mean

θ
(Percent)
Slope Down
Toward North

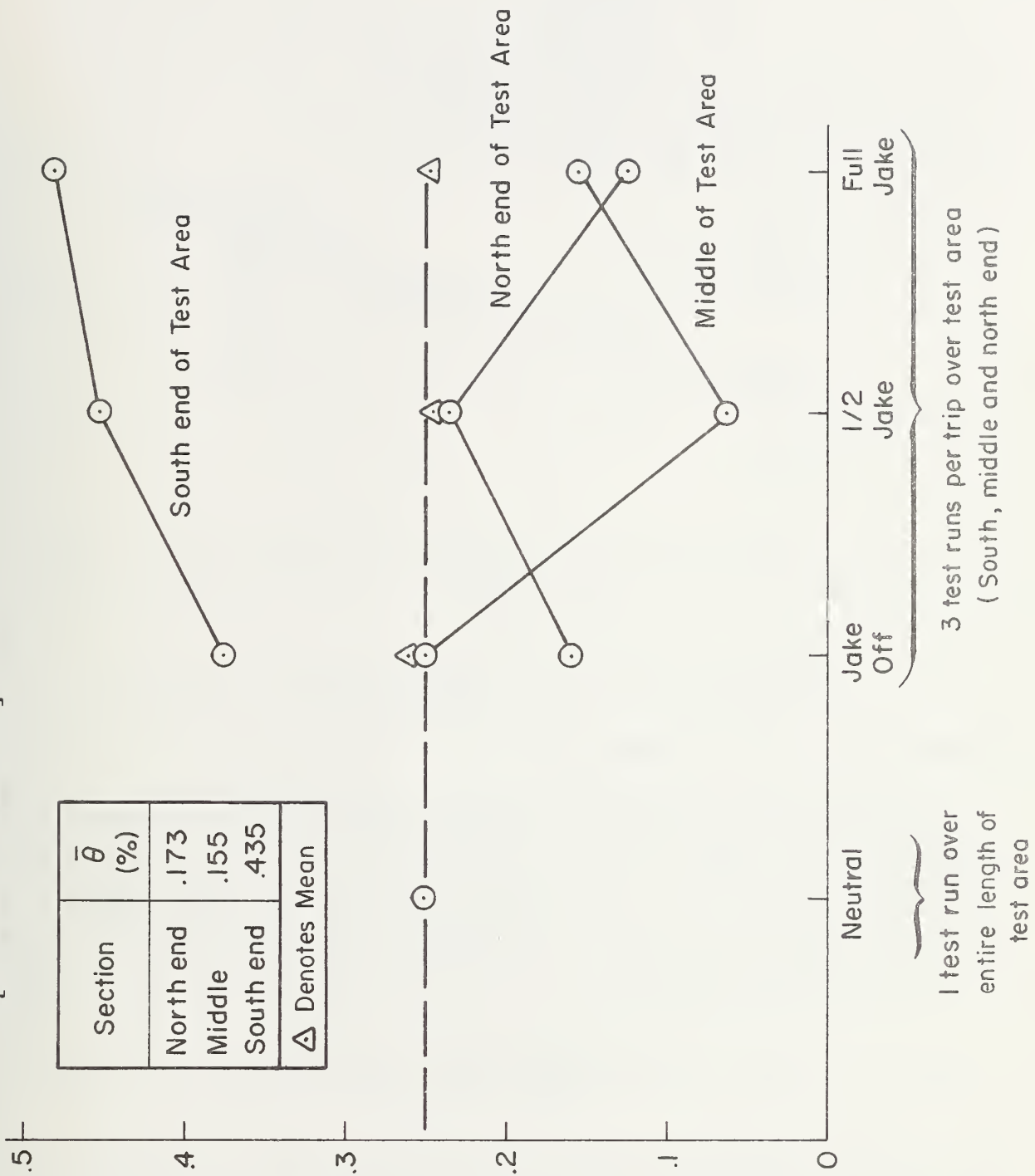


Figure B-12. Apparent Slope of Adobe Rd. Test Area.

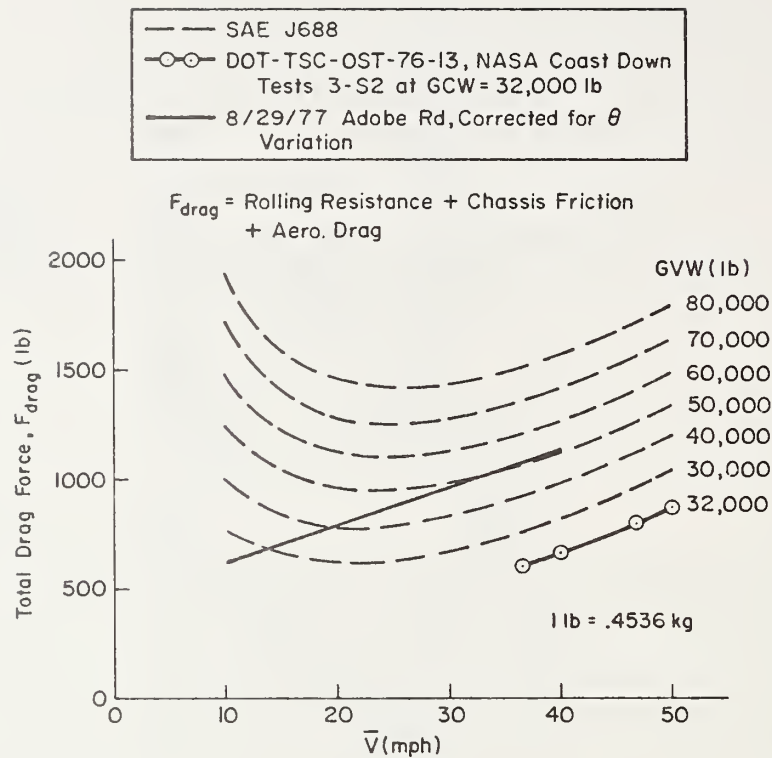


Figure B-13. Variation of F_{drag} with Speed

Determination of Engine Braking Force

An example of the results of a coast-down test with engine braking (transmission in 5th gear, 1/2 engine brake setting) is shown in Fig. B-14. Since these test runs covered relatively small distances, slope changes during the run were neglected. To determine the engine braking force, the following relation was used:

$$F_{eng} = -F_{drag} + \left[\frac{W}{g} + \frac{nI_w}{R^2} + I_{eng} \left(\frac{G_i}{R} \right)^2 \right] a_x \quad (B-5)$$

which includes, in addition to the rotational inertia effect of wheel assemblies, the effect of rotating engine and clutch parts as well. Data from

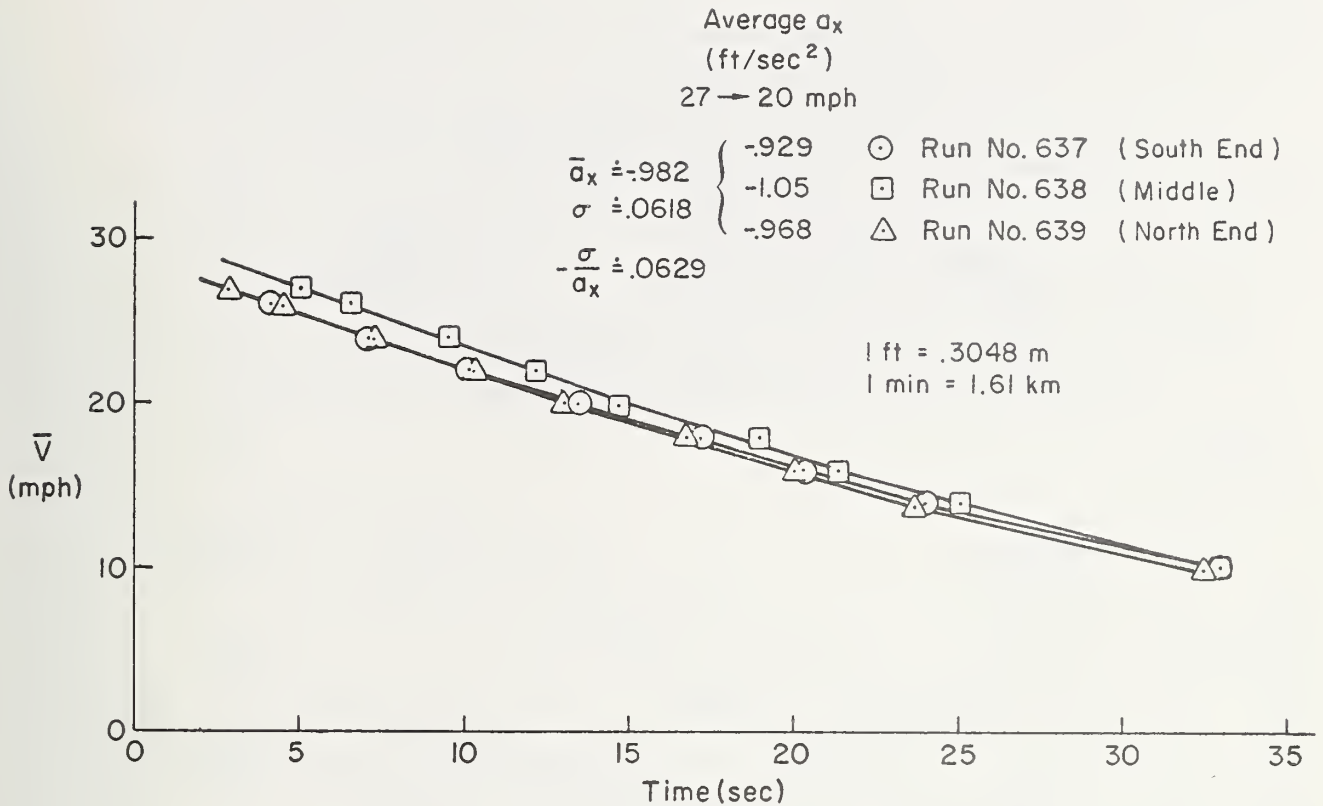


Figure B-14. Coast-Down Test Data for Determination of Engine Braking

Western Highway Institute (Ref. 11) indicate that the engine and clutch contribution is comparable to that of the wheel assemblies by themselves. The coast-down test results indicate that for all settings of the engine brake (off, half, and full), the engine braking force is constant with engine speed in the engine's operating range (1400 to 1900 rpm). These data, converted to the more convenient power absorption form,

$$HP_{eng} = F_{eng}V/550 \tag{B-6}$$

are plotted versus engine speed for each engine brake setting in Fig. B-15.

Engine braking was also measured by a second technique in which the engine brake switch position was changed while running downhill. The incremental change in braking force was determined from the instantaneous

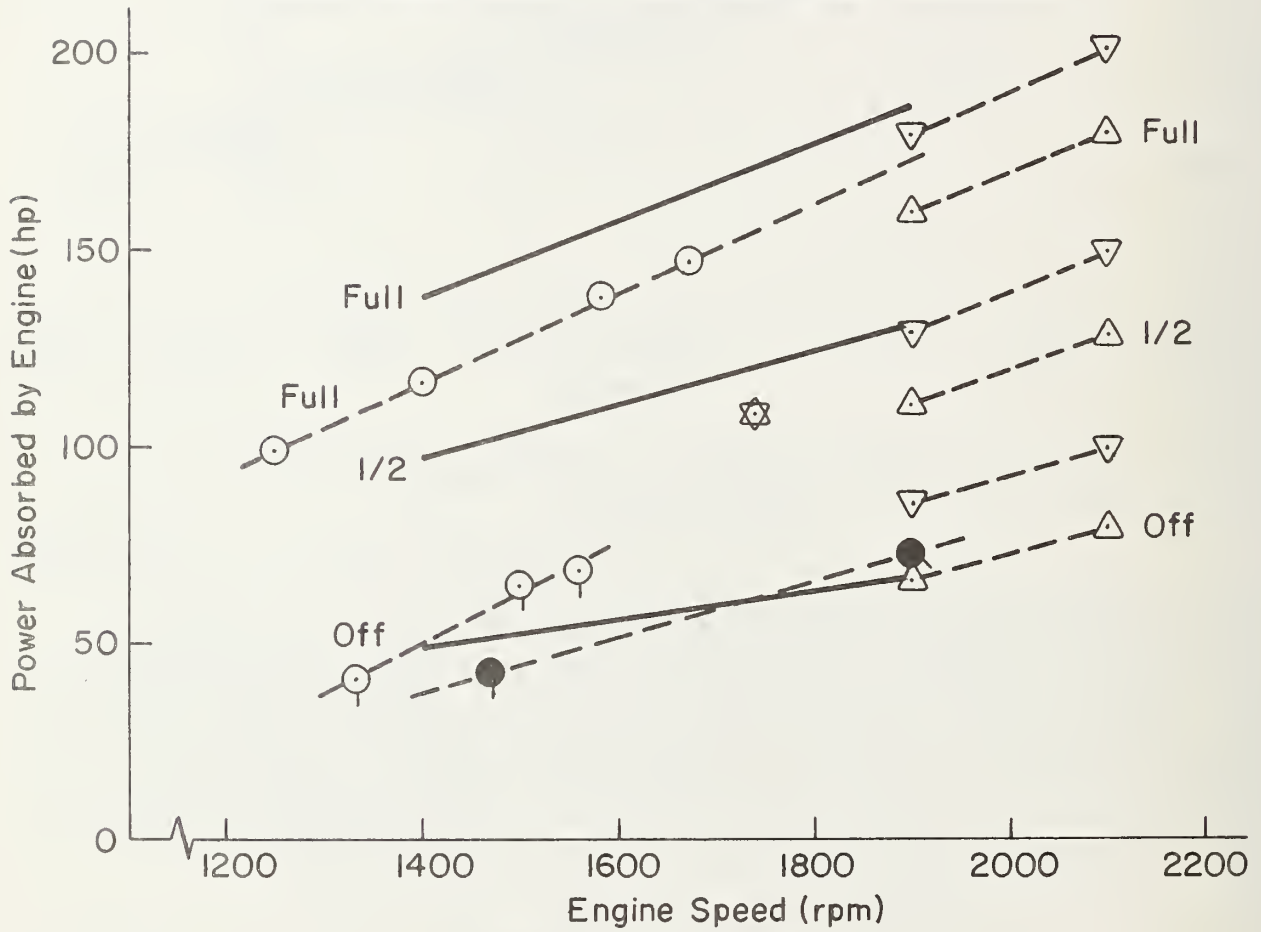
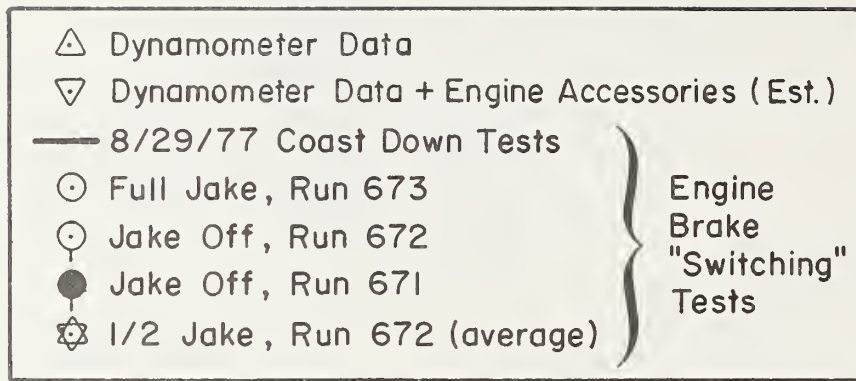


Figure B-15. Results of Engine Braking Tests

change in acceleration at the instant of "switching." The results of these tests, also presented in Fig. B-15, show a similar but somewhat lower power absorption than do the coast-down tests.

The above results compare well with dynamometer test data supplied by the engine brake manufacturer when corrected for the effect of power absorbing accessories, including the air compressor and engine fan. The final values used for engine power absorption were 73 hp (54,458 W) with the engine brake off and an additional 50 hp (37,300 W) for each half engine brake setting at the nominal engine speed, 1900 rpm, see Fig. B-16.

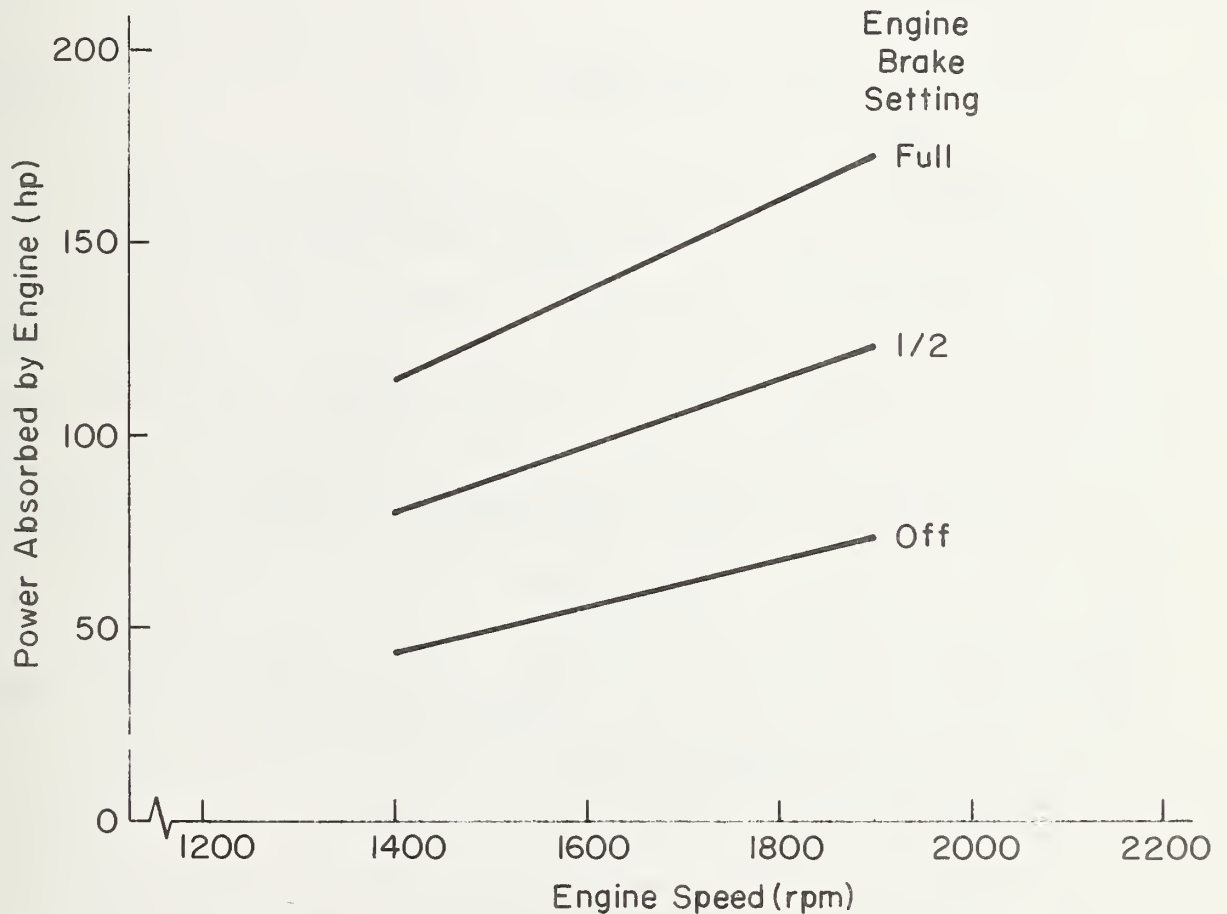


Figure B-16. Final Estimate of Engine Braking Capacity

Determination of Effective Heat Transfer Coefficient

In a cool-down test the brake temperature is governed by the temperature equation, Eq. 5, with $F_B = 0$. Thus,

$$T = T_0 e^{-K_1 t} + T_\infty (1 - e^{-K_1 t}) \quad (B-7)$$

where

K_1 is the inverse thermal time constant

To extract the inverse thermal time constant from the cool-down test data, this equation is rewritten as:

$$\ln \left(\frac{T - T_\infty}{T_0 - T_\infty} \right) = -K_1 t \quad (B-8)$$

From this relation it follows that if experimentally measured values of the parameter $\ln[(T - T_\infty)/(T_0 - T_\infty)]$ are plotted versus time, a straight line of slope $-K_1$ should result. Such a plot is shown in Fig. B-17 for the left side brakes at $\bar{V} = 51.5$ mph (82.4 kph). Five distinct lines result, one for each brake, since each brake has slightly different heat capacity and heat transfer characteristics. The fact that a straight line fits the data well in each case indicates that the heat transfer model is a good representation of the actual physical situation. Other data at other speeds (Figs. B-18 through B-20) indicate some concave upward curvature for some brakes, that is, a steeper initial slope. This indicates a higher heat transfer rate at high temperatures, which is consistent with radiant heat transfer effects (Ref. 33). Since a steeper slope indicates a higher cooling rate, it can be seen that the tractor front brakes and the trailer brakes cool faster than the tractor drive axle brakes.

The variation of K_1 with speed presented in Fig. B-21 has the general character of the data presented by Limpert (Ref. 9), but shows less difference between high and low speed values. While there is theoretical and

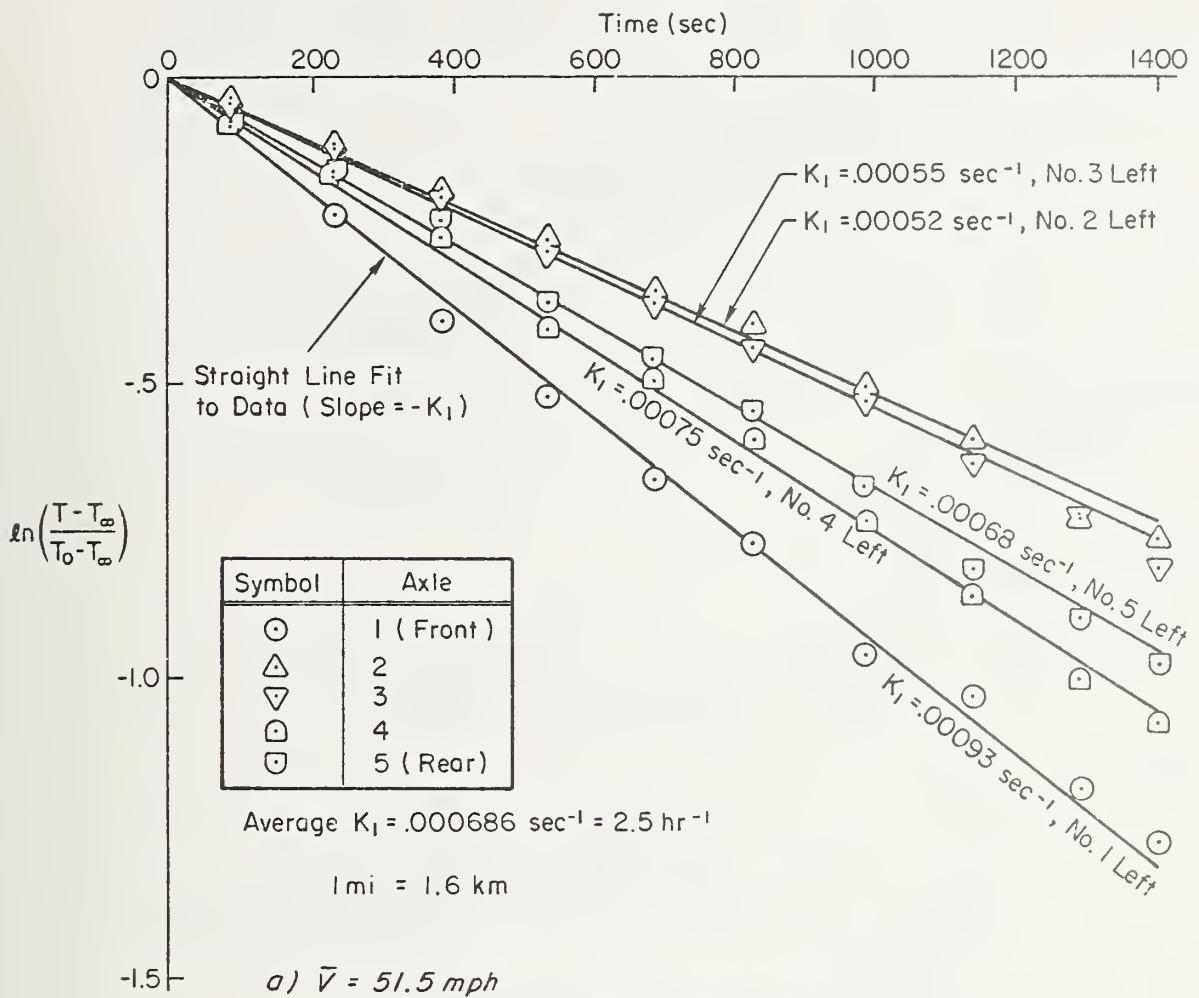


Figure B-17. Example of Cool-Down Data Analysis; K_1 Extraction ($\bar{V} = 51.5 \text{ mph}$, Left Side Brakes)

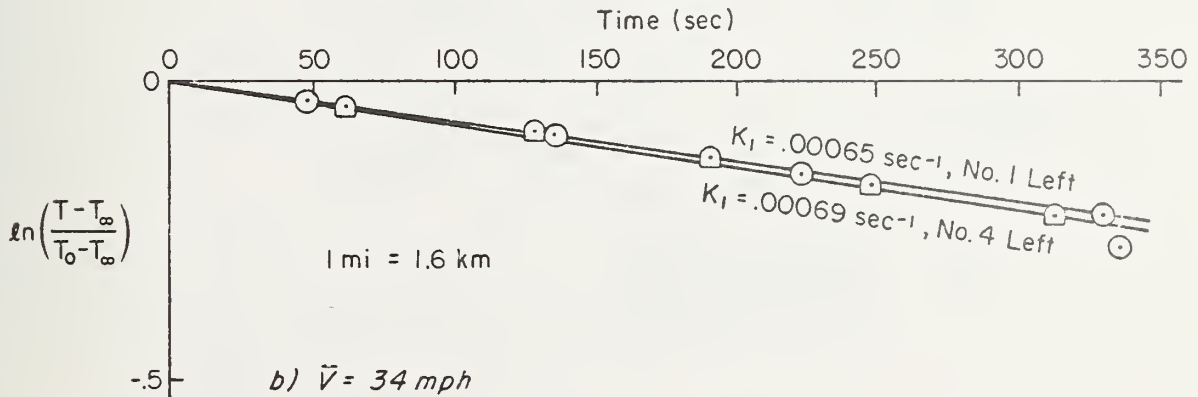


Figure B-18. Example of Cool-Down Data Analysis; K_1 Extraction ($\bar{V} = 34 \text{ mph}$, Left Side Brakes)

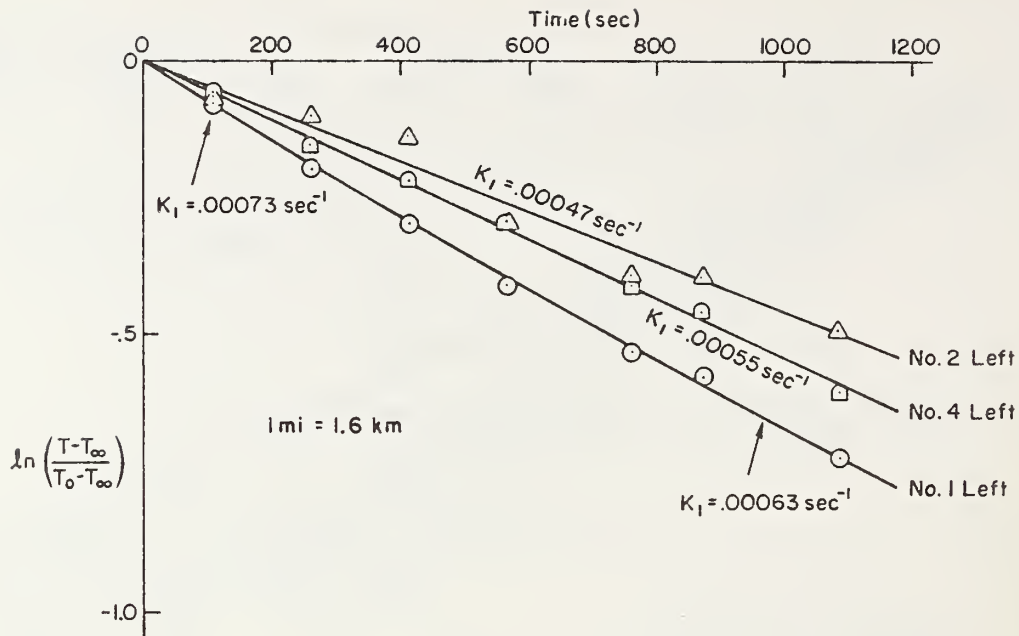


Figure B-19. Example of Cool-Down Data Analysis; K_1 Extraction ($\bar{V} = 20$ mph, Left Side Brakes)

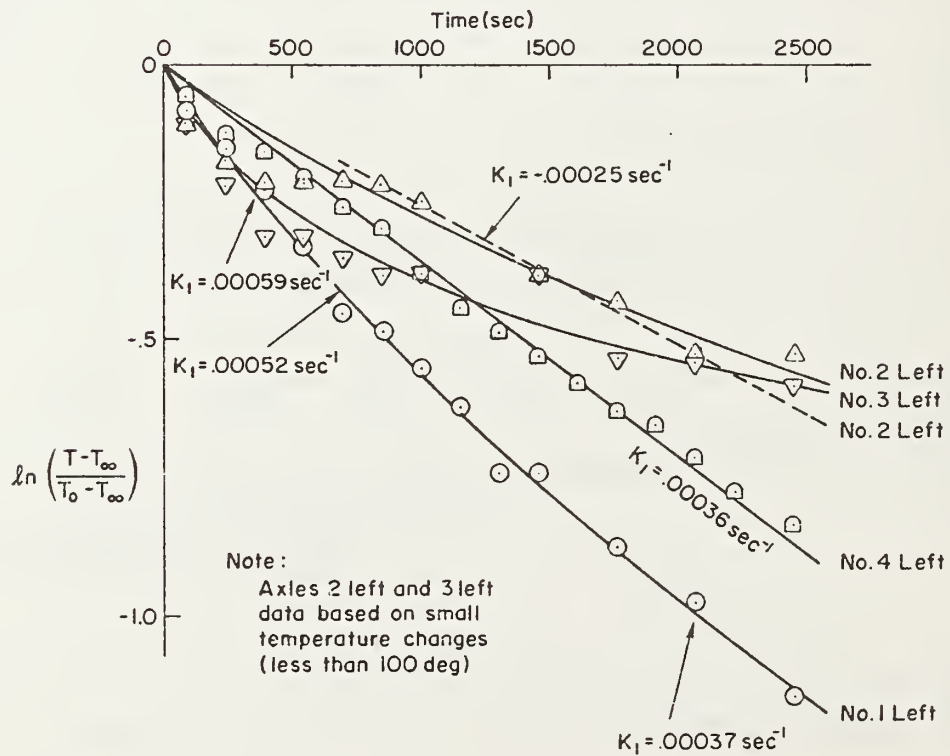


Figure B-20. Example of Cool-Down Data Analysis; K_1 Extraction ($\bar{V} = 0$, Left Side Brakes)

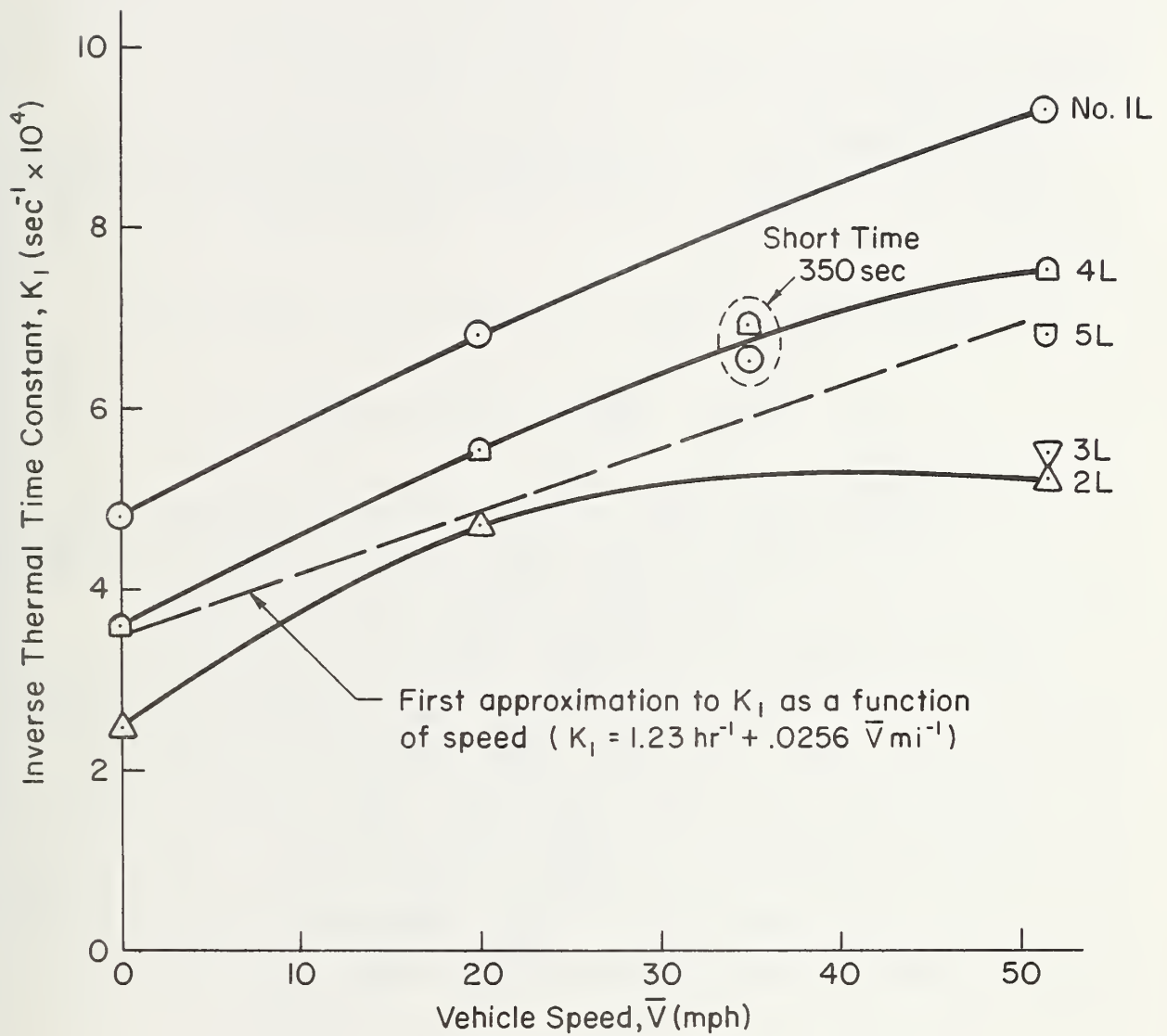


Figure B-21. Variation of Inverse Thermal Time Constant, K_1 , with Speed.

experimental evidence for the curved variation of K_1 with speed, it was felt that a linear approximation was adequate for data analysis. The final empirical formula for K_1 is:

$$K_1 = 1.23 \text{ hr}^{-1} + 0.0256 \bar{V} \text{ mi}^{-1} \quad (\text{B-9})$$

Analysis of Hill Descent Tests

At the most basic level, analysis of the hill descent data was aimed at correlating brake temperature with the power absorbed by the brake system during hill descent.

The brake power absorbed in each hill descent was computed from:

$$\text{HP}_B = \frac{F_D V}{550} = \frac{V}{550} [W\theta - F_{\text{drag}}] - \text{HP}_{\text{eng}} \quad (\text{B-10})$$

Since HP_{eng} is fixed at known levels, θ is determined from the hill geometry and F_{drag} is known as a function of V and gear selection; the required power absorption can be computed for each hill descent, Fig. B-22.

To correlate observed brake temperatures with the power input to the brakes first required some treatment of the large variation in temperatures among the various brakes. The most obvious approach was to average the brake temperatures on all brakes, because this is theoretically the appropriate first approximation, the accuracy of the approximation depending on having similar values of K_1 for the individual brakes. While there is variation in K_1 among the brakes (see Fig. B-22), the effect is nonetheless of secondary importance; thus, temperature averages were used for data correlation purposes.

As a first attempt at correlating brake temperatures with power into the brakes, the temperature rise during a descent was plotted versus $F_D V$. However, this turned out not to correlate very well, and therefore is not recommended except as the crudest of measures. The reason temperature rise does not correlate well with power input is that the temperature rise is dependent on the initial temperature (at the top of the hill). It was

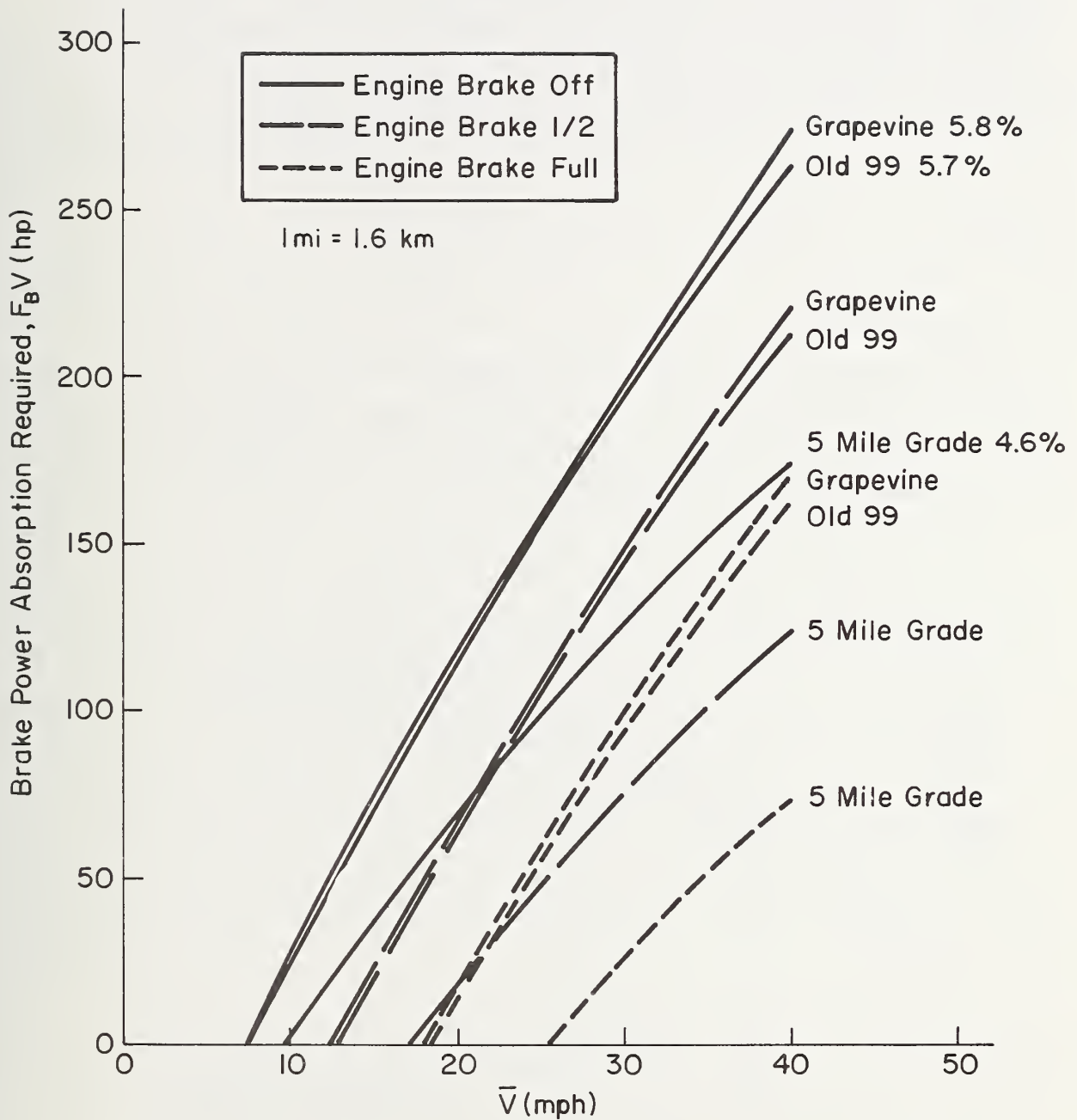


Figure B-22. Brake Power Absorption as a Function of Speed and Engine Brake Setting for Several Hills

expected that the temperature at the bottom of the hill would be strongly dependent on the initial temperature, but the dependence of temperature rise on initial temperature was somewhat of a surprise. The explanation for this is now well understood and can be described as follows. The average brake temperature during a hill descent has a nonlinear variation with time (or distance along the hill), as sketched in Fig. B-23. For the example shown, the temperature at the bottom of a hill of length L_1 is T_2 if the initial temperature was T_1 ; and it is T_3 if the initial temperature was T_2 . From the sketch it is easy to see that the temperature rise, $T_3 - T_2$, is less than $T_2 - T_1$ (for the same length hill). It is also easy to see that the temperature rise is associated with the slope of the curve, and therefore for any temperature curve that decreases in slope at the higher temperatures the temperature rise will decrease with increasing initial temperatures. It is pointed out that this feature of the temperature curve will always exist because it is the nature of heat transfer that higher temperatures result in more heat flow out of a body. Thus, the heat flow out of the brakes has a strong influence on brake temperature.

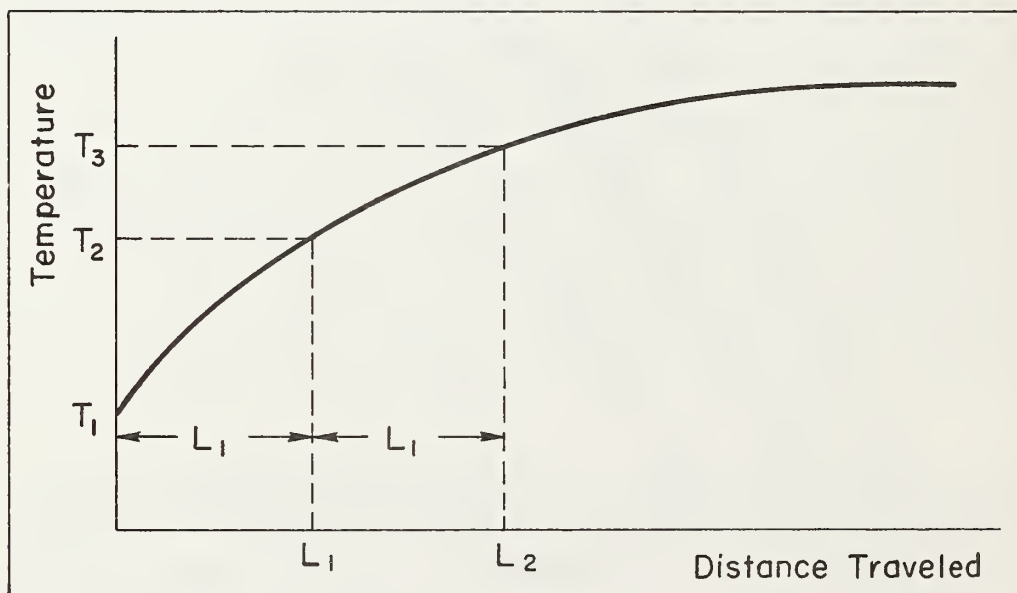


Figure B-23. Sketch of Average Brake Temperature as a Function of Distance Traveled (During Steady Braking at a Given Speed)

Since temperature rise is not recommended as a correlation parameter, the question remains as to what temperature parameter is correlated with power into the brakes. As alluded to above, to answer this we need to consider the heat "rejection" characteristics of the brakes. But this was already included in the derivation of the fundamental thermodynamic equation (Eq. 5). Therefore, we will use Eq. 5, rearranged to put the power absorption, $F_B V$, on one side of the equation and an expression called T^* (involving the thermodynamic variables) on the other side. Thus,

$$T^* \equiv \frac{T - T_0}{1 - e^{-K_1 L / \bar{V}}} + (T_0 - T_\infty) = K_2 F_B V \quad (B-11)$$

It can be seen that if T^* is computed for each hill descent and plotted against power absorption the result should be, if the temperature equation is valid, a straight line through the origin with slope, K_2 . Making these computations and plots not only checks the validity of the temperature model, but also provides a means of extracting the parameter K_2 from the data. The parameter K_2 is the inverse of the total convective heat transfer parameter, hA_c , which is a function of speed. Thus, separate T^* versus $F_B V$ plots must be made for each hill descent speed. Such plots are shown in Fig. B-24. It can be observed that in all cases the data are well correlated by a straight line through the origin as required by the theory. From each plot a value of K_2 is determined from the slope (Fig. B-25). From these values the convective heat transfer parameter was computed and plotted as a function of speed in Fig. B-26. The data indicate a linear increase in heat transfer with speed which can be fitted with the empirical equation:

$$\frac{1}{K_2} = hA_c = 0.100 + 0.00208\bar{V} \quad \frac{hp}{^\circ F} \quad (B-12)$$

1 mi = 1.6 km

○ Grapevine ; □ Old 99 ; △ 5 Mile Grade

$$T^* = T - T_0 + \frac{(T_0 - T_\infty)(1 - e^{-K_1 L / V})}{K_1}$$

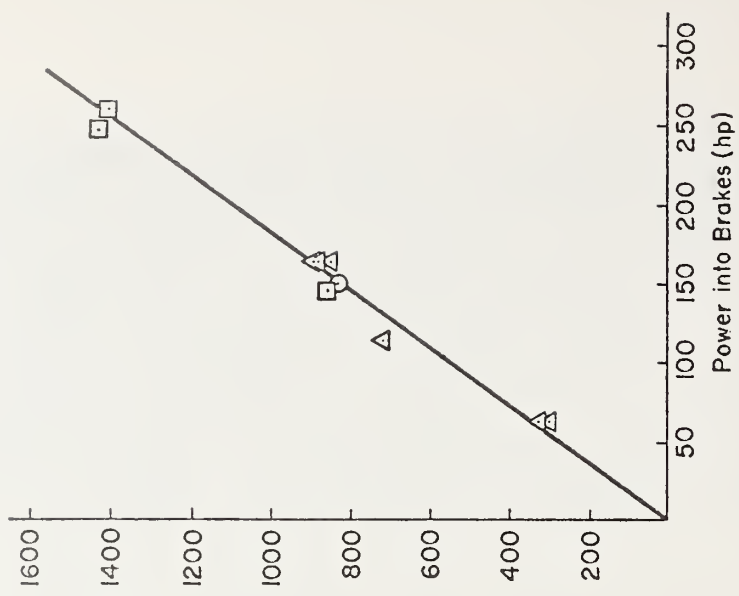
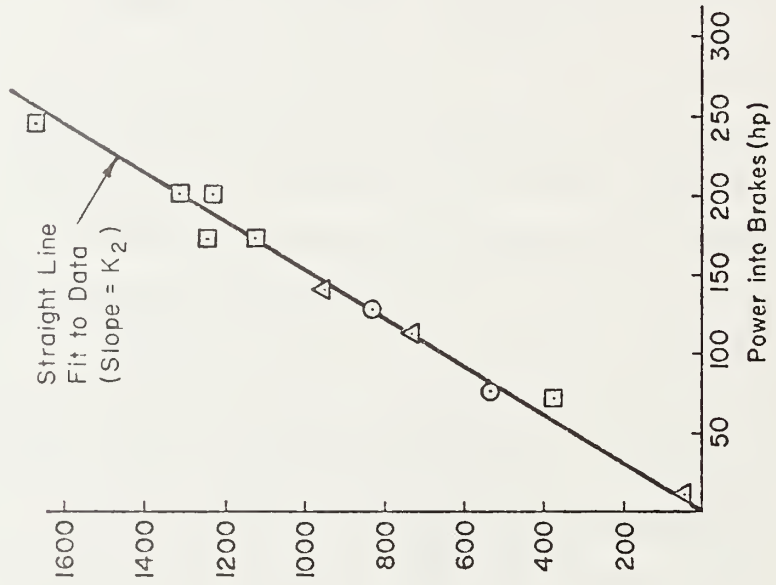
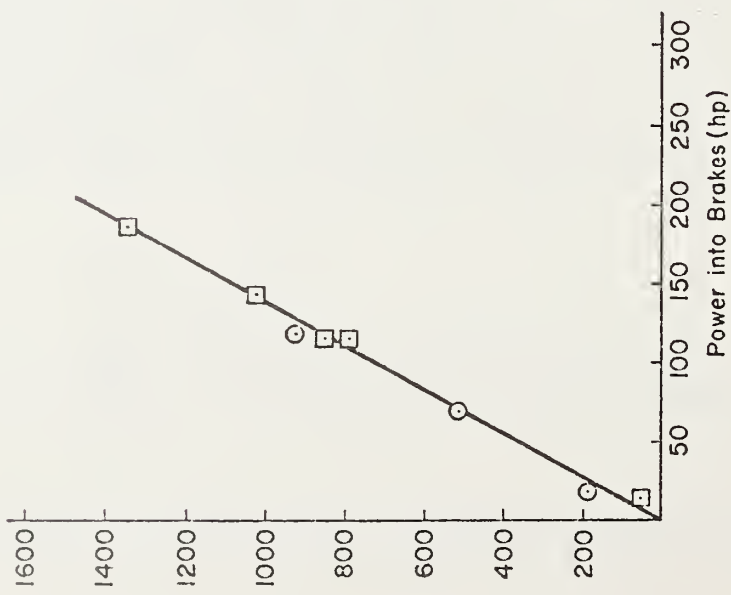


Figure B-24. Plot of Measured Temperature Data vs. Computed Braking Horsepower ($F_B V$)

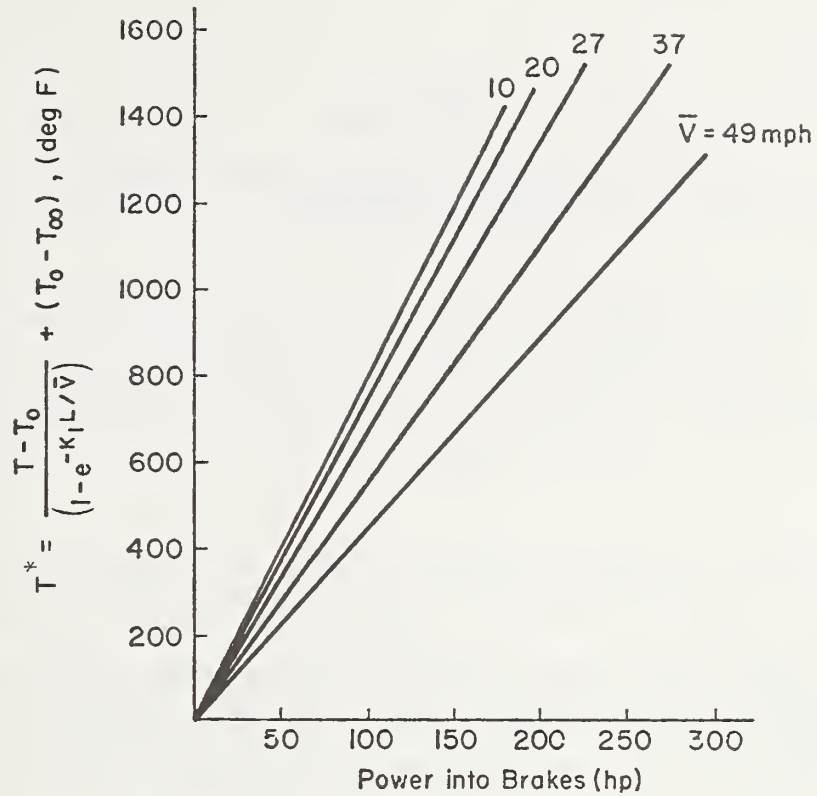


Figure B-25. Summary of Straight Line Fits to Temperature Data (Slope of Line = K_2)

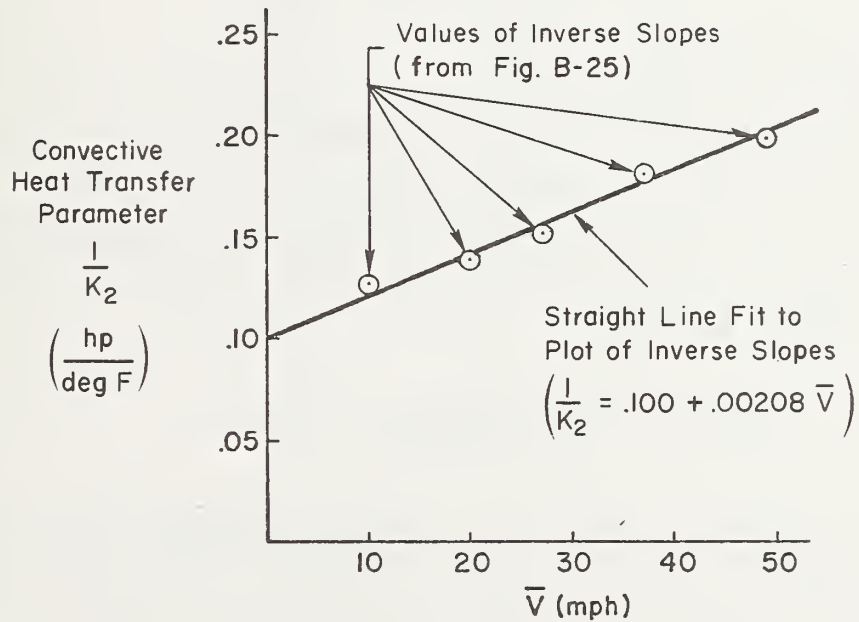


Figure B-26. Variation of the Convective Heat Transfer Parameter, $1/K_2$, with Speed (Derived from T^* Versus $F_B V$ Plots)

Since

$$K_1 = \frac{hA_c}{m_B C}$$

and

$$\frac{1}{K_2} = hA_c$$

it follows that

$$K_1 = \frac{1}{K_2} m_B C \quad (B-13)$$

From theoretical considerations it can be shown that the total effective heat capacity, $m_B C$, is not a function of speed. Thus, Eq. B-13 indicates that K_1 and $1/K_2$, which individually are functions of speed, should differ only by a constant factor equal to $m_B C$. Since empirical expressions for K_1 and $1/K_2$ were derived from independent experiments, their ratio can be used as an additional check of the temperature model, i.e.,

$$m_B C = \frac{K_1}{1/K_2} = \frac{1.23 + 0.0256\bar{V}}{0.100 + 0.00208\bar{V}} \cdot \frac{1.23(1 + 0.0208\bar{V})}{0.1(1 + 0.0208\bar{V})} = 12.3 \frac{^{\circ}\text{F}}{\text{HP-hr}} \quad (B-14)$$

which is independent of speed as required.

As a result of knowing how to compute the power absorbed by the brakes, and having equations for the thermodynamic constants K_1 and K_2 , it is possible to go back to the basic temperature equation (Eq. 5) and solve for brake temperature as a function of time (or distance traveled) as a truck descends a grade. That is,

$$T = T_0 e^{-K_1 L / \bar{V}} + (T_{\infty} + K_2 F_B V)(1 - e^{-K_1 L / \bar{V}})$$

Figure B-27 shows an example comparison of measured (average) brake temperatures with those computed with Eq. B-15 for a descent of the Grapevine at 20 mph (32 kph). The excellent agreement in both general shape and numerical value is indicative of the validity of the overall technique for estimating brake temperatures on grades.

APPENDIX C

EXTENSION OF THE TRUCK DOWNGRADE BRAKING MODEL TO COMPLEX GRADES

Brake temperature change over the i th grade segment may be calculated from Eq. 18 since θ_i and \bar{V}_i will be approximately constant. A T profile for the entire grade may be generated by using $T_{O1} = 150^\circ \text{ F}$ and the recursion formula

$$T_{O_i} = T_{f_{i-1}} \quad (\text{C-1})$$

if \bar{V}_i is specified. \bar{V}_i will generally be specified arbitrarily for braking intervals, but it is necessary to develop a procedure for estimating speed on non-braking (possibly upgrade) intervals. This may be done by assuming that the driver always uses the maximum engine output power to minimize time on a non-braking interval.

$$\frac{W}{g} \ddot{x} = W\theta_i - F_{\text{NB}}(\bar{V}_i) + F_x \quad (\text{C-2})$$

$$F_{\text{NB}} = F_{\text{drag}} = F_0 + F_1 \bar{V}_i \quad (\text{C-3})$$

For uphill sections

$$375\text{HP}_{\text{max}} = (F_x V_i)_{\text{max}} \quad (\text{C-4})$$

$$F_{x_{\text{max}}} = 375\text{HP}_{\text{max}} / \bar{V}_i \quad (\text{C-5})$$

Assume $\ddot{x} \equiv 0$ on uphill section

$$W\theta_i - F_0 - F_1\bar{V}_i + \frac{375\text{HP}_{\text{max}}}{\bar{V}_i} = 0 \quad (\text{C-6})$$

$$\bar{V}_i^2 + \frac{(W\theta_i - F_0)}{-F_1} \bar{V}_i + \frac{375\text{HP}_{\text{max}}}{-F_1} = 0 \quad (\text{C-7})$$

$$\bar{V}_i = -\frac{B}{2} \pm \frac{\sqrt{B^2 - 4C}}{2}$$

where

$$B = \frac{W\theta_i - F_0}{-F_1}$$

$$C = \frac{375\text{HP}_{\text{max}}}{-F_1} \quad (\text{C-8})$$

This equation produces the family of speed curves in Fig. C-1. For use in the simplified multigrade procedure (Appendix E) this family of curves may be approximated as

$$\bar{V}_i = 50 + 500 \theta_i \quad (\text{C-9})$$

This computational approach can be made quite efficient by organization into a formal algorithm as shown in the flow chart of Fig. C-2. Furthermore the calculations can be made quite rapidly (more rapidly than the time required for the descent of a typical hill in a real truck) by programming the algorithm on a programmable calculator or digital computer. For purposes of development in this program, the procedure was programmed in FORTRAN 4 on the STI PDP-11 digital computer (see BTEMP program listing, Page C-5). This program produces output both in tabular form and in the form of computer plotted temperature and grade profiles. For use in field calculations, this program has been implemented on a programmable calculator.

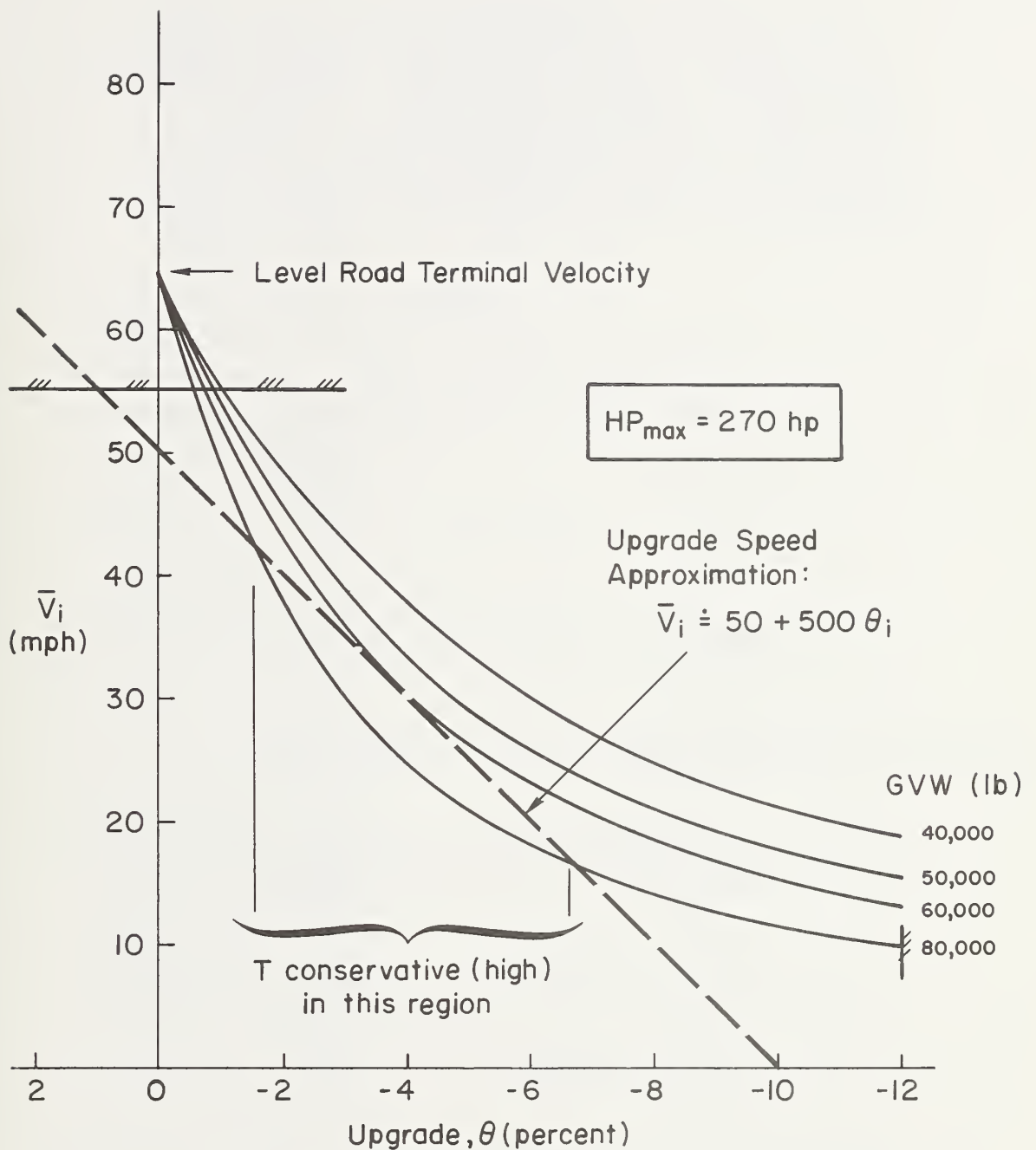


Figure C-1. Maximum Upgrade Speed at Maximum Power as a Function of θ

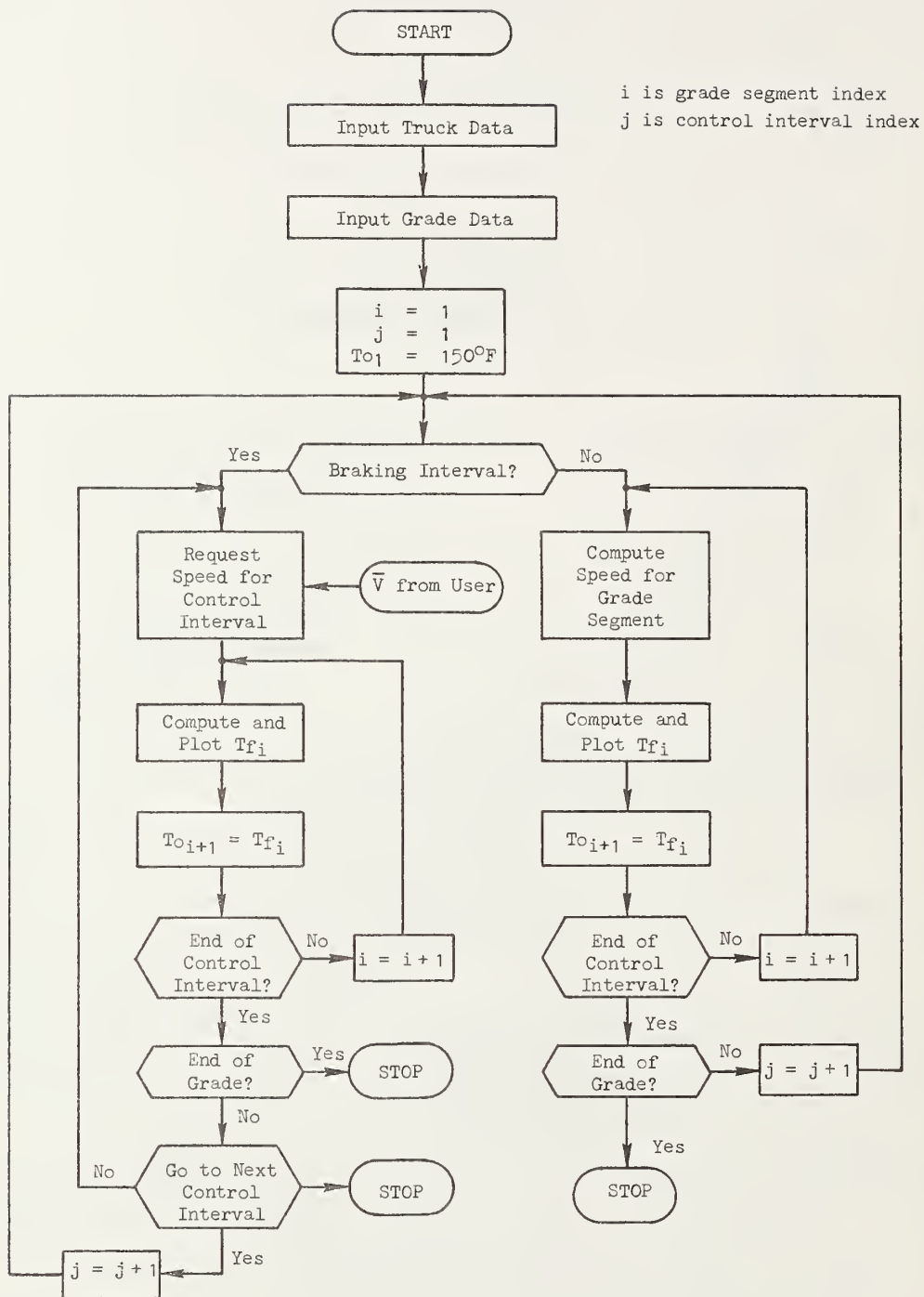


Figure C-2. Flow Chart for Simulation Program

```

C
C   BRAKE TEMPERATURE PROFILE PROGRAM, PDP-11
C
C   TIM, SC1106, 6/8/78, REVISED 6/27/78, 7/15/78
C   PROGRAM PLCTS TEMPERATURE PROFILE ON MULTIGRADE HILL.
C   HILL IS DIVIDED INTO CONTROL INTERVALS SEPARATED BY
C   CONTROL POINTS. CONTROL INTERVALS ARE EITHER "UPGRADE"
C   OR "DOWNGRADE". UPGRADE INTERVALS HAVE NO BRAKING INPUT
C   AND THE SPEED (< OR = 55MPH) ON EACH SLOPE SEGMENT IS
C   DETERMINED TO GIVE ZERO ACCELERATION WITH MAXIMUM ENGINE
C   OUTPUT. DOWNGRADE INTERVALS HAVE BRAKING TO MAINTAIN A
C   CONSTANT SPEED. SPEED(S) ARE SPECIFIED FOR EACH DOWNGRADE
C   INTERVAL BY USER.
C
0001   DIMENSION FNAME(4),IDATE(5)
0002   DATA IT,IP,ID,IN,IS,IY/'T','P','D','N','S','Y'/
0003   REAL KRET
0004   COMMON TKDT(15),SFPT(40,3),VJ(40),THETA(125),DIST(125),
*ISFPT(40),DSFPT(40),KRET,SFX,SFY,TAMB,W,CRLSWH(40),ET
0005   CALL ASSIGN(20,'KB:/C')
0006   CALL DATE(IDATE)
0007   WRITE(20,2) IDATE
0008   REWIND 20
0009   2 FORMAT(15X,5A2)
0010   WRITE(20,4)
0011   REWIND 20
0012   4 FORMAT(5X,'STI BRAKE TEMPERATURE PROFILE PROGRAM')
C
C   DATA INPUT
C
C   SET SWITCH FOR AUTOMATIC SPEED DETERMINATION ON "UPGRADE" INTERVAL
C
0013   WRITE(20,70)
0014   REWIND 20
0015   70 FORMAT(5X,'AUTOMATIC SPEED SET ON "UPGRADES"? (Y OR N) : '$)
0016   READ(20,42) IAUTO
0017   REWIND 20
0018   WRITE(20,6)
0019   REWIND 20
0020   6 FORMAT(5X,'ENTER TRUCK DATA FILE (DX1:FILNAM.DAT) : ', $)
0021   READ(20,8) (FNAME(I),I=1,4)
0022   REWIND 20
0023   8 FORMAT(4A4)
0024   CALL ASSIGN(21,FNAME)
0025   DO 10 I=1,15,5
0026   10 READ(21,12)TKDT(I),TKDT(I+1),TKDT(I+2),TKDT(I+3),TKDT(I+4)
0027   12 FORMAT(5E)
0028   CALL CLOSE(21)
0029   WRITE(20,14)
0030   REWIND 20
0031   14 FORMAT(5X,'ENTER SLOPE PROFILE FILE (DX1:FILNAM.DAT) : ', $)
0032   READ(20,16) (FNAME(I),I=1,4)
0033   REWIND 20
0034   16 FORMAT(4A4)

```

FORTRAN IV

```

0035      CALL ASSIGN(21,FNAME)
0036      READ(21,17)NGDP
0037      17 FORMAT(I)
0038      DO 18 J=1,NGDP
0039      18 READ(21,20) THETA(J),DIST(J)
0040      20 FORMAT(2E)
0041      CALL CLOSE(21)
0042      WRITE(20,24)
0043      REWIND 20
0044      24 FORMAT(5X,'ENTER SHIFT POINT FILE(DX1:FILLAM.DAT) : ',5)
0045      READ(20,26) (FNAME(I),I=1,4)
0046      REWIND 20
0047      26 FORMAT(4A4)
0048      CALL ASSIGN(21,FNAME)
0049      READ(21,17) NSF
0050      DO 28 J=1,NSF
0051      READ(21,30) SFPT(J,1),SFPT(J,2),SFPT(J,3)
0052      ISFPT(J)=SFPT(J,1)
0053      DSFPT(J)=SFPT(J,2)
0054      GRESWB(J)=SFPT(J,3)
0055      28 IF(IAUTO.NE.1Y) GRESWB(J)=0.
0057      30 FORMAT(3E)
0058      CALL CLOSE(21)
0059      WRITE(20,32)
0060      REWIND 20
0061      32 FORMAT(5X,'ENTER T0,TAMB,W,KRET : ',5)
0062      READ(20,34) T0,TAMB,W,KRET
0063      REWIND 20
0064      34 FORMAT(4E)
0065      WRITE(20,35)
0066      REWIND 20
0067      35 FORMAT(5X,'ENTER SCALE FACTORS; SFX(MI/IN),SFY(LEG/IN) : ',5)
0068      READ(20,31) SFX,SFY
0069      WRITE(7,31) SFX,SFY
0070      31 FORMAT(2E)
0071      REWIND 20
C
C      INITIALIZE FOR FIRST SHIFT INTERVAL
C
0072      ET=0.
0073      TJ = T0
0074      J=1
0075      CALL CLOSE(20)
0076      CALL PLOIF(30,20)
0077      CALL P0FF
C
C      CONTROL INTERVAL 'UPGRADE' OR 'DOWNGRADE'?
C
0078      36 IF(GRESWB(J).NE.0) GO TO 60
C
C      REQUEST OUTPUT OPTION FROM USER, SET SWITCHES
C
0080      38 WRITE(20,40)
0081      REWIND 20

```

FORTRAN IV

```

0082      40 FORMAT(5X,'WHAT NOW? T,P,D,N,S : ', $)
0083      READ(20,42) ICSWH
0084      REWIND 20
0085      42 FORMAT(A1)
0086      WRITE(7,80) ICSWH
0087      80 FORMAT(5X,'ICSWH(MAIN)= ',A4)

      C
      C      PICK OPTION FOR 'BRARING' INTERVAL
      C

0088      IF(ICSWH.EQ.IS) GO TO 50
0090      IF(ICSWH.EQ.IN) GO TO 45
0092      IF(ICSWH.NE.IT.AND.ICSWH.NE.IP.AND.ICSWH.NE.ID) GO TO 36
0094      IF(ICSWH.EQ.IT) CALL BRARN(TJ,V,J,T,1)
0096      IF(ICSWH.EQ.IP) CALL BRARN(TJ,V,J,T,2)
0098      IF(ICSWH.EQ.ID) CALL BRARN(TJ,V,J,T,3)
0100      GO TO 36
0101      45 CALL BRARN(TJ,V,J,T,4)
0102      TJ=T
0103      VJ(J) = V
0104      J=J+1
0105      GO TO 36
0106      60 CALL CLINE(TJ,J,T)
0107      TJ=T
0108      J=J+1
0109      JMAX = NSP-1
0110      IF(J.GT.JMAX) GO TO 50
0112      GO TO 36
0113      50 STOP
0114      END

```

```

C
C      SUBROUTINE BRAKN
C
C      COMPUTES TEMPERATURE PROFILE OVER A "DOWNGRADE" CONTROL INTERVAL.
C      USER INPUTS DESIRED SPEED FOR ENTIRE INTERVAL.
C
0001      SUBROUTINE BRAKN(TJ,V,J,T,IOSWH)
0002      REAL K1,K2,KRET
0003      COMMON TKDT(15),SFPT(40,3),VJ(40),THETA(125),DIST(125),
*ISFPT(40),LSFPT(40),KRET,SFX,SFY,TAMB,W,GRLSWH(40),ET
0004      DIMENSION TPLT(125)
0005      WRITE(7,20) IOSWH
0006      20 FORMAT(5X,'IOSWH(BRAKN)= ',I)
0007      WRITE(20,2)
0008      REWIND 20
0009      2 FORMAT(5X,'ENTER SPEED (MPH) : ',,$)
0010      READ(20,4) V
0011      REWIND 20
0012      4 FORMAT(1E)
0013      K1 = TKDT(1) + TKDT(2)*V
0014      K2 = TKDT(3)/K1
0015      FLRAG = TKDT(6) + TKDT(7)*V + TKDT(8)*V**2
0016      HPENG = TKDT(11) + TKDT(12)*KRET
0017      IK1 = ISFPT(J)
0018      IRE = ISFPT(J+1)-1
0019      X=DIST(IK1)/SFX
0020      Y=TJ/SFY
0021      CALL PON
0022      CALL PLOT(X,0.,3)
0023      CALL PLOT(X,Y,4)
0024      CALL POF
0025      5 T=TJ
0026      TMAX=0.
0027      DO 6 I=IK1,IKF
0028      THETA(I) = THETA(I+1)
0029      HPB = ((W*THETA(I)-FLRAG)*V/375.)-HPENG
0030      FX=375.*HPB/V
0031      IF(HPB.LT.0.) HPB=0.
0033      DL = DIST(I+1)-DIST(I)
0034      DT=DL/V
0035      IF(ICSWH.EQ.4) ET=ET+DT
0037      T = T + (TAMB-T+K2*HPB)*(1-EXP(-K1*DL/V))
0038      TPLT(I)=T
0039      IF(T.GT.TMAX) XTMAX=DIST(I+1)
0041      IF(T.GT.TMAX) TMAX=T
0043      IF(IOSWH.EQ.3.OR.IOSWH.EQ.4) WRITE(20,10) J,1,THETA(I),DIST(I),V,
*DT,ET,FX,HPB,T
0045      10 FORMAT(5X,'BRAKE',2I4,2X,F9.6,2X,F6.2,2X,F5.1,2X,F8.6,2X,F6.3,2X,
*f7.0,2X,F6.0,2X,F6.0)
0046      6 CONTINUE
0047      CALL PON
0048      IF(ICSWH.EQ.1.OR.IOSWH.EQ.3) GO TO 21
0050      DO 18 I=IK1,IKF
0051      X=DIST(I+1)/SFX

```

FCRIRAN IV

```
0052      Y=IPLT(I)/SFY
0053      CALL PLOT(X,Y,2)
0054 \    18 CONTINUE
0055 \    21 CALL POFB
0056      WRITE(20,8) V,XIMAX,TMAX
0057      8 FORMAT(5X,'V= ',F5.1,' MPH   X= ',F6.2,' MILES   TMAX= ',F6.1)
0058      RETURN
0059      END
```

```

C
C   SUBROUTINE CLIME
C     TIM, S01106, 6/27/78
C
C     ROUTINE COMPUTES SPEED AND BRAKE TEMPERATURE ON
C     "UPGRADE" CONTROL INTERVAL ON EACH UPGRADE
C     SECTION, THE SPEED IS THAT FOR ZERO ACCELERATION AT
C     MAXIMUM ENGINE POWER OUTPUT.
C
0001   SUBROUTINE CLIME(TJ,J,T)
0002   REAL KRET,K1,K2
0003   COMMON TKDT(15),SFPT(40,3),VJ(40),THETA(125),DIST(125),
*ISFPT(40),DSFPT(40),KRET,SFX,SFY,TAME,V,GRDSWH(40),ET
0004   DIMENSION TPLT(125)
C
C     INITIALIZE INDICIES, COORDINATES, ETC. TO BEGIN
C     CONTROL INTERVAL.
C
0005   IK1=ISFPT(J)
0006   IKF=ISFPT(J+1)-1
0007   X=DIST(IK1)/SFX
0008   Y=TJ/SFY
0009   CALL PON
0010   CALL PLOT(X,0.,3)
0011   CALL PLOT(X,Y,4)
0012   CALL POFF
0013   CV=-375.*TKDT(13)/TKDT(7)
0014   T=TJ
C     CALCULATE TEMPERATURE PROFILE OVER CONTROL INTERVAL
0015   DO 2 I=IK1,IKF
0016   THETA1=THETA(I+1)
0017   EV=-(V*THETA1-TKDT(6))/TKDT(7)
0018   V=-(EV/2.)+(EV**2-4.*CV)**.5/2.
0019   IF(V.GT.55.) V=55.
0021   K1=TKDT(1)+TKDT(2)*V
0022   K2=TKDT(3)/K1
0023   FDRAG=TKDT(6)+TKDT(7)*V+TKDT(8)*V**2
0024   HPENG=TKDT(11)+TKDT(12)*KRET
0025   HPX=((V*THETA1-FDRAG)*V/375.)-HPENG
0026   FX=375.*HPX/V
0027   DL = DIST(I+1)-DIST(I)
0028   LT=DL/V
0029   ET=ET+LT
0030   T=T+(TAME-T)*(1-EXP(-K1*DL/V))
0031   TPLT(I)=T
0032   WRITE(20,14) J,I,THETA1,DIST(I),V,DT,ET,FX,HPX,T
0033   14 FORMAT(5X,'NONBRAKE',2I4,2X,F9.6,2X,F6.2,2X,F5.1,2X,F8.6,2X,F6.3,2X,
*F7.0,2X,F6.0,2X,F6.0)
0034   2 CONTINUE
0035   CALL PON
0036   DO 20 I=IK1,IKF
0037   X=DIST(I+1)/SFX
0038   Y=TPLT(I)/SFY
0039   CALL PLOT(X,Y,4)

```

FCFTRAN IV

0040 20 CONTINUE
0041 CALL PCFF
0042 RETURN
0043 END

APPENDIX D

DERIVATION OF \bar{V}_{\max} APPROXIMATION

APPROXIMATION OF HP_B

1. Write exact HP_B equation from Eq. 19

$$HP_B = \frac{F_B \bar{V}}{375} = \frac{(W\theta - F_{\text{drag}}) \bar{V}}{375} - HP_{\text{eng}} \quad (D-1)$$

$$F_{\text{drag}} = 450 + 17.3 \bar{V} \text{ lb} \quad (\text{from Eq. 22}) \quad (D-2)$$

$$HP_{\text{eng}} = 73 \text{ hp} \quad (\text{from Eq. 23, with retarder off}) \quad (D-3)$$

$$\begin{aligned} HP_B &= \frac{(W\theta \bar{V} - 450 \bar{V} - 17.3 \bar{V}^2)}{375} - 73 \text{ hp} \\ &= -73 + .00267(W\theta - 450.) \bar{V} - .04613 \bar{V}^2 \text{ hp} \end{aligned} \quad (D-4)$$

2. Plot exact HP_B equation (solid curves in Fig. D-1).
3. Make best linear approximation to each exact $W\theta$ curve by fitting straight lines through 20-40 mph region with common origin $HP_B = -34$.
4. Plot slope $[d(\text{approx. } HP_B)/d\bar{V}]$ of approximating lines vs. $W\theta$ (Fig. D-2).
5. Compute approximate HP_B

$$\begin{aligned} HP_B &\doteq (\text{approx. } HP_B)_{V=0} + \frac{\Delta(\text{approx. } HP_B)}{\Delta \bar{V}} \bar{V} \\ &= -34 + (-3.8 + .0026 W\theta) \bar{V} \quad \text{hp} \end{aligned} \quad (D-5)$$

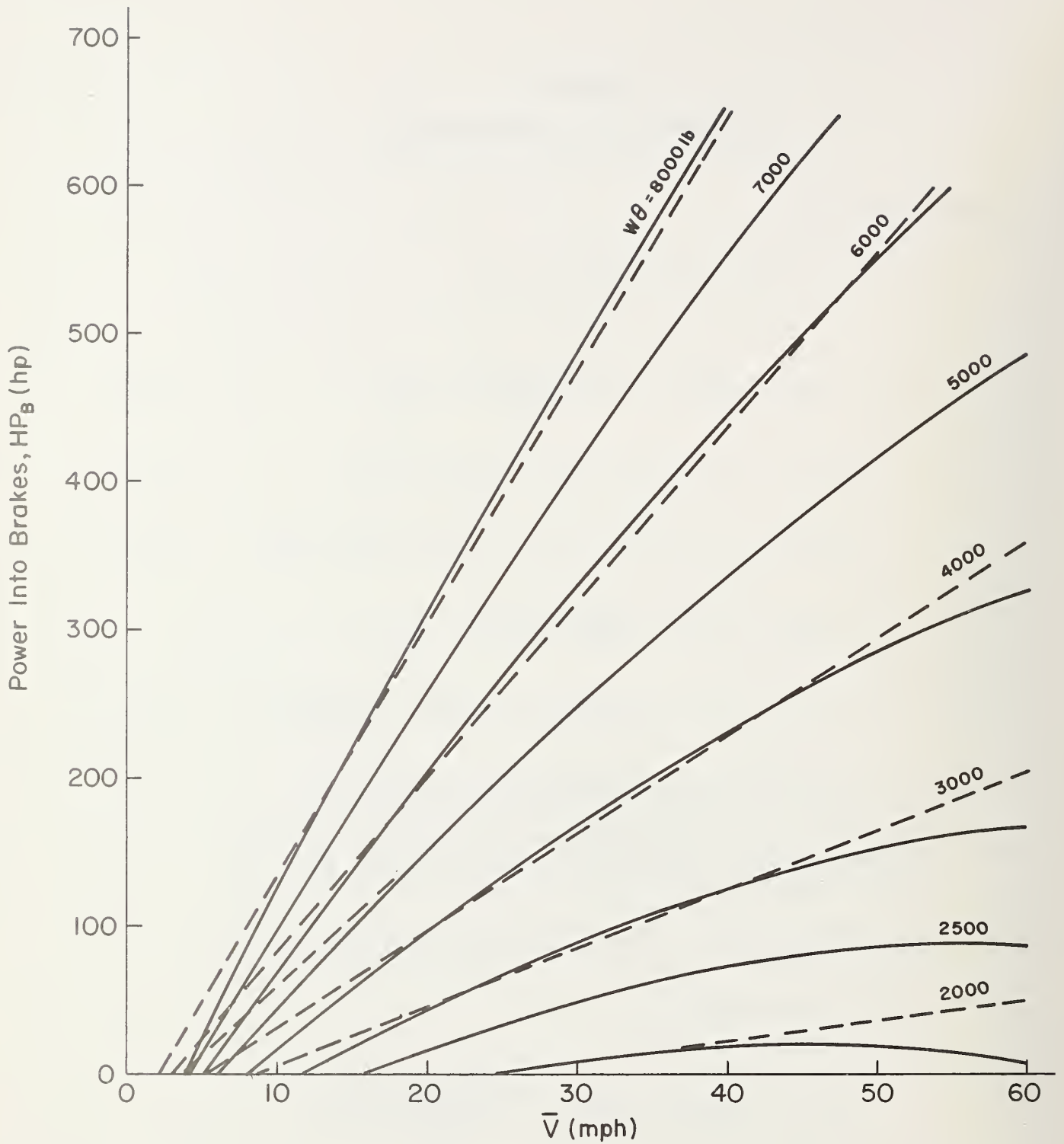


Figure D-1. Exact (solid lines) and Approximate (dashed lines) Brake Power Required Curves

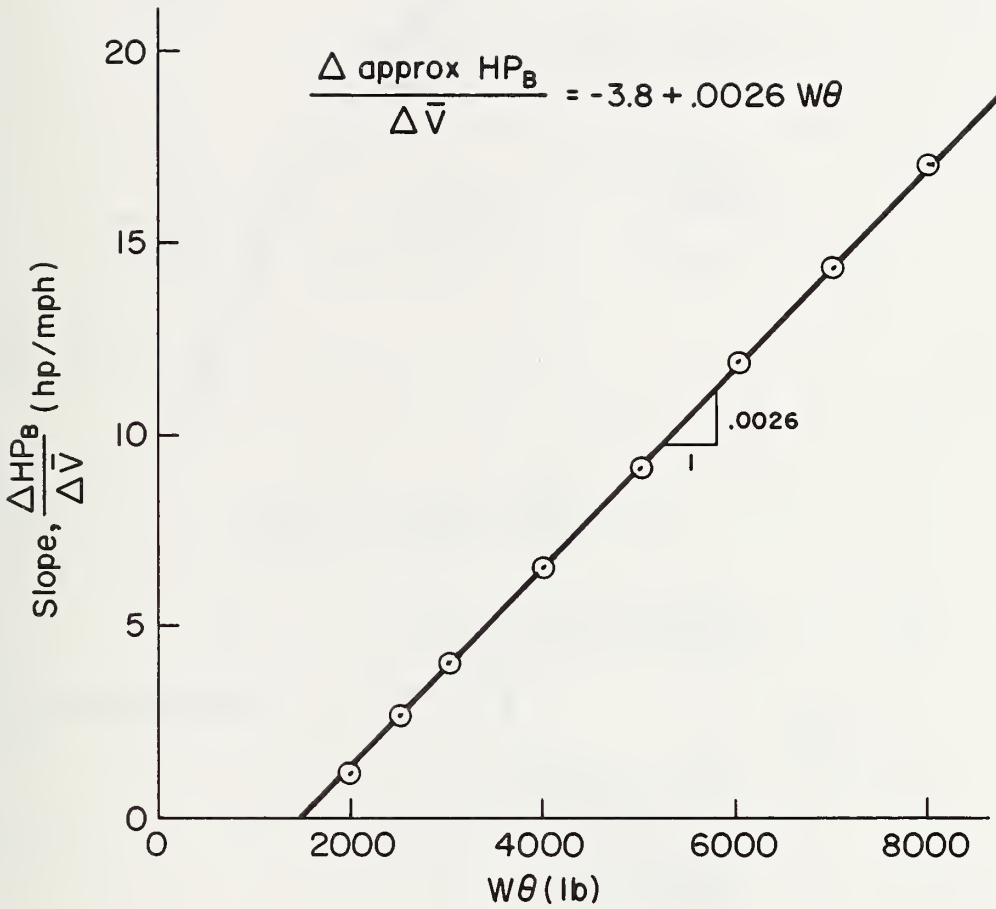


Figure D-2. Variation of Speed Derivative of HP_B Approximation Versus $W\theta$

APPROXIMATION OF $1 - e^{-K_1 L/\bar{V}}$ WITH PADÉ FORM

Letting $y = K_1 L/\bar{V}$, the modified Padé approximation of $1 - e^{-y}$ is

$$\begin{aligned}
 (1 - e^{-y}) &\doteq 1 - \frac{1 + Ay}{1 + By} \\
 &= \frac{1 + By - 1 - Ay}{1 + By} = \frac{\alpha_1 y}{1 + \alpha_2 y} \\
 &= \frac{\alpha_1 K_1 L/\bar{V}}{1 + \alpha_2 K_1 L/\bar{V}} = \frac{\alpha_1 K_1 L/\bar{V}}{(\bar{V} + \alpha_2 K_1 L)/\bar{V}} = \frac{\alpha_1 K_1 L}{\bar{V} + \alpha_2 K_1 L} \quad (D-6)
 \end{aligned}$$

where $\alpha_1 = B' - A'$ and $\alpha_2 = B'$. The domain of interest for y is indicated in Fig. D-3.

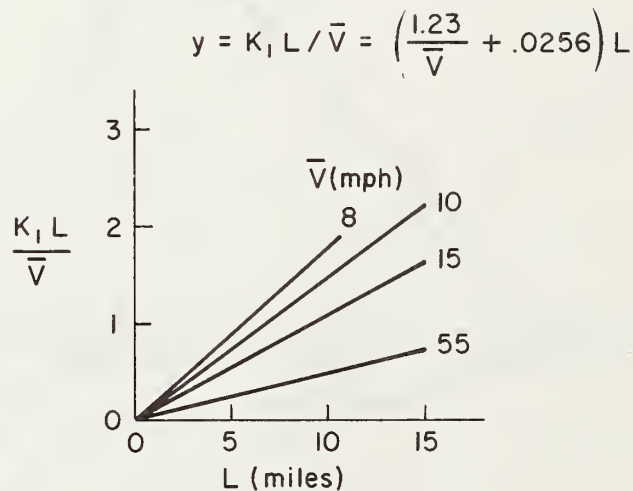


Figure D-3. Domain of Interest for x

Best fit in domain of interest is dashed line in Fig. D-4: $\alpha_1 = 1.15$, $\alpha_2 = 0.80$.

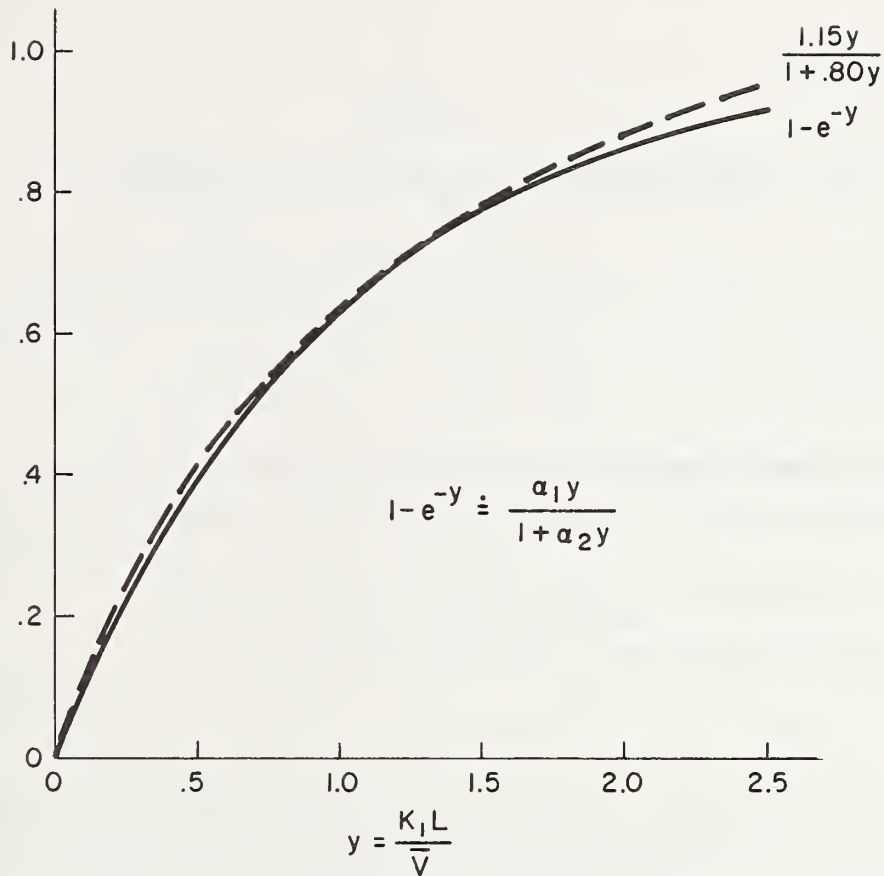


Figure D-4. Comparison of Function $1 - e^{-y}$ With Its Padé Approximation

\bar{V}_m APPROXIMATION

$$T - T_0 = (T_\infty - T_0 + K_2 HP_B) \left(1 - e^{-K_1 L / \bar{V}} \right) \quad (D-7)$$

where

$$K_1 = \delta_0 + \delta_1 \bar{V} = 1.23 + .0256 \bar{V} \quad \frac{1}{\text{hr}} \quad (\text{from Eq. 20})$$

and

$$K_1 K_2 = 12.3 \quad ^\circ\text{F}/\text{hp} - \text{hr} \quad (\text{From Eq. 20 and 21})$$

$$HP_B \doteq \beta_0 + (\beta_1 + \beta_2 W\theta) \bar{V} = -34 + (-3.8 + .0026W\theta) \bar{V}$$

Therefore Eq. D-7 may be written as

$$(T - T_0) - (T_\infty - T_0) \left(\frac{\alpha_1 K_1 L}{\bar{V} + \alpha_2 K_1 L} \right) - [\beta_0 + (\beta_1 + \beta_2 W\theta) \bar{V}] K_2 \left(\frac{\alpha_1 K_1 L}{\bar{V} + \alpha_2 K_1 L} \right) = 0 \quad (D-8)$$

which implies

$$(T - T_0)[\bar{V} + \alpha_2(\delta_0 + \delta_1\bar{V})L] - (T_\infty - T_0)\alpha_1(\delta_0 + \delta_1\bar{V})L - [\beta_0 + (\beta_1 + \beta_2W\theta)\bar{V}][K_2K_1]\alpha_1L = 0 \quad (D-9)$$

Rearranging

$$\begin{aligned} & \overbrace{\{(T - T_0) + \alpha_2\delta_1L - (T_\infty - T_0)\alpha_1\delta_1L - (\beta_1 + \beta_2W\theta)[K_1K_2]\alpha_1L\}}^A \bar{V} \\ & \underbrace{\{(T - T_0)\alpha_2\delta_0L - (T_\infty - T_0)\alpha_1\delta_0L - \beta_0[K_2K_1]\alpha_1L\}}_B L = 0 \end{aligned} \quad (D-10)$$

$$\begin{aligned} \bar{V} & \doteq \frac{-B}{A} = \frac{\{(T - T_0)(.80)(1.23)L - (T_\infty - T_0)(1.15)(1.23)L + 34(12.3)(1.15)L\}L}{\left\{\left(\frac{T - T_0}{L}\right) + (.80)(.0256) - (T_\infty - T_0)(1.15)(.0256) - (-3.8 + .0026W\theta)(12.3)(1.15)\right\}} \\ & = \frac{-.984(T - T_0) + 1.415(T_\infty - T_0) - 480.9}{\left(\frac{T - T_0}{L}\right) + .020 - .0294(T_\infty - T_0) - 14.1(-3.8 + .0026W\theta)} \\ & = \frac{-482 + 1.415(T_\infty - T_0) - .984(T - T_0)}{53.6 - .0367W\theta - .0294(T_\infty - T_0) + (T - T_0)/L} \end{aligned} \quad (D-11)$$

Thus for

$$T_\infty = 90^\circ \quad \text{and} \quad T_0 = 150^\circ$$

$$\bar{V} \doteq \frac{-837.5}{55.4 - .0367W\theta + 275/L} \quad (D-12)$$

APPENDIX E

EXTENSION OF THE GSRS TO MULTIGRADE HILLS

To this point the GSRS has been considered for single grades of constant slope. Of course, on any real grade the slope varies continuously. If these variations in slope are sufficiently small, the grade may be adequately represented as a single grade of constant slope. However, on more complex grades the question of representing a grade by averaging the slope on one or more subintervals becomes a difficult issue. True multigrade hills, which have significant nonbraking intervals where partial brake cooling occurs, represent the most complex problem.

The problems in extending the GSRS to complex grades arise from the additional complexities in the downgrade braking model. Specifically, two of the basic assumptions made in deriving the integrated form of the braking model, Eq. 18, are not valid in general for complex grades. First, θ is not a constant and furthermore may be less than the threshold value, θ_0 , resulting in a nonbraking, $HP_B \equiv 0$, interval. Secondly, the descent speed may not be constant everywhere on the grade. On upgrade sections the prohibition against downshifting does not apply and, in fact, speed may be reduced through downshifting on steep upgrades. The prohibition against downshifting does still apply to braking intervals and thus they are constant speed intervals; however, the speed may be different on each braking interval if the driver shifts between them.

To develop multigrade GSRS procedures, a real multigrade, the Donner grade on I-80 in California, was used as an example case. The altitude profile of this grade was measured using the altimeter technique discussed in Appendix B. These measurements produced 104 altitude-distance pairs (i.e., 103 grade segments) which when plotted produce the altitude profile shown in Fig. 13a. A slope profile was then determined by computing the slope on each grade segment as the change in altitude on the segment divided by the segment length, Fig. 13b.

For a simple initial examination of the effect of this complex geometry on brake temperature, a temperature profile was calculated for a typical truck (80,000 lb, no retarder) at a constant 37 mph using the sequential calculation procedure, Appendix C, Fig. E-1. Obviously the use of a constant speed is an idealization; however, general trends so obtained are meaningful. The most important characteristic of this temperature profile is that it is not monotonic but instead consists of a complex pattern of heating and cooling.

An obvious first concern is the extent to which the grade representation may be simplified by appropriated slope averaging over groups of grade segments. To consider this problem, three approximate representations were made in which the original 103 grade segments were simplified into 47, 25, and 6 constant slope segments respectively. In each case the averaged segments were picked to be the apparent "best fit" of the grade. Brake temperature profiles at 37 mph were then calculated and compared to the profile for the original ("exact") representation, Fig. E-1.

It can be seen that as the number of averaged segments decreases, the approximation of the exact temperature profile deteriorates. Furthermore a reduction in the number of segments generally results in a lower temperature estimate. The basic conclusion here is that care must be taken in averaging grade data and that some physical rationale for averaging is needed.

As has been noted previously, brake cooling will occur on nonbraking intervals; thus a first step would be to avoid including significant braking and nonbraking intervals in a single averaged grade segment. To illustrate, consider an 8 mile multigrade consisting of 8 alternating 7 percent downgrades and 7 percent upgrades as shown in Fig. E-2a. Obviously if the multigrade is averaged over the entire grade length, i.e., from 0 to 8 miles, the slope would be 0. Thus if the brake temperature was computed from the average slope there would be zero temperature rise. However, when the temperature profile is computed for the actual grade profile, Fig. E-2b, the temperature rise at the end of 8 miles is 540° F. The reason for this net temperature gain is that the temperature rise on the braking intervals is greater than the cooling which occurs on the nonbraking intervals.

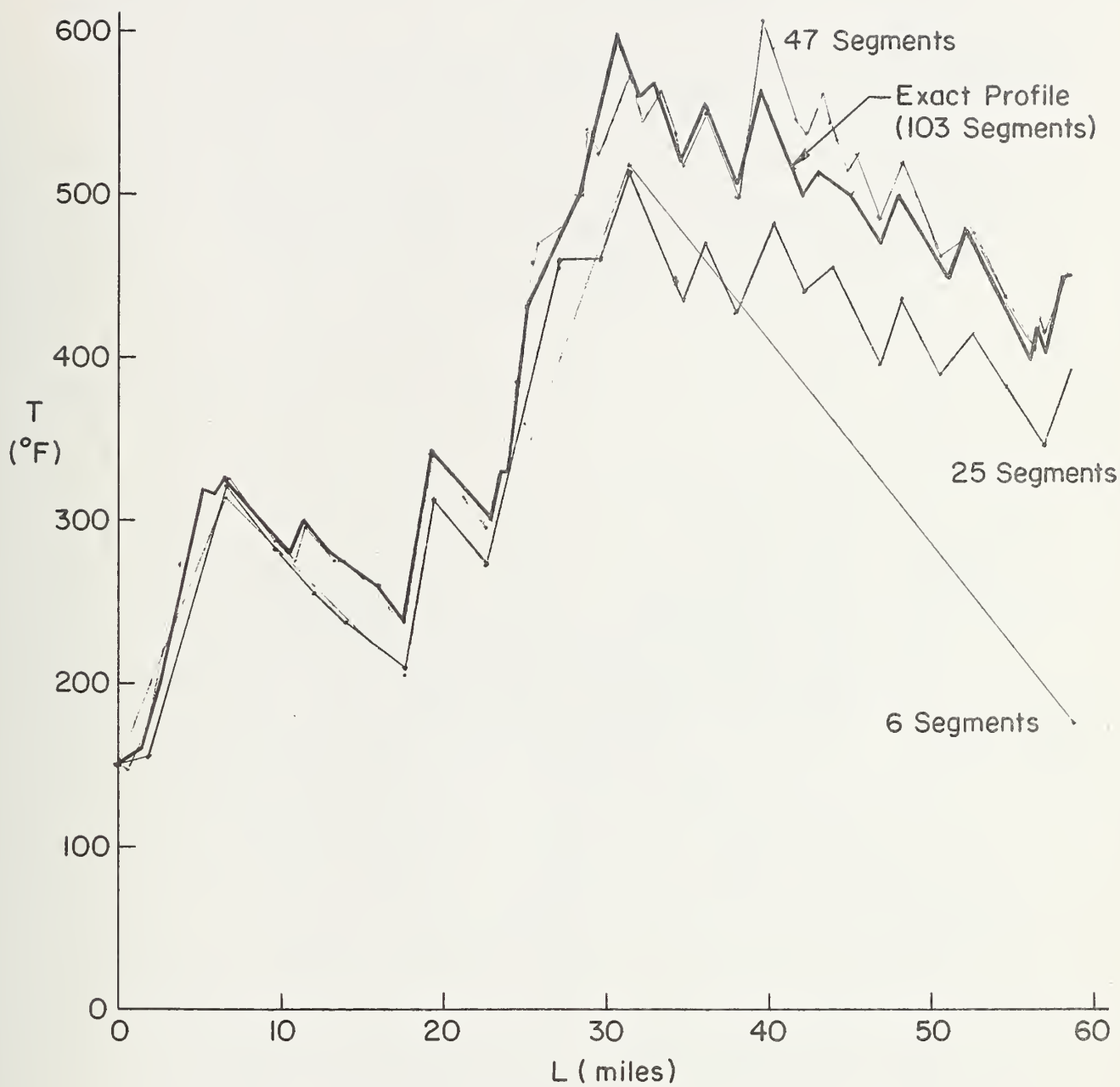
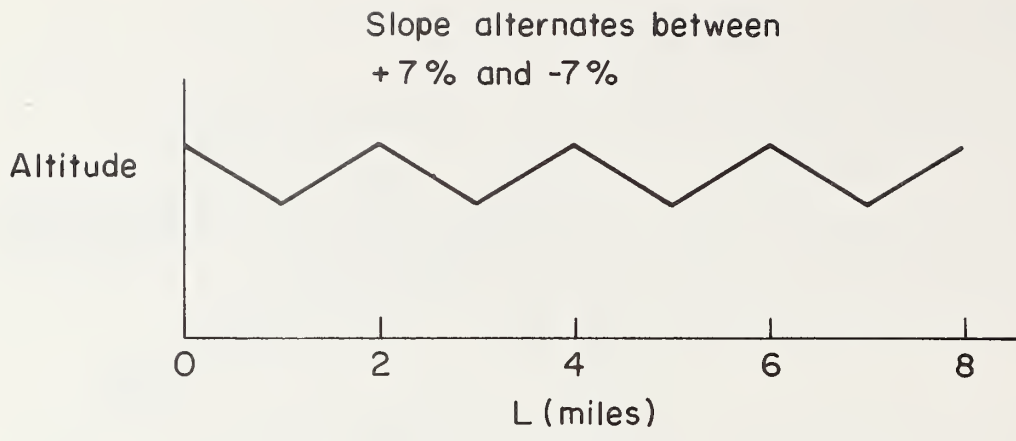
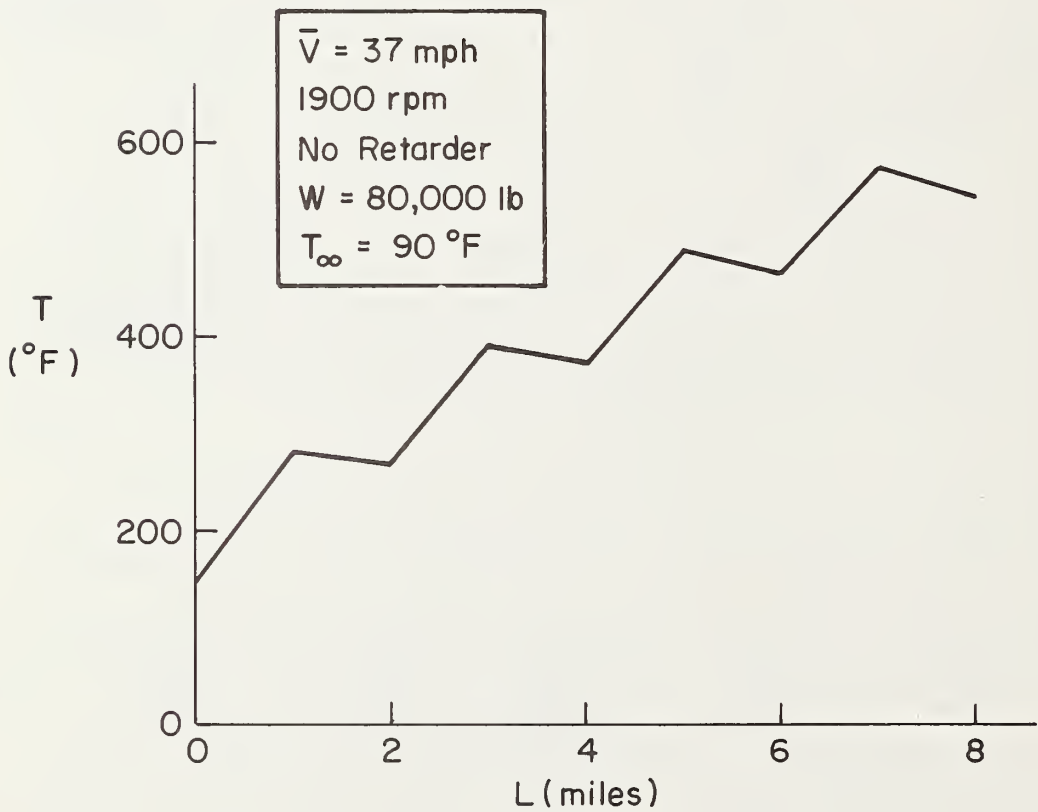


Figure E-1. Brake Temperature Profiles on the Donner Grade for 3 Approximate Representations Compared to the "Exact" Profile



a)



b)

Figure E-2. Hypothetical Multigrade with Zero Average Slope Which Produces a Non-Zero Temperature Rise

The foregoing considerations imply that we can view a multigrade hill as a series of constant speed braking intervals separated by nonbraking intervals on which the driver is free to shift as required. Thus the control problem for the driver is simply to select the correct speed for his truck on each braking interval, and the requirement for the GSRs is to aid the driver in each speed selection. This may be accomplished by placing GSR and/or WSS signs at the beginning of each braking interval. Drivers will use these signs in exactly the same manner as for a single grade hill. The differences between single grade and multigrade hills will only affect the highway engineer who must generate the signs.

This approach requires that a unique set of braking intervals be defined; however, the actual braking intervals change with θ_0 which is a function of W and \bar{V} (see Fig. 20). This effect may be considered an additional weight effect which takes the form of a threshold nonlinearity. It appears that the best procedure for treating this problem is to define the braking intervals according to the θ_0 for a "worst case" truck, i.e., an 80,000 lb truck descending at 30 mph. Under this strategy, a multigrade will contain the largest possible percentage of braking intervals. For trucks operating at less than the maximum 80,000 lb weight and/or at speeds other than 30 mph, there will in general be portions of the "worst case" braking intervals where braking will not be required.

With a unique set of braking intervals defined in this manner, the generation of GSR/WSS signs becomes a matter of determining \bar{V}_{\max} at any weight on any braking interval. There are two primary problems in determining \bar{V}_{\max} . First the slope may vary on a braking interval and thus the maximum brake temperature may not occur at the end of the braking interval which violates the basic GSR assumption that $T_{\max} = T_{\text{fin}}$. It is still possible to define \bar{V}_{\max} from the more general constraint that $T_{\max} \leq T_{\text{lim}}$, Eq. 26, but \bar{V}_{\max} is now more difficult to calculate. The second problem in determining \bar{V}_{\max} is that the initial brake temperature on each braking interval, T_{0j} , will in general be different. The subtle aspect of this problem is that there are many (actually an infinite number) of possible T_{0j} distributions for which the $T_{\max} \leq T_{\text{lim}}$ constraint may be satisfied if speed is chosen correctly on each braking interval. However, before \bar{V}_{\max} can be determined for a braking interval, T_{0j} must be specified and

thus some rationale must be developed for defining a T_{Oj} distribution. It is important to note here that the procedures to follow for determining \bar{V}_{\max} are independent of the specific T_{Oj} distribution used but rather only require that some distribution be specified.

A rationale for picking a T_{Oj} distribution may be derived from considering the optimal control problem, i.e., seeking the distribution that will lead to a safe descent in minimum time. The optimal control problem for multigrade hills is quite complex and a general rigorous solution to the problem is beyond the scope of this program. However, an intuitive understanding of the requirements for optimality can be obtained by considering an example multigrade with two constant slope braking intervals separated by a nonbraking interval just long enough for downshifting but not long enough for any significant cooling to occur. Specifically, a 7 percent 3.6 mi braking interval (index $j = 1$) separated by a short non-braking interval ($j = 2$) from a 5 percent 8.4 mi braking interval ($j = 3$). As individual single grades, these two braking intervals would be of comparable severity.

The first step is to compute the final temperature on the first braking interval, T_{f1} , as a function of speed, \bar{V}_1 . This is plotted as a dashed line in Fig. E-3 and shows that $\bar{V}_1 \leq 15$ mph for $T_{f1} \leq T_{lim}$. Since cooling on the non-braking interval is negligible, this curve also gives the variation of T_{O3} with \bar{V}_1 . Using this T_{O3} curve we may compute contours of T_{f3} as a function of \bar{V}_3 for different values of \bar{V}_1 (solid lines in Fig. E-3).

From the intersection of these contours (solid curves in Fig. E-3) with the T_{lim} line, the T_{lim} line may be transformed into the $\bar{V}_1 - \bar{V}_3$ plane as the solid line in Fig. E-4. This line, for $V_1 < 15$ mph, is the locus of \bar{V}_1, \bar{V}_2 pairs for which $T_{\max} = T_{f3} = T_{lim}$. The optimal descent strategy is thus the \bar{V}_1, \bar{V}_2 pair which minimizes time on the grade. This pair may be found by plotting contours of constant descent time for the entire multigrade, Δt , where

$$\Delta t = \frac{L_1}{\bar{V}_1} + \frac{L_3}{\bar{V}_3} \quad (E-1)$$

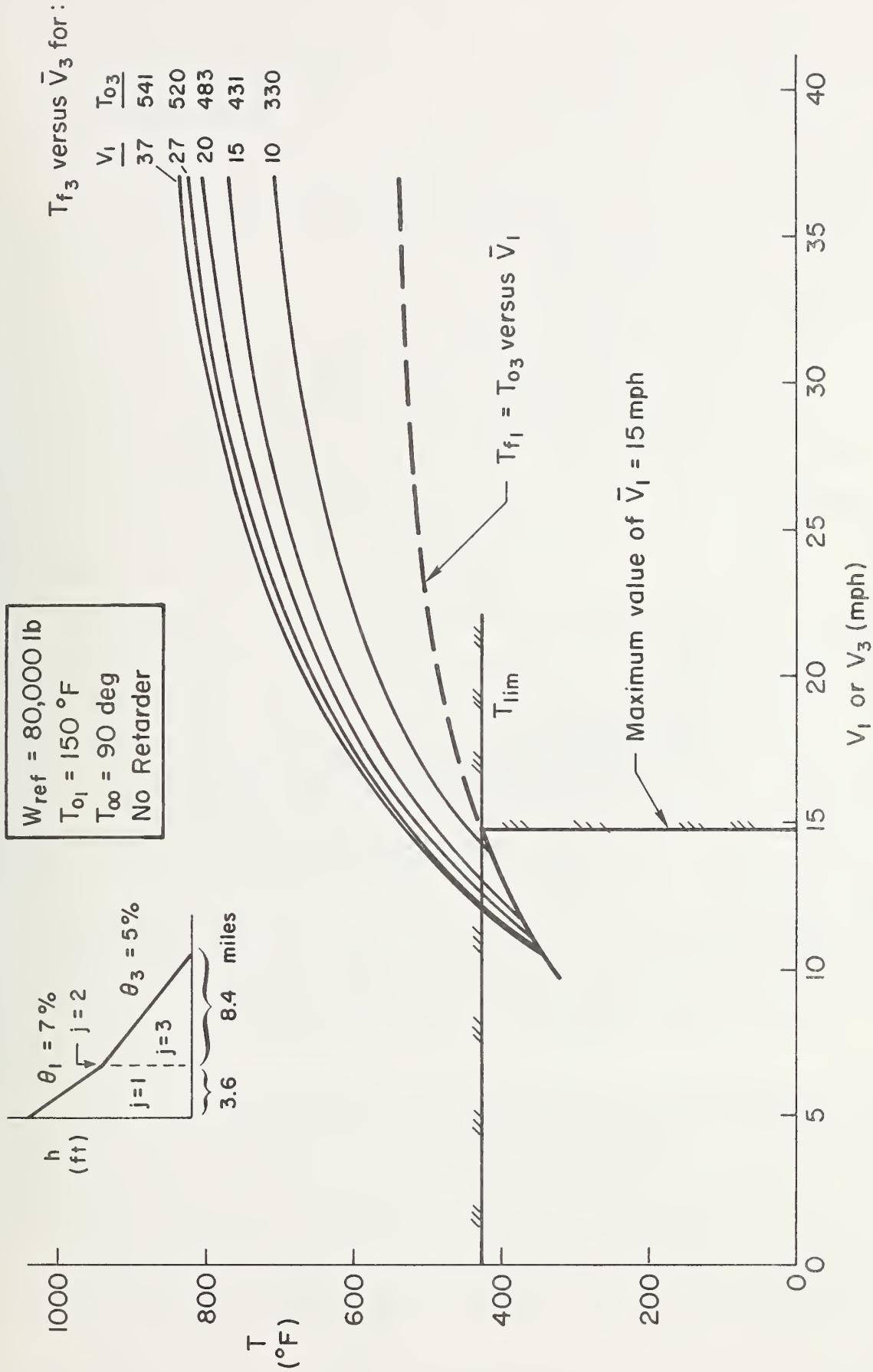


Figure E-3. Determination of T_{f3} as a Function of \bar{V}_1 and \bar{V}_3

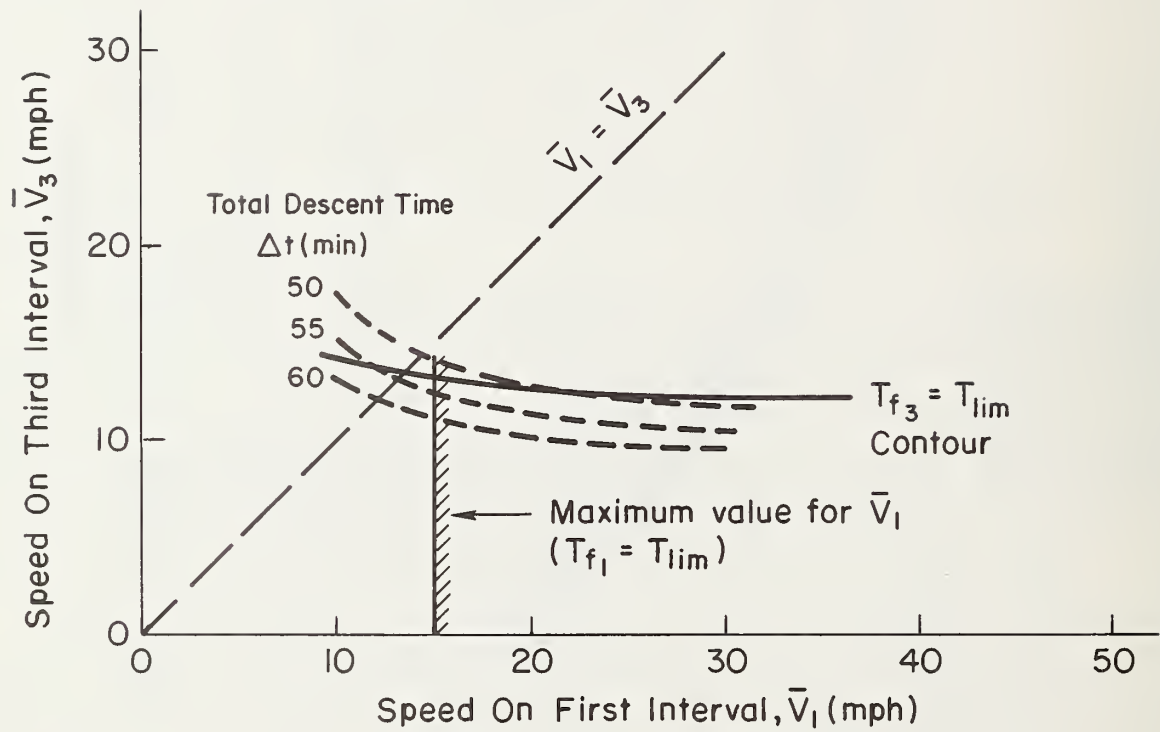
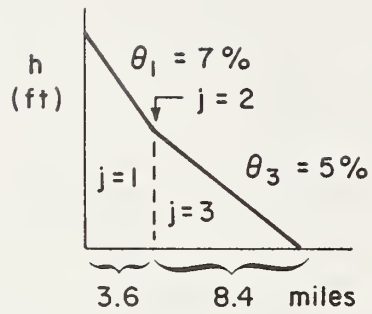


Figure E-4. Determination of \bar{V}_1, \bar{V}_3 Pair Which Produces Minimum Descent Time

Several descent time contours have been plotted (dashed lines) in Fig. E-4, and it may be seen that the minimum time of descent occurs when the maximum value of \bar{V}_1 , 15 mph, is used. That is, the first braking interval should be driven just as if it were a single grade, i.e., with $\bar{V}_1 = \bar{V}_{\max}$, so that $T_{f_1} = T_{lim}$. The second ($j = 3$) braking interval should then be driven at the speed which will maintain brake temperature at T_{lim} .

These calculations have been repeated with the braking intervals reversed and with two geometrically identical braking intervals with the same result, namely, that the first braking interval should be driven fast enough to make $T_{f_1} = T_{lim}$ and the second braking interval driven to maintain $T = T_{lim}$. The descent time advantage of the optimal strategy is not large compared to a $\bar{V}_1 = \bar{V}_2$ descent for these examples. However, if the first braking interval were less severe so that V_1 could be larger, the optimal strategy would have a much larger advantage.

For multigrades consisting of more than two braking intervals, the optimization problem is conceptually the same as in the examples above; however, the simple graphical procedure cannot be used. Instead it would be necessary to use formal optimization techniques such as dynamic programming which is beyond the scope of this program. The "fast-first" descent, however, can be extended to the general multigrade case and it appears that this may be the optimal strategy. That is, each braking interval will be driven at the speed (\bar{V}_{\max}) which makes $T_{f_j} = T_{lim}$ (or if this is not possible for a shallow downgrade at $V_j = 55$ mph). On the basis of these considerations, the fast-first descent strategy will be used to extend the GSRS to multigrade hills, with the understanding that the basic procedures which follow would work as well with any other descent strategy.

Having established the fast-first descent rationale, there still remains a problem in defining V_{\max} on certain braking intervals, i.e. the determination of T_{\max} when it does not occur at the end of the interval due to large θ variations. The most straightforward procedure for defining \bar{V}_{\max} in this case would be to simply calculate the temperature profile over the braking interval for several speeds, using the sequential procedure of Appendix C,

and picking \bar{V}_{\max} ; as the \bar{V}_j value which makes $T_{\max,j} = T_{\text{lim}}$ (see Fig. E-5). These calculations are tedious to perform manually, but are accomplished quickly and efficiently (including plotting) when programmed on a digital computer (the BTEMP program in Appendix C). This procedure is referred to as the "simulation" procedure since it simulates a field test for empirical determination of \bar{V}_{\max} . This simulation procedure can define in minutes \bar{V}_{\max} values that would take days or weeks to determine with an actual instrumented truck.

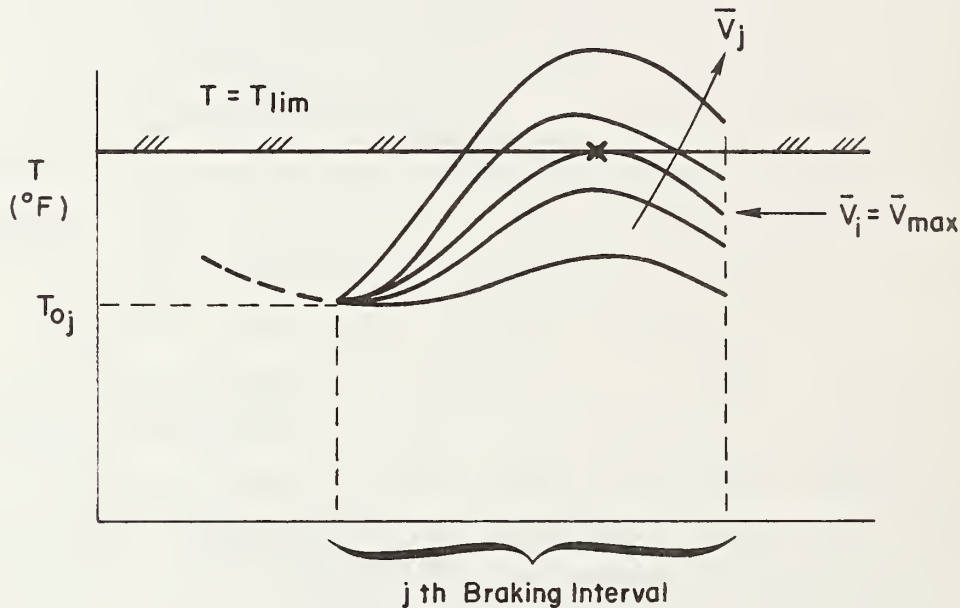


Figure E-5. Iterative Determination of $\bar{V}_{\max,j}$

The determination of \bar{V}_{\max} (at 80,000 lb) along the Donner grade, using the BTEMP program on the STI PDP-11 digital computer, is illustrated by the T profile in Fig. E-4. To start a \bar{V}_{\max} run, the engineer inputs the truck parameters, grade geometry, and truck weight. A trial speed is selected for the first braking interval ($j = 1$), and the computer calculates and plots the temperature profile. With a few speed iterations it can be seen that T_{lim} is not reached even at the speed limit, thus $\bar{V}_{\max,1} = 55$ mph. The program then automatically calculates the speeds and temperature profile for the following nonbraking interval ($j = 2$) to define T_{0j} . The engineer then repeats the speed iteration process sequentially along the grade to define a \bar{V}_{\max} for each braking interval. The \bar{V}_{\max} values at 80,000 lb, Fig. E-6, may be immediately converted to

GSR values for each braking interval using the GSR categories developed in Section IV-D (see Table E-1).

TABLE E-1. GSR CATEGORIES AT W = 80,000 lbs

V_{\max} at 80,000 lb	GSR
39-55 mph	1
33-39	2
28-33	3
23-28	4
20-23	5
17-20	6
14-17	7
12-14	8
10-12	9
Less than 10	10

The weight-specific speeds for each WSS sign would be generated in a similar manner except that the limiting weight for each weight class would be used in the calculations instead of the 80,000 lb representative weight.

The simulation procedure is quite powerful and convenient to use when implemented on a minicomputer. However, it is still highly desirable to simplify this procedure as much as possible and in particular to make the multigrade procedures more like the single grade procedures. The problem of variations in T_{Oj} cannot be eliminated; however, some useful approximations can be made in the determination of T_{\max} . It has been noted that variations in θ over a braking interval may result in a non-monotonic T profile which could produce a T_{\max} on the interior of the interval. Such a non-monotonic profile would require $dT/dx < 0$ for some significant portion of the interval. This derivative may be computed from the differential form of the brake temperature equation, Eq. 9, as

$$\frac{dT}{dx} = \frac{HP_B}{m_B C V} - \frac{hA_c}{m_B C} (T - T_\infty) \quad (E-2)$$

Thus it may be seen that on a severe braking interval, where HP_B tends to be large, dT/dx will tend to be positive except possibly where $T \doteq T_{lim}$. The implication is that T will increase in a roughly monotonic way on braking intervals; consequently, we may approximate T_{max_j} as T_{f_j} . Numerical experimentation on the Donner grade supports this conclusion (see the $j = 7$ braking interval in Fig. E-6).

However, to make this approximation for T_{max_j} really useful, a simple formula is needed for computing T_{f_j} . Such an expression may be derived through the use of an "equivalent" slope concept. The equivalent slope, θ_{equiv} , for a braking interval of length L_j is defined as the constant slope braking interval of length L_j which would have the same T_{f_j} as the interval in question. As the variation in θ over an interval goes to zero, θ_{equiv} approaches the geometric average slope

$$\theta_{ave} \equiv \frac{\text{change in altitude on interval in ft}}{5280 \times (\text{interval length in miles})} \quad (E-3)$$

θ_{equiv} may be computed by the procedure indicated schematically in Fig. E-7a and E-7b.

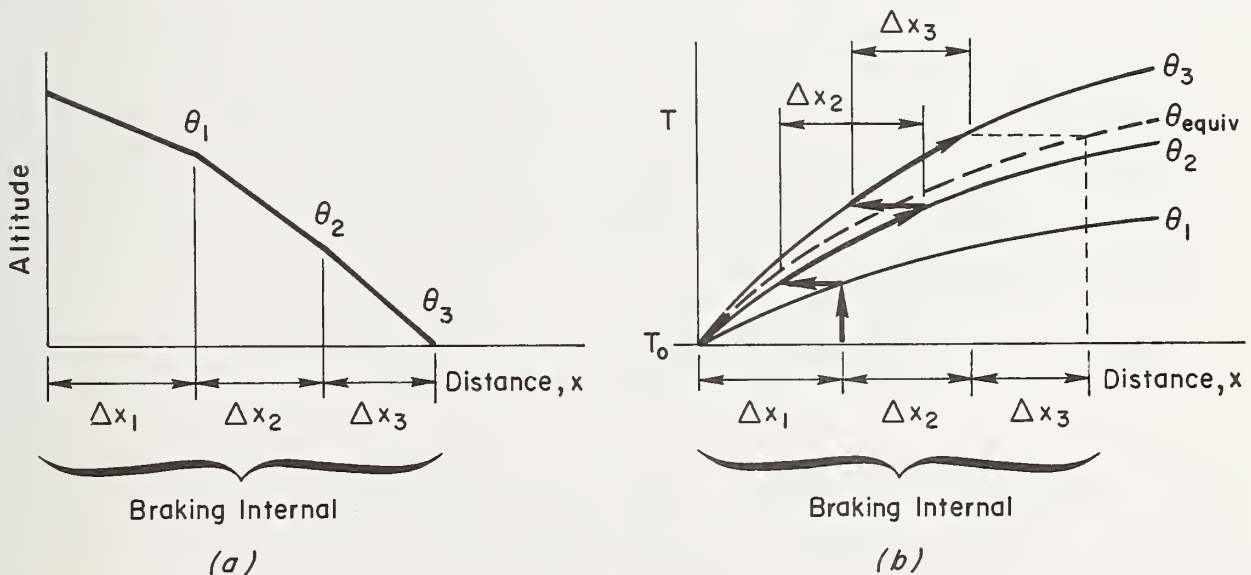


Figure E-7. Graphical Procedure for Computing θ_{equiv}

Alternatively, an analytic expression may be derived for θ_{equiv} by the use of Duhamel's integral as

$$\theta_{\text{equiv}_j} = \left\{ \frac{e^{-(K_1/\bar{V})L_j}}{e^{-(K_1/\bar{V})L_j} - 1} \right\} \sum_{i=1}^n \theta_i \left[e^{(K_1/\bar{V})x_i} - e^{(K_1/\bar{V})x_{i-1}} \right] \quad (\text{E-4})$$

where i is the grade (measurement) segment index. It can be seen from Eq. E-4 that θ_{equiv} is, strictly speaking, a function of \bar{V} ; however, it has been found that this variation may be neglected for practical work.

The determination of T_{f_j} from θ_{equiv_j} is not really practical because the calculation of θ_{equiv} is as complex as the calculation of the temperature profile. However, by making θ_{equiv} calculations for some real and hypothetical grades, it has been found that for real grades θ_{ave} is generally a reasonable approximation for θ_{equiv} . For instance, a typical value for θ_{equiv} on the Airport grade section of the Donner grade ($j = 7$ in Fig. E-6) is $\theta_{\text{equiv}} = 0.0451$ which is almost identical to the geometric average, $\theta_{\text{ave}} = 0.0452$, even though the slope variation is quite complex.

The practical implication of this result is that we may generally represent braking intervals for computation of \bar{V}_{max} as constant slope downgrades with $\theta = \theta_{\text{ave}}$. Furthermore, the nonbraking intervals may also be treated as constant slope, constant speed intervals with $\theta = \theta_{\text{ave}}$ and an average speed, \bar{V}_j , given by

$$\bar{V}_j = 50 + 500 \theta_{\text{ave}_j} \quad \text{mph} \quad (\text{E-5})$$

which is developed in Appendix C. Thus a multigrade may be simply approximated as a series of constant slope, constant speed intervals which allows T_{f_j} on each interval to be calculated in one step from Eq. 18.

On each braking interval $\bar{V}_{\max j}$ and the corresponding T_{fj} may be determined by calculating T_{fj} for several values of \bar{V}_j as shown in Fig. E-8.

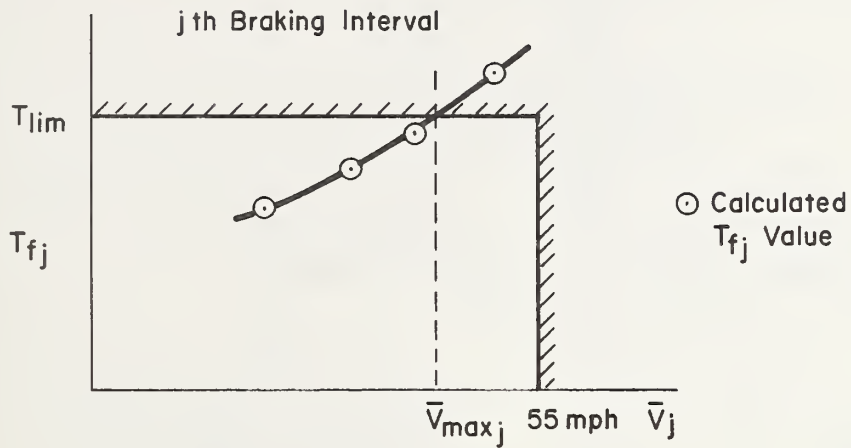


Figure E-8. Calculation of \bar{V}_{\max} for j th Braking Interval

If the T versus \bar{V} curve intersects the T_{\lim} line (as shown in Fig. E-8), the speed at the intersection is \bar{V}_{\max} and $T_{fj} = T_{\lim}$. If the curve intersects the speed limit line, $\bar{V}_{\max} = 55$ mph and the temperature at the intersection is T_{fj} .

\bar{V}_{\max} may now be determined for each braking interval by use of the sequential procedure shown in the flow chart of Fig. E-9. This procedure is analogous to the sequential calculation in the simulation method, Fig. C-2, except that now each calculation step is made over an entire braking or nonbraking interval rather than a grade segment. By computing \bar{V}_{\max} on each braking interval with this procedure, GSR and WSS signs may be generated in the same way as they were generated using the complete simulation procedure.

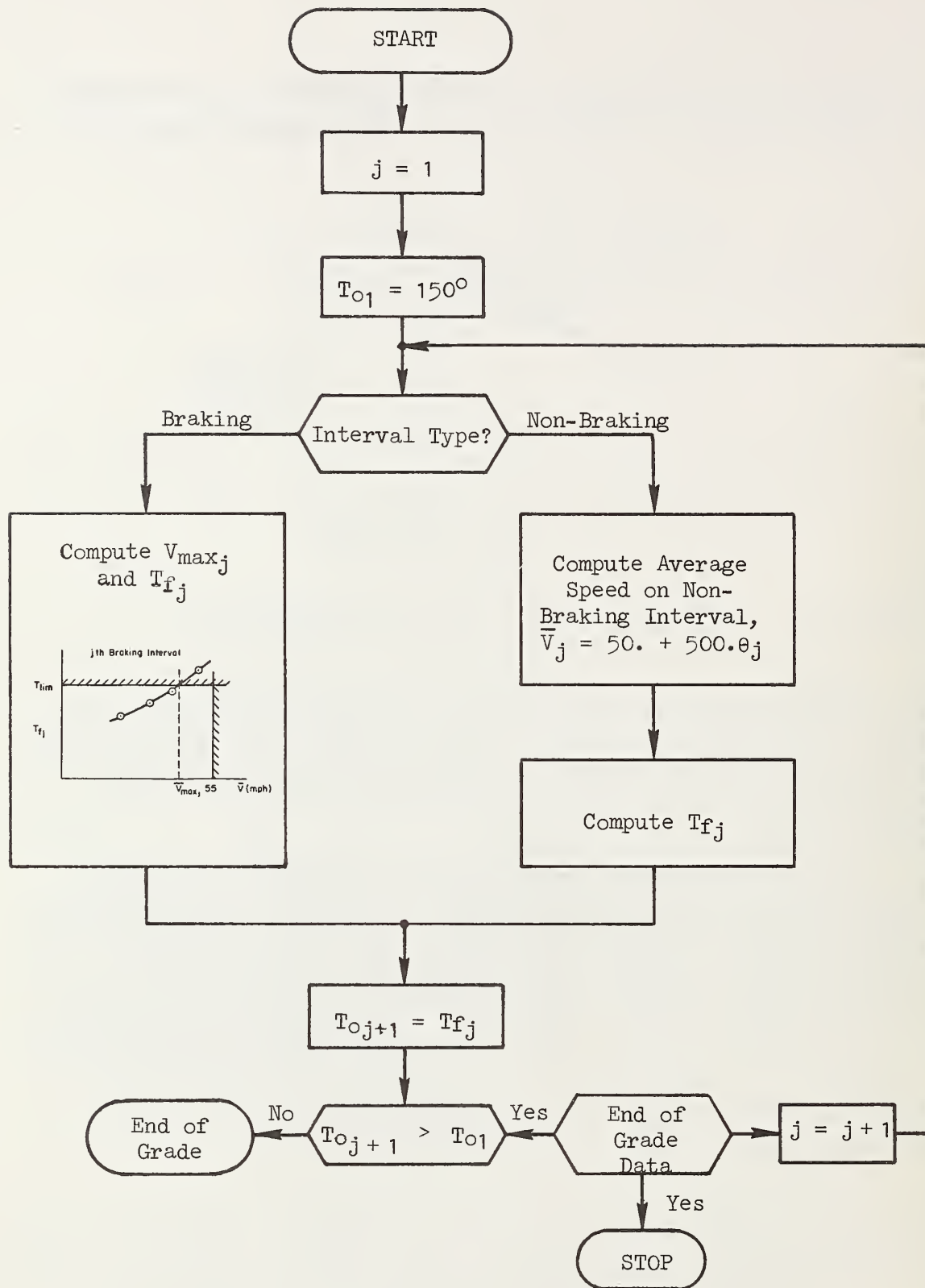


Figure E-9. Flowchart for Simplified Procedure for Estimating \bar{V}_{max} on Braking Interval

FEDERALLY COORDINATED PROGRAM (FCP) OF HIGHWAY RESEARCH AND DEVELOPMENT

The Offices of Research and Development (R&D) of the Federal Highway Administration (FHWA) are responsible for a broad program of staff and contract research and development and a Federal-aid program, conducted by or through the State highway transportation agencies, that includes the Highway Planning and Research (HP&R) program and the National Cooperative Highway Research Program (NCHRP) managed by the Transportation Research Board. The FCP is a carefully selected group of projects that uses research and development resources to obtain timely solutions to urgent national highway engineering problems.*

The diagonal double stripe on the cover of this report represents a highway and is color-coded to identify the FCP category that the report falls under. A red stripe is used for category 1, dark blue for category 2, light blue for category 3, brown for category 4, gray for category 5, green for categories 6 and 7, and an orange stripe identifies category 0.

FCP Category Descriptions

1. Improved Highway Design and Operation for Safety

Safety R&D addresses problems associated with the responsibilities of the FHWA under the Highway Safety Act and includes investigation of appropriate design standards, roadside hardware,

the quality of the human environment. The goals are reduction of adverse highway and traffic impacts, and protection and enhancement of the environment.

4. Improved Materials Utilization and Durability

Materials R&D is concerned with expanding the knowledge and technology of materials properties, using available natural materials, improving structural foundation materials, recycling highway materials, converting industrial wastes into useful highway products, developing extender or substitute materials for those in short supply, and developing more rapid and reliable testing procedures. The goals are lower highway construction costs and extended maintenance-free operation.

5. Improved Design to Reduce Costs, Extend Life Expectancy, and Insure Structural Safety

Structural R&D is concerned with furthering the latest technological advances in structural and hydraulic designs, fabrication processes, and construction techniques to provide safe, efficient highways at reasonable costs.

6. Improved Technology for Highway Construction

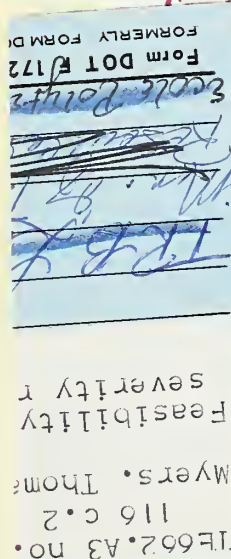
Category 6 is concerned with the research, development, and implementation of highway construction technology to increase productivity, reduce energy consumption, conserve dwindling resources, and reduce costs while improving the methods of construction.

7. Improved Technology for Highway Maintenance

Category 7 addresses problems in preserving existing highways and includes activities in maintenance, traffic services, management, and equipment. The goal is to maximize operational efficiency and safety to the traveling public while conserving resources.

8. Studies

Category 8, not included in the seven-volume official statement of the FCP, is concerned with HP&R and NCHRP studies not specifically related to FCP projects. These studies involve R&D support of other FHWA program office research.



61. Single

copies of the introductory volume are available without charge from Program Analysis (HRD-3), Offices of Research and Development, Federal Highway Administration, Washington, D.C. 20590.

DOT LIBRARY



00056477

